



Πανεπιστήμιο Κύπρου
University of Cyprus

DEPARTMENT OF BIOLOGICAL SCIENCES

Establishment and use of a revised embryo staging, novel *in vitro* assays for pluripotency, potency and specification for investigating early mammalian ectoderm germ layer development in wildtype and gene knockout mouse embryos

XENIA HADJIKYPRI

A Dissertation Submitted to the University of Cyprus in Partial Fulfilment of the Requirements for the Degree of Doctor of Philosophy

SEPTEMBER 2024

XENIA HADJIKYPRI

VALIDATION PAGE

Doctoral Candidate: Xenia Hadjikypr

Doctoral Thesis Title: Establishment and use of a revised embryo staging, novel *in vitro* assays for pluripotency, potency and specification for investigating early mammalian ectoderm germ layer development in wildtype and gene knockout mouse embryos.

The present Doctoral Dissertation was submitted in partial fulfillment of the requirements for the Degree of Doctor of Philosophy at the Department of Biological Sciences and was approved on the 17.03.2023 by the members of the Examination Committee.

Examination Committee:

Research Supervisor: Dr. Pantelis Georgiades, Associate Professor, Department of Biological Sciences, UCY.

.....

Committee Member: Dr. Paris Skourides, Professor, Department of Biological Sciences, UCY.

.....

Committee Member: Dr. Chrysoula Pitsouli, Associate Professor, Department of Biological Sciences, UCY.

Committee Member: Dr Petros P. Petrou, Associate Professor, The Cyprus Institute of Neurology and Genetics.

Committee Member: Dr Vasiliki Gkretsi, Associate Professor, Department of Life Sciences, European University Cyprus.

DECLARATION OF DOCTORAL CANDIDATE

The present doctoral dissertation was submitted in partial fulfilment of the requirements for the degree of Doctor of Philosophy of the University of Cyprus. It is a product of original work of my own unless otherwise mentioned through references, notes, or any other statements.

Xenia Hadjikyprí

XENIA HADJIKYPRÍ

Title

Establishment and use of a revised embryo staging and novel in vitro assays for pluripotency, potency and specification, for investigating early ectoderm development in wildtype and geneknockout mouse embryos.

XENIA HADJIKYPRRI

ABSTRACT [in the English language]

The ectoderm, together with the other two embryonic germ layers (mesoderm and endoderm, collectively known as mesendoderm), are the progenitors of all tissues of the foetus/new-born. Ectoderm is the least understood mammalian germ layer. Its development begins within that part of the epiblast epithelium (progenitor of foetus/new-born) whose cells: (a) are fated to form ectodermal derivatives, mainly neural and surface ectoderm tissues, and (b) remain within the epiblast, as they do not exit it through the primitive streak during gastrulation to form mesendoderm. This project focused on investigating early mammalian ectoderm development using the mouse as a model by studying the development of anterior epiblast, which is fated to mainly form brain and head surface ectoderm, the earliest-formed ectodermal derivatives. The differentiation of epiblast cells into their differentiated cell types, such as ectodermal derivatives, is preceded by important spatio-temporally regulated developmental events. Specifically, epiblast cells, which are initially pluripotent (they are capable of differentiating to all the cell types derived from all three embryonic germ layers) and have a certain specification state (the cell type they are programmed to differentiate), gradually: (a) restrict their potency (reduce the collection of cell types they are capable of differentiating to), and therefore stop being pluripotent, and (b) have to change their specification if it is not according to what they differentiate into during normal development. However, these developmental events during early mouse ectoderm development are poorly understood and were the main interest of this project. Investigating them, not only requires the use of assays for pluripotency, potency and specification, but also knowing when these events occur. The latter requires employment of embryo staging: the subdivision of development into a specific temporal sequence of embryos with different structural features called stages, which unlike embryonic age (time elapsed since fertilization) are an accurate index of the degree of development reached. The study of early ectoderm development, therefore, could benefit from a more refined embryo staging of the period during which it occurs. The six major findings of this study are the following.

First, using novel combinations of external embryo features and gene expression validation, a revised embryo staging for the period from just before gastrulation until the late headfold stage was established. It resulted in subdividing this period into fifteen stages, as opposed to the existing nine ones. This new staging includes the hitherto unidentified stage of gastrulation initiation and, unlike existing staging, subdivides the pre-headfold period into stages without being depended on the timing of allantoic bud presence/size as a diagnostic feature since the latter is not applicable across all mouse strains.

Second, new *in vitro* pluripotency and potency assays for mouse postimplantation tissues that are simpler and faster than existing ones, were established using explant culture and gene expression validation. Both assays identify whether the tested postimplantation tissue is pluripotent, but only the potency assay identifies the potency of non-pluripotent tissues.

Third, the first specification assay for mouse embryo tissues was established by culturing explants under completely defined culture conditions that are considered neutral, so as to allow the manifestation of the programmed differentiation of the tested tissue.

Fourth, combining our revised staging, our novel pluripotency/potency assays and marker gene expression, we show for the first time that during anterior epiblast development the following take place. (i) The earliest loss of pluripotency occurs at pre-headfold-2 (PH2) stage, the earliest stage when primitive streak reaches its full length. This is the earliest stage when anterior-proximal epiblast restricts its potency to only ectodermal fates (neural and surface ectoderm fates) and this bipotent ectoderm state is marked by co-expression of the pluripotency-related markers *Fgf5* (low levels) and *Oct4* and the early surface ectoderm marker *Dlx5*, at a time before expression of the earliest neural genes *Six3* and *Hesx1*. In contrast, the anterior-distal epiblast at this stage is still pluripotent and expresses *Fgf5* (high levels), *Oct4*, but not *Dlx5*. (ii) At pre-headfold-3 (PH3) stage, the previously pluripotent anterior-distal epiblast also restricts its potency to ectodermal fates and this coincides with low level expression of *Fgf5* in this part of anterior epiblast, suggesting that low expression of *Fgf5* marks anterior epiblast with bipotent ectodermal potency. The earliest anterior neural markers *Six3/Hesx1* start being expressed in anterior-proximal epiblast at this stage, suggesting neural plate formation. (iii) At pre-headfold-4 (PH4) stage, there is further restriction of potency of the entire anterior epiblast fated to become brain (most proximal edge of anterior epiblast is fated to form surface ectoderm) to only neural fates. This coincides with undetectable *Fgf5* expression in anterior epiblast, suggesting that the earliest loss of *Fgf5* expression marks neurally committed anterior epiblast.

Fifth, using our specification assay, we show that just prior to gastrulation (exact stage needs further clarification), the pluripotent anterior-proximal and anterior-distal epiblast regions (previously shown to be fated towards mainly non-neural ectoderm and neural derivatives, respectively), are specified differently: the former is specified mainly towards surface ectoderm fates and the latter towards neural fates.

Lastly, we used our pluripotency assay on the anterior epiblast of *Ets2* gene knockout embryos, an *in vivo* system for studying influences from early trophoblast (extraembryonic progenitor tissue of the placenta) on embryo development. This is because unpublished data from our lab showed that early ectoderm development requires

signals from the trophoblast, since the anterior epiblast of these mutants fails to express neural genes (indicating failure of neural induction) and coexpresses *Fgf5*, *Oct4* and *Dlx5*. Our pluripotency assay revealed that anterior epiblast of these mutants is not pluripotent. Taken together with our finding that coexpression of *Fgf5*, *Oct4* and *Dlx5* marks the transient, ectodermally bipotent anterior-proximal epiblast state, it is suggested that anterior epiblast of these mutants may be 'stuck' or confined at this state and that the role of trophoblast signalling might be to promote exit from this state, so as to allow further ectodermal development.

It is concluded that the revised staging and the new pluripotency/potency/specification assays developed here are useful tools for mouse developmental biologists in general, and the results of their application to early ectoderm development have contributed to the understanding of this important developmental process.

Τίτλος

Δημιουργία και χρήση αναθεωρημένου συστήματος σταδιοποίησης εμβρύων και νέων *in vitro* τεστ κυτταρικής πληθοδυνητικότητας, δυνητικότητας και προσδιορισμού για διερεύνηση της ανάπτυξης του πρώιμου εκτοdéρματος χρησιμοποιώντας έμβρυα ποντικών άγριου τύπου και 'gene knockout'.

XENIA HADJIKYPRU

ΠΕΡΙΛΗΨΗ [ABSTRACT in the Greek language]

Το εκτόδεσμα, μαζί άλλες δύο εμβρυϊκές βλαστικές στιβάδες (μεσόδεσμα και ενδόδεσμα, από κοινού γνωστά ως μεσενδόδεσμα), είναι οι πρόγονοι όλων των ιστών του εμβρύου/νεογέννητου. Το εκτόδεσμα είναι η λιγότερο κατανοητή βλαστική στιβάδα των θηλαστικών. Η ανάπτυξη του αρχίζει μέσα στο τμήμα εκείνο του επιβλαστικού επιθηλίου (προγονικός ιστός του εμβρύου/νεογέννητου) του οποίου τα κύτταρα: (α) προορίζονται να σχηματίσουν εκτοδερμικά παράγωγα, κυρίως νευρικούς και επιφανειακούς εκτοδερμικούς ιστούς, και (β) παραμένουν μέσα στον επιβλάστη, καθώς δεν εξέρχονται από αυτόν μέσω της πρωτογενούς αυλάκωσης κατά τη διάρκεια της γαστρίδωσης για να σχηματίσουν το μεσενδόδεσμα. Η μελέτη αυτή επικεντρώθηκε στη διερεύνηση της πρώιμης ανάπτυξης του εκτοδέματος των θηλαστικών χρησιμοποιώντας το ποντίκι ως μοντέλο, μελετώντας την ανάπτυξη του πρόσθιου επιβλάστη, ο οποίος προορίζεται να σχηματίσει κυρίως τον εγκέφαλο και το επιφανειακό εκτόδεσμα του κεφαλιού, τα οποία είναι τα πρώτα εκτοδερμικά παράγωγα που εμφανίζονται. Οι διαφοροποιήσεις των κυττάρων του επιβλάστη στους διαφοροποιημένους κυτταρικούς τύπους τους, όπως αυτοί των εκτοδερμικών παραγώγων, προηγούνται από σημαντικά χωροχρονικά-ρυθμιζόμενα αναπτυξιακά γεγονότα. Συγκεκριμένα, τα κύτταρα του επιβλάστη, τα οποία είναι αρχικά πληθοδυνητικά (είναι ικανά να διαφοροποιηθούν σε όλους τους κυτταρικούς τύπους που προέρχονται και από τις τρεις εμβρυϊκές βλαστικές στιβάδες) και έχουν μια συγκεκριμένη κατάσταση προσδιορισμού (ο κυτταρικός τύπος στον οποίο είναι προγραμματισμένα να διαφοροποιηθούν), σταδιακά: (α) περιορίζουν την δυναμικότητά τους (μειώνουν τη συλλογή των κυτταρικών τύπων στους οποίους είναι ικανά να διαφοροποιηθούν) και επομένως παύουν να είναι πληθοδυνητικά, και (β) πρέπει να αλλάξουν τον προσδιορισμό τους εάν αυτός δεν είναι σύμφωνος με το σε τι διαφοροποιούνται κατά τη διάρκεια της φυσιολογικής ανάπτυξης. Ωστόσο, αυτά τα αναπτυξιακά γεγονότα κατά την ανάπτυξη του πρώιμου εκτοδέματος των ποντικών είναι ελάχιστα κατανοητά και αποτέλεσαν το κύριο ενδιαφέρον αυτής της μελέτης. Η διερεύνησή τους, όχι μόνο απαιτεί τη χρήση δοκιμασιών για την πληθοδυνητικότητα, τη δυναμικότητα και τον προσδιορισμό, αλλά και τη γνώση του πότε συμβαίνουν αυτά τα γεγονότα. Το τελευταίο απαιτεί τη χρήση συστήματος σταδιοποίησης των εμβρύων: την υποδιαίρεση της ανάπτυξης σε μια συγκεκριμένη χρονική ακολουθία εμβρύων με διαφορετικά δομικά χαρακτηριστικά που ονομάζονται στάδια, τα οποία σε αντίθεση με την εμβρυϊκή ηλικία (χρόνος που έχει παρέλθει από τη γονιμοποίηση) αποτελούν ακριβή δείκτη του βαθμού ανάπτυξης που έχει επιτευχθεί. Η μελέτη της ανάπτυξης του πρώιμου εκτοδέματος, επομένως, θα μπορούσε να ωφεληθεί από μια πιο εκλεπτυσμένη εμβρυϊκή σταδιοποίηση της περιόδου κατά την οποία λαμβάνει χώρα. Τα έξι σημαντικότερα ευρήματα της παρούσας μελέτης είναι τα ακόλουθα.

Πρώτον, χρησιμοποιώντας νέους συνδυασμούς εξωτερικών χαρακτηριστικών του εμβρύου και επικύρωσης της γονιδιακής έκφρασης, καθορίστηκε μια αναθεωρημένη σταδιοποίηση του εμβρύου για την περίοδο από λίγο πριν από τη γαστριδίωση έως το headfold στάδιο, η οποία οδήγησε στην

υποδιαίρεση αυτής της περιόδου σε δεκαπέντε στάδια, σε αντίθεση με τα προυπάρχοντα εννέα στάδια. Αυτή η νέα σταδιοποίηση περιλαμβάνει το μέχρι σήμερα μη αναγνωρισμένο στάδιο της έναρξης της γαστριδίωσης και, σε αντίθεση με την υπάρχουσα σταδιοποίηση, υποδιαιρεί την pre headfold περίοδο σε στάδια χωρίς να εξαρτάται από το χρόνο παρουσίας/μέγεθους του allantoic bud ως διαγνωστικό χαρακτηριστικό, δεδομένου ότι το τελευταίο δεν είναι εφαρμόσιμο σε όλα τα στελέχη ποντικών.

Δεύτερον, καθιερώθηκαν νέες δοκιμασίες *in vitro* πληθοδυνητικότητας και δυναμικότητας για ιστούς ποντικών μετά την εμφύτευση, οι οποίες είναι απλούστερες και ταχύτερες από τις υπάρχουσες, με τη χρήση καλλιέργειας εκφυτευμάτων και επικύρωσης γονιδιακής έκφρασης. Και οι δύο δοκιμασίες προσδιορίζουν αν ο εξεταζόμενος μεταεμφυτευτικός ιστός είναι πληθοδυνητικός, αλλά μόνο η δοκιμασία δυναμικότητας προσδιορίζει την ισχύ των μη πληθοδύναμων ιστών.

Τρίτον, καθιερώθηκε η πρώτη δοκιμασία προσδιορισμού για ιστούς εμβρύου ποντικού με καλλιέργεια εκβλαστήσεων υπό πλήρως καθορισμένες συνθήκες καλλιέργειας που θεωρούνται ουδέτερες, έτσι ώστε να επιτρέπεται η εκδήλωση της προγραμματισμένης διαφοροποίησης του εξεταζόμενου ιστού.

Τέταρτον, συνδυάζοντας το αναθεωρημένο σύστημα σταδιοποίησης, τις νέες δοκιμασίες πληθοδυνητικότητας /δυναμικότητας και την έκφραση γονιδίων δεικτών, δείχνουμε για πρώτη φορά ότι κατά την ανάπτυξη του πρόσθιου επιβλάστη λαμβάνουν χώρα τα εξής. (i) Η πρωιμότερη απώλεια της πληθοδυνητικότητας συμβαίνει στο στάδιο pre-headfold-2 (PH2), το πρωιμότερο στάδιο κατά το οποίο η πρώιμη αυλάκωση φτάνει στο πλήρες μήκος της. Αυτό είναι το πρωιμότερο στάδιο κατά το οποίο ο προσθιο-εγγύς επιβλάστης περιορίζει τη δραστηριότητά του μόνο σε εκτοδερμικές μοίρες (νευρικές και επιφανειακές εκτοδερμικές μοίρες) και αυτό σηματοδοτείται από τη συν-έκφραση των σχετικών με την πληθοδυνητικότητα δεικτών *Fgf5* (χαμηλά επίπεδα) και *Oct4* και του πρώιμου επιφανειακού εκτοδερμικού δείκτη *Dlx5*, σε χρόνο πριν από την έκφραση των πρώιμων νευρικών γονιδίων *Six3* και *Hesx1*. Αντίθετα, ο προσθιο-απομακρυσμένος επιβλάστης σε αυτό το στάδιο εξακολουθεί να είναι πληθοδυνητικός και εκφράζει το *Fgf5* (σε υψηλά επίπεδα), το *Oct4*, αλλά όχι το *Dlx5*. (ii) Στο στάδιο pre-headfold-3 (PH3), ο προηγούμενος πληθοδυνητικός προσθιο-απομακρυσμένος επιβλάστης περιορίζει επίσης την ικανότητά του σε εκτοδερμικές μοίρες και αυτό συμπίπτει με χαμηλά επίπεδα έκφρασης του *Fgf5* σε αυτό το τμήμα του πρόσθιου επιβλάστη, γεγονός που υποδηλώνει

ότι η χαμηλή έκφραση του *Fgf5* σηματοδοτεί τον πρόσθιο επιβλάστη με διποτική εκτοδερμική ικανότητα. Οι πρώιμοι πρόσθιοι νευρικοί δείκτες *Six3/Hesx1* αρχίζουν να εκφράζονται στον πρόσθιο-εγγύς επιβλάστη σε αυτό το στάδιο, γεγονός που υποδηλώνει το σχηματισμό νευρικής πλάκας. (iii) Στο στάδιο pre-headfold-4 (PH4), υπάρχει περαιτέρω περιορισμός της ικανότητας ολόκληρου του πρόσθιου επιβλάστη που προορίζεται να γίνει εγκέφαλος (εκτός πιθανώς από το πιο εγγύς άκρο της, το οποίο προορίζεται για επιφανειακό εκτόδερμα) μόνο σε νευρικές μοίρες. Αυτό συμπίπτει με μη ανιχνεύσιμη έκφραση του *Fgf5* στον πρόσθιο επιβλάστη, γεγονός που υποδηλώνει ότι η πρώιμη απώλεια της έκφρασης του *Fgf5* σηματοδοτεί τον νευρικά δεσμευμένο πρόσθιο επιβλάστη.

Πέμπτον, χρησιμοποιώντας τη δοκιμασία προσδιορισμού μας, δείχνουμε ότι λίγο πριν από τη γαστριδίωση (το ακριβές στάδιο χρειάζεται περαιτέρω διευκρίνιση), οι πληθοδυνητικές περιοχές του πρόσθιο-εγγύς και πρόσθιο-απομακρυσμένου επιβλάστη (που προηγουμένως είχε αποδειχθεί ότι προδιαγράφονται κυρίως προς μη νευρικό εκτόδερμα και νευρικά παράγωγα, αντίστοιχα), προσδιορίζονται διαφορετικά: η πρώτη προσδιορίζεται κυρίως προς τις μοίρες του επιφανειακού εκτοδέρματος και η δεύτερη προς τις νευρικές μοίρες.

Τέλος, χρησιμοποιήσαμε τη δοκιμασία πληθοδυνητικότητας μας στον πρόσθιο επιβλάστη εμβρύων με knockout γονίδιο *Ets2*, ένα *in vivo* σύστημα για τη μελέτη των επιδράσεων του πρώιμου τροφοβλάστη (εξωεμβρυϊκός προγονικός ιστός του πλακούντα) στην ανάπτυξη του εμβρύου. Αυτό συμβαίνει επειδή αδημοσίευτα δεδομένα από το εργαστήριό μας έδειξαν ότι η ανάπτυξη του πρώιμου εκτοδέρματος απαιτεί σήματα από την τροφοβλάστη, καθώς ο πρόσθιος επιβλάστης αυτών των μεταλλαγμένων εμβρύων αποτυγχάνει να εκφράσει νευρικά γονίδια (υποδεικνύοντας αποτυχία της νευρικής επαγωγής) και συν-εκφράζει τα *Fgf5*, *Oct4* και *Dlx5*. Η δοκιμασία πληθοδυνητικότητας μας αποκάλυψε ότι ο πρόσθιος επιβλάστη αυτών των εμβρύων δεν είναι πληθοδυνητικός. Σε συνδυασμό με τη διαπίστωση μας ότι η συνεκφραση των *Fgf5*, *Oct4* και *Dlx5* σηματοδοτεί την παροδική, εκτοδερμικά διποτική κατάσταση του πρόσθιο-εγγύς επιβλάστη, προτείνεται ότι ο πρόσθιος επιβλάστης των μεταλλαγμένων αυτών εμβρύων μπορεί να είναι "κολλημένος" σε αυτή την κατάσταση και ότι ο ρόλος της σηματοδότησης του τροφοβλάστη μπορεί να είναι η προώθηση της εξόδου από αυτή την κατάσταση, ώστε να επιτραπεί η περαιτέρω ανάπτυξη.

Συμπεραίνεται ότι οι αναθεωρημένες δοκιμασίες σταδιοποίησης και πληθοδυνητικότητας/δυνητικότητας/προσδιορισμού που αναπτύχθηκαν στην μελέτη αυτή αποτελούν χρήσιμα εργαλεία για τους αναπτυξιακούς βιολόγους ποντικών γενικά και τα αποτελέσματά της εφαρμογής τους στην ανάπτυξη του πρώιμου εκτοδέρματος συνέβαλαν στην κατανόηση αυτής της σημαντικής αναπτυξιακής διαδικασίας.

ACKNOWLEDGEMENTS

Firstly, I would like to thank my supervisor Dr. Pantelis Georgiades for all his huge support and guidance throughout all the years of my PhD. Also, all my colleagues from the lab and all my friends and family members for their continuous support and love! A huge thank you and special dedication to my forever partner Philippos, for being there for me all these years!

XENIA HADJIKYPRRI

Table of Contents

Contents

CHAPTER 1. INTRODUCTION	1
1.1 Overview of early mouse development.....	1
1.2 Developmental potency and specification	3
1.3 Embryo staging	5
1.4 Gastrulation.....	5
1.5 The ectoderm germ layer	9
1.6. Formation of the neural tube: primary and secondary neurulation	18
1.7. The Anterior Primitive Streak and its derivatives	21
1.7.1 The Node	23
1.7.2 The role of the Node in the Definitive Ectoderm.....	25
1.7.3 The Anterior Mesendoderm (AME).....	27
1.7.4 The role of the AME in Definitive Ectoderm.....	27
1.7.5 The Head Process.....	30
1.8 Overview of Extraembryonic Tissues.....	31
1.8.1 The Extraembryonic Ectoderm (ExE).....	33
1.8.2 The ExE and its role in Epiblast and VE patterning	34
1.8.3 The role of the AVE on the establishment of the Definitive Ectoderm.....	36
1.9. The <i>Ets2</i> gene: Introduction to its structure and expression	37
1.9.1 <i>Ets2</i> null type-I and type-II mutant embryos	38
1.10 Discrepancies regarding the early development of the ectoderm germ layer and the need to establish a more comprehensive mouse embryo staging system.....	41
CHAPTER 2. METHODOLOGY.....	44
2.1 Mice and embryo collection.....	44
2.2. Mouse tails genotyping	45
2.3. Microsurgery and culture of Epiblast embryonic explants	46
2.4 Whole mount RNA <i>in situ</i> Hybridization	47
2.5 One colour RNA in situ hybridization	53
2.6 Double colour whole-mount RNA in situ hybridization	55
2.7 Clearing method of staged embryos.....	56
2.8 RNA Preparation and quantitative PCR Analysis.....	56
2.9 Quantitative Real Time PCR (qPCR).....	56
2.10 ExE and VE ablation of embryos and the accurate generation of epiblast explants..	58
CHAPTER 3. SCIENTIFIC AIMS AND HYPOTHESES	59
3.1. Specific Aim 1	59
3.2 Specific Aim 2	60
3.3 Specific Aim 3 (3A and 3B).....	60

3.4 Specific Aim 4 (4A and 4B).....	61
3.5 Specific Aim 5	62
3.6 Specific Aim 6 (6A and 6B).....	63
3.7 Specific Aim 7	64
CHAPTER 4. RESULTS	65
4.1 Specific Aim 1, its hypothesis and its results:	65
4.2 Specific Aim 2, its hypothesis and its results:	92
4.3 Specific Aim 3 (A and B), its hypothesis and its results:	108
4.4 Specific Aim 4 (A and B), its hypothesis and its results:	122
4.5 Specific Aim 5, its hypothesis and its results:	151
4.6 Specific Aim 6 (A and B), its hypothesis and its results:	155
4.7 Specific Aim 7, its hypothesis and its results:	161
DISCUSSION	167
PUBLICATIONS	177
FUTURE EXPERIMENTS	178
ANNEXES.....	179
REFERENCES	181

Table of Figures

Figure 1: Early murine development from the blastocyst to gastrulation stage.....	3
Figure 2: Mouse embryo gastrulation.....	8
Figure 3: Gastrulation gives rise to the three primary germ layers of the embryo.....	12
Figure 4: Overview of molecular markers in early neural plate border specification.....	18
Figure 5: Formation and patterning of the murine neural tube	20
Figure 6: Signalling in the mouse embryo during gastrulation influences pluripotent epiblast cell fate decisions.....	22
Figure 7: Neural induction in the mouse embryo from E6.0 to E8.5	29
Figure 8: The Extraembryonic Tissues – the ExE and VE	33
Figure 9: Ets2 expression profile	38
Figure 10: Morphological classification of type I and type II Ets2 mutant conceptuses	40
Figure 11: Epiblast patterning defects in Ets2 type-II and type I mutant embryos.....	41
Figure 12: The different angles that isolated conceptuses can be visualized.....	67
Figure 13: The classification of embryos depends on the presence or absence of amnion closure ..	68
Figure 14: Thickened anterior VE (AVE) stage embryo	70
Figure 15: Immature Pre-Streak (preS) stage embryo	71
Figure 16: Mature Pre-Streak (preS) stage embryos.....	72
Figure 17: Nascent Stage (NS) embryos.....	74
Figure 18: Early Streak (ES) stage embryo.....	75
Figure 19: Mid-Streak-1 (MS1) stage embryo.....	76
Figure 20: Mid-Streak-2 (MS2) stage embryo.....	77
Figure 21: Late-Streak-1 (LS1) stage embryos.....	78
Figure 22: Late-Streak-2 (LS2) stage embryos.....	79
Figure 23: The classification of embryos depends on the presence/absence of head process and its relative location within the distal tip area	81
Figure 24: The classification of embryos depends on the presence of either immature or mature morphological node.....	82
Figure 25: The use of the size of Allantoic bud as a morphological criterion for embryonic staging	84
Figure 26: The classification of embryos depends on the presence of headfold.....	85
Figure 27: Pre- Headfold - 1 (PH1) stage embryo	86
Figure 28: Pre-Headfold – 2 (PH2) stage embryo.....	87
Figure 29: Pre- Headfold – 3 (PH3) stage embryo.....	88
Figure 30: Pre- Headfold - 4 (PH4) stage embryo	89
Figure 31: Early-Headfold (EH) stage embryo.....	90
Figure 32: Late-Headfold stage (LH) embryo.....	90
Figure 33: Spatiotemporal expression of Fgf5 from early streak to late headfold.....	94
Figure 34: Spatiotemporal expression of Dlx5 from early streak to late headfold	96
Figure 35: Spatiotemporal expression of Hesx1 from early streak to late headfold	99
Figure 36: Spatiotemporal expression of Six3 from pre-headfold-1 to late headfold.....	100
Figure 37: Spatiotemporal expression of Sox1 from pre-headfold-3 to late headfold	101
Figure 38: Spatiotemporal expression of Bra from pre-headfold-1 to late headfold	103
Figure 39: Spatiotemporal expression of Sox2 from pre-headfold-1 to Late Headfold.....	105
Figure 40: Establishment of pluripotency assay	113
Figure 41: Establishment of pluripotency assay RNA in situ hybridization.	114
Figure 42: RT-qPCR analysis of marker gene expression of anterior explants cultured in pluripotency assay conditions of anterior epiblast explants from E6.5 pre-streak embryos (pluripotent explants) after culture for 48h in pluripotency conditions	115
Figure 43: Application of pluripotency assay based on live morphology of explant outgrowths for identification of earliest stage when pluripotency is lost from anterior epiblast explants derived from mid-streak (MS) to early headfold (EH) stages.....	119
Figure 44: Application of pluripotency assay based on gene expression assessed by RNA in situ hybridization in explant outgrowths for identification of earliest stage when pluripotency is lost from anterior epiblast explants derived from mid-streak (MS) to pre-he	120
Figure 45: Establishment of neural potency assay: Live morphology of outgrowths of anterior epiblast explants from E6.5 pre-streak (positive control - pluripotent epiblast) cultured up to 72h	

under neural potency culture conditions (N2/B27 and SB43 on FBS)	126
Figure 46: Establishment of neural potency assay: RNA in situ hybridization for gene expression analysis of outgrowths of anterior epiblast explants from E6.5 pre-streak cultured for up to 48h under neural potency conditions (N2/B27, SB43 on FBS)	127
Figure 47: RT-qPCR analysis of marker gene expression of anterior epiblast explants from E6.5 Pre-Streak embryos cultured in neural potency assay culture conditions (N2/B27 + SB43) for 48h	128
Figure 48: Establishment of surface ectoderm potency assay: Live morphology of outgrowths of anterior epiblast explants from E6.5 pre-streak cultured up to 96h under surface ectoderm potency culture conditions (N2/B27 + SB43 + BMP2 on FBS).....	130
Figure 49: Establishment of surface ectoderm potency assay: RNA in situ hybridization for gene expression analysis of outgrowths of anterior epiblast explants from E6.5 pre-streak cultured for up to 48h under surface ectoderm potency conditions (N2/B27 + SB43 + B	131
Figure 50: RT-qPCR analysis of marker gene expression of anterior epiblast explants from E6.5 Pre-Streak embryos cultured in surface ectoderm potency assay culture conditions (N2/B27 + SB43 + BMP2) for 48h.....	132
Figure 51: Establishment of mesendoderm potency assay: Live morphology of outgrowths of anterior epiblast explants from E6.5 pre-streak cultured up to 96h under mesendoderm potency culture conditions (N2/B27 + BMP2 on FBS).....	134
Figure 52: Establishment of mesendoderm potency assay: RNA in situ hybridization for gene expression analysis of outgrowths of anterior epiblast explants from E6.5 pre-streak cultured for 48h under mesendoderm potency conditions (N2/B27 + BMP2 on FBS).....	135
Figure 53: RT-qPCR analysis of marker gene expression of anterior explants from anterior epiblast of Pre-Streak embryos cultured in predominantly mesendoderm differentiation culture conditions (N2/B27 + BMP2) for 48h.....	136
Figure 54: RT-qPCR analysis of marker gene expression of proximal anterior explants from Early Headfold (EH) embryos cultured in all three conditions of the potency assay for 2 days	137
Figure 55: RT-qPCR analysis of marker gene expression of proximal and distal anterior explants of Mid Streak (MS), Late Streak (LS) and Pre Headfold 1 (PH1) and anterior distal of Pre Headfold-2 (PH2) explants cultured in all three conditions of the potency assay	144
Figure 56: Figure 56: RT-qPCR analysis of marker gene expression of proximal anterior explants of Pre Headfold 2 (PH2) and anterior proximal and distal explants of Pre – Headfold 3 (PH3) cultured in all three conditions of the potency assay for 2 days.....	146
Figure 57: RT-qPCR analysis of marker gene expression of proximal anterior and proximal distal explants of Pre Headfold 4 (PH2) and Early Headfold (EH) cultured in all three conditions of the potency assay for 2 days	149
Figure 58: Gene expression assessed by RNA in situ hybridization of the Ets2 type II E8.3 mutant embryos and wildtype E8.25 embryos	153
Figure 59: Gene expression assessed by RNA in situ hybridization of the Co expression of Dlx5 and Fgf5 (Non neural ectoderm and pluripotency related epiblast markers, respectively) during normal development at the Pre Headfold-1 (PH1) and Pre Headfold-2 (PH2) stages	154
Figure 60: Live morphology and RNA in situ hybridization for gene expression analysis of outgrowths of anterior epiblast explants from pre-streak (pluripotent epiblast) and anterior Ets2 -/- type II epiblast.....	156
Figure 61: Live morphology and Gene expression of anterior epiblast explants of Ets2 type II E8.3 mutants cultured using the surface ectoderm (N2/B27 + SB43 + BMP2 on FBS) and mesendoderm potency assay (N2/B27 + BMP2 on FBS) culture conditions for 2 days.....	159
Figure 62: Live morphology and Gene expression of anterior proximal epiblast explants from E6.5 Pre-Streak embryos cultured under the specification assay culture conditions (N2/B27 on Fibronectin) for 24, 48h and 72h.....	164
Figure 63: Live morphology and Gene expression of anterior distal epiblast explants from E6.5 Pre-Streak embryos cultured under the specification assay culture conditions (N2/B27 on Fibronectin) for 24h and 48h	165
Figure 64: Model for the existence of the transient, ectodermally bipotent anterior-proximal epiblast state at PH2 stage and the transient, ectodermally bipotent anterior epiblast state at the PH3 stage during mouse embryonic development.....	176

Table of Tables

Table 1: Primers for the wildtype and Ets2 mutant allele that were used in mouse tails and embryo genotyping.....	46
Table 2: Restriction enzymes and polymerases for anti-sense probes that were used for each gene	52

XENIA HADJIKYPRRI

Abbreviations

AC: Amniotic cavity	Fgf: Fibroblast Growth Factor
ACP: Anterior chordal plate	ICM: Inner cell mass
Al: Allantois	Krt18: Keratin 18
Am: Amnion	MET: Mesenchymal to epithelial transition
AME: Anterior Mesendoderm	MGO: Mid gastrula organiser
AN: Anterior Notochord	MHP: Median hinge point
A-P axis: Anterior-posterior axis	mTE: Mural trophectoderm.
AVE: Anterior Visceral Endoderm	NC: Notochord
BMPs: Bone morphogenetic proteins	NE: Neuroepithelium
Bra/T: Brachyury	NMPs: Neuromesodermal progenitors
Ch: Chorionic	PD: Proximo-distal
CNS: Central nervous system	PNS: Peripheral nervous system
DE: Definitive Endoderm	PrCP: Prechordal plate
DLHP: Dorsolateral hinge point	PrE: Primitive endoderm
dpc: Days post-coitum	PS: Primitive Streak
DVE: Distal Visceral Endoderm	pTE: Polar trophectoderm
E: Embryonic day	PX: Paraxial mesoderm
EC: Exocoelomic cavity	TE: trophectoderm
EGO: Early gastrula organiser	VE: Visceral endoderm
EMT: Epithelial-to-mesenchymal transition	WISH: Whole mount in situ hybridization
EPC: Ectoplacenta Cone	
EPI: Epiblast	
EpiSCs: Epiblast stem cells	
ESCs: Embryonic stem cells	
EXE: Extraembryonic ectoderm	

Embryonic stages abbreviations:

AVE: Thickened anterior VE

PreS: Immature / Mature pre-streak

NS: Nascent streak

ES: Early streak

MS1: Mid-streak-1

MS2: Mid-streak-2

LS1: Late-streak-1

LS2: Late-streak-2

PH1: Pre-Headfold-1

PH2: Pre-Headfold-2

PH3: Pre-Headfold-3

PH4: Pre-Headfold-4

EH: Early- Headfold

LH: Late-Headfold

Gene abbreviations:

Bra - T brachyury, T-box transcription factor T

Dlx5/6 - Distal-Less Homeobox 5/6

Fgf5 - Fibroblast Growth Factor 5

Hesx1 - HESX Homeobox 1

K8/18 - Keratin 8/18

Oct4 - POU Class 5 Homeobox 1

Six3 - SIX Homeobox 3

Sox 1 - SRY-Box Transcription Factor 1

Sox2 - SRY-Box Transcription Factor 2

CHAPTER 1. INTRODUCTION

1.1 Overview of early mouse development

The early mouse development commences when the zygote undergoes several mitotic cell divisions, so that by embryonic (E) day 2-3 (E2-3) 8-16 identical blastomeres now constitute the embryo (Loebel et al., 2003; Nagy et al., 2003). Being totipotent, these cells have the ability to differentiate into all embryonic and extraembryonic tissues that will contribute to the future embryo. By 3.0 dpc, the embryo compacts to form what is now called the morula, establishing the first time appeared apical-basal polarisation of the embryo (Alarcon, 2010). Due to passive diffusion of water molecules by 3.5 dpc, a blastocoelic cavity forms and the embryo is now known as the blastocyst (Watson and Barcroft, 2001) consisting of an outer trophectoderm (TE) multipotent population and an inner cell mass (ICM) pluripotent population.

Following implantation at embryonic day 4.5 (E4.5), the TE of the expanded blastocyst will give rise to the placenta progenitors, that is the extraembryonic ectoderm (ExE) and the ectoplacental cone (EPC) in response to Fgf4 signalling (Haffner et al., 1999). The outside cells forming the ICM will differentiate into the Primitive Endoderm (PrE) while the remaining will form the Embryonic Ectoderm or pluripotent epiblast (EPI) which is the precursor of the fetus (Saiz and Plusa 2013). The extraembryonic tissues (TE and PrE) are necessary for the proper development of the embryo as the progenitors of the placenta structure that protects the embryo and mediates the nutrient and gas exchange as well as the disposal of waste products (Haffner et al., 1999).

The early postimplantation embryo at E5.5 has now adopted the relatively simple form of a cup shape known as the egg cylinder (Arnold and Robertson, 2009; Nichols and Smith, 2012). Consisting of three epithelial tissues, the epiblast is found at the distal half, the ExE at the proximal half, while the Visceral Endoderm, a tissue derived from the PrE, encapsulates the other two tissues. Specifically, what is defined as embryonic VE (emVE) is associated with the epiblast, while the extraembryonic VE (exVE) surrounds the ExE. The VE will differentiate into the yolk sac placenta, an extraembryonic structure necessary prior to the establishment of the definitive placenta (Georgiades et al. 2002). Once specified, the VE cells found at the embryonic distal tip migrate proximally on one side towards the embryonic-extraembryonic junction (where EPI and ExE meet), forming the anterior visceral endoderm (AVE) (Nowotschin and Hadjantonakis, 2010). This proximal orientated cell migration occurs rapidly and results in a unilateral repositioning of emVE cells that convert the proximal-distal (P-D) axis into an anterior posterior (A-

P) axis (Nowotschin and Hadjantonakis, 2010) (Stower and Srinivas, 2014). This rotation of axis establishes a gradient of Wnt and Nodal signalling marking the site of primitive streak (PS) formation within the epiblast that is found diagonally to the AVE. The PS defines the posterior site of the embryo and therefore the site of gastrulation (Tam and Loebe 2007).

XENIA HADJIKYPRU

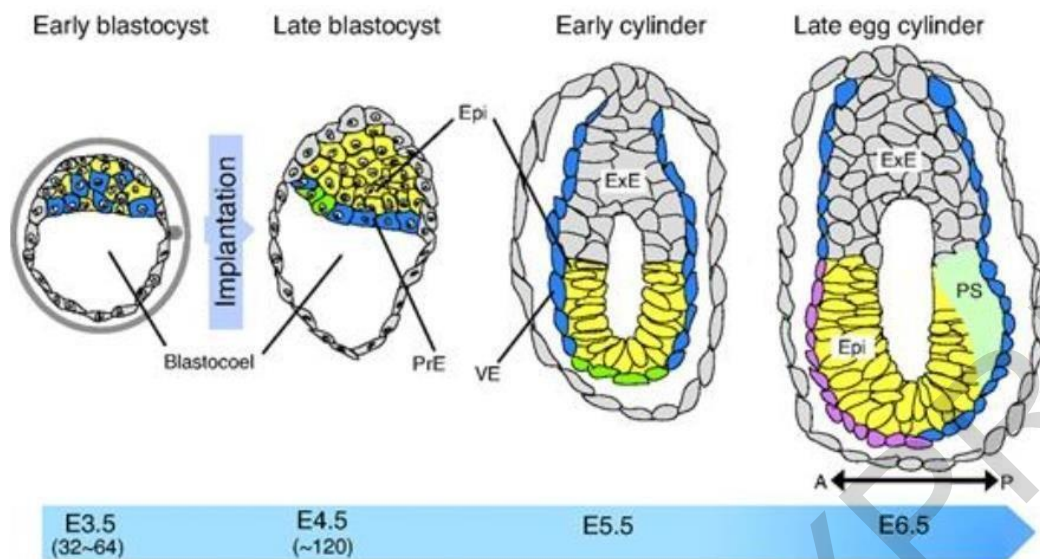


Figure 1: Early murine development from the blastocyst to gastrulation stage.

Morphological and cellular events taking place from the E3.5 stage blastocyst stage to the E6.5 early gastrulation stage. AVE, anterior visceral endoderm; DVE, distal visceral endoderm; Epi, epiblast; Exe, extra-embryonic ectoderm; PrE, primitive ectoderm; PS, primitive streak; VE, visceral endoderm. (Adapted from Katsuyoshi Takaoka and Hiroshi Hamada, 2012)

1.2 Developmental potency and specification

In addition to morphogenesis events guiding development, during these early stages, what also takes place are changes in cell potency and specification.

Cell or tissue potency refers to cells that can differentiate. It is defined as the collection of cell types/tissues, a cell or tissue is capable of differentiating to. At the beginning of mammalian development, the zygote and its early descendants are totipotent, meaning that they can differentiate to all cell types of the conceptus. As development progresses, potency becomes gradually restricted. For example, the epiblast (progenitor of fetus) is initially pluripotent, that is, it can differentiate to all cell types of the fetus/newborn, but not to the majority of extraembryonic tissues. During development different embryonic cell types usually have different potencies (De Los Angeles et al., 2015). Mouse embryonic stem cells and epiblast stem cells (the *in vitro* analogues of preimplantation and early postimplantation epiblast, respectively) are pluripotent (De Los Angeles et al., 2015).

Cell or tissue specification also refers to cells that can differentiate. The specification status of a cell/tissue can be defined as the collection of cell types/tissues it is

programmed to differentiate to (that is, how it differentiates in the absence of external influences). During development, before cells differentiate according to their fate, they have to change their specification status (if it is not the same as their fate), so that it becomes the same as their fate. Embryonic cell types from different embryonic regions and/or different stages usually have different specification status (Bedzhov et al., 2014).

To study cell potency in vivo heterotopic grafting and in vitro explant studies (Li et al., 2013) have been widely used. Pluripotency investigation studies have used the techniques of teratoma derivation. A teratoma is a benign tumour consisting of a mixture of differentiated tissues and derivatives of the three germ layers. Experimental teratomas are derived from early mammalian embryos that were transplanted into ectopic sites of the adult animal (Bulic-Jakus et al., 2015). Pluripotency has also been defined by the ability of cells to form germline chimeras. Indeed, the production of chimeras—animals made up of cells originating from two zygotes—is another major experimental type for assessing stem cell potency/pluripotency (Nagy et al., 1993). Cell specification assessment has been achieved through in vitro culture of embryonic explants into chemically defined medium (Li et al., 2015) ensuring the absence of exogenous factors affecting cell fate.

1.3 Embryo staging

To study developmental events during animal embryogenesis, such as cell/tissue changes, potency, specification, or differentiation is important to acknowledge all involved spatiotemporal aspects, in other words, when and where these events occur. Therefore, to efficiently study the extent of embryonic development, embryonic staging systems should be established.

Although chronological age of embryos (i.e., the amount of time in hours, days or weeks elapsed from fertilization) is still widely used, it is not an accurate indicator of the extent of developmental progression. This is because there is variation in the degree of developmental progression between embryos having the same chronological age. Instead, a more accurate way of defining developmental progression is based on structural embryonic features. These are used to subdivide development into a temporal sequence of different stages (Fujinaga M. et al., 1992).

Indeed, embryo staging, is usually based on a unique set of structural features defining each stage. However, since development is a continuous process, any existing embryo stage could be improved by subdividing it into more stages if new combinations of structural features are used. This would further improve our understanding of developmental progression processes.

1.4 Gastrulation

As mentioned above, gastrulation commences with the appearance of the primitive streak (PS) in the posterior side of the embryo. The PS is a dynamic structure consisting of two components: a midline(axial) strip of posterior epiblast whose cells (unlike the rest of the epiblast) undergo Epithelial to Mesenchymal transition (EMT) and mesenchymal cells situated between EMT epiblast and its subadjacent emVE that are derived from EMT epiblast and are actively migrating away from this

region (find references in BBRC paper). During gastrulation, which is under way by the early streak(ES) stage at around E6.5), epiblast cells destined to form the endoderm and mesoderm embryonic germ layers (the other being the ectoderm) exit the epiblast through the EMT epiblast part of the PS(ref). Gastrulation is a well-coordinated process of fate specification involving spatial organisation and morphogenesis (Morgani et al, 2018). It is a development event of great importance and a prerequisite of organogenesis, as the epiblast transforms into the three embryonic germ layers (ectoderm, mesoderm and endoderm) resulting in the establishment of the main body plan of the animal (Baron

2005).

During the time of gastrulation, some epiblast cells undergo EMT, to ingress through the PS and emerge as cells of either the Mesoderm or the Endoderm germ layer (Loebel et al., 2003; Arnold and Robertson, 2009). The cells that will not ingress through the PS will form the third multipotent germ layer, the Definitive Ectoderm. The cells of the mesoderm and endoderm germ layers migrate laterally and anteriorly away from the PS as mesodermal wings. Specifically, the middle area will predominately contribute to the lateral plate mesoderm and heart mesoderm, while the anterior part will contribute to the axial mesoderm (midline). This midline constitutes the mesoderm part of the prechordal plate (PrCP) which will eventually localise underneath the most anterior part of the forebrain and the anterior notochord (AN) that is situated underneath the posterior forebrain, midbrain and anterior hindbrain. (Robb and Tam 2004). Moreover, mesodermal cells migrate proximally, forming the extraembryonic mesoderm (Williams et al., 2012), which will generate the visceral yolk sac, amnion, and chorion. Conclusively, mesodermal cells will organise into cardiac mesoderm, axial mesoderm of the PrE-plate and notochord, paraxial mesoderm, intermediate mesoderm as well as lateral plate mesoderm. Every one of these mesodermal regions undergoes segmentation. The most evident and profound segmentation is seen to occur in the paraxial trunk mesoderm, in which each segment becomes a complete separate somite. The remaining of the mesodermal regions will develop into the cardiovascular and lymphatic system, the embryonic connective tissue, the cells of the skeletal muscles, the majority of the urogenital system, and the lining of the peritoneal, the pericardial and the pleural cavities. Subsequently, the endoderm forms the primitive gut tube consisting of three subregions: foregut, midgut and hindgut, which will give rise to the epithelial cells constructing the lining of the digestive and respiratory gut (Fu et al., 2021).

The EMT process, defined by the loss of cell-to-cell contacts and loss of the basal membrane of epiblast cells, is a highly coordinated process regulated by signalling pathways such as Nodal, Wnt, BMP, and FGF (Ciruna and Rossant, 2001; Ciruna et al., 1997; Huelsken et al., 2000). Proper combination of signals will allow the expression of a transcription factor network that achieves the switch from E-Cadherin to N-Cadherin expression, adoption of a mesenchymal profile and therefore the migration of cells away from the primitive streak. These transcription factors include the *Eomes* and *Snail1* which both target and repress E-cadherin (Arnold et al., 2008; Cano et al., 2000; Costello et al., 2011). Another transcription factor of high significance during this process is *Brachyury/T*

that reliably marks the posterior side of the PS throughout gastrulation. In the lack of *T*, posterior mesoderm is specified but is unable to exit the primitive streak, resulting in a

build-up of tail bud cells and a loss of posterior somites (Rashbass et al., 1991; Wilson et al., 1995). The expression of *Sox2* is downregulated in the PS epiblast before *Snail1* expression, a switch that was shown to be necessary but not sufficient for mesoderm migration (Bazzi et al., 2017; Ramkumar et al., 2016).

The growth factor Nodal that is secreted by VE acts on VE surrounding ExE to promote its own expression (Le Good et al., 2005). At E6.0 Nodal expression is restricted to the posterior side of the primitive ectoderm assisting in the induction of the primitive streak (Shen et al., 2007) This is achieved by stimulating the expression of PS genes *Mixl1* and *Gooseoid (Gsc)* (Yamamoto et al., 2001; Izzi et al., 2007). Following this, Nodal signalling is also essential for mesendoderm specification of epiblast pluripotent cells that move through the streak (Ben-Haim et al., 2006; Shen, 2007).

Pro-Nodal acts on the ExE to induce the expression of the growth factor BMP4, which then causes ExE to secrete Wnt3 (Beck et al., 2002; Le Good et al., 2005). Wnt3 as an activator of the canonical Wnt pathway causes β -catenin to translocate to the nucleus which induces the transcription of *T* and *Nodal* to the posterior side of the embryo. This results in the expression of Nodal, BMP4, and Wnt3 that are maintained along the posterior axis of the embryo, ensuring the establishment, maintenance and elongation of the PS.

Failure of the gastrulation process results in embryonic lethality just after implantation (Loebel et al., 2003). Embryos shown to lack functional Nodal, Wnt, and/or BMP4 signalling showed delayed and/or failure to initiate PS formation together with abnormal mesendoderm development (Tortelote et al., 2013; Miyamoto et al., 2015; Yoon et al., 2015).

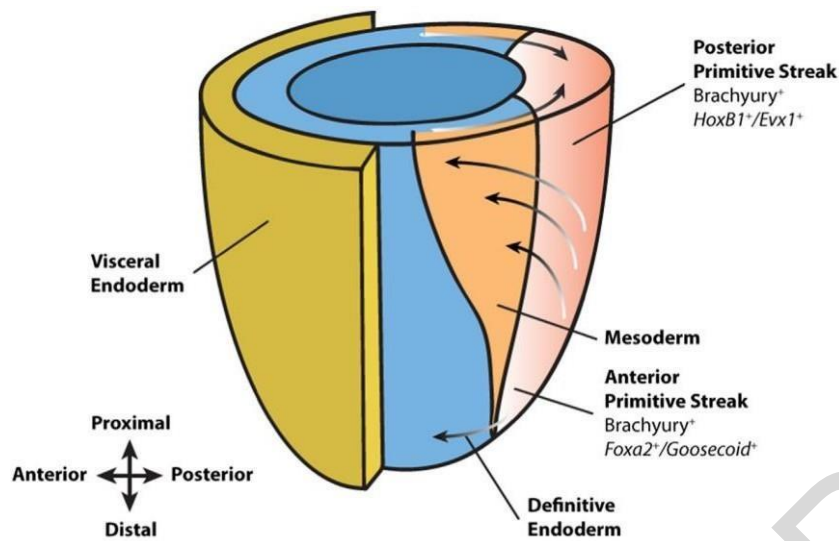


Figure 2: Mouse embryo gastrulation

Early primitive streak (PS) formation at E6.5 day. The posterior region of the PS co expresses *Bra/HoxB1/Evx1*. The anterior region co expresses *Bra Foxa2/Gsd*. Epiblast cells enter the anterior PS (black arrows on top of the embryo) and generate cardiac mesoderm. (Adapted from R. Duellen, M. Sampaolesi 2017).

1.5 The ectoderm germ layer

During gastrulation the epiblast cells that do not ingress through the PS constitute the ectoderm germ layer, that is defined by its fate of not forming mesoderm nor endoderm and which accounts for about 45 percent of the total epiblast cell population. Ectoderm, as its name indicates, is the outer-most germ layer of vertebrate embryos, although in mice this layer is initially the innermost and becomes the outermost after embryo turning at around E8.5.

More specifically, the ectoderm germ layer is the epiblast region fated to form ectodermal derivatives from the time of its pluripotency until the stage when it commences differentiation towards ectodermal derivatives. Before it starts differentiating to these derivatives the ectoderm germ layer restricts its potency and may change its specification in a spatiotemporally dependent manner. In this project the study of the early ectoderm development will be investigated, that is the earliest epiblast region to develop that is fated to ectodermal derivatives.

Therefore, the study of the early ectoderm development, involving when, where and how the initially pluripotent and undifferentiated epiblast cells are fated to form ectodermal derivatives is based on:

(a) its restriction of potency (b) its change of specification and (c) its differentiation towards neural or non-neural fates.

The development of this germ layer involves several poorly understood developmental events including restriction of epiblast potency from pluripotent to a bipotent status (towards neural and non-neural ectoderm fates) and eventually further restriction to only neural and only non-neural ectoderm fates. Specifically, this involves patterning of epiblast destined for ectoderm into lineage progenitors for neural, non-neural/epidermis, neural crest and placodes cell derivatives (Plouhinec et al. 2017). During ectoderm development several important events take place such as neural induction (that results in neural plate formation) and neurulation (bending of neural plate to form the neural tube), both of which involve molecular and morphogenetic changes initiated by spatial regionalization in the ectoderm.

The ectoderm is fated to form the epidermis, the central nervous system (CNS) including the brain and spinal cord, as well as the neural crest (NC) cells and the sensory placodes. NC cells arise from the border of the neural plate (NP) generating multiple derivatives such as the peripheral nervous system, pigment cells, endocrinal cells, and craniofacial structures (Liu JA and Cheung M 2016). The placodes are found to be specialised ectodermal thickenings emerging around the anterior neuralplate (NP), responsible to form sensory organs, including lens, inner ear, cranial ganglia, and olfactory epithelium (Schlosser G. et al. 2015). The diversification of ectodermal specification begins around gastrulation and early neurulation by signalling interactions found within the ectoderm or between the ectoderm and the mesoderm (Plouhinec et al. 2017).

The early development of the ectoderm germ layer includes loss of epiblast pluripotency and the formation of the brain neural plate, the initial sign of the development of CNS. While this is a developmental event of tremendous importance, mammalian neural commitment is thought to be one of the most challenging and poorly understood processes of developmental biology. Even though a number of publications have studied how the mammalian neurectoderm produces mature neural cells, little is known about the molecular signatures of the non-pluripotent ectoderm germ layer and that of the neural plate, as well as the mechanisms governing their formation (Rachel A. Shparberg et al 2019).

No study to date has shown the exact time point in murine development of the ectoderm initiation furthermore the lack of any validated molecular marker of this germ layer makes its study even more challenging.

A study using mouse epiblast explants cultured in serum free/chemically defined media, demonstrated that a region within the developing ectoderm layer that restricted its potency (from pluripotent to neural and surface ectoderm fates) resides in the anterior proximal region of the E7.0 embryo (Li et al., 2013). This region is sometimes called the bipotent ectoderm. It was suggested that the bipotent ectoderm residing in the anterior proximal region of the E7.0 embryo can either become epidermis or neural plate, depending on the levels of BMP signalling provided (Li et al. 2013). Following Nodal inhibition and in the presence of BMP4 this cell population could differentiate towards non-neural ectoderm lineages, while in the absence of BMP4 the neural fate was promoted. This is however, a very transient developmental phase because by the E7.5 (Early Headfold) stage, the anterior epiblast had not responded to any more of the BMP cues provided, meaning that the ectodermal subdivision into its derivatives has already taken place. The roles of BMP4 and Nodal signalling in neural induction were also confirmed in a later study using epiblast stem cells (EpiSCs) also cultured under the same

serum free conditions (Li et al. 2015). Inhibition of Nodal signalling over a short period of time allowed mouse embryonic derived epiblast stem cells (ESD-EpiSCs) to differentiate into either neural or epidermal ectoderm derivatives, depending on the absence or presence of BMP signalling respectively. The role of BMP4 signalling into lineage commitments was also confirmed using *BMPR1a*^{-/-} embryos that showed failure to produce surface ectoderm derivatives but instead promoted the expression of genes driving neurectoderm differentiation (Davis et al., 2004; Di-Gregorio et al., 2007).

XENIA HADJIKYPRIS

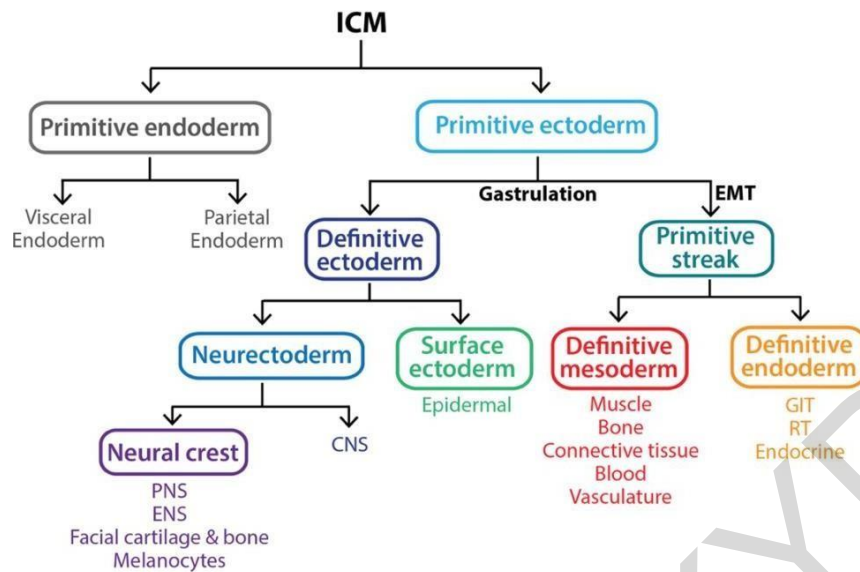


Figure 3: Gastrulation gives rise to the three primary germ layers of the embryo

Gastrulation results in the ingression of cells through the PS to form the mesoderm and endoderm germ layers. The remaining primitive ectoderm cells that do not move through the PS give rise to the definitive ectoderm germ layer, which further differentiates into the surface ectoderm and neurectoderm in response to the presence and absence of BMP4 signalling, respectively. Key: CNS, central nervous system; ENS, enteric nervous system; GIT, gastrointestinal tract (epithelial lining); PNS, peripheral nervous system; RT, respiratory tract (epithelial lining). (Adapted by Shparberg RAGlover HJ and Morris MB. 2019).

As mentioned above, an early event in mouse ectoderm development begins in anterior epiblast (fated to form brain and head surface ectoderm/epidermis) at around E7.0 with loss of pluripotency and acquisition of the bipotent ectoderm character (ability to differentiate towards neural/epidermal but not mesoendodermal fates) where Nodal signalling is low or completely absent (Li et al., 2013). This poorly understood lineage due to both its transient nature *in vivo* and the lack of molecular markers has not been extensively studied. To date, very few studies have attempted to understand ectodermal development and neural commitment at this stage of development. A relatively recent

study suggested that a population of ectodermal precursors has been established *in vitro* (Liu et al., 2018). Derived from EpiSCs and cultured in the presence of Nodal inhibitor SB431542, these cells showed a gene expression profile comparable to that of the E7.0–7.5 anterior embryo as well as active chromatin marks in both the promoter regions of neurectoderm and surface ectoderm genes (Liu et al., 2018). Thus, these cells are thought to represent an *in vitro* equivalent population of the definitive ectoderm germ layer, primed to differentiate to neurectoderm under suitable conditions.

Stem cell studies show that SRY-Box Transcription Factor 1 (*Sox1*) is the earliest neurectoderm marker expressed in differentiated mouse Embryonic Stem Cells (mESCs) (Aubert et al., 2003). When mESCs are cultured under conditions allowing neurectoderm differentiation (these include low plating density and serum-free media supplemented with N2B27), they firstly show rapid downregulation of POU Class 5 Homeobox 1 (*Oct4*) (Ying et al., 2003; Lowell et al., 2006). Under these same culture conditions, about more than half of the mESCs showed expression of *Sox1* (as measured by a GFP reporter cell line) after 4 days of culture, followed by the expression of the early neural progenitor marker Nestin one day later (Lowell et al., 2006).

Moreover, when *Sox1* is forcibly expressed in mESCs it causes the differentiation to neurectoderm lineage (Suter et al., 2009), while siRNA knock-down of *Sox1* in neurectoderm cells activate differentiation to *Pax6* positive radial glia (RG) cells (Suter et al., 2009). RG cells are considered the primary progenitor cell population of the developing and post-natal Central Nervous System (CNS). Firstly, they give rise to neurons (around E10.0–14.5), followed by the production of glial cells, astrocytes and oligodendrocytes (E15.0) (Kriegstein and Gotz, 2003; Anthony et al., 2004). Overexpression of the gene *Pax6* in mESCs causes the differentiation to BLBP+ /Vimentin+ RG cells that will later give rise to β III-tub+ /NeuN+ post-mitotic neuronal cells (Suter et al., 2009). *Pax6* is therefore an essential regulator in affecting the switch between embryonic neuroepithelial self-renewal and radial glial cell differentiation (Sansom et al., 2009).

A number of molecules shown to enable neurectoderm formation in the mouse embryo (such as chordin, noggin, and follistatin) are shown to be antagonists of BMP4 signalling, which further prevent downstream SMAD signalling. Studies demonstrate that neurectoderm production from ESCs emerge by a default mechanism of differentiation (1) SMAD4^{-/-} mESCs cultured under serum-free conditions give rise to Nestin+ neural progenitor population followed by β III-tub+ neurons within 24h (Trapepe et al., 2001). (2) mESCs and Human ESCs cultured in the presence of BMP antagonist noggin or chordin differentiate into neural progenitor cells within the first day of culture (Gratsch and O’Shea, 2002, Dottori and Pera, 2008). (3) mESCs plated at low density and cultured

under chemically defined conditions for a period of 4 hours differentiate to *Sox1*+ neurectoderm, followed by their differentiation into Nestin+ neural progenitors and β III-tub+neurons after an additional 20 hours of culture, at the expense of endodermal mesodermal cell types (Smukler, 2006). Interestingly enough this, neural differentiation occurs even when mESCs are cultured in PBS.

Other studies have also examined instructive factors that stimulate neurectoderm production. Specifically, retinoic acid (RA) is frequently used for in vitro differentiation of mESCs and hESCs purposes into the neural cell lineage (Engberg et al., 2010; Stavridis et al., 2010;). In mESCs, RA acts through ERK signalling, firstly by downregulating *Oct4* expression (Gu et al., 2005), followed by the regulation of Fgf signalling. Fgf4 is the primary activator of ERK signalling in mESCs. This pathway prepares mESCs for differentiation and when conditions are suitable permits them to progress to an early primitive ectoderm like (EPL) population (Stavridis et al., 2007), a differentiation process corresponding to the *in vivo* ICM to PrE transition. Following a high but short Fgf4-mediated ERK activity, RA was seen to gradually downregulate the expression of Fgf4 and ERK, which was also accompanied by an increase in *Sox1*+ neurectodermal cells (Stavridis et al., 2010; Rizvi et al., 2017). In a similar manner, mouse EpiSCs cultured in the addition of ERK inhibitor PD032590 for 24 hours, show a reduction in *Oct4* expression levels, increased expression of *Sox1* and a significant increase in the numbers of *Sox1*-GFP+ cells compared to their untreated counterparts (Yu et al., 2018). Inhibition of ERK activity was shown to decrease the expression of mesendoderm markers such as *Mixl1*, *Bra*, *FoxA2* and *Sox17*, and inhibits the translocation of β -catenin to the nucleus so as to prevent an EMT from happening — a key feature characteristic of the definitive ectoderm-derived cells (Yu et al., 2018).

Studies using Human ESCs (hESCs) demonstrate similar findings. Fgf-mediated ERK1/2 signalling activates the Poly-(ADP-ribose)-Polymerase-1 (PARP-1), which then binds directly to the *Pax6* promoter (the first human neurectoderm marker, followed closely by the expression of *Sox1*) (Pankratz et al., 2007; Zhang et al., 2010), giving rise to neurectoderm induction (Yoo et al., 2011). Inhibition of Fgf receptor through pharmacological means before the onset of neurectoderm induction lowers significantly the percentage of *Pax6* and *Sox2* positive cells. Collectively, complex, time-dependent alteration of ERK activity is necessary for proper progression to neurectoderm.

The Notch signalling pathway has also been involved in neurectoderm induction, regulation of neurectoderm proliferation as well as neuronal differentiation (Lowell et al., 2006; Souilhol et al., 2015; Boareto et al., 2017; Roese-Koerner et al., 2017). As seen in the embryo, Notch works together with Fgf signalling from around E7.5 to ensure the maintenance of the neuroepithelial pool, while inhibiting neurogenesis (Lowell et al.,

2006; Souilhol et al., 2015). Notch is activated when cleaved by γ -secretase and then binds to its reciprocal membrane receptor on a nearby cell (Kopan, 2012). The now activated Notch Intracellular domain (NotchIC) moves to the nucleus where it acts as a transcriptional regulator of downstream target genes, including *Hes1* and *Hes5* (Ohtsuka et al., 1999). Inhibition of Notch signalling in mESCs results in the prevention of differentiation of *Oct4* positive cells into *Sox1*-GFP positive neuroectoderm cells (Ying et al., 2003).

Genetic removal of the NotchIC binding partner, RBPJ, results in very few cells expressing the pan-neural marker *Sox2* as well as *Pax6* (Lowell et al., 2006). In the presence of the inhibitor DAPT, a significant increase in the expression of p63, an early surface ectoderm commitment marker, is

observed in hESCs (Tadeu and Horsley, 2013). This could suggest that Notch is not only essential for neural induction but also acts as a fate mediator of the definitive ectoderm lineage by restricting surface ectoderm derivation.

As mentioned above the ectoderm germ layer also gives rise to neural crest and placodal cells. Neural crest and placode cells arise in close contact with the neural plate border, a strip of embryonic ectoderm found in between zone of the surface ectoderm and the neural plate, which will eventually form the central nervous system (Koontz et al 2022). Within the neural plate border region, signals from both the surface ectoderm and the neural plate specify the pre-placodal region (PPR) and the region of presumptive neural crest.

During the time of neurulation, neural crest and placode cells remain in close proximity. When neural tube closure occurs, however, neural crest cells undergo an EMT transition and migrate throughout the entire body. On the other hand, placodes, remain within the ectoderm germ layer as regional thickenings, then gradually invaginate or ingress, to become committed to a number of different placodal lineages. These include, from anterior to posterior: adenohypophysis of the pituitary gland, olfactory, lens of the eye, trigeminal, otic, and epibranchial tissues (Koontz et al 2022). During the duration of the development of the sensory system, the activity between the migratory neural crest and placode cells aims to generate some of the most complex factors of the peripheral system.

In the chick embryo, cells of the neural plate border co-express markers of distinct lineages including neural crest and placode (Roellig et al 2017). Gradually, specific gene regulatory networks guide the cells towards their distinct fates (Riddiford 2016, Sanchez et al., 2015). However, a neural plate border signature is clearly evident only when neurulation commences, with distinct lineages arising during the time of neural tube closure (Williams et al., 2022).

The expression and / or inhibition of WNTs, FGFs, and BMPs are seen again to play an essential role in the delineation of these different embryonic regions. In the presumptive surface ectoderm, WNT and BMP activity is high, while the expression of WNT and BMP agonists increases more medially, decreasing at the same time the levels of WNT and BMP in the pre-neural region (Pera and Kessel 1999, Pieper et al., 2012).

While still exploring the chick embryo, FGF expression is also critical for a pre-neural fate (Streit and Stern 1999). WNT, FGF, and BMPs influence the expression of a group of both markers for both neural and non-neural markers areas. For instance, early expression of *Sox2*, *Erni*, *Otx2* and *Geminin* marks the pre-neural domain. Moreover, *Gbx2* was seen to be involved in neural crest formation and expression, while specific transcripts of this gene have been localised in the PPR (Kuriyama et al., 2009). On the contrary, expression of Distal-Less Homeobox 5 and 6 genes (*Dlx5/6*) mark the early non-neural region (McLarren et al 2003).

The interplay between the neural and non-neural ectoderm is considered to be very important for neural plate border formation and subsequent generation of neural crest and placode cells. Indeed, when neural plate tissue is transplanted onto non-neural ectoderm, it induces the formation of both neural crest and placode cells (Selleck and Fraser 1995).

Furthermore, stimuli arising from WNT, BMP, FGF and Retinoic Acid (RA) activity is also critical for vertebrate neural plate border induction (Yardley and Castro 2012). By the early gastrulation stages, neural and non-neural domains are established (Li et al., 2013). Due to the secretion of inducing signals which include WNTs and BMPs, distinct neural plate border factors such as *Tfap2*, *Pax3 / 7*, *Dlx3 / 5*, and *Msx1 / 2* are expressed in a gradient between the non-neural and neural domains (Moody and LaMantia 2015, Pera et al., 1999, Shen et al., 1997). These instrumental factors aim to induce the neural plate border region, where both the pre-placodal and pre-neural crest cells will arise.

Studies have shown that the neural plate border displays intermediate levels of BMP signalling, and that the levels of BMP and BMP antagonists shape the specification of the placodal and neural crest cells (Croze et al., 2011, Garnett et al., 2012., Grove and LaBonne 2014). For instance, in explant experiments using the *Xenopus* animal cap, increased levels of the BMP antagonist Noggin caused the expression of placodal markers, neural crest genes were seen to be expressed in the presence of Noggin at intermediate levels, while the expression of neural plate genes required the presence of high Noggin levels (Brugmann et al., 2014, Park and Jeannot 2008).

Pre-placodal cells are characterised by relatively downregulated expression of BMP, and higher expression of *Eya* and *Six* genes. These are seen to be expressed at the most lateral portion of the neural plate border (Ahrens and Schlosser 2005, Brugmann et al., 2004).

Specifically, *Six1* and *Eya1* are necessary for the correct specification of the PPR. The relative levels of *Six1* are important to determine whether a cell will give rise to neural crest or placode. Over-expression of *Six1* broadens the pre-placodal area at the expense of the neural crest one, while downregulation of *Six 1* levels results in the reduction of the pre-placodal region (Ahrens and Schlosser 2005, Brugmann et al., 2004). FGF signalling also exhibits a critical role for the induction of the PPR. Lack of FGF signalling causes the levels of WNT and BMP signalling to expand or reduce the PPR, while the presence of FGF is necessary for the expression of placode markers such as *Six* and *Eya* (Brugmann et al., 2004, Hintze et al., 2017, Litsiou et al., 2015).

The middle section of the neural plate border derives the premigratory neural crest cells, which are specified by a group of genes such as *FoxD3*, *Snai1/2*, *Twist*, *Sox10*, and *Ets1* ([Barembaum and Bronner, 2013, Khudyakov and Bronner-Fraser, 2009, Sauka-Spengler and Bronner-Fraser, 2008, Simoes Costa, 2012). These genes activate factors critical for EMT, and this allows cells to dissociate from the dorsal neural tube and commence their migration. *FoxD3* receives instructive signals from the genes (*Pax3/7* and *Msx1*) that specify the neural plate border, which directly attach to enhancers that regulate neural crest fate in the head and trunk region (Simoes Costa, 2012).

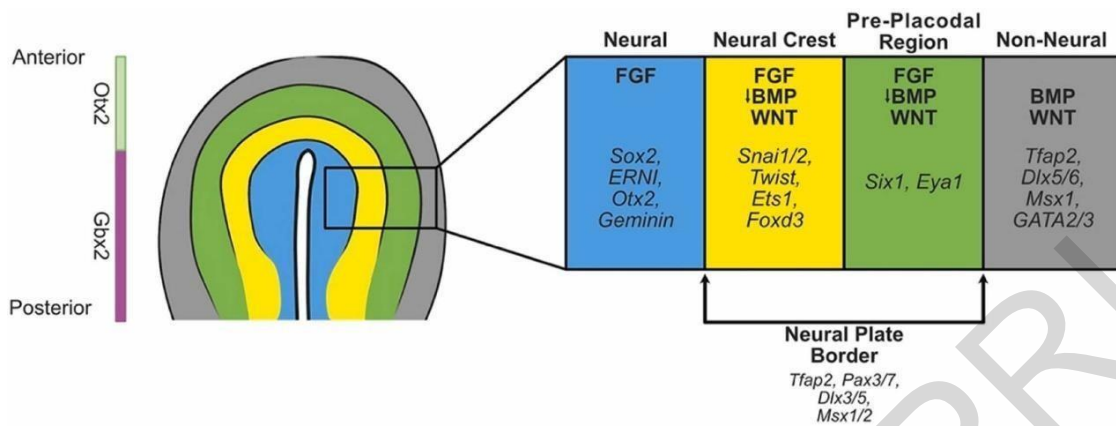


Figure 4: Overview of molecular markers in early neural plate border specification

Schematic diagram showing genes related to ectodermal patterning during the emergence of the neural plate border in the chick embryo. Neural plate border markers become detectable, in between the neural (blue) and non-neural ectoderm (grey). During early neurulation, neural plate border, neural crest progenitors (yellow) and pre-placodal ectoderm (green) emerge. (Adapted from Koontzet et al., 2022)

1.6. Formation of the neural tube: primary and secondary neurulation

Neurulation is an essential event of embryogenesis that is completed with the formation of the neural tube (NT), the precursor of the brain and spinal cord. The dorsal side of the definitive ectoderm, the open neural plate, is induced to differentiate and develop bilateral neural folds at its junction with the non-neural ectoderm. The elevation of these folds causes them to come into contact in the dorsal midline and fuse to generate the neural tube, which becomes surrounded by future epidermal ectoderm (Copp et al., 2003), that was previously seen to flank the neural plate. This process, called Primary neurulation, creates the brain (mindbrain, hindbrain and forebrain) and most part of the spinal cord.

Although the Primary neurulation process varies between species, mammals, birds and amphibians, they all undergo a Secondary Neurulation process in a similar manner. This involves NT progenitor cells found in the developing tail bud to form a neuroepithelium (NE) surrounding a lumen, without neural folding (Copp et al., 2015). More specifically, the tail bud is made up of a stem-cell population representing the remaining of the retreating PS. Mesenchymal cells in the dorsal region of the tail bud undergo epithelialization and condensation to give rise to the secondary neural tube, the continuous lumen with that of the primary neural tube (Schoenwolf, G. C. 1984).
Secondary

neurulation generates the lowest part of the spinal cord, including most of the sacral and the entire coccygeal region.

These neurulation processes involve not only the cells of the Neuroepithelium but also the tissues surrounding them. Indeed, the non-neural ectoderm, mesoderm and notochord have all been shown to be implicated in the regulation of NT closure (NTC).

During the time of primary neural tube formation different levels of morphogen activity serve to pattern this structure dorsoventrally. By E8.5, the ventral side of the neural tube (i.e., the side closest to the underlying notochord and prechordal plate) transitions to form the floor plate due to Sonic hedgehog (Shh) released from the node, prechordal plate and notochord before neural tube formation (Shparberg et al., 2019). The floor plate now acts as a primary signalling centre of Shh production up until E14.5 (Echelard et al., 1993; Ding et al., 1998) establishing a gradient to assist in ventral side patterning of the neural tube (Litingtung and Chiang, 2000; Gilbert, 2006; Ribes et al., 2010).

A small cluster of cells in contact with the overlying non-neural surface ectoderm forms the roof plate, partly due to BMP4/7 signalling from this overlying structure of surface ectoderm. The roof plate secretes BMPs and other morphogens acting as a dorsal organiser establishing dorsal-ventral gradients (Gilbert, 2006). The floor plate, notochord and prechordal plate alter these gradients by the release of BMP antagonists such as chordin and noggin (McMahon et al., 1998; Placzek and Briscoe, 2005). In the future spinal cord, this morphogen gradient activity contributes to establishing a series of neural cell types running ventral to lateral. Mice lacking functional Shh signalling, show node and notochord function disruptions, followed by floor plate formation inability (Ding et al., 1998), resulting in abnormal CNS patterning (Chiang et al., 1996). Shh mutant mice also display craniofacial, visual, and axial abnormalities (Chiang et al., 1996;). Similarly, other studies show that lack of function roof plate cells leads to CNS patterning disruption. Genetic ablation of roof plate cells in E9.5 mouse embryos, disrupts the gradient activity of BMPs leading to failure of dorsal interneurons formation (Jessell et al., 2000; Wine-Lee et al., 2004).

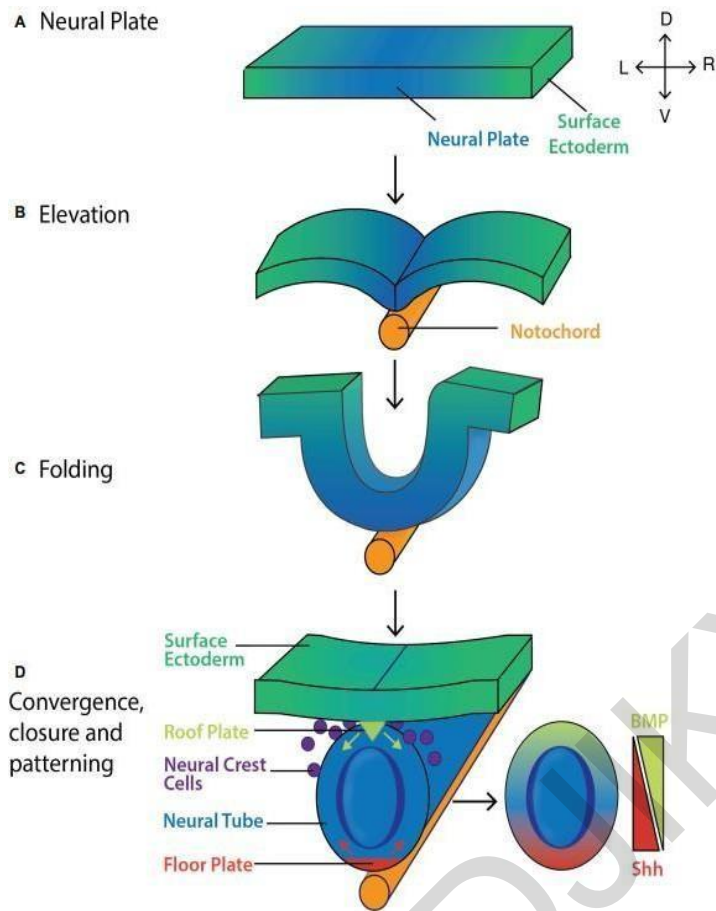


Figure 5: Formation and patterning of the murine neural tube

(A) The pseudostratified columnar like epithelium of neural plate forms by E7.5. The lateral edges of the neural plate (B) elevate and (C) fold by E8.0 before (D) their convergence at the midline and closing by E8.5. Shh (red arrowheads) and BMP inhibitors released from the floor plate, and BMP4/7 (green arrowheads) secreted from the roof plate act to pattern the neural tube along its ventro-dorsal axis, giving rise to the spinal cord. Key: V, ventral; D, dorsal; L, left; R, right. Adapted by ShparbergRA, Glover HJ and Morris MB (2019).

1.7. The Anterior Primitive Streak and its derivatives

Gastrulation initiation is marked by the appearance of the PS in embryos' posterior side. As described above epiblast cells that undergo EMT, ingress through the PS so as to give rise to either the mesoderm or endoderm germ layers. Clonal analysis of germ layer formation and fate mapping studies during pre-streak and early-streak stages reveal that PS cells can be divided into three different regions: posterior, middle and anterior PS cells with each region displaying different fates (Lawson, Meneses et al., 1991). The most posterior mesoderm populations that are patterned in response to signals from the ExE and specifically BMP4, will give rise to the extraembryonic mesodermal tissues of the chorion, the visceral yolk sac and blood islands (Winnier et al., 1995). The embryonic structures that is the lateral plate, the paraxial and cardiac mesoderm, emerge later from the middle and anterior parts of the streak. Finally, pluripotent epiblast cells that migrate through the anterior tip of the PS (named the APS progenitors) will give rise to the midline axial mesendoderm tissues that will make up the prechordal plate (PCP), the notochord and the node together with the Definitive Endoderm cell lineage (Arnold and Robertson 2009).

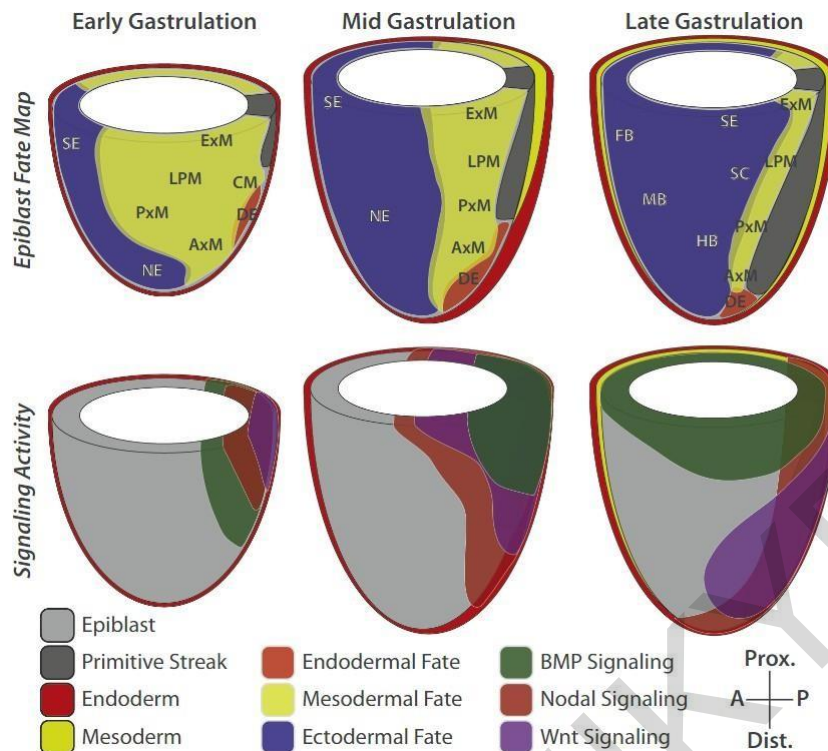


Figure 6: Signalling in the mouse embryo during gastrulation influences pluripotent epiblast cell fate decisions

Regions of the epiblast are shown to have reproducible lineage fates, resulting in fate maps for consecutive stages during gastrulation (top row). These fates are determined by the signalling cues arising from neighbour cells and guide cells to ingress through and migrate away from the PS (bottomrow). Hence, the synergistic mechanisms of fate and signalling activity are instructive into guiding specification of different lineages during development. Keys: DE, definitive endoderm; CM, cardiac mesoderm; ExM, extraembryonic mesoderm; LPM, lateral plate mesoderm; PxM, paraxial mesoderm, AxM, axial mesoderm; SE, surface ectoderm; SC, spinal cord; NE, neurectoderm; FB, forebrain; MB, midbrain; HB, hindbrain. (Adapted from Bardot and Hadjantonakis 2020).

1.7.1 The Node

In the murine embryo, the node of the late-streak to early-bud stage embryo has been shown to have organizing activity shown by its ability to induce left/right axis formation after heterotopic transplantation (Beddington, 1994). Described as organizer, or node, is a transient structure comprised of a ciliated cell population of around 250 cells visible at the distal tip region of the embryo at E7.5 that disappears by E9.0. The node, having a unique cell morphology characterized by a small columnar pit shape in its centre, is surrounded by cells covered by an endoderm surface layer. Cell labelling and transplantation assays have demonstrated that the cells of the node will form the trunk notochord (Kinder et al., 2001; Sulik et al., 1994). Once the notochord tissue with the characteristic rod-like shape has been laid down along the anterior-posterior (A/P) axis, it acts not only as a structural core for the embryo, but also as a secretion point of signalling molecules patterning the surrounding tissues. To this extent, it was shown that the notochord functions to pattern the overlying neural tube creating a dorsal-ventral (D/V) axis within the newly formed central nervous system (CNS) (Jessell, 2000).

Evidence coming from vertebrate studies showed that the notochord derives from progressively different stages of the organiser tissue, the node. Mouse fate mapping assays demonstrated that the anterior mesendoderm, consisting of the prechordal plate (PCP) and the anterior head process (AHP) notochord, is formed from early (EGO) and mid-gastrula organizer (MGO) (Kinder et al., 2001). The same study also showed that the node of later stages, will form the more posterior axial mesoderm. Chick embryo experiments revealed that in a similar manner, the organizer, Hensen's node, becomes successively more restricted in its Anterior-Posterior axis contribution. Specifically, the early-stage node can form the head process and notochord, while later stage node can only contribute to the posterior notochord (Selleck and Stern, 1991). Both studies emphasise the complexity of the organiser contributions to different notochord regions along the A/P axis.

Additional time-lapse and genetic analysis experiments revealed how the notochord is formed in the mouse. It was demonstrated that there are three different regions of the notochord that can develop by different morphogenetic processes and that these are governed by different genetic control (Yamanaka et al., 2007).

The anterior head process (AHP) is formed by notochord progenitors found anterior to the forming node in the early streak embryo and directly accumulate in the midline without reaching the node. The trunk notochord again derived from the node, was shown to be formed by Medio Lateral axis intercalation behaviour. Lastly, node derived cells form the tail notochord that migrate posteriorly and are maintained at the caudal end point

of the trunk notochord. (Yamanaka et al., 2007). Despite these observed different origins, the node derived notochord tissue does not display any notable differences in morphology nor in gene expression along the A/P axis while maintaining its one continuous rod-like shape.

A unique structure to amniotes, that is the AHP, forms between the PCP and trunk notochord, beneath the midbrain and rostral hindbrain (Rowan et al., 1999). Although the AHP displays a similar genetic profile to trunk notochord (*Gsc*⁻, *T*⁺), unlike the PCP (*Gsc*⁺, *T*⁻) lineage analysis suggests that the PCP and AHP both derive from the EGO/MGO cell populations but not the definitive node (Kinderet al., 2001). This was again confirmed by time-lapse live imaging analysis showing that the AHP forms by independent mechanisms of clustering of dispersed progenitors rostral to the node (Yamanaka et al., 2007). The PCP and AHP have a common high Nodal activity requirement in axial mesoderm formation, and are not formed if the Nodal signal is decreased (Vincent et al., 2003).

1.7.2 The role of the Node in the Definitive Ectoderm

The anterior neural tissue is firstly formed and moves away from the gastrula organizer. This molecularly distinct gastrula organiser progresses to become the node, a morphologically identifiable structure that retains the neural inducing ability of its predecessor. The role of the node up until E9.0 is the distribution of Nodal in a clockwise direction throughout the embryo to set the left-right embryonic axis (Zhou et al., 1993; Sulik et al., 1994; Collignon et al., 1996; Okada et al., 1999; Yamanaka et al., 2007; Babu et al., 2013). Through the node there is anterior migration of primitive ectodermal cells that will form the mesodermal prechordal plate and notochord. (Sulik et al., 1994). These important developmental structures are signalling centres that guide the overlying formation of the neural plate followed by the patterning of the neural tube. Node and/or notochord failure of formation results in embryonic lethality (Ang and Rossant, 1994).

At around E7.0 the node is the secretion point of BMP4 antagonists, such as Chordin, Noggin, and Follistatin that lower the BMP4 gradient reaching the distal tip originating from the proximal ExE (Bachiller et al., 2000; Brazil et al., 2015). The cells found closer to the node that receive low or zero BMP4 signals will differentiate into the neural plate expressing *Sox1* followed by the expression of another neural marker *Pax6* (Timmer et al., 2002; Suter et al., 2009). The neural plate is morphologically recognised as a pseudostratified columnar sheet of neuroepithelium that is placed symmetrically along the anterior midline of the embryo. The induction of the neural plate not only requires the node driven reduction of BMP4 levels but it also needs signalling cues from the underlying mesodermal tissue, the notochord and the prechordal plate (Gilbert, 2006), together with the inhibition of ERK activity (Yu et al., 2018). The anterior proximal epiblast receives higher BMP4 activity, allowing for the activation of the SMAD1/5/8 signalling pathway. SMAD complexes will then bind to epidermal DNA response regions resulting in the transcription and expression of genes related to surface ectoderm specification. These genes include members of the keratin family: early markers *K8*, *K18*, and *K19*, followed by the more mature epidermal markers, *K14* and *K17* (Troy and Turksen, 2005; Harvey et al., 2010). By E7.5, this embryonic region is said to be fully committed to either surface ectoderm or neurectoderm while the levels of BMP4 no longer promote nor inhibit lineage commitment as cells are already specified (Li et al., 2013).

The node was shown to induce neural tissue posteriorised by local influences, while it can also induce ectopic posterior neural axis development upon transplantation to the posterior region of an embryo (Beddington, 1994; Tam and Steiner, 1999). Interestingly, transplantation of the node to the chick's embryo anterior region was shown to induce a

secondary neural axis having both anterior and posterior neural tissue (Knoetgen et al., 2000). This could be explained by a species-specific mechanism.

Studies in mutants that showed preservation of early gastrula organiser activity, with the node failing to form (*FoxA2*^{-/-}, *Fgf8*^{-/-}, *Cripto*^{-/-}), anterior neural structures develop into posterior neural tissues (Klingensmith et al., 1999). This observation can suggest that early anterior neural tissue is induced by the gastrula organiser migrating anteriorly, while the later formed node continues the same function but closer to posteriorising factors (Levine and Brivanlou 2007).

XENIA HADJIKYPRRI

1.7.3 The Anterior Mesendoderm (AME)

The AME is a compacted two layered stripe of the anterior axial tissue midline mesendoderm (also known as axial mesendoderm) situated right next to the anterior edge of the PS at the LS embryo. The AME is composed of the PrCP (anterior region AME) which is localised underneath the forebrain and of the anterior notochord (posterior region AME; also known as the anterior head process) which is found underneath the midbrain and hindbrain. The AME progenitors are located in the Early Gastrula Organizer (EGO) and the anterior part of the epiblast outside the EGO (Robb and Tam, 2004). The EGO is found in the posterior epiblast anterior to the newly formed PS at E6.5. Fate mapping studies show that the EGO constitutes a heterogeneous cell population of progenitors that will give rise to the AME, the cranial and heart mesoderm and foregut endoderm. Specifically, the progenitors of the AME are found in the anterior part of EGO. During gastrulation and as the PS elongates anteriorly, the AME progenitors within the EGO are displaced anteriorly and later merge to the anterior end side of the PS to give rise to the Mid Gastrula Organizer (MGO). The MGO cells will then migrate anteriorly to eventually form the AME (Kinder et al., 2001).

1.7.4 The role of the AME in Definitive Ectoderm

The AME and its role in patterning the brain has been extensively studied. Experimental data indicate that the anterior midline tissue of the LS stage murine embryo that is the AME, together with the ventral neurectoderm play a role in the maintenance and refinement of the head region patterning. Heterotopic transplantation of this region was shown to induce anterior neural markers in the host tissue, most likely due to the presence of the AME within the transplant (Camus et al., 2000). When AME tissue was surgically removed, this demonstrated that the tissue has a role in the maintenance of the segmental features of the neural axis and the following regionalisation of the forebrain. Removal of the rostral portion of AME results in abnormal morphogenesis and patterning of the forebrain while ablation of the caudal region modifies the genetic profile of prechordal plate and the future ventral diencephalon (Camus et al., 2000).

After anterior neural tissue specification during gastrulation, this tissue must be maintained by the underlying AME, the node derivative. This maintenance is possible to occur through multiple mechanisms, including a continuous BMP inhibition. The outcome of this regulation is the anterior neural ridge induction and specification, that is a signalling centre expressing Fgf8, Shh, and Foxg1 (Levine and Brivanlou 2007).

The role of the AME was first examined following the observation that co-culture of explants derived from anterior mesendoderm tissue from head-fold stage embryos induces anterior neural tissues (Ang and Rossant, 1993). AME explants from Mid Streak embryos also retain this ability but showing lower anterior neural tissue efficiency (Ang and Rossant, 1993).

While AME can cause the induction of anterior neural tissue, it appears to have a more important role in the maintenance of this fate. In explants of later stage embryos, it was shown that although the forebrain has already been specified, markers of forebrain development disappear following prolonged culture or treatment with exogenous BMPs. This phenotype was rescued when these explants were co-cultured with AME tissues. (Yang and Klingensmith, 2006).

A number of experiments using mouse mutants reveal the necessity of this ongoing maintenance by the AME as defects in mesendoderm generally cause anterior neural truncations and loss of forebrain markers after gastrulation. The double mutant $Gdf1^{-/-}$; $Nodal^{+/-}$ does not properly induce mesendoderm resulting in forebrain defects (Andersson et al., 2006). In another mutant study the Hex1 mutant, the AME is induced but fails to migrate anteriorly. The subsequent loss of anterior mesendoderm beneath the forebrain tissue results in failure to support and therefore maintain this tissue (Martinez Barbera et al., 2000). The signalling factors chordin and noggin are required in the mesendoderm to maintain the BMP inhibition contributing to forebrain development. This was demonstrated when $Chordin^{-/-}$; $Noggin^{+/-}$ embryos, lacking these factors in the AME resulted in failure of forebrain tissue maintenance (Anderson et al., 2002).

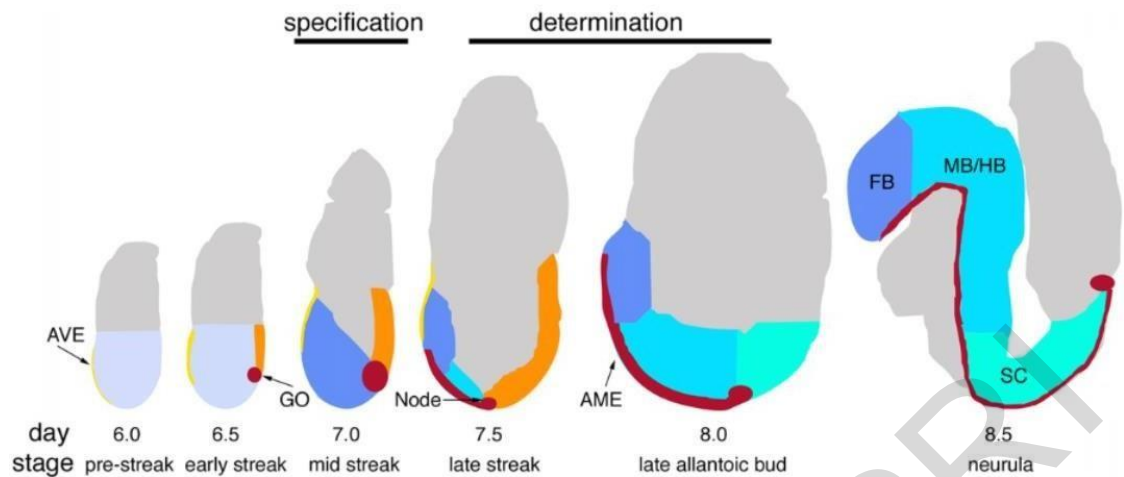


Figure 7: Neural induction in the mouse embryo from E6.0 to E8.5

The epiblast of the pre and early streak mouse embryo exists in a pre-neural state (light blue). At pre-streak stages the anterior visceral endoderm (AVE - yellow) is present overlying the anterior epiblast. As gastrulation commences, the early PS (orange) forms in the posterior side of the embryo, with the early gastrula organizer (EGO - maroon) present anteriorly to the streak. By MS stages, the AVE has migrated proximally and the PS has elongated distally. At late streak stages anterior neural precursors (blue) represent on the anterior proximal and distal side the specification of neural tissue. The node is found at the distal end of the embryo while AME (maroon) extends anteriorly from the node during LS and later stages. Anterior neural tissue determination is completed by the late allantoic bud stage. At E8.5 stage neural tissue is comprised of the forebrain (FB, blue), midbrain (MB, light blue), hindbrain (HB, light blue), and spinal cord (SC, turquoise). The AME underlying these neural tissue structures is required for their maintenance. Image not drawn to scale. Adapted from Levine, A.H. Brivanlou (2007).

1.7.5 The Head Process

At the Late Streak stage, a transient sub-epiblast compact thickening/bulge can be found in the posterior half of the distal tip of the embryonic region (Rivera-Pérez et al., 2010; Downs et al., 1993) and is thought to represent the anteriorly migrating population of axial mesoderm precursors of AMEs as well as the ventral layer of the mature node (Downs et al., 1993; Lawson et al., 2016; Kinder et al., 2001; Robb and Tam 2004; Poelmann 1981).

During the process of neurulation, the head process cells become flattened and form the so-called midline mesoderm tissue underlying the neural groove of the cephalic neural tube (Meier and Tam, 1982).

It remains unclear how the head process is formed during the stages of gastrulation. In the chick embryo, the continuity of the head process with the node might imply that the cells of the head process could be produced by the anterior movement of cells deriving from the node (Psychoyos and Stern, 1996). The node residing at the anterior end of the PS regresses along the cranio-caudal axis leaving a trail of cells forming the notochord (Catala et al., 1996). This extends to the posterior side from the junction with the head process.

Two other mechanisms can explain the head process formation. First, the head process formation may be due to the contribution of mesodermal wings derived cells as they fuse at the midline from the embryo's two sides (Tam et al., 1993). However, some genes of the later head process (Brachyury, Gsc, Lim1 and Otx2) are expressed in the tissues prior to the emergence of mesodermal wings at the midline. This could suggest that some components of the head process are guided by sources different from the node and the PS (Tam and Behringer 1997).

A second possibility suggested is that the head process tissue may be derived from the anterior endoderm. During notochord formation, the future notochordal cells are initially organised into a structure immediately anterior to the node (that is the notochordal plate). The notochordal plate neighbouring with the endoderm and the notochord is formed as its cells move to a mesodermal location and are re-organized into a cord (Sulik et al., 1994). It cannot be excluded that the head process can also be formed in a similar manner from the anterior endoderm and that the expression of early head process genes is in the endodermal precursor of this tissue (Tam and Behringer 1997).

1.8 Overview of Extraembryonic Tissues

At around E4.5 the trophoctoderm (TE) will give rise only to the extraembryonic tissues, the extraembryonic ectoderm (ExE), chorion, and ectoplacental cone (EPC) (Gardner, 1983; Gardner et al., 1973). While all these extraembryonic structures have proven trophic and homeostatic features throughout development, studies have shown that many also play significant roles in lineage segregation as well as in embryonic tissues patterning during early developmental stages.

Implantation stimulates the polar TE to proliferate so as to form the EPC. The EPC acts as the point of the embryo attachment to the endometrial wall. These maternal cells will then respond by proliferation and decidualisation to be able to completely surround the forming conceptus (Ramathal et al., 2010).

During E4.5 to E5.0, the embryo also goes through changes in both size and morphology, specifically elongating from the attachment point to the maternal wall, the EPC (the proximal EPC region) to form an elongated structure having a clear proximal–distal axis (Rossant, 2004). The polar TE also forms the ExE found distally to the EPC. During the same time, epiblast cells proliferate to form the cup-like morphology, also described above, with the margin of this tissue next to the newly formed ExE (Tam & Loebel, 2007).

As the embryo continues to develop due to the appearance of the newly-formed ExE and expansion of the epiblast, these tissues expand distally towards the blastocoel cavity (Copp, 1979). The cells of the PrE that were initially seen to be in contact only with the epiblast cells, are now seen to expand distally to envelope the entire outer surface of the egg cylinder embryo as a continuous single-cell layered epithelium known as the Visceral Endoderm (VE). The region of the VE surrounding the epiblast at the distal half of the embryo is described as the Epiblast VE (Epi VE), whereas the more proximal VE covering the ExE, as the Extraembryonic VE (ExE VE). The VE layer is described as a continuous single cell monolayer with either columnar, cuboidal, or squamous epithelial cell morphology depending on stage and location (Stower and Srinivas 2018).

By E5.5 a morphological change in the subset of Epiblast - VE at the distal tip of the embryo becomes noticeable as their morphology changes from cuboidal to columnar (Srinivas et al., 2004). These cells form the what is now known as the distal visceral endoderm (DVE) and have an essential role in the conversion of the proximal–distal asymmetry to the anterior–posterior asymmetry of the embryo (Thomas & Beddington, 1996). The directed proximal movement of DVE cells from the distal point towards one side of the egg cylinder embryo, results in the relocation of these cells at the boundary of epiblast and ExE (Srinivas et al., 2004). At this region, these cells are now referred to as the anterior visceral

endoderm (AVE) as it can direct anterior patterning in the underlying epiblaston the anterior side of the embryo. AVE is regarded as a specialized signalling centre having a characteristic columnar morphology at E5.75 (Thomas & Beddington, 1996). AVE was also shown to be required for the PS formation and gastrulation. AVE cells acting as a signalling centre secrete antagonists of Nodal, BMP and Wnt, while the opposite side of the embryo receives Nodal and Wnt signals stimulating the formation of the PS. Thus, AVE positioning interferes with the radial embryo symmetry and acts to define the anterior-posterior axis (Stower and Srinivas 2018).

DVE/AVE cell migration is a complex process involving cell translocation and coordinated divisions (Antonica et al., 2019). Confocal time-lapse imaging analysis studying embryos that expressed fluorescent nuclear protein H2B-EGFP and adherens junction marker PLEKHA7-EGFP showed global collective VE cell rearrangements that was initiated by apical constriction of DVE cells (Shioe et al., 2017).

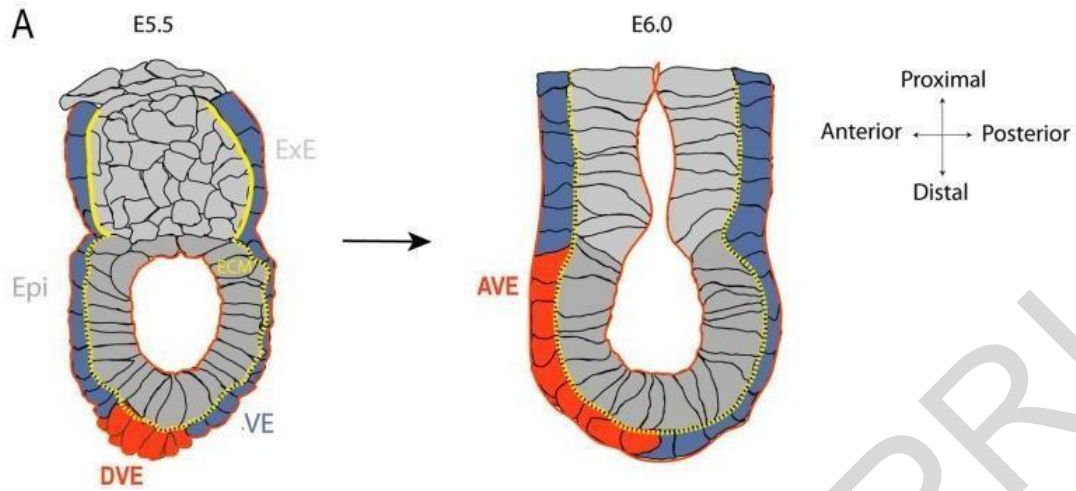


Figure 8: The Extraembryonic Tissues – the ExE and VE

At E5.5 the mouse embryo is already implanted and composed of three distinct cell lineages: epiblast (EPI), extra-embryonic ectoderm (ExE), and visceral endoderm (VE). The embryo has the egg cylinder morphology with proximal-distal axis. The distal end consists of embryonic pluripotent Epiblast cells. The proximal side comprises the ExE and the EPC. The embryonic epiblast and the extraembryonic ExE tissues are covered by the continuous VE outer layer. (Adapted by Omelenchenko Tatiana 2022).

1.8.1 The Extraembryonic Ectoderm (ExE)

Following implantation, the TE develops into two different trophoblast types: the mural trophoblast (mTE), surrounding the blastocyst cavity, and the polar trophoblast (pTE), overlying the entire ICM. pTE cells will give rise to trophoblast stem cells (TSCs) which proliferate to form the EXE. The mTE cells will differentiate into primary trophoblast giant cells (TGCs) which will eventually form a network of blood connections at the embryo's periphery ensuring the diffusion of oxygen and nutrients between maternal and embryonic circulation (Bedzhov et al., 2014).

The ExE found more distally to the epiblast differentiates into the EPC. This tissue will derive secondary trophoblast giant cells (TGCs) as well as spongiotrophoblasts (Tanaka, Kunath et al., 1998). Together, EXE and EPC make up the pre-placental trophoblast (PPT), which constitutes the progenitor of the trophoblast compartment of the placenta (Georgiades and Rossant 2006). During gastrulation, the extraembryonic mesoderm will give rise to the extraembryonic tissues, the allantois, the mesodermal part of the chorion and that of the visceral yolk sac. Taken together the EXE and the extraembryonic mesoderm form the posterior amniotic fold, which forms the amnion by later stage, another structure with a protective role to the embryo. By later stages and towards the completion of gastrulation the EXE forms a bilayer, named the chorion with the extraembryonic mesoderm and

becomes detached from the epiblast. At E8.5, the allantois fuses with the chorion at its basal layer of the chorion to form the chorioallantoic placenta by E9.5-E10. The chorioallantoic attachment is a crucial step in the development of the labyrinth that will allow the exchange of gases and nutrients between fetal and maternal blood vessels (El-Hashash, Warburton et al. 2010).

The placenta, being the first organ to form during mammalian embryogenesis, is essential for the appropriate exchange of gases, nutrients and waste products between the mother and the foetus. Any interference with its formation and function due to genetic or environmental stimuli affects the development of the embryo and can lead to fetal growth retardation and lethality, in both mice and humans (Rossant and Cross 2001).

1.8.2 The ExE and its role in Epiblast and VE patterning

The ExE derives from the polar TE, and while it has an extraembryonic fate, it also plays a key role in the patterning process of the adjacent epiblast and VE during early development. The role of the ExE in this patterning was revealed through the study of early E5.5 embryos using dissected embryonic and abembryonic halves. This led to the Epiblast and VE tissues expressing markers of the Distal VE in an abnormal and unrestricted manner (Rodriguez et al., 2005). This suggested that an ExE inhibitory signal normally prevents the proximal VE differentiation toward the DVE fate. BMP signalling released from the ExE has been proposed to be the repressive signal that will prevent the DVE-like fate in the remaining VE. Therefore, this model suggests that the DVE will only format the distal region of the egg cylinder embryo, furthest to the origin of the repressive signal source, that is the ExE. (Rodriguez et al., 2005; Yamamoto et al., 2009).

Other studies have also described the ExE as a source of BMP signalling. Specifically, the ExE expresses BMPs such as BMP8b and BMP4 (Winnier et al., 1995; Ying and Zhao, 2001), while knockout experiments showed that BMP4 has an important role as *Bmp4*^{-/-} embryos show a loss of expression of the mesodermal marker *T* and failure of gastrulation (Ben-Haim et al., 2006; Winnier et al., 1995).

BMP signalling in the ExE is maintained by epiblast's NODAL signalling, and in a mutual way BMP from the ExE is necessary for correct epiblast development and PS formation (Ben-Haim et al., 2006). NODAL is also needed to induce the formation of the DVE (Brennan et al., 2001). The VE also expressing NODAL has epiblast patterning effects. Loss of NODAL expression in this tissue, as seen through VE-specific knockout mice (Kumar et al., 2015), led to a reduction of epiblast NODAL followed by developmental arrest (Kumar et al., 2015). The DVE will later feedback on NODAL in a negative feedback manner through the secretion of inhibitors of the NODAL pathway including

CER1 and LEFTY1 (Brennan et al., 2001). This leads to the conclusion that although there is an initial mutual interaction between the epiblast and the VE tissues to maintain epiblast's NODAL signalling, this is followed by repressive interaction once epiblast patterning is completed.

The regulatory mechanisms between the epiblast, ExE and the VE have been described in another study using knockouts of the *Sall4-a* isoform, a transcription factor expressed exclusively in ExE and VE at E5.0. The mutants showed loss of *Bmp4* expression in the underlying ExE. *Bmp4* dramatic reduction in the ExE resulted in loss of NODAL expression in the epiblast as well as a failure of DVE induction (Uez et al., 2008). This study proposed that a series of synergistic mechanisms exist between these tissues to induce and sustain the expression of BMP4 and NODAL as well as to induce the DVE at the embryo's distal tip region that will subsequently feedback on the epiblast to contribute to its patterning by Nodal and WNT inhibition (Stower and Srinivas 2018).

ExE trophoblast signalling is not only required for the initiation of gastrulation (Georgiades and Rossant 2006) (Mesnard et al., 2011), but also for gastrulation progression controlling mechanisms including PS elongation, completion of mesoderm EMT processes and anterior PS derivative development (Polydorou and Georgiades 2013). Further evidence comes from studies exploring again the Nodal signalling pathway. The ExE is the source of the proteases *Spc1* (Furin) and *Spc4* (Pace4) (Beck et al., 2002), responsible to cleave the Nodal preprotein to its functional form. Mutations of both these genes lead to the abolishment of active Nodal production resulting in arrested gastrulation. Another study using *Nodal*^{-/-} epiblast cells and mutant embryos, showed precocious neural differentiation reporting a possible role of Nodal in averting the emergence of anterior neural fates prior to gastrulation (Camus et al., 2006). This could suggest an early role of trophoblast signalling in inhibiting neural fates.

1.8.3 The role of the AVE on the establishment of the Definitive Ectoderm

Together with their roles in PS formation and mesendoderm appearance, Nodal, BMP4 and Wnt3 signalling are also required for the anterior movement of the Distal Visceral Endoderm (DVE) in E5.5 embryo from the distal tip region, and by E6.0 its differentiation to anterior visceral endoderm(AVE) (Ben-Haim et al., 2006; Stuckey et al., 2011; Hoshino et al., 2015). The AVE located at the anterior side of the embryo promotes the formation of the definitive ectoderm due to the secretion of Nodal antagonists such as Cerberus-like 1 (Cer1) and Left-right determining factor 1 (Lefty1), and the Wnt antagonist Dickkopf1 (Dkk1) (Rodriguez et al., 2005; Kong and Zhang, 2009; Stower and Srinivas, 2014; Hoshino et al., 2015). Therefore, the Nodal, Wnt and BMP4 signalling cues present on the embryo's posterior side are disrupted on the anterior region of the embryo so that the primitiveectoderm cells of the pluripotent epiblast that are anteriorly located, fail to undergo EMT and do not migrate through the PS that is located posteriorly. The role of Nodal inhibition to the formation of the DE was again confirmed when E6.5 embryos cultured *ex vivo* in the presence of the Nodal inhibitor SB431542 (Inman et al., 2002), showed failure to produce mesendodermal cells on the posterior side. Further to this notion, *Nodal*^{-/-} epiblast explants were unable to form mesoderm while instead differentiated prematurely into neurectoderm by E6.5 (Lu and Robertson, 2004; Camuset al., 2006).

1.9. The *Ets2* gene: Introduction to its structure and expression

This study uses *Ets2*^{-/-} transgenic mice to accomplish some of its aims and for this reason it is necessary to present a brief introduction regarding the gene's structure, function and expression. *Ets2* is a member of the Ets domain family of transcription factors that was originally identified on a region of homologous sequence with the *v-ets* oncogene encoded by the E26 avian erythroblastosis and myeloblastosis virus. More than 30 members of Ets family transcription factors have been identified in living organisms. The Ets transcription factors were shown to act as activators or in some cases repressors by identifying the GGA core motif in their target gene's promoter, so as to guide several biological processes such as cellular proliferation, differentiation, embryonic development, apoptosis and oncogenic transformation (Sharrocks et al., 1997; Wasyluk et al., 1998). A subgroup of Ets proteins, including *Drosophila* P2 and vertebrate Ets1 and *Ets2*, have an N-terminal pointed domain which is involved in interfering with the Ras signalling via a conserved site of MAPK phosphorylation (Wasyluk et al., 1997; Yang et al., 1996). This phosphorylation enhances their ability to activate the transcription of target genes by binding to sequences known as Ras responsive elements (RREs) and serum response elements (SREs) that can be found in the promoter region of many genes (Brunner, Ducker et al., 1994).

Ets2 is expressed in different cell types in the duration of early mouse development. *Ets2* expression was detected in early postimplantation mouse embryo (E5.0), specifically localised in the ExE while later on in development (E5.5 and E6.75) in the ExE and EPC. By E7.75, the expression of *Ets2* becomes downregulated from trophoblastic compartments and begins its appearance in the PS (Yamamoto et al., 1998; Georgiades and Rossant 2006). In the E8.5 embryo, *Ets2* is expressed in the paraxial mesoderm and in limb buds, while during stages of late embryogenesis is seen to be expressed in the CNS. During the course of organogenesis *Ets2* is detected in the epithelial layers of the kidneys, lungs and gut with its expression showing downregulation following bone formation. Moreover, increased levels of *Ets2* expression were found in the cortical region of the thymus while its expression pattern is maintained throughout adult life. In the adult mouse, its expression is restricted to specific areas of the brain and is also detected in mammary glands, the uterine wall and in the lung alveolar structures. In humans, *Ets2* expression is also located in the brain, and the ovaries (Maroulakou and Bowe 2000).

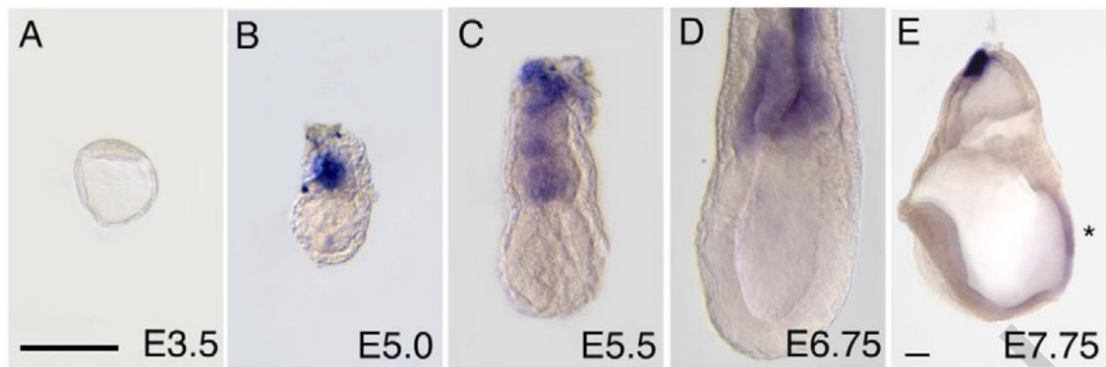


Figure 9: *Ets2* expression profile

(A-E) *Ets2* expression from E3.5 pre-implantation to E7.75 early head-fold stage. *Ets2* is not expressed in the PE before implantation. Beginning at E5.0 its expression is found in the ExE and by E5.5 in both the ExE and the EPC. In the early head-fold stage it also expressed in the PS (asterisk). (Adapted from Georgiades and Rossant 2006)

1.9.1 *Ets2* null type-I and type-II mutant embryos

To better understand its significant role in early development, transgenic mice (*Ets2*^{-/-}) carrying a targeted deletion for this gene have been generated, the animal model used in this study. This was done when all or part of the gene's three exons coding for the Ets DNA binding domain were replaced by the pMC1NeoA selectable gene. These homozygous mutant embryos present an abnormal cone-shaped structure, growth retardation and resorption by E9.5, deficiencies in trophoblastic development resulting in a smaller EPC, failure of proliferation and no chorion formation (Yamamoto, Flannery et al., 1998; Maroulakou and Bowe 2000). Additional analysis of these mutant embryos revealed the presence of two main phenotypes: type-I and type-II (Georgiades and Rossant 2006). This study's results mainly focus on type II mutant embryos.

Both phenotypes represent an excellent *in vivo* animal model for investigating trophoblastic influences on early mouse development. The following evidence supports this notion: a) *Ets2* gene expression is being restricted only in trophoblastic tissues during early mouse development as seen above; b) the generation of chimaeras was achieved by aggregation of *Ets2*^{-/-} embryonic stem (ES) cells (contribute only to the epiblast) with tetraploid (4n) wild-type *Ets2*^{+/+} mouse embryos (contribute to the extraembryonic tissues); this aggregation of cells was able to rescue *Ets2*^{-/-} mutant mice as these appear to be viable; c) lentivirus-mediated-trophoblast specific expression of *Ets2* restore embryonic development in *Ets2*^{-/-} embryos (Okada et al., 2007). *Ets2*^{-/-} type-I mutant embryos, representing the more severe phenotype of both types. They fail to express ExE markers such as *Cdx2*, *Bmp4*, *Errb*, *Spc4* (*Pace4*) from at least E5.5 onwards, they do not initiate gastrulation while their DVE does not migrate to the anterior side of the embryo

(Georgiades and Rossant 2006). Type-II mutant embryos lose trophoblastic signalling around E6.7, but are able to form PS and AVE. Nonetheless, they also represent gastrulation progression defects including inappropriate gene expression within the newly formed PS, failure at elongating the PS up to the distal tip of the embryo, complete mesoderm formation and incorrect development of anterior PS derivatives (Polydorou and Georgiades 2013).

XENIA HADJIKYPRRI

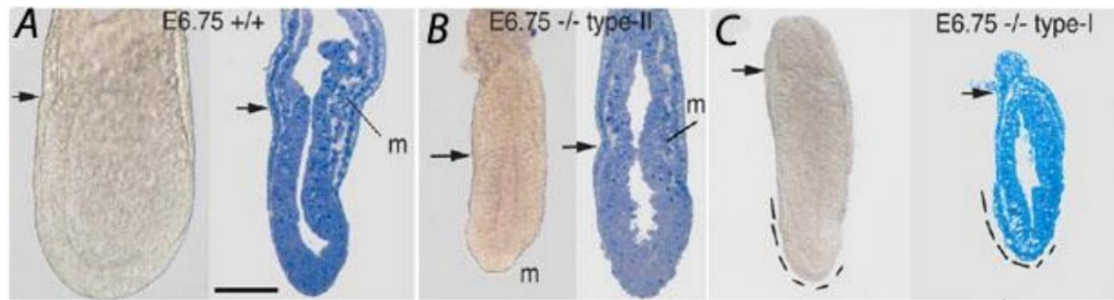


Figure 10: Morphological classification of type I and type II *Ets2* mutant conceptuses

A) wild-type, B) type-II and C) type-I. On the left of each panel are whole mount pictures and on the right are sagittal semithin sections of the same embryo. Note the absence and presence of mesoderm in type-I and type-II mutant respectively. (Adapted from Georgiades and Rossant 2006).

Ets2^{-/-} type-I mutant embryos do not express ExE markers such as *Cdx2*, *Bmp4*, *Erbb*, *Spc4* (*Pace4*) from E5.5 and onwards, show failure to initiate gastrulation and DVE failure of migration to the anterior side of the embryo. In chimaera experiments, where diploid wild type ES aggregate with tetraploid *Ets2*^{-/-}, show arrested development with defects similar to those seen in E7.75 type-I mutants, when their expression patterns of *Bra*, *Hex* and *Oct4* are compared. Additionally, E5.5 trophoblast-ablated embryos display similar epiblast defects as in the case of type-I suggesting that ExE signalling is required for the initiation of gastrulation (Georgiades and Rossant 2006).

On the other hand, *Ets2*^{-/-} type-II mutant embryos lose ExE signalling at around E6.7. These embryos, in contrast to their type I counterparts, form a PS and AVE but present gastrulation progression defects that include incorrect gene expression profile within the newly formed PS, failure of PS elongation up to the distal tip as well as improper development of anterior PS derivatives. More specifically, these mutants fail to execute DE, AME and node formation (Polydorou and Georgiades 2013).

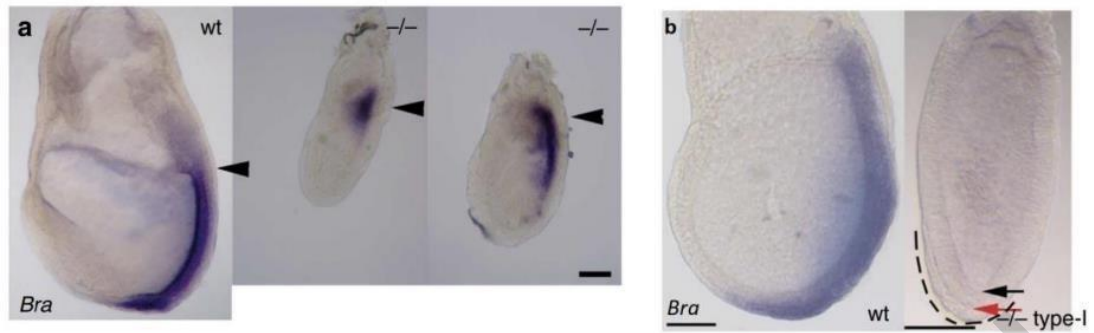


Figure 11: Epiblast patterning defects in *Ets2* type-II and type I mutant embryos

(a) *Bra* expression of E7.75 wt control embryo (left panel) and E7.75 type II mutants. Note the defective PS elongation. (b) *Bra* expression of E7.75 wt control embryo (left panel) and E7.75 type I mutant. Note the complete absence of PS. (Adapted from Polydorou and Georgiades 2013).

1.10 Discrepancies regarding the early development of the ectoderm germ layer and the need to establish a more comprehensive mouse embryo staging system

Ectoderm development is a poorly understood process with great importance, as it is the very first step in the generation of the most complicated structure known to science, that is, the central nervous system (CNS-brain and spinal cord) (Wilson S.I. and Edlund T. 2001). The ectoderm, being one of the three classic germ layers in the early mouse embryo, has the capacity not only to develop into the central nervous system but also to epidermis, placodes and neural crest cells (Plouhinec et al. 2017). The fact that it is a very transient phase in development together with the lack of any validated molecular markers, makes it the least understood germ layer in mouse embryonic development. This project will advance our knowledge around this fascinating whilst still largely unexplored time in development, focusing on the novel influences that extraembryonic tissues have on the ectoderm germ layer.

Studying early ectoderm development means investigating the changes in specification/potency and differentiation that the epiblast region fated to form ectodermal derivatives goes through. Through this project's results changes in pluripotency/potency/specification during early development are investigated.

These still unexplored aspects of the early ectoderm germ layer development arise mainly due to the fact that there is no validated *in vivo* marker (e.g., gene/protein expression marker), of the aforementioned germ layer, based on either single or combination of more than one gene expression patterns and secondly, due to the lack of any *in vivo* marker

identifying the entire neural plate when it first appears. Although *Sox1* is considered to be the most widely used neural progenitor marker (Kan et al., 2004), it is not described as a marker for the newly formed neural plate.

As mentioned above, the only study that reported the existence of a region within the developing ectoderm layer that restricted its potency (from pluripotent to neural and surface ectoderm fates) in the murine embryo suggested that this exists in the anterior proximal half of the embryo at the No bud (NO)/ Early bud (EB) stage (E7.0) (Li et al., 2013). This region is sometimes called the bipotent ectoderm. However, a contrasting study using a pluripotency assay based on the ability of epiblast fragments to generate epiblast stem cells or teratocarcinomas when transplanted elsewhere, reported that the fragment of the anterior-proximal epiblast is still pluripotent at NO/EB stages and loses its pluripotency at the early headfold stages (Osorno et al., 2012).

In addition, the NO/EB stage should actually be considered as a period of several substages, containing at least three substages according to Kaufman's Atlas, while there is also an additional stage before the early headfold stage (Lawson and Wilson, 2016). The timing of appearance of the bipotent ectoderm is in dispute as the testing for this was done only using early streak and NO/EB stages (Li et al., 2013), but not the intermediate substages, that could be very informative regarding the ectoderm development and the neural plate formation. On the other hand, a study using entire epiblast fragments to form epiblast stem cells, showed that pluripotency was reduced at the earlier LS stage, suggesting that a region of the LS epiblast may have already lost its pluripotency (Kojima et al., 2014).

In order to answer all of these questions, functional assays to test the pluripotency, potency and specification of specific epiblast regions at specific developmental stages, based on the latest most comprehensive mouse staging system found in the literature (Lawson and Wilson, 2016) must be done. However, this staging system is not based on live images of embryos but only on images of cleared wholemount embryos or on their sagittal sections. Previous established staging systems also including the above mentioned, depend on the development and size of the Allantoic bud – an extraembryonic structure to define the different developmental stages (Downs and Davies, 1993, Rivera-Perez et al., 2010, Lawson and Wilson, 2016). Nevertheless, some mouse strains show the appearance of the Allantoic bud prior to amnion closure, while some other strains include a stage where no Allantoic bud has formed even after amnion closure. This might be due to strain variation, the synchrony between amnion closure and development of Allantoic bud, or a combination of both. In addition, the use of Allantoic bud as the only criterion to stage the embryos might be a source of errors as there is no accepted definition of the Allantoic bud size, i.e it is not known when the Early bud (EB) ceases to exist and

grows to form the late bud (LB). For all the above-mentioned reasons, a more detailed, refined and comprehensive staging system of the murine embryo describing in detail the stages involved in the early ectoderm germ layer development should be established.

XENIA HADJIKYPRU

CHAPTER 2. METHODOLOGY

2.1 Mice and embryo collection

ICR mice and mice heterozygous for the *Ets2* gene were kept under standard housing conditions (light conditions 6:00-18:00 and dark conditions 18:00-6:00). At noon, the day following fertilization it is assumed that the embryos are aged E0.5. Pregnant females sacrificed on E5.5 (around 12:00-13:00 of the fifth day), E6.5 (around 12:00-13:00 of the sixth day), E7.5 (around 12:00-13:00 of the seventh day) and E8.3 (around 8:00-9:00 of the eighth day). *Ets2* ^{-/-} type-I and type-II embryos were generated by inter-crossing *Ets2* parental heterozygous mice. The conceptuses dissected out from the decidua using fine tip forceps and the Richert's membrane was mechanically removed using tungsten needles 30G (Sigma, Z192341). Dissection was carried out in culture medium F-12 nutrient mixture (Invitrogen, 21765) containing 10% fetal bovine serum (FBS) (Biosera, S1810) and 1M HEPES pH 7.4 (Sigma, 7364-45-9). Isolated embryos immediately after dissection or embryos after culture were at first fixed in 4% paraformaldehyde (Sigma, P6148) O/N at 4 degrees followed by wash in 1XPBST {PBS plus 0.1% TWEEN 20 (Sigma, P1379)}. Dehydration of the embryos followed (25%, 50%, and 75% methanol in PBT) to be stored at -20 degrees in 100% methanol for up to 6 months.

Ets2 ^{-/-} embryos were distinguished from their wildtype counterparts (*Ets2* ^{+/+} or *Ets2* ^{+/-}) based on previous findings (Polydorou and Georgiades 2013). The *Ets2* ^{-/-} mutant embryos were recognised during dissection due to their relatively small size, the reduced accumulation of maternal blood around their site of implantation and a V-shaped attachment of the Richert's membrane at the distal tip of the embryo (Georgiades and Rossant 2006). Type-I mutant embryos have a thick DVE which fails to move to the anterior side, do not have ExE trophoblast and do not form a PS/mesoderm. On the other hand, type-II mutant embryos form an AVE, even if appeared defective in most cases (does not reach the embryonic-extraembryonic junction), have a smaller ExE trophoblast, form a PS/mesoderm but present gastrulation progression defects. Moreover, type-II mutants do not form any recognizable allantoic bud, amnion or node. The maximum number of mutant embryos isolated per litter was four, where most of them were type-II.

2.2. Mouse tails genotyping

The heterozygosity of the parent mice determined by PCR analysis of genomic DNA derived from the mouse tails. For genomic DNA extraction the Extract-N Amp™ Tissue PCR Kit (Sigma, XNAT2). The kit includes the tissue preparation, the extraction and the neutralization solutions. Genomic DNA that had been extracted from mouse tail (~ 1 cm) when incubated in 12,5µl tissue preparation solution and 50µl extraction solution (1:4) for 15 min at 37°C. Then the samples were heated at 95°C for 3 min and then mixed with the neutralization solution (50µl) prior to PCR reaction.

Two separate PCR reactions with a primer set that produced either the wild-type (220bp) or mutant (200bp) sequences (Yamamoto et al., 1998, Georgiades and Rossant 2006) were performed. The PCR reaction conditions are as follows: 94°C for 3 min; 35 cycles of 94°C for 30 sec, 64°C for 30 sec and 72°C for 45 sec; then 72°C for 5 min. For the detection of the wild-type and the mutant DNA sequences, the primers that were used, presented in Table 1.

	Forward Primer (EtsA)	Reverse Primers	Length
Wt	5-CGTCCCTACTGGATGACAGCGG-3	5-TGCTTTGGTCAAATAGGAGCCACTG-3	220bp
		EtsB	
Ets2	5-CGTCCCTACTGGATGACAGCGG-3	5-AATGACAAGACGCTGGGCGG-3	200bp
		Neo	

Table 1: Primers for the wildtype and *Ets2* mutant allele that were used in mouse tails and embryo genotyping

The PCR mix for the detection of the **mutant** sequence (10µl reaction) was:

6.5µl H₂O (Gibco, RNase and DNase free), 2µl genomic DNA, 1µl enzyme buffer, 0.2µl dNTPs(10mM), 0.1µl Neo (10mM), 0.1µl EtsA (10mM), 0.1µl Tag Polymerase (Takara).

The PCR mix for the detection of the **wild type** sequence (10µl reaction) was:

6.5µl H₂O (Gibco, RNase and DNase free), 2µl genomic DNA, 1µl enzyme buffer, 0.2µl dNTPs, 0.1µl EtsA (10mM), 0.1µl EtsB (10mM), 0.1µl Tag Polymerase (Takara).

Following PCR analysis, the samples were run on 1X TAE/1% (Life Technologies, 24710-030) Agarose gel (Sigma, A0169) at 120 V for 30 minutes for the detection of the heterozygous and homozygous *Ets2* mice.

2.3. Microsurgery and culture of Epiblast embryonic explants

Following embryo isolation, the generation of epiblast explants required the embryos to be incubated for 15 minutes at 4°C in Trypsin – pancreatin solution (Gibco, 13151-014) and then transferred to 1xPBS (Ca²⁺, Mg²⁺ free). This procedure followed by mouth pipetting allowed the VE of the embryos to be peeled away while the ExE and EPC were cut off from the epiblast tissue using a glass pulled needle. The epiblast tissue was then bisected into its anterior and posterior parts. This was followed by bisection of the anterior part into its anterior proximal and anterior distal halves while the same was done using the posterior part.

Epiblast explants were then used for the needs of potency/pluripotency and specification assays (Annex – Figure 1). The specification assay was done on Fibronectin (Corning - CLS356008) coated plates (coating for 24 hours) (5mg/ml) while the pluripotency and potency assays were done on Fetal

Bovine Serum (FBS) (Sigma- F2442) coated plates (coating for at least 24hours). The composition of the chemically defined medium N2B27 used for all the assays were as follows: 25% DMEM lowglucose without phenol red (Invitrogen, 11880-028), 25% Ham's F12 Nutrient Mix with GlutaMax (Gibco, 31765) and 50% Neurobasal A without phenol red (Gibco, 12349), supplemented with 0,5X of N2 supplement (100X stock, Gibco, 17502-048), 0,5X of B27 supplement (50X stock, Gibco, 17504,), Streptomycin 5000µg/ml-Penicillin 5000 units/ml and 100 µM β- mercaptoethanol. Medium was changed every 48 hours.

Proteins and Inhibitors used:

- BMP2 (10 ng/ml, R&D Systems, 314-BP-010)
- Human FGF2 (10 ng/ml, NBP2-34921, Novus)
- Nodal/Activin: Inhibitor SB431542 (2 µM, 1614/1 – R&D Biosystems)
- Wnt Inhibitor XAV939 (10 µM X3004 Sigma-Aldrich)

2.4 Whole mount RNA *in situ* Hybridization

Single-colour and double-colour whole-mount RNA *in situ* hybridization (ISH) was carried out as previously described (Georgiades and Rossant 2006). The RNA probes were labelled either with digoxigenin or fluorescein and were detected using alkaline phosphatase conjugated antibodies that catalyse a chromogenic reaction with different chromogenic substrates, producing blue/purple or red/orange products respectively.

2.4.1 Preparation of Digoxigenin and Fluorescein-labelled probes

The cDNA-containing plasmids linearized using specific restriction enzymes. Antisense Digoxigenin or/and Fluorescein-labelled RNA probes are synthesized by *in vitro* transcription (IVT) from linearized plasmid template using bacteriophage RNA polymerases (T7, T3, SP6, Roche) and a ribonucleotide mixture in which the UTPs are labelled with Digoxigenin (DIG-11-UTP, Roche, 11277073910) or Fluorescein (Fluorescein-12-UTP, Roche, 11427857910). The polymerase was chosen based on the orientation of the cDNA with respect to the RNA promoters that flank it and it was used to transcribe the chosen plasmid cDNA template. For whole-mount RNA ISH antisense probes were used for the detection of the gene of interest. For this project the probes that were used for the detection of *Bra*, *Oct4*, *K8*, *K18*, *Sox2* and *Gsc* were as bacterial stocks stored at - 80oC (Georgiades and Rossant, 2006). Also *Dlx5* (supplied by Biosciences) were sent to the lab as bacterial stocks. From these bacterial stocks at first the plasmidDNA templates were purified using Midi-Preppreparation (see below), then were linearized

using unique restriction enzymes (see below) and finally the RNA probes were prepared using IVT. The plasmid DNA templates for *Hesx1*, *Fgf5*, *Six3* (kindly provided by Dr Tristan Rodriguez), *Sox1* (kindly provided by Dr. Stavros Malas) have been sent in the form of a DNA spot on a piece of Whatman 3MM paper. For those probes at first the plasmid DNA templates were released from the paper and then bacteria (DH5A) were transformed with these DNA templates (see below). Afterward the plasmid DNAs were purified using Midi-prep preparation then linearized using unique restriction enzymes and finally the RNA probes were prepared using IVT.

XENIA HADJIKYPR

2.4.2 Bacterial transformation with plasmid DNA

To transform competent bacteria with plasmid DNA the “Subcloning Efficiency DH5a Competent cells” were used (Invitrogen). The plasmid DNA was added (concentration varies from 1ng-10ng) in a 1.5ml Eppendorf tube which contained 50µl of the bacteria were incubated for 30 min on ice. Then the bacteria were heat shocked by placing them in a water bath at 42°C for 20 sec. Under sterile conditions 950µl of SOC medium (a medium suitable for growing freshly transformed bacteria) were transferred in a tube and incubated at 37°C at 225rpm incubator with shaking platform for 1 hour. Following incubation, the bacteria under aseptic conditions were spread on plates contained LB agar (Invitrogen, 22700025) and antibiotic (Ampicillin - Sigma, A95-18-5G, 100mg/ml), and were grown so as to get individual colonies at 37°C incubator overnight. The next day individual colonies were picked up and were transferred in a tube which contained 2.5ml LB growth (Invitrogen, 12780-052)/2.5µl Amp. Then, the bacteria colonies were incubated at 37°C at 225rpm incubator with a shaking platform overnight (O/N) (12-16 hours). Finally, the bacterial cultures were then used for re-growing them and 20µl (from 2.5 ml LB/Amp cultures) were added in flasks that contained 50ml LB growth/50µl Amp, so as to be used for Midi-preparation.

2.4.3 DNA purification using Midi-Preparation

The “NucleoBond Xtra Midi 50 preps” plasmid purification kit (Machery-Nagel, 740410.50) was used to purify plasmid DNA. Each “NucleoBond Xtra column” contains a “column filter” and a “column” situated at the base of the syringe and this is the filter that will trap the DNA. This “column” contains silica resin beads and provides a high overall positive charge that permits the negatively charged phosphate backbone of plasmid DNA to bind with high specificity. The basic principle of this system is that the bacterial cells were first lysed by an optimized set of buffers based on the NaOH/SDS lysis method. After equilibration of the “NucleoBond Xtra column”, the entire lysate was loaded by gravity flow and simultaneously was cleared by the specially designed “column filter”. The plasmid DNA was bound to the “NucleoBond Xtra silica resin” and following efficient washes the plasmid DNA was eluted, precipitated, and easily dissolved in water for further use. The kit’s protocol is as follows: the bacterial cultures that were grown at 37°C at 225 rpm, pellet by centrifugation at 5500g (rcf) for 15 min at 4°C and the supernatant was completely discarded. The bacterial pellet was resuspended completely in 8ml resuspension buffer (RES) with RNaseA by

pipetting the cells up and down. In this suspension 8ml of Lysis Buffer (LYS) was added, mixed gently by inverting the tube 5 times and the mixture was incubated for 5 min at RT. 12ml of Equilibration buffer (EQU) was applied onto the rim of the “column” and was allowed to empty by gravity flow. 8ml of the Neutralization (NEU) buffer was added to the suspension buffer (the bacterial lysate appeared less viscous and more homogeneous) which was then transferred to the equilibrated “column” and was allowed to empty by gravity flow. The “column filter” and the “column” were washed by adding 5ml of EQU buffer and then the “filter column” was discarded. The “column” was then washed by added 8ml of washing (WASH) buffer. To elude the plasmid DNA, 5ml of elution buffer (ELU) was added to the “column” and the DNA was then collected in a 50 ml centrifuge tube. For the precipitation of the plasmid DNA, 3.5ml of room temperature isopropanol was added to the 5ml of eluted DNA, the mixture was let for 2 min at RT and then centrifuged at 15,000 rcf at 4°C for 30 min. The supernatant was then removed carefully and the DNA pellet was washed twice using 70% ethanol in H₂O and dried at RT for approximately 2-3 min. The DNA pellet was then dissolved in 50µl H₂O (RNase-free/DNase free). The concentration of the DNA was calculated using the spectrophotometer and finally the purified DNA was stored at -20°C until used.

The DNA template that was purified using the Midi-prep method was then linearized to be later used for In Vitro Transcription (IVT). For each DNA template a unique restriction enzyme was used (shown in Table 2). To reach a final volume of 100µl the concentrations that were used for the restriction reaction mixture were as follows: 10mg DNA, 1X buffer, ddH₂O and enzyme (50units amount). The mixture was incubated at 37°C O/N. Afterwards, 100 µl of Phenol:Chloroform: Isoamylalcohol (25:24:1) (Sigma, P3803) was added in the sample, followed by vortex and centrifugation for 10 min at 12000 rcf. The upper phase was then transferred in a new tube and 500µl cold isopropanol together with 50µl RNase free 3M Sodium Acetate pH 5.2 were added in the sample. The sample was left for at least 1 hour at -20°C (preferably O/N). Then the mixture was centrifuged at 15 000 rcf for 30 min at 4°C and the DNA pellet was washed twice with 70% Ethanol in Gibco H₂O and was left to air dry. The pellet was resuspended in 20µl Gibco H₂O. To test for proper digestion, 1µl of the digested and 0.5µl of the undigested (control) DNA was loaded on a 1XTAE/1% Agarose gel and run at 120 V for 30 min. Appropriate size of bands revealed successful digestion.

2.4.4 In vitro transcription for making the RNA probe

Anti-sense Digoxigenin-labelled and Fluorescein-labelled RNA probes were synthesized by IVT using the linearized plasmid template, RNA polymerases (T7, T3 or SP6, Roche – see Table 2) and a ribonucleotide mixture in which the UTPs were labelled either with Digoxigenin or Fluorescein. The transcription mixture (10 μ l) contained 0.5 μ g of linearized template cDNA (1 μ l), 1 μ l transcription buffer (10X), 1 μ l DIG/Fluorescein RNA labelling mix, 0.5 μ l RNase Inhibitor, 0.5 μ l RNA polymerase and 6 μ l of RNase free ddH₂O. Transcription was performed for at least 3 h at 37°C for T3 and T7 and at 40°C for Sp6. Following incubation 50 μ l 4% LiCl, 80 μ l DEPC H₂O and 400 μ l isopropanol (mixed and 50 incubated at -20°C for 1h) were added to the probes. RNA was then precipitated. The RNA pellet was then washed twice with 70% Ethanol in DEPC H₂O and it was left to air dry. The pellet was resuspended in 55 μ l DEPC H₂O. To test the success of IVT, 5 μ l of the probe was run on 1% TAE agarose gel (RNase free). The remaining amount of the RNA probe was stored at -80°C for later use.

Gene	Restriction Enzymes	Polymerase for anti- sense probe
<i>Id1</i>	BamHI	T3
<i>Sox1</i>	EcoRV	Sp6
<i>Dlx5</i>	NotI	T3
<i>Nodal</i>	BamHI	T7
<i>Fgf5</i>	BamHI	T3
<i>Six3</i>	XbaI	T3
<i>Sox2</i>	EcoRI	T3
<i>K8</i>	XbaI	T3
<i>K18</i>	XbaI	T3
<i>Bra</i>	XbaI	T7
<i>Oct4</i>	XhoI	T7
<i>Gsc</i>	SacI	T3
<i>Sox17</i>	Hind3	T7
<i>Flk1</i>	XbaI	Sp6
<i>Msp1</i>	XhoI	T3
<i>Pax6</i>	EcoRI	T3
<i>Cer1</i>	SalI	Sp6
<i>Hesx1</i>	BamHI	T3

Table 2: Restriction enzymes and polymerases for anti-sense probes that were used for each gene

2.5 One colour RNA in situ hybridization

Day 1: Rehydration, permeabilization, post-fixation, pre-hybridization, hybridization. Embryos rehydrated through a methanol series (100% methanol, 75% methanol in PBT, 50% methanol in PBT, 25% methanol in PBT, 100% PBT), permeabilized by incubation at RT with Proteinase K (10mg/ml, Roche, 03115836001) in PBT for 2.5 – 6.5min (depending on embryonic stage). Epiblast explants were permeabilized using RIPA buffer for 15 minutes. The rest of the protocol remains the same both for embryos and explant cultures. This was followed by 3X5min washes in PBT, post fixation of samples in 0.2% Glutaraldehyde (Sigma, Cat. No. G6257) in 4% PFA for 20min, followed by 5h incubation in Prehybridization solution (DEPC-treated H₂O, Ultrapure formamide, 20XSSC RNase-free pH4.5, 10mg/ml tRNA (Roche), 50mg/ml Heparin, 10% RNase-free SDS) in 67°C hybridization oven and 3 x O/N incubation of hybridization solution containing the probe in 67°C hybridization oven.

Day 2: Post-hybridization washes, RNase step, pre-block and antibody incubation.

Following O/N hybridization, the embryos were washed 3x with Solution I (Formamide, 20X RNasefree SSC pH4.5, RNase free H₂O and 10% SDS) for 30 min at 67°C. Then they were washed 3x with TNT solution (ddH₂O, 5M NaCl, 1M TrisCl pH7.5, and 0.1% Tween 20) for 5 min at RT followed by incubation with RNaseA in TNT solution at 37°C for 1hour. The embryos were then washed 3x with Solution II (Formamide, 20X RNase-free SSC pH4.5, RNase-free H₂O and 10% SDS) at 67°C followed by 3x incubation with MAB solution pH 7.5 (ddH₂O, 1M Maleic acid, 200mM Levamisole, 5M NaCl and 0.1% Tween20) for 5 min at RT. They were then incubated in pre-block solution containing MAB/Block (MAB solution and 1% Blocking reagent, Roche) with 0.1% Sheep Serum for 3 hours at RT and finally were incubated overnight with the antibody (1:1000, Anti-Digoxigenin-AP, Fab fragments, Roche) at 4°C rocking in the dark.

Day 3: Post-antibody washes

The embryos were washed 3x with MAB solution for 10 min at RT, then 6x for 1 hour at RT and finally were left in MAB solution overnight at 4°C rocking.

Day 4: Visualization of the probe signal

Embryos were washed 3x with NTMT solution (ddH₂O, 1M TrisCl pH 9.5, 1M MgCl₂, 200mM Levamisole and 0.1% Tween 20) for 10 minutes at RT. Then the embryos were incubated in TBS staining solution containing 1M TrisHCl pH9.5, 1M MgCl₂, 5M NaCl plus INT/BCIP (Alkaline Phosphates substrate producing red/orange color, Roche) in the dark. The colour development time varies depending on the probe (from 2 hours to 48h). The embryos following colour development were washed 2x with PBT for 10 min at RT

followed by post fixation in 4% pfa and through a series of 50% and 75% glycerol in PBS for 10 minutes each. The embryos were documented as photos were taken using the inverted microscope Zeiss Axiovert 200M with AxioVision software.

XENIA HADJIKYPRIS

2.6 Double colour whole-mount RNA in situ hybridization

Day 1: Rehydration, permeabilization, post-fixation, pre-hybridization, hybridization. The procedure is exactly the same as in single colour whole-mount RNA in situ hybridization except the last step. At the end, the embryos were incubated in the hybridization solution containing the appropriate amount of both RNA probes. The one was fluorescein-labelled and the other one was digoxigenin-labelled RNA probe.

Day 2: Post-hybridization washes, RNase step, pre-block and incubation with the first antibody. After the post-hybridization washes and the RNase step, the embryos were then incubated in pre-block solution overnight with the first antibody (1:1000, Anti Fluorescein AP, Fab fragments, Roche) at 4°C rocking in the dark.

Day 3: Post-antibody washes with MAB solution.

Day 4: Visualization of the RNA Fluorescein-labelled probe signal. The embryos were washed with NTMT solution. Then the embryos were incubated in TBS staining solution containing 1M TrisHCl pH9.5, 1M MgCl₂, 5M NaCl plus INT/BCIP (Alkaline Phosphates substrate producing red/orange colour, Roche) in the dark. The colour development time for Fluorescein-labelled probes varies depending on the probe. The embryos were documented as photos were taken using the inverted microscope Zeiss Axiovert 200M with AxioVision software. After documentation they were then used for the development of the digoxigenin-labelled probes.

Day 5: Dehydration, Rehydration, pre-block and incubation with the second antibody. Embryos were dehydrated and then rehydrated through a methanol series (100% methanol, 75% methanol, 50% methanol, 25% methanol in RNase-free PBT (1X RNase-free PBS with 0.1% Tween 20) for 5 min at RT for the removal of the orange colour of the embryos. Then they were washed 3x in RNase-free PBT for 5 min at RT. To remove any alkaline phosphatases the embryos were incubated in RNase-free PBT for 1 hour at 70°C (hybridization oven). After the alkaline phosphatases heat inactivation, the samples were washed 3x with MAB solution pH 7.5 for 5 min at RT and then incubated in pre-block solution overnight with the second antibody (Anti-Digoxigenin-AP, Fab fragments, Roche) at 4°C rocking in the dark.

Day 6: Post-antibody washes with MAB solution.

Day 7: Visualization of the RNA digoxigenin-labelled probe signal. Embryos were washed with NTMT solution and then they were incubated in BM purple in the dark for the development of the digoxigenin-labelled probes. The BM purple removes a phosphate and turns the substrate purple. The embryos documented as photos were taken using the inverted microscope Zeiss Axiovert 200M with AxioVision software.

2.7 Clearing method of staged embryos

Following collection of embryos at the desired developmental stage and documentation of live morphology, they were fixed at 4% PFA, overnight at 4°C. The following day, embryos were dehydrated through a series of Methanol dilutions (1x PBST, 25% Methanol in 1x PBS, 50% Methanol in 1x PBS, 75% Methanol in 1x PBS and 100% Methanol) and then stored in 100% Methanol at -20°C. Stored embryos were then rehydrated again through Methanol dilutions (100% Methanol, 75% Methanol in 1x PBS, 50% 39 Methanol in 1x PBS and 25% Methanol in 1x PBS) and finally washed twice in 1x PBST. Rehydrated embryos were post-fixed in 0.2% Glutaraldehyde/4% PFA for 20 minutes at RT. Following this, they were washed twice in 1x PBST and incubated in a pre-warmed solution containing Ultrapure formamide, 20x RNase-free SSC pH4.5, DEPC-treated H₂O and 10% RNase-free SDS for 1 hour at RT. Then, the embryos were washed twice in 1x PBST, fixed at 4% PFA, rinsed once in 1x PBST and finally transferred into 50% and finally at 75% Glycerol. Embryos were oriented according to the orientation of their live morphology and photographs were taken at different magnifications using the inverted microscope Zeiss Axiovert 200M and the AxioVision software. Corresponding live embryos were also witnessed using the inverted microscope Zeiss Axiovert 200M and the AxioVision software.

2.8 RNA Preparation and quantitative PCR Analysis

At least four epiblast explant tissues or epiblast explant cultures were pooled together for RNA extraction. The desired tissue or explant outgrowth was used as a source of total RNA which was extracted using the NucleoSpin® RNA XS kit from Macherey Nagel (MN 740902.250). The whole process was repeated three times (three biological replicates). 100ng of total RNA were then used per reverse transcription reaction using random hexamers and oligo dT primer, according to the manufacturer (PrimeScript™ RT reagent Kit – Perfect Real Time, TaKaRa).

2.9 Quantitative Real Time PCR (qPCR)

For each reaction (each gene was measured in duplicate for each condition, using three biological replicates), 15ng of cDNA were used per reaction in a total volume of 25ul as follows:

- 15ng of template cDNA
- Up to 20µl PCR grade H₂O
- 1:1 forward and reverse primer mixture (300nM each primer)
- 10µl KAPA SYBR FAST qPCR Master Mix (2x) Universal

- 0.4 μ l 50X ROX High

Cycle thresholds (C_t) for each reaction were obtained and transformed into gene expression foldchange according to the formula: $\text{Fold change} = 2^{\Delta\Delta C_t}$, where $\Delta\Delta C_t = \Delta C_t(\text{GOI treated})$

$- \Delta C_t(\text{GOI mock}) - \Delta C_t(\beta\text{-actin mock})$. Where GOI = Gene of interest. C_t values were

relatively calculated to the house keeping gene $\beta\text{-actin}$.

The appropriate volumes of qPCR Master mix, template and primers were transferred to each well of a PCR plate. The following parameters were used:

- Enzyme activation at 95 °C during 20 sec - 3 min (1 cycle)
- Denaturation at 95 °C 30 seconds
- Annealing at 60 °C \geq 20 seconds
- Extension at 72 °C 5 minutes

Do 40 cycles of Denaturation/Annealing/Extension

- Dissociation according to instrument guidelines

2.10 ExE and VE ablation of embryos and the accurate generation of epiblast explants

The microsurgical technique during which the ExE is removed was evaluated to confirm the accuracy of the procedure. ExE ablated embryos were used to confirm the accuracy of the ExE ablation procedure when *Cdx2* was undetectable in the samples. To evaluate the efficiency of the microsurgical VE ablation procedure ISH experiments were conducted to confirm the absence of any VE cells contained in the samples. The transthyretin (*Ttr*) gene was used, known to be expressed specifically in the VE. *Ttr* was undetectable in the VE- ablated embryos suggesting no VE cell contamination.

CHAPTER 3. SCIENTIFIC AIMS AND HYPOTHESES

General aim of project: To better understand early mammalian ectoderm development using the mouse as a model by studying the development of anterior epiblast, which is mainly fated to form brain and head surface ectoderm, the earliest ectodermal derivatives to develop. It can be divided into **seven** Specific aims whose goal is to better describe and provide functional explanations about the emergence and development of the ectoderm germ layer using the mouse embryo as a model. In order to do that, *in vivo* and *ex vivo* approaches were employed.

Importance of general aim: Early ectoderm development, that is, the spatiotemporal changes in potency and specification and appearance of neural plate (neural induction) within anterior epiblast (progenitor of earliest ectodermal derivatives to develop: brain and head surface ectoderm) are underexplored and not precisely known. Moreover, trophoblastic influences on early ectoderm development are poorly understood.

3.1. Specific Aim 1

To establish a revised staging for period from just before gastrulation to early headfold for the discovery of more stages using new combinations of morphological criteria.

Importance of specific aim 1: Developmental staging systems have been used by researchers to understand the continuous process of embryonic development by dividing the different developmental phases into discernible blocks aiding the analysis of mouse embryos and reproducibility of the experiments (Fujinaga et al., 1992, Downs and Davies, 1993, Rivera-Perez et al., 2010, Theiler, 1972; Lawson and Wilson, 2016). Existing developmental staging systems for the period from just before gastrulation until the late headfold stage depend on external features of mainly live whole mouse embryos (Fujinaga et al., 1992, Downs and Davies, 1993, Rivera-Perez et al., 2010, Theiler, 1972; Lawson and Wilson, 2016). The most widely used stages from just before initiation of gastrulation up to late headfold stage divide development of this period into 9 stages (Downs and Davies, 1993, Rivera-Perez et al., 2010) or 10 stages (Lawson and Wilson, 2016). Moreover, gastrulation initiation, a significant developmental event, has not been linked to a specific developmental stage so far. A more defined staging system will also assist in identifying the exact developmental phase of the earliest loss of anterior epiblast pluripotency, that coincides with the onset of the ectoderm germ layer development. Pre-headfold stages are currently heavily based on the existence and size of the extraembryonic feature, the allantoic bud, whose size is not easily distinguished.

Moreover, allantoic bud size shows heterochrony amongst different mouse strains. Pre headfold developmental period marks an important phase during which important ectodermal events are thought to occur such as neural induction and appearance of bi-potent ectoderm. **Hypothesis of specific aim 1:** We hypothesized that if by using novel combinations of morphological embryonic criteria, achieves to subdivide this period of development into more stages than existing staging systems, then this aim will be achieved.

3.2 Specific Aim 2

To use this revised staging system to better define the spatio-temporal expression of genes that are informative of significant developmental events such as the onset of gastrulation and early ectoderm development.

Importance of specific aim 2: This more comprehensive staging system will be further validated by the use of informative gene expression patterns that will give clues regarding early ectoderm development. These genes include pluripotency related genes, early neural, early surface ectoderm and mesoderm genes.

Hypothesis of specific aim 2: We hypothesized that if by using this novel embryonic staging system validated with gene expression achieves to provide information regarding important developmental events, then the aim will be achieved.

3.3 Specific Aim 3 (3A and 3B)

This Specific Aim is divided into two (A and B) parts:

Specific Aim 3A: To establish a new *in vitro* pluripotency assay for testing pluripotency of postimplantation mouse explant tissues that is simpler and faster than existing *in vitro* pluripotency assays, for the purposes of using it to identify the earliest loss of pluripotency during ectoderm development.

Importance of specific aim 3A: During early embryo development, including early ectoderm germ layer development within anterior epiblast, one of the most fundamental events that takes place is the spatio-temporally controlled restriction of potency. As a result, there is loss of pluripotency (loss of ability to differentiate to derivatives of all three embryonic germ layers) since the epiblast is initially pluripotent (Slack, 2012). Understanding when and where this pluripotency loss takes place within anterior epiblast (progenitor of brain and head surface ectoderm) is important for understanding early ectoderm development.

Pluripotency assays are used to identify whether a tissue is pluripotent or not without being necessarily informative about the potency state of the tested tissue in the event that it is found not to be pluripotent. In addition to the existing, but technically difficult and relatively time-consuming, *in vivo* pluripotency assays (experimental teratomas and generation of embryo chimeras) (Beddington et al., 1986; Huang et al., 2012), there is only one widely used *in vitro* pluripotency assay. The latter relies on the ability of the tested postimplantation tissue explants to generate epiblast stem cell lines: if it can, it is pluripotent, if it cannot, it is considered non-pluripotent (Kojima et al., 2014). However, this assay is time-consuming (culture takes several weeks) and the fact that it involves disruption of intercellular contacts in the initial tissue explant may have a drawback. This is because loss of intercellular contacts affects cell behaviour and therefore it is unknown if potency is not affected.

Hypothesis of specific aim 3A: We hypothesized that if a new *in vitro* pluripotency assay is established, we would expect the explant culture conditions that comprise it to: (a) maintain the pluripotency of pluripotent postimplantation tissues during culture and (b) not result in a pluripotent phenotype during culture if a non-pluripotent tissue is used.

Specific Aim 3B: To use of this novel pluripotency assay in conjunction with our revised embryo staging to assess the underexplored issue of when pluripotency is first lost in anterior epiblast during ectoderm development.

Importance of specific aim 3B: Identifying the hitherto unknown earliest stage when pluripotency is lost from anterior epiblast during early ectoderm development is crucial for understanding its development. This is because before the initially pluripotent anterior epiblast differentiates to its ectodermal derivatives, it must first lose its pluripotency.

Hypothesis of specific aim 3B: We hypothesized that if the earliest stage where our pluripotency assay culture conditions result in anterior epiblast explant outgrowth not having a pluripotent phenotype at the end of culture should be the stage where pluripotency is first lost from at least part of anterior epiblast.

3.4 Specific Aim 4 (4A and 4B)

This Specific Aim is divided into two (A and B) parts:

Specific Aim 4A: To establish an *in vitro* potency assay for testing potency of postimplantation mouse epiblast explant tissues that is simpler and faster than existing *in vitro* potency assays, for the purposes of using it to identify the potency status of anterior epiblast during ectoderm development.

Importance of specific aim 4A: Developmental potency is a fundamental property of cells that are capable of differentiation, as is the case for anterior epiblast. It can be defined as the complete set of cell types/cell lineages/cell fates to which a cell/tissue (or its descendants) is capable of differentiating. When a cell/tissue loses its pluripotency its potency is said to be restricted because it can differentiate towards one or some, but not all, lineages (Slack, 2012).

The establishment of this potency assay includes advances over the currently ones used. A tissue potency assay is more informative than a pluripotency assay in the sense that although both assays establish whether a tissue is pluripotent, a potency assay also informs about the potency of the tested tissue in the event when it is not pluripotent.

Hypothesis of specific aim 4A: We hypothesized that if a new *in vitro* potency assay is established, we would expect the different explant culture conditions to give rise to: (a) neural fates (b) surface ectoderm fates (c) mesendodermal fates.

Specific Aim 4B: To use of this *in vitro* potency assay in conjunction with our revised embryo staging to assess the potency status of the anterior epiblast during ectoderm development.

Importance of specific aim 4B: The use of the potency assay developed here allowed for the identification of the exact time of loss of pluripotency and the restriction of potency of anterior proximal and anterior distal epiblast. This is important as loss of pluripotency and restriction of potency signifies important events during ectoderm development of the anterior epiblast.

Hypothesis of specific aim 4B: We hypothesized that if by using the potency assay, not all three embryonic germ layer derivatives can be derived, then pluripotency can be considered as lost and restriction of potency can be assessed.

3.5 Specific Aim 5

This specific aim stems from our unpublished data concerning the trophoblast-caused anterior epiblast phenotype seen in E8.3 *Ets2* type II mutants (Annex – Figure 2). This phenotype shows the coexpression of the early surface ectoderm marker *Dlx5* and the pluripotency related gene marker *Fgf5* in the absence of neural gene (*Sox1*) expression marker.

To determine whether this defective trophoblast-caused ectoderm phenotype seen in E8.3 *Ets2* mutants, represent a pathological phenotype (that is, one that is not encountered during normal development), or a phenotype also seen during normal development at an earlier stage prior to neural induction.

Importance of specific aim 5: This aim was addressed by examining the expression of *Sox1*, *Dlx5* and *Fgf5* in wildtype embryos just before amnion closure. This stage was identified based on our new mouse embryo staging system we developed described above to show a similar ectodermal phenotype as the one seen in *Ets2* mutants. This aim will investigate for the first time if the co expression of *Dlx5* and *Fgf5* exists during normal development.

Hypothesis of specific aim 5: By examining whether the never-before-seen anterior epiblast ectoderm phenotype of the mutants, we hypothesized that if this is encountered during normal development of anterior epiblast at an earlier stage than E8.3, it would suggest that the role of trophoblast signaling is to promote the exit of anterior epiblast from this state.

3.6 Specific Aim 6 (6A and 6B)

This Specific Aim is divided into two (A and B) parts:

Specific Aim 6A: To use our pluripotency assay to examine whether the anterior epiblast of E8.3 *Ets2*^{-/-} type-II mutants (a time when control embryos develop beyond the late headfold stage and reach the early somite period) is pluripotent or not.

Importance of aim 6A: This is important because if it is pluripotent, it would mean that anterior epiblast in the mutants is ‘stuck’ or confined at the pluripotency state and therefore the role of trophoblast should be to promote exit from pluripotency so as to differentiate to neural and surface ectoderm fates. If it is not pluripotent, the suggestion would be that it is the bipotent ectoderm state because our data shows coexpression of *Fgf5/Dlx5* in the mutants and this is also observed during normal development at PH2 stage where we showed that anterior-proximal epiblast is at a bipotent ectoderm state.

Hypothesis of specific aim 6A: We hypothesized that if during the pluripotency assay on mutant anterior epiblast, the live morphology of its explant outgrowths and the expression of pluripotency-related genes *Oct4* and *Fgf5* after 48h culture on FBS under pluripotency maintenance conditions, are as in the pluripotent control anterior epiblast from pre-streak embryos (that is, flat compact outgrowth with indistinguishable intercellular boundaries expressing *Fgf5* and *Oct4* throughout the outgrowth), then it is pluripotent. If not, it is not pluripotent.

Specific Aim 6B: To use our potency assay to examine the potency of anterior epiblast of E8.3 *Ets2* type-II mutants.

Importance of specific aim 6B: This is important because it will be informative about

the role of trophoblast in early ectoderm development. For example, if potency is that of bipotent ectoderm this would mean that in the mutants it is halted at this state and trophoblast signalling is required for further restriction of potency so that neural and surface ectoderm differentiation can occur.

Hypothesis of specific aim 6B: If during the potency assay on mutant anterior epiblast, the live morphology of its explant outgrowths and the expression of neural related genes, surface ectoderm related and mesoderm related after 48h culture on FBS under potency assay culture conditions, are as in the pluripotent control anterior epiblast from pre-streak embryos, then it is pluripotent. If not, then it can be suggested that the anterior epiblast of these mutants has restricted its potency towards specific fates.

3.7 Specific Aim 7

To develop the first fully serum-free and chemically defined specification assay for testing the specification status of mammalian tissues and use it to identify the hitherto unknown specification status of anterior-proximal and anterior-distal epiblast in pre-streak mouse embryos, which is fated to predominantly ectodermal fates.

Importance of specific aim 7: Since no chemically defined/serum-free mammalian specification assays exist, the specification status of E6.5 pre-streak anterior epiblast (anterior-proximal and anterior-distal fragments) was examined here for the first time.

Hypothesis of specific aim 7: We hypothesized that if the explant outgrowth of anterior-proximal and anterior-distal epiblast of pre-streak mouse embryos differentiates into neural, epidermal and/or mesodermal fates this would be the tissue's specification status.

CHAPTER 4. RESULTS

In this chapter, each of the specific aims is stated, followed by its hypothesis and its results.

4.1 Specific Aim 1, its hypothesis and its results:

Specific Aim 1

This specific aim was achieved by establishing a revised staging for period from just before gastrulation to early headfold for the discovery of more stages using new combinations of morphological criteria.

Hypothesis of specific aim 1

New set/combination of embryonic morphological features were used to define new developmental stages that established a more comprehensive murine embryonic staging system for the period just before gastrulation initiation and during it up to the late headfold stage.

Results of specific aim 1

The establishment of a revised embryo staging system

Developmental staging systems have been used by researchers to understand the continuous process of embryonic development by dividing the different developmental phases into discernible blocks aiding the analysis of mouse embryos and reproducibility of the experiments (Fujinaga et al., 1992, Downs and Davies, 1993, Rivera-Perez et al., 2010, Theiler, 1972; Lawson and Wilson, 2016). Existing developmental staging systems for the period from just before gastrulation until the late headfold stage depend on external features of whole mouse embryos (mainly live) (Fujinaga et al., 1992, Downs and Davies, 1993, Rivera-Perez et al., 2010, Theiler, 1972; Lawson and Wilson, 2016). The most widely used stages from just before initiation of gastrulation up to late headfold stage divided development of this period into 9 stages (Downs and Davies, 1993, Rivera-Perez et al., 2010) or 10 stages (Lawson and Wilson, 2016).

To establish a new developmental staging system, the cleared morphology of the mouse embryos was correlated with their live counterparts based on morphological criteria, some of which have never been used previously. These morphological criteria are detected when isolated conceptuses are viewed from different angles of their embryonic region, the region 'below' the embryonic- extraembryonic junction (explained further below). This

can be viewed either at its widest side (referred here as ‘sideview’), or their narrowest side (referred here as ‘front-to-back view’ when viewed from the anterior) (Figure 12).

XENIA HADJIKYPRRI



Figure 12: The different angles that isolated conceptuses can be visualized

A cleared embryo placed in side-view with the anterior side at the left. The black arrow points the embryonic-extraembryonic junction and the anterior side of the embryo. The same embryo seen in front-to-back view. All panels are of the same magnification (16 x magnification).

- **Amnion presence**

The PS as the first morphological landmark of gastrulation, is characterized by a thickening of the posterior epiblast, close to the embryonic-extraembryonic junction. PS cells undergo an epithelial- to-mesenchymal transition resulting in the emergence of mesoderm (Beddington RS and Robertson EJ 1999) including both embryonic and extraembryonic mesoderm of the chorion, amnion, yolk sac and allantois. The amnion is an extraembryonic membrane found around the foetus of amniotes (Schmidt W. 1992). The presence of an amnion is considered to have firstly occurred when the proamniotic canal has finally vanished resulting in the absence of free space within this region. This firstly occurs during a stage named ‘between late streak/early bud and neural plate stage’ (Pereira et al., 2011) or ‘10c/11a (Lawson and Wilson, 2016), in our staging system Pre-Headfold 1. At this stage, the proamniotic canal is sealed, creating three new cavities, the ectoplacental EPC cavity, the exocoelomic cavity and the amniotic cavity. Both sideviews and front-to-back views were used to confirm the presence of an amnion (Figure 13). This is because in some cases, sideviews suggest the presence of an amnion while front-to-back views show that there is still a narrow proamniotic canal present. This could happen just before amnion closure. All cases considered to have amnion; the amnion was detected directly as it appeared as a dark continuous zone at the level of the embryonic

- extraembryonic junction that extended from the posterior side of the embryo to the anterior side. Front to back views confirmed this observation as the presence of amnion was seen as a continuous dark zone expanding from one side of the embryo to the other along the embryonic extraembryonic junction. In all cases of using cleared embryos the amnion was also seen, but it was no longer dark in all cases.

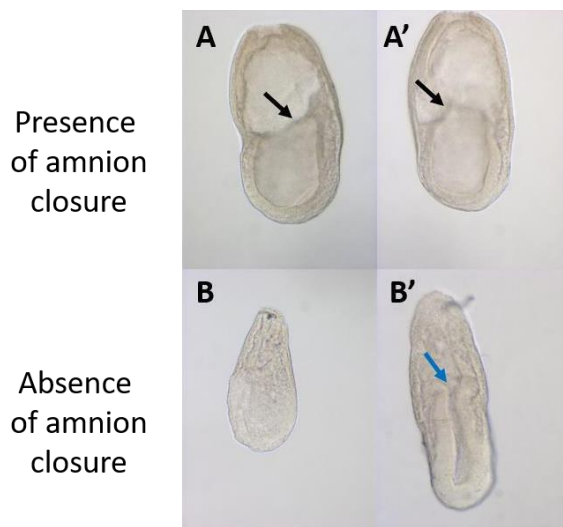


Figure 13: The classification of embryos depends on the presence or absence of amnion closure

A and B are sideview whereas A' and B' are front to back views. A and A' show presence of amnion, seen as a continuous dark line (black arrows). B and B' amnion is not present as a gap in the proamniotic canal is visible, signifying its absence (blue arrow) (B'). All images are of cleared embryos. Panels A, A' and B (16x magnification) Panel B' (25x magnification).

Classification of stages in post-implantation embryos

Based on several morphological criteria and observations described below, 15 embryonic stages during this period were classified; 9 stages in the Pre-Streak classification, 4 stages in the pre-headfold classification and 2 stages in the Headfold classification.

Perigastrulation stages - before amnion closure (the identification of 9 substages)

Understanding and studying fundamental mammalian embryonic events that take place during early gastrulation such as streak initiation and extension, mesendoderm formation, AME and node formation is very crucial. Some of these events can be addressed using this staging system.

1. Thickened anterior VE (AVE) stage (n=6)

These embryos, also described in Lawson and Tam (2016) as AVE eggcylinder, show similar embryonic VE thickness throughout their PD length that can be seen on one side of the embryonic region in all embryos (Figure 14). No mesodermal wedge was observed in these stages. There was no opacity in embryonic region and distal extraembryonic region in any embryo but opacity of proximal extraembryonic region was observed in all embryos. The PD length of embryonic region is approximately equal to its midpoint orthogonal width (length/width ratio from 5 embryos, ranging from 0.90 to 1.01).

Asymmetric circumferential constriction of VE at junction (either one on the anterior side only or in both sides but deeper or more abrupt on the anterior side) was observed in all embryos. The posterior-distal EXE is not separated from posterior distal extraembryonic VE by tissue (extraembryonic mesoderm) and this was seen in all embryos. No *Bra* expression observed.

XENIA HADJIKYPRIS

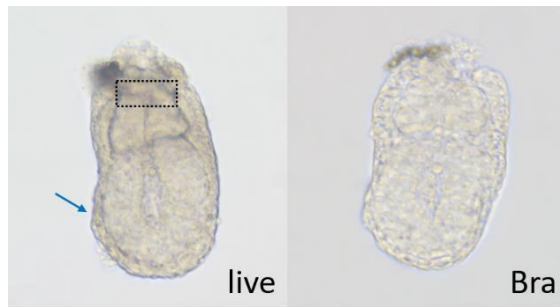


Figure 14: Thickened anterior VE (AVE) stage embryo

Live morphology and gene expression of *Bra* of the same embryo. Blue arrow showing anterior VE thickness. Dotted box showing opacity of the proximal extraembryonic region. No *Bra* expression. All images are of the same magnification (20 x magnification).

2. Immature pre-streak (preS) stage (n=13)

This is a new stage described here that can be placed between AVE and Pre-Streak stages of Tam et al 2010. Similar to the previous AVE stage, these *Bra*-negative embryos, showed no mesodermal wedge, no opacity but translucent embryonic region in all embryos but opacity in proximal only extraembryonic region (Figure 15). There was also asymmetric circumferential constriction of VE at junction (either one on the anterior side only or in both sides but deeper or more abrupt on the anterior side) in the vast majority of these. The posterior-distal EXE not separated from posterior distal extraembryonic VE by tissue (extraembryonic mesoderm) in all embryos. The new features of this stage include the observed bilateral thickness of proximal embryonic VE (prVE) relative to more distal embryonic VE seen in all embryos. Another feature regards embryonic size. The embryonic PD length ranged from being approximately equal (4/13 embryos) or longer (up to 36% longer in 9/13) than its orthogonal midpoint width (from 13 embryos studied).

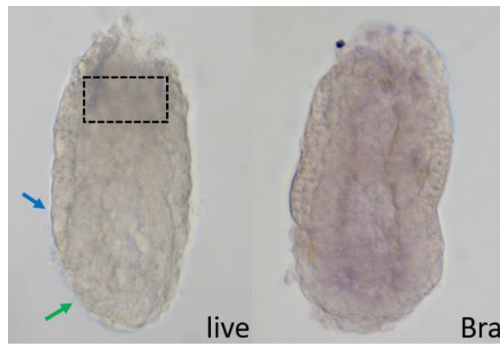


Figure 15: Immature Pre-Streak (preS) stage embryo

Live morphology and gene expression of *Bra* of the same embryo. Bilateral thickness of proximal embryonic VE on both anterior and posterior sides (blue arrow). Thin distal embryonic VE (green arrow). Dotted box showing opacity of the proximal extraembryonic region. No *Bra* expression. All images are of the same magnification (20 x magnification).

3. Mature pre-streak (preS) stage (n=34)

This is a new stage described here that can be placed between AVE and Pre-Streak stages of Tam et al 2010. All embryonic features remain the same as described in Immature preS stage except: Tissue opacity that is now present in the entire extraembryonic region (34/34) and may (13/34) or may not (21/34) expand into proximal extremity of both anterior and posterior embryonic region at an approximately equal PD extent (Figure 16). This opacity in proximal extraembryonic region was darker than that of distal extraembryonic region in most (25/34) embryos. These embryos although *Bra* negative show *Sox2* expression throughout the epiblast, consistent with absence of streak. Moreover, the source of extraembryonic opacity at mature preS stage is due to extraembryonic VE being opaquer than EXE, epiblast and embryonic VE.

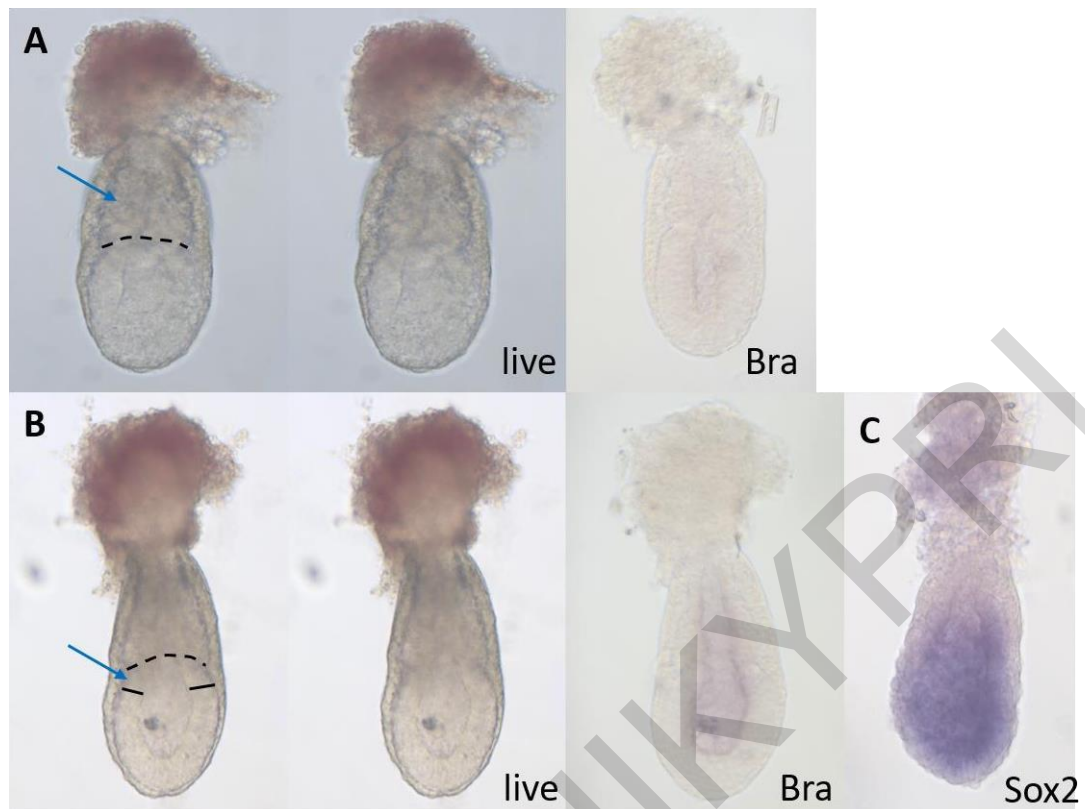


Figure 16: Mature Pre-Streak (preS) stage embryos

(A) Live morphology and *Bra* expression of the same embryo. (B) Live morphology and *Bra* expression of the same embryo. (C) *Sox2* expression. Opacity only in the entire extraembryonic region (A) (blue arrow). Opacity expanding into the proximal area of embryonic region (B) (blue arrow). No *Bra* expression (B right panel). *Sox2* expressed in the entire epiblast (C). Dotted line showing embryonic-extraembryonic junction. All images are of the same magnification (20 x magnification).

4. Nascent streak (NS) stage (n=14)

This is a new stage never described elsewhere, that provides the first morphological criteria for identifying from live embryos those embryos with streak prior to mesoderm formation. Although previous authors named this stage “pre-streak” stage (Lawson, 2016; Tam, 2010), this is misleading because there is presence of primitive streak seen by *Bra* expression at the posterior proximal side (Figure 17). All embryonic features remain the same as described in Immature pre Streak stage except: The PD length of tissue opacity in posterior embryonic region is now appreciably longer than that in the anterior side and this is associated with presence of *Bra* in embryonic region, thereby allowing for the first time the identification of PS prior to mesoderm formation in live embryos. Distal limit of posterior embryonic opacity coincides with distal limit of *Bra* expression, thereby allowing for the first time the identification of anterior end of PS in live embryos at this stage. PD length of *Bra* or tissue opacity in posterior embryonic

region ranges from 22% to 46% of the total PD length of the embryonic region. *Sox2* downregulation in posterior epiblast was observed that coincides with appearance of pre-mesoderm streak at this stage. Specifically, *Sox2* is expressed throughout epiblast except in proximal-posterior region where the streak is. This is important because it shows that at NS stage when pre-mesoderm PS first appears, there is concomitant downregulation of *Sox2*, which in previous stages (see mature pre-streak stage) is expressed throughout the epiblast. Therefore, consistent with previous studies that state that onset of *Bra* and downregulation of *Sox2* signifies PS initiation (Morgani et al., 2017), our data show for the first time that this occurs in vivo at the NS stage prior to mesoderm formation.

XENIA HADJIKYPRRI

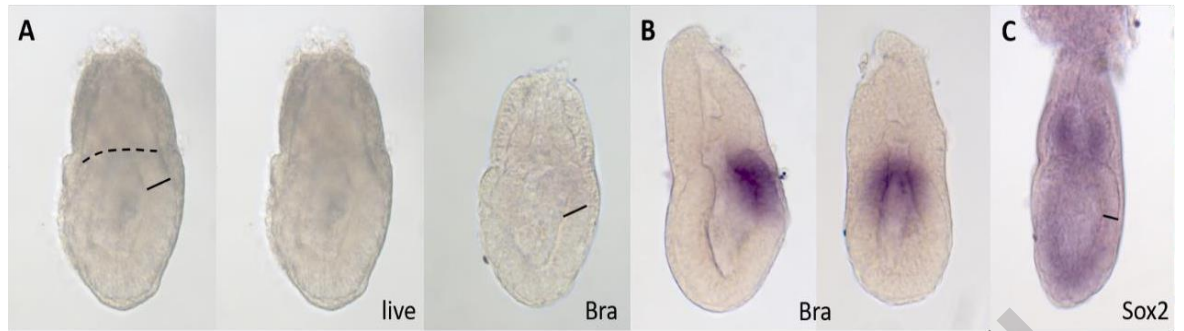


Figure 17: Nascent Stage (NS) embryos

(A) Live morphology and *Bra* expression of the same embryo. (B) *Bra* expression. (C) *Sox2* expression. Posterior embryonic region tissue opaqueness (A left panel) associated with presence of *Bra* in embryonic region (A right panel). Some embryos show further expansion of posterior embryonic region opaqueness evident by the expansion of *Bra* expression in PD length (B left panel). Pro amniotic canal present (B right panel – front to back views). Downregulation of *Sox2* expression in posterior proximal epiblast (C). All images are of the same magnification (20 x magnification).

5. Early streak (ES) stage (n=17)

This previously described stage shows similar features to the NS stage except: Mesoderm formation (bumpy/rough tissue appearance in at least proximal-posterior embryonic region as opposed to the smooth and continuous appearance of distal tip epiblast, seen in both live and in situ/cleared embryos) is present in side-views of all embryos studied (Figure 18). This was confirmed from front-back views, seen by extra tissue between proximal epiblast and proximal VE, as reported previously (Downs 1993, Tam 2000). Another new feature included the distal limit of mesodermal wing coincided with distal limit of epiblast *Bra* in all embryos so mesodermal wings can be used to detect the length of streak at this stage. Mesodermal wings constitute migrating mesodermal tissue that first spreads over posterior streak epiblast and then continues laterally towards anterior epiblast. Posterior-distal ExE is separated from posterior distal extraembryonic VE by tissue (extraembryonic mesoderm) in all embryos studied. PD length reached by distal limit of posterior embryonic opaqueness coincides with distal limit of *Bra* expression seen in all embryos studied. This indicates that at the ES stage (streak maximum length up to 50% that of embryonic region, as indicated by previous authors), the distal limit of posterior embryonic opaqueness and the distal limit of

mesodermal wings could be both used as new morphological features for identifying the PD length of streak in live embryos.

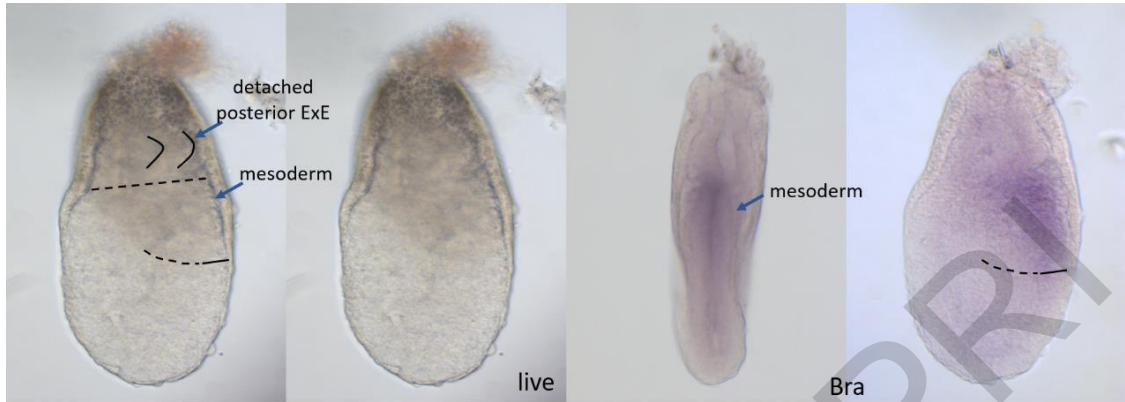


Figure 18: Early Streak (ES) stage embryo

Live morphology and *Bra* expression of the same embryo. Mesoderm formation seen both in sideways (1st panel) and front to back views (3rd panel). Detached posterior distal ExE from distal extraembryonic VE (1st panel). *Bra* expression (4th panel) coincides with posterior embryonic opaqueness. *Bra* expression also coincides with distal limit of mesodermal wings (dotted black line in epiblast). All images are of the same magnification (20 x magnification).

6. Mid-streak-1 (MS1) (n=15)

This is a new substage of previously described mid streak stage (Downs 1993, Tam 2010 and Lawson2016) (Figure 19). At this stage, the distal limit of posterior opaqueness is no longer indicative of the length of the streak as it was in previous stages. This is because the PD length reached by distal limit of posterior embryonic opaqueness does not coincide with distal limit of *Bra* expression in all embryos. At this stage, the streak ranges from 53% to 61% based on *Bra* expression. Streak length at this stage was statistically longer than ES stage. On the other hand, mesodermal wings PD length also ranged from 53% to 61%. This indicates that at the MS1 stage the distal limit of mesodermal wings is still a reliable morphological feature for identifying the PD length of streak in live embryos. *Sox2* downregulation in posterior epiblast colocalizes with the presence of the streak, so that this gene could be used to estimate streak length.



Figure 19: Mid-Streak-1 (MS1) stage embryo

(A) Live morphology and *Bra* expression of the same embryo (B) *Sox2* expression. Posterior tissue opaqueness (black line - A left panel) no longer coincides with *Bra* expression (A right panel). Primitive streak more than 50% of embryonic region based on *Bra* expression (A right panel). Mesodermal wing distal limit coincides with streak length (black epiblast dotted line - A right panel). *Sox2* absence at streak location (B). All images are of the same magnification (20 x magnification).

7. Mid-streak-2 (MS2) (n=12)

This is a new substage of the previously described mid streak stage (Downs 1993, Tam 2010 and Lawson 2016). The new features of this stage include the statistically significant increase of the the mean streak length in MS-2 embryos (66.8%) compared to the previous stage based on *Bra* expression and the distal limit of the mesodermal wings (Figure 20). Another new feature of this substage include the presence of a thickened lower layer that appears close to, but proximal to the distal tip area in the posterior region of the embryo seen in all embryos. The thickest part of this lower layer is proximal to the posterior half of distal tip and may or may not extend into the posterior half of the latter. This lower layer was seen just anterior to the distal end of the streak and does not express *Bra* meaning it does not contain the mesodermal progenitors of AME.

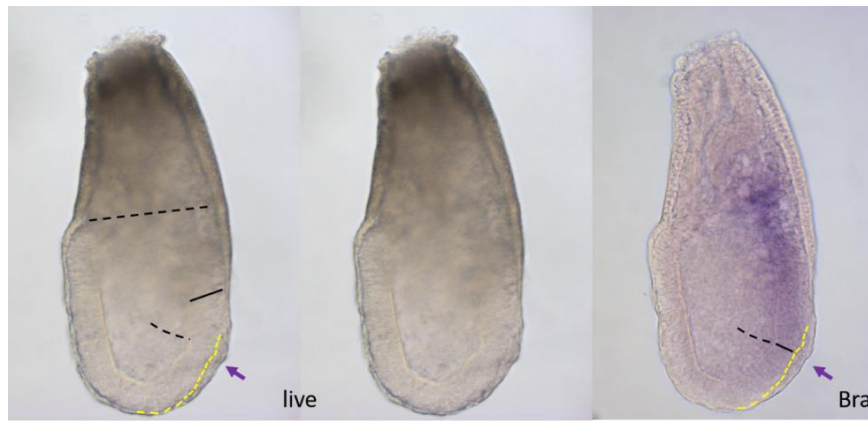


Figure 20: Mid-Streak-2 (MS2) stage embryo

Live morphology and *Bra* expression of the same embryo. Presence of a thickened lower layer closeto, but proximal to the distal tip area in the posterior region (purple arrow). Dotted yellow line indicates epiblast outer layer. Primitive streak more than 50% of embryonic region based on *Bra* expression (right panel). Mesodermal wing distal limit coincides with streak length (black epiblast dotted line). All images are of the same magnification (20 x magnification).

8. Late-streak-1 (LS1) (n=12)

This is a new substage of previously described late stage; late streak is the stage defined by having head process (thickened lower layer) in the distal tip region and exocoelomic cavity (Downs 1993, Tam 2010 and Lawson 2016) (Figure 21). The new features of this stage described here include that the thickest part of lower layer expanded into the posterior half of distal tip in all embryos. The StreakPD length is found above the distal tip area and coincides with mesodermal wing distal limit and distal limit of epiblast Bra. The streak length is significantly longer than MS-2 stage. *Bra* expression is now present in lower layer and expands more anteriorly than the streak marking the Axial Mesoderm (AME). The lower layer is still covered by VE as *Bra* in lower layer is covered by a *Bra*-negative thin lower layer. *Sox2* downregulation in posterior epiblast colocalizes with the presence of the streak and consistent with the extent of the streak.



Figure 21: Late-Streak-1 (LS1) stage embryos

(A) Live and clear views of the same embryo. (B) *Bra* expression. (C) *Sox2* expression. Thickened lower layer expanded into the posterior half of the distal tip (purple arrow – A). Presence of exocoelomic cavity (red asterisk panel A – clear). Proamniotic canal present (black arrow, far right panel A – clear). Mesodermal wing (dotted black line in amniotic canal) (far left panel A) coincides with streak PD length evident by *Bra* expression (B). *Bra* expression also present in lower layer marking the AME. *Sox2* absence in posterior epiblast (C). All images are of the same magnification (16 x magnification).

9. Late-streak-2 (LS2) (n= 17)

This is a new substage of previously described Late-Streak stage Early Bud stage (Lawson and Wilson 2016). This stage was based on the presence of the extraembryonic feature allantoic bud which we found here that it was not consistently seen in all embryos. This stage was also previously defined by another new feature that is the presence of a larger exocoelomic cavity which again was difficult to observe in all live embryos. Our new feature of this stage includes the further expansion of the Streak PD length based on epiblast *Bra* expression that has not reached its full length yet (Figure 22) The streak length was again found to be significantly longer than that of the LS-1 stage based on *Bra* expression. Mesodermal wing distal limit no longer coincides with *Bra* expression. Lower layer is now completely exposed and this was evident by *Bra* expression in the entire lower layer and absence of *Bra* negative thin lower layer. *Sox2* downregulation in posterior epiblast colocalizes with the presence of the steak. The posterior AME (sometimes called anterior head process), which is defined as *Bra*-positive axial mesoderm continuous with the head process that extends more anteriorly than the mid-point of the distal tip (Yamanaka et al., 2007; Polydorou and Georgiades 2013), forms during this stage, but not before (not present in the LS1 stage).

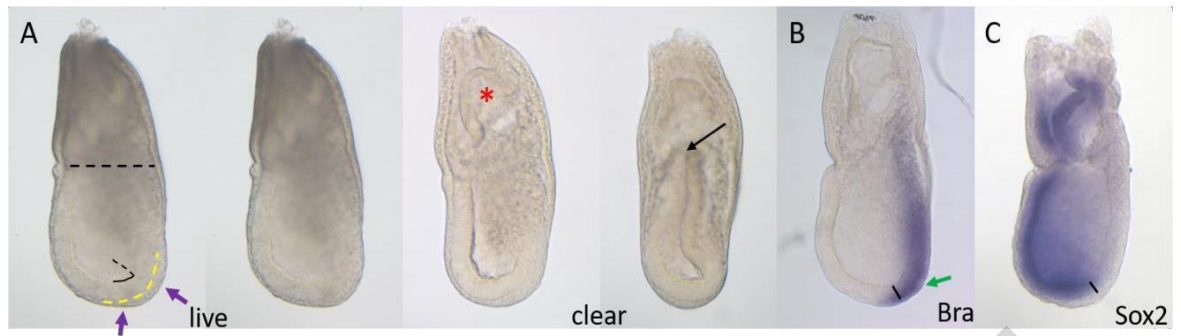


Figure 22: Late-Streak-2 (LS2) stage embryos

(A) Live and clear views of the same embryo. (B) *Bra* expression. (C) *Sox2* expression. Thickened lower layer expanded into the posterior half of the distal tip (purple arrow – A). Presence of exocoelomic cavity (red asterisk panel A - clear). Proamniotic canal present (black arrow far right panel A – clear). Mesodermal wing (dotted black line in amniotic canal) expanded but does not coincide with streak PD length evident by *Bra* expression (B). *Bra* expression also present in lower layer marking the AME. *Sox2* absence in posterior epiblast (C). All images are of the same magnification (16 x magnification).

Morphological criteria employed for the identification of the pre headfold developmental stages of mouse embryos

The set of morphological criteria and observations for the classification of embryos at peri gastrulation stages from amnion closure until the late headfold (approximately E8.5) for the mouse ICR strain, are presented and described below. All are presented at the resolution of the inverted microscope. These set of morphological criteria are:

- **Presence of head process**

Another criterion used was the presence of a morphological head process and its localization either in the posterior side or the middle point of the embryo's distal tip. This feature was applicable to the late streak stages and pre-headfold stages following amnion formation and was only seen when embryos were documented sideways (Figure 23). The head process could be visualized as soon as it formed at the mid to late streak stage. It appeared as a small, ventrally directed bulge at the embryonic distal tip. When the embryos were seen from side-views, the head process was the thickening of the tissue underneath (or distal to) the epiblast within the embryonic distal tip area. The latter area was defined as the tissue found below (distal to) the imaginary line that is perpendicular to the PD axis and situated at the level of the outer surface of the distal epiblast. This thickening was considered present if any region of the below-epiblast tissue of the distal tip region was thicker than its counterparts in more anterior and posterior regions. If the widest region of this thickening overlapped with the midpoint of the distal tip, it was considered to denote a 'middle head process'. If its thickest region was localized within the posterior

side of the distal tip without extending under the midpoint of the distal tip, it was then considered as 'posterior head process'. If there was no such thickness within the distal tip region, it was assumed that there is no morphologically distinguishable head process. This could mean that a head process does not exist or that it exists but cannot be identified from wholemount viewing. Head process was clearly observed in all embryos in both live and cleared views. Therefore, this criterion was employed in our staging system to distinguish between the Mid to Late streak stage and Late Streak stage, in which the head process is confined in the distal posteriorside, and the other Late streak Stage 2 in which the head process is localized in the middle distal area.

XENIA HADJIKYPRRI

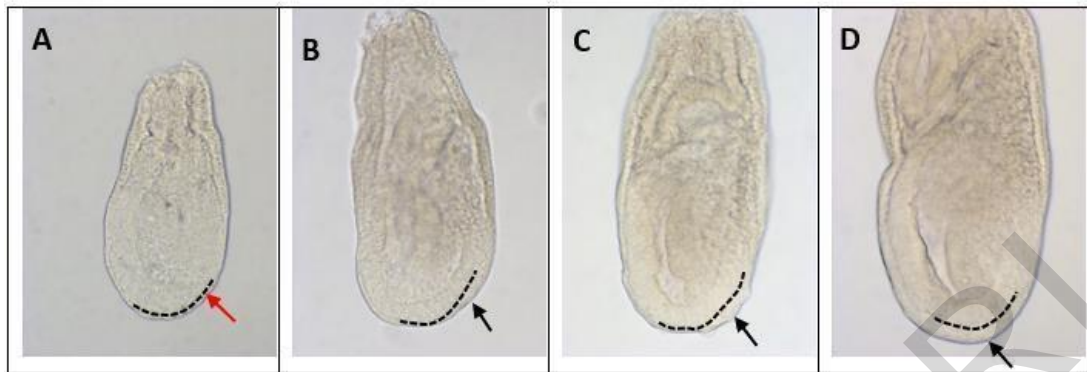


Figure 23: The classification of embryos depends on the presence/absence of head process and its relative location within the distal tip area

(A) shows no head process. Red arrow indicates its absence. (B) and (C) head process is present (black arrows) and located on the anterior side of the distal tip area. (D) head process extended to the distal tip area (black arrow). All images are side-views. Dotted black line marks outer epiblast membrane. All panels are of cleared embryos and of the same magnification (25 x magnification).

- **Presence of morphological node**

The next criterion was the presence of a morphological node and the identification of its stage. This feature can be distinguished by the presence of immature and the presence of mature (or morphological) node (Figure 24). The immature node is the non-morphologically identifiable precursor of the mature node. The mature node appeared as a dorsally directed indentation confined at the ventral surface of the lower layer underneath the middle-distal epiblast.

Its appearance occurs following amnion formation, i.e., at ‘Pre-headfold’ stages, and it gradually deepens up to the early somite stages (Bellomo et al., 1996, Downs and Davies, 1993, Yamanaka et al., 2007). Notably, the ventral surface of the middle distal epiblast (upper layer of mature node) is also curved dorsally towards the amniotic cavity and this feature seems to emerge earlier than that of the lower layer (Bellomo et al., 1996, Poelmann, 1981).

An immature node was considered present if live or cleared embryos having an amnion were viewed from front-to-back and their ventral surface of the upper layer of the distal tip epiblast was slightly curved dorsally but there was no presence of a dorsally directed indentation on the ventral surface of the lower layer.

When embryos were seen in front-to-back and a dorsally directed curve was observed in both the ventral layer of the epiblast and the ventral layer of the lower layer, it was thought that mature node was morphologically present. In some cases, when this mature state of node was more conspicuous, it was also visible when the embryos were seen in side-views. This was observed when there was a slight indentation dorsally of the outer lower layer at the distal tip region. Nevertheless, this dorsally directed indentation was reliably assessed only from front-to-back views since it was not consistently determined from side-views.

The observations made on cleared and live views agree in all embryos that have these features and in all embryos that do not have them. This criterion was employed to distinguish between certain pre-headfold stages as the appearance of immature and mature node happens during these stages.

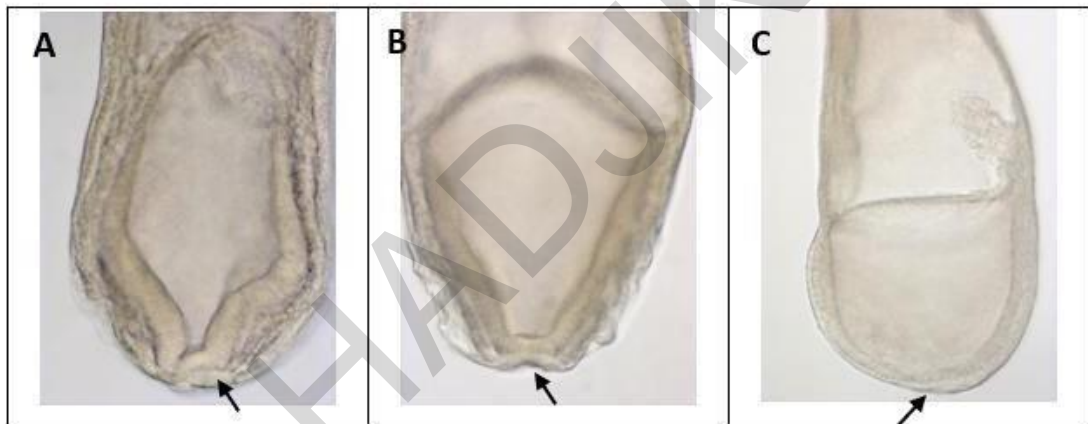


Figure 24: The classification of embryos depends on the presence of either immature or mature morphological node

The black arrow in (A) indicates an indentation of the upper layer of distal tip epiblast that is the immature node. The black arrow in (B) indicates the dorsally directed curve of both the ventral layer of the epiblast and the ventral layer of the lower layer that is the mature node. (C) is the same embryo as (B) when seen side-view. Mature node can be seen as a slight indentation of the distal tip area (C). All panels are of cleared embryos. (A) and (B) are of the same magnification (10 x magnification 2,5 optovar), while (C) (16 magnification).

- **Presence of allantoic bud**

Another feature that is usually employed by other staging systems available in the literature is the presence of the extraembryonic structure, the allantoic bud, either as an early bud or a late bud. This feature can be identified when embryos are seen side-views. An allantoic bud was considered present if there was a tissue protrusion extending from

the proximal limit of the primitive streak into the exocoelomic cavity. It was classified as no bud when no protrusion was visible, as **Early bud** if the shape of the bud was a hemisphere and not extending up to the midline of the anterior - posterior axis of the exocoelomic cavity, as **Mid bud** when it resembled a short, elongated tissue but still not extending up to the midline and as **Late bud** when this tissue projected freely into the exocoelomic cavity and was extending up to the midline and further of the anterior-posterior axis. However, there is no established definition of when early bud ends and late bud begins (Downs and Davies, 1993, Rivera-Perez et al., 2010). The presence of allantois from live side-view was seen only in about half the number of embryos examined ranging from late streak to late headfold stages whereas in cleared side-view was seen in all counterparts (Figure 25). Since this criterion was not consistently seen in all live views and because the length (size) of the bud was subjective, it was not employed as a criterion for this current staging system.



Figure 25: The use of the size of Allantoic bud as a morphological criterion for embryonic staging

(A) is an embryo representing No bud, (B) Early bud, (C) Mid bud and (D) Late bud. The black arrows indicate the tip of the allantoic bud for size estimation. All images are of cleared embryos and of the same magnification (16 x magnification).

- **Presence of headfold**

Moreover, another criterion to be used in this staging system was the presence of a headfold which was applicable to all stages with an amnion. Initially, the headfold emerges as a thickening of the anterior ectoderm region, due to the thickening of the neural folds which begin to project dorsally into the amniotic cavity. When this was observed, the embryo was considered to be at the Early headfold stage (Fujinaga et al., 1992, Downs and Davies, 1993). The headfold becomes even more conspicuous when, in addition to the aforementioned thickening, there is a foregut invagination, a dorsally directed indentation of the outer layer of the anterior region of the embryo (Figure 26). It becomes more pronounced as the thickened ectoderm is further pushed into the amniotic cavity due to folding of its underneath side (Kojima et al., 2014b) (Snell and Stevens, 1966). The presence of these features was inspected from side-view in both live and cleared embryos.

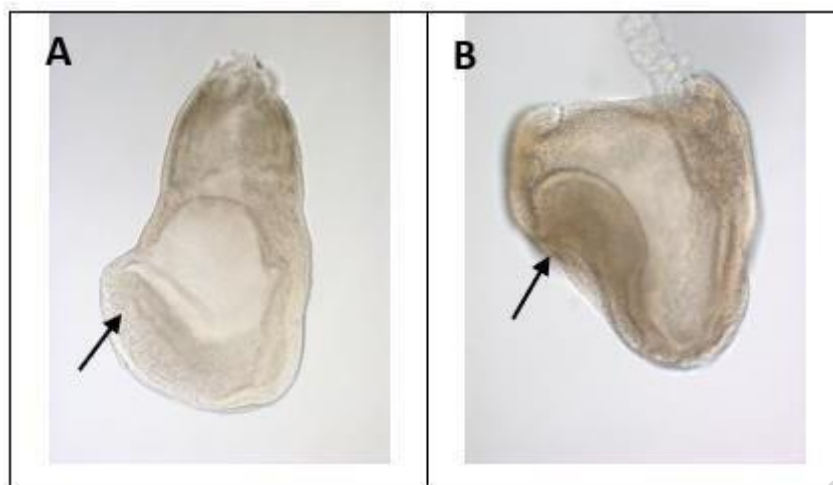


Figure 26: The classification of embryos depends on the presence of headfold

Embryo (A) represents an Early Headfold stage as seen by the thickened anterior epiblast (black arrow). Embryo (B) is at the Late Headfold stage with the black arrow indicating the foregut invagination. All images are of cleared embryos and of the same magnification (10 x magnification).

Pre-headfold stages - after amnion closure (the identification of 4 substages)

All embryos which had a completely formed amnion were classified as pre-headfold.

1. 'Pre-headfold - 1' (PH1) (n=24)

This is the earliest stage during the embryo development that a fully formed amnion was present (Figure 27). The proamniotic canal is at this time point sealed which created two new cavities; the proximal ectoplacental cavity i.e the chorionic cavity and the distal amniotic one. At this stage in which the amnion was just formed, the length of the embryonic region was equal to its width ($L=W$). Exocoelomic cavity was present although not constantly seen in live morphology. The head process was present and again the thickest part of this lower layer expanded into the posterior half of the distal tip in all embryos. When seen in front to back views amnion formation was evident because a continuous black line is observed between the two canals. Another feature here includes the shape of the inner epiblast when embryos are seen in front to back views. Shape of distal epiblast region (area where inner surface of left and right distal epiblast sides are clearly tilted away from each other) is "open U". Specifically, it consists of 2 sides and 1 base, all of approximately equal size with transition between sides and base being smooth, thereby giving an open U shape. In addition, there was no presence of a morphological node.

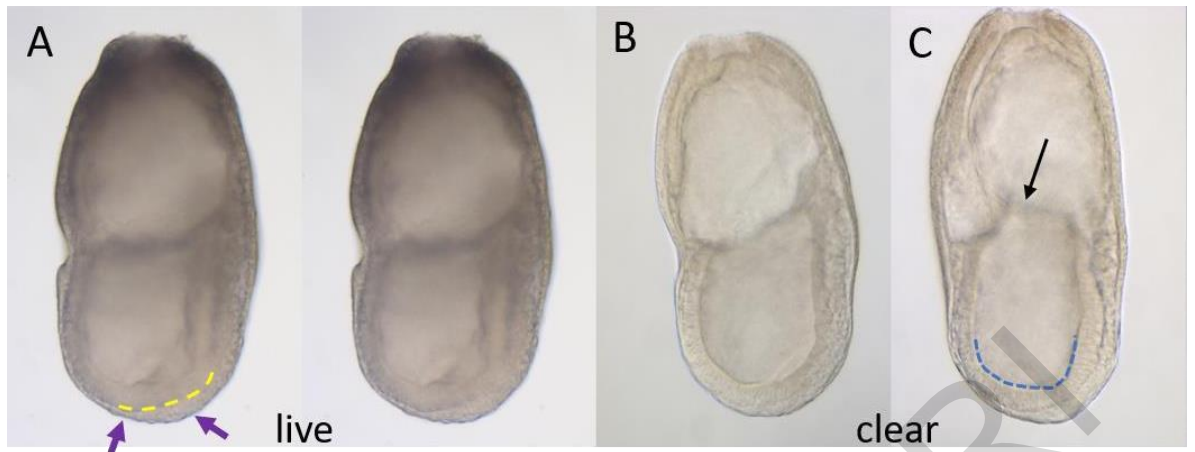


Figure 27: Pre- Headfold - 1 (PH1) stage embryo

Showing the same embryo of (A) Sideways live views. (B) Sideways clear views. (C) Front to backclear views. Thickened lower layer expanded into the posterior half of the distal tip (A - purple arrow). Amnion formation seen by continuous black line (black arrow - C). Inner epiblast of the distal third region when seen from front to back has a U shape (dotted blue line - C). All images are of the same magnification (16 x magnification).

2. 'Pre-headfold-2' (PH2) (n=18)

Compared to the pre-headfold 1, the only noticeable difference observed here was the presence of morphologically distinct head process at the middle region of the distal tip of the egg cylinder evidently by the thickening of the lower layer found beneath the distal tip region (Figure 28). Specifically, the lower layer underneath the midpoint of distal epiblast is as thick or thicker than lower layer found in posterior part of distal tip, while lower layer in anterior part of distal tip remains thinner. The inner surface of the epiblast of the distal-third region when viewed from front to back, had a U shape similar to Pre-Head 1. In addition, there was no presence of a morphological node.



Figure 28: Pre-Headfold – 2 (PH2) stage embryo

Showing the same embryo of (A) Sideways live views. (B) Front to back live views. (C) Sideways clear views. (D) Front to back clear views. Thickened lower layer expanded into the distal tip area showing the same thickness (A and C - purple arrow). Inner epiblast of the distal third region when seen from front to back has a U shape (dotted blue line – B). All images are of the same magnification (16 x magnification).

3. 'Pre-headfold 3' (PH3) (n=29)

Embryos which were classified in this stage were observed to have width exceeding their embryonic region length ($W > L$) for the first time. For the first time there was appearance of an immature morphological node as an indentation of the outer layer of the epiblast at the distal tip area. Specifically, the middle of the distal tip region where the inner surface of lower layer and the outer surface of epiblast curve in a proximal direction. At this stage there was a change of shape of the inner epiblast surface. Specifically, the inner surface of the distal-third region of the epiblast in front-to-back view had the shape of a V. Specifically, it consists of 2 sides and 1 base, with length of sides being much longer than that of base, thereby giving a characteristic V shape. An immature morphological node was still apparent (Figure 29).

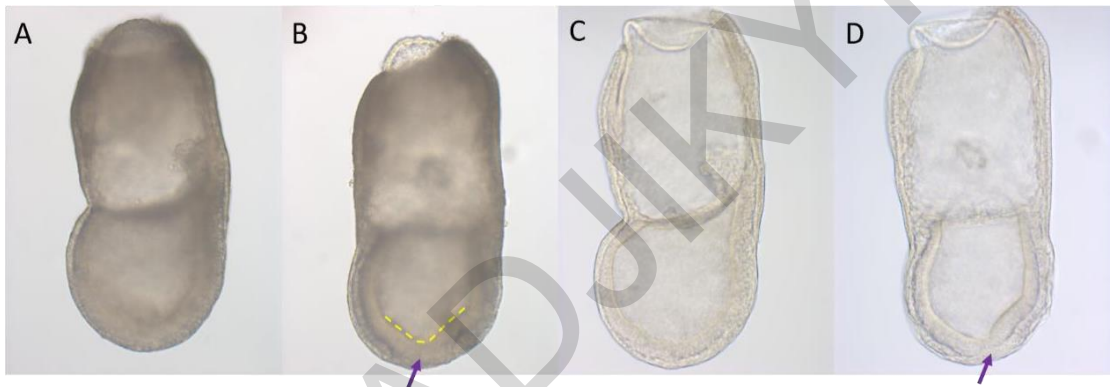


Figure 29: Pre- Headfold – 3 (PH3) stage embryo

Showing the same embryo of (A) Sideways live views. (B) Front to back live views. (C) Sideways clear views. (D) Front to back clear views. Immature morphological node seen at front to back views (B and D – purple arrow). Inner epiblast of the distal third region when seen from front to back has a truncated V shape (dotted yellow line – B). All images are of the same magnification (16 x magnification).

4. 'Pre-headfold - 4' (PH4) (n=20)

Classification of embryos in this stage was dependent on the presence of mature morphological node that was evident when the embryo was seen both from sideways and front to back views. The mature node is characterised by the external surface of node that also becomes curved in a proximal direction (Figure 30). It was also observed that an alteration in the inner surface of the epiblast occurred in the distal-third embryonic region of these embryos that now acquire a truncated V shape.

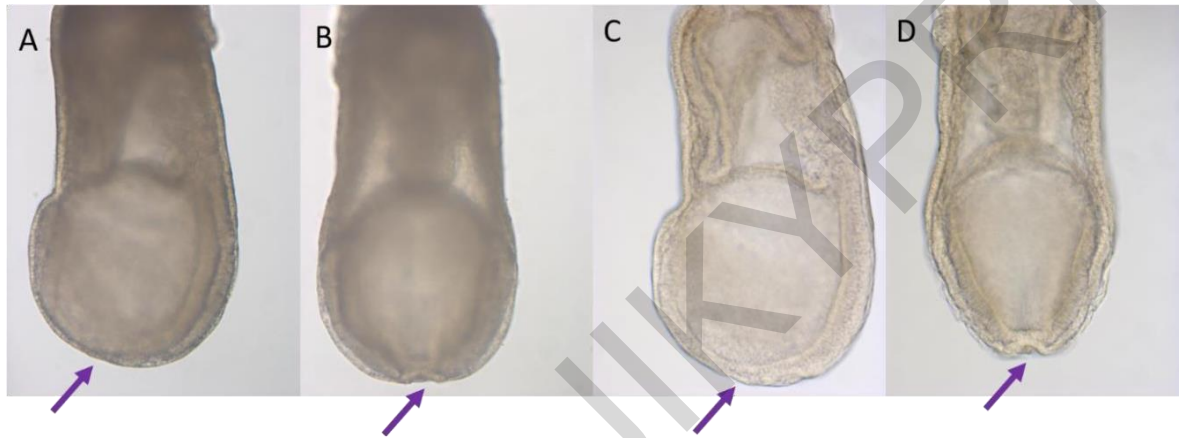


Figure 30: Pre- Headfold - 4 (PH4) stage embryo

Showing the same embryo of (A) Sideways live views. (B) Front to back live views. (C) Sideways clear views. (D) Front to back clear views. Mature morphological node seen at both sideways and front to back views (purple arrow). All images are of the same magnification (16 x magnification).

Headfold stages (2)

1. 'Early - Headfold' (EH) (n=12)

At this stage the embryos are characterised by the curvature of the outer surface of VE of the anterior-proximal fifth epiblast region that is clearly more pronounced than that of the remaining anterior region (Figure 31). When seen from sideways, the anterior-proximal epiblast is no longer close to the anterior endoderm, but has curved so that its inner surface is curved towards the amniotic cavity and there is mesoderm tissue between it and the anterior endoderm region. Mature node can be seen as an indentation both in sideways and front to back views. Another distinctive morphological characteristic of this stage was the presence of a late neural groove. The midline crease extended beyond the midpoint of the PD axis of the embryonic region when the embryos were seen in front-to-back views.



Figure 31: Early-Headfold (EH) stage embryo

Showing the same embryo of (A) Sideways live views. (B) Front to back live views. (C) Sideways clear views. (D) Front to back clear views. Mature morphological node seen at front to back views. Curvature of anterior proximal epiblast (black arrow – A and C). Late neural groove (purple arrow –B and D). All images are of the same magnification (16 x magnification).

2. Late Headfold (LH) (n=9)

The presence of more pronounced headfold with a conspicuously sigmoidal shape of the anterior ectoderm and the appearance of a shallow foregut invagination in the outer layer of the anterior region of the embryo (Figure 32), allowed to distinguish between the embryos of the ‘Late Headfold’ stage from those reported of the ‘Early Headfold’ stage. Foregut invagination is an inwardly directed dent in the outer surface of anterior endoderm.

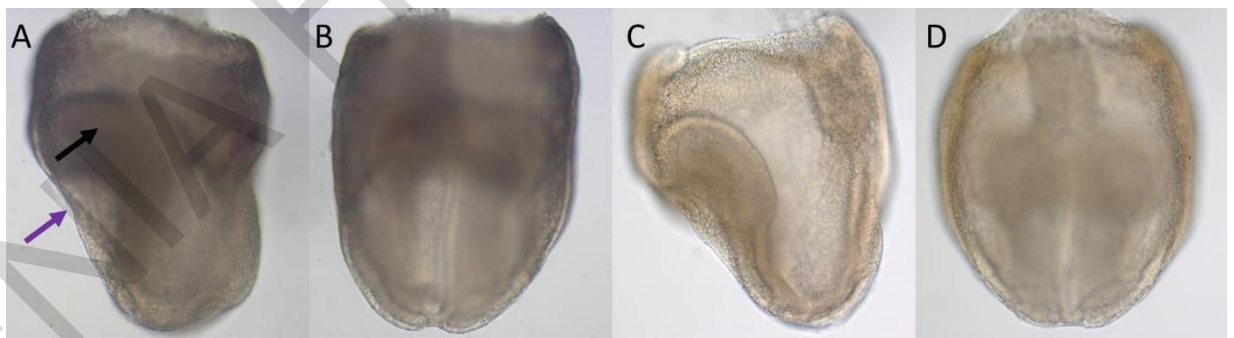


Figure 32: Late-Headfold stage (LH) embryo

Showing the same embryo of (A) Sideways live views. (B) Front to back live views. (C) Sideways clear views. (D) Front to back clear views. Mature morphological node seen at front to back views. Sigmoidal shape of the anterior ectoderm (black arrow – A) and shallow foregut invagination (purple arrow – A). All images are of the same magnification (16 x magnification).

Conclusions Regarding Specific Aim 1:

Using novel combinations of external embryo features, a revised embryo staging for the period from just before gastrulation until the late headfold stage was established here that resulted in subdividing this period into fifteen stages, as opposed to the existing nine stages. This new staging includes the hitherto unidentified stage of gastrulation initiation and, unlike existing staging, subdivides the pre-headfold period into stages without being depended on timing of allantoic bud presence/size as a diagnostic feature since the latter is not applicable across all mouse strains.

XENIA HADJIKYPRIS

4.2 Specific Aim 2, its hypothesis and its results:

Specific Aim 2

The revised staging system described above can be used to better define the spatio-temporal expression of genes that are informative of significant developmental events such as the onset of gastrulation and early ectoderm development.

Hypothesis of specific aim 2

If by using this novel embryonic staging system validated with gene expression achieves to provide information regarding important developmental events, then the aim will be achieved.

Results of specific aim 2

Gene expression profile of Pre - Streak Pre - Headfold and Headfold embryos using the revised embryo staging system

During the process of ectoderm germ layer formation, loss of pluripotency, restriction of potency and consequently acquisition of specificity are necessary and gradual processes. To obtain a more detailed overview of these progressive procedures, the aforementioned staging system was applied to examine the expression patterns of different genes involved in pluripotency, the ectoderm germ layer development and its differentiation into its immediate ectodermal derivatives. The spatiotemporal expression profiles of epiblast related gene Fibroblast Growth Factor 5 (*Fgf5*) and of primitive streak marker T brachyury, T-box transcription factor T (*Bra*) were examined. As this more comprehensive staging system was established for the first time, the primitive streak marker *Bra* was utilized to confirm the extension of PS before amnion closure. Furthermore, early neural gene markers SIX Homeobox 3 (*Six3*), HESX Homeobox 1 (*Hesx1*), *Sox1*, and SRY-Box Transcription Factor 2 (*Sox2*) and *Dlx5* that marks the early non-neural ectoderm derivatives were examined and described below, as observed in each developmental stage identified in the previous section. Examination of each gene in each developmental stage demonstrated the following spatiotemporal patterns and these expression patterns are presented in the Figure panels below.

Fgf5

Fibroblast growth factor 5 (*Fgf5*) is a well-known post implantation epiblast marker and its expression is largely associated with epiblast differentiation and loss of stemness, thus FGF5 is in most cases undetectable in mESCs (Mossahebi-Mohammadi M. et al., 2020). During mouse development, FGF5 is shown to be transiently expressed during different stages (Haub and Goldfarb, 1991). It was also reported that FGF5 is expressed during the

time of cellular commitment to primitive ectoderm but its expression is not found in the ICM (Hayashi et al., 2007) and that autocrine FGF5 may have a role during gastrulation to preserve the mobility of cells to promote all three germ layer emergence (Hebert et al., 1991).

Fgf5 expression pattern was examined using embryos staged according to the above-mentioned staging system. Strong expression of *Fgf5* in the entire epiblast was evident at early streak. Expression in posterior epiblast was progressively downregulated (beginning from posterior-proximal regions) from mid-streak stage onwards until pre-headfold-4 where it was absent from entire posterior epiblast (Figure 33). Specifically, it becomes downregulated (but not extinct) in most proximal anterior epiblast at PH1 and PH2 while at PH3 stage this low-level expression extends to entire anterior epiblast. By PH4 stage it is absent from the entire anterior epiblast except its midpoint (sections of embryo can confirm this expression).

The earliest down-regulation of *Fgf5* expression within anterior epiblast was seen at pre-Headfold-1 in its most proximal region where the level of expression was lower relative to more distal regions (Figure 33). This reduced expression in most proximal anterior epiblast was maintained at pre-Headfold-2 stage, but by pre-headfold-3 most anterior epiblast showed reduced expression (Figure 33). By Pre-headfold-4, *Fgf5* expression was almost undetectable in entire anterior epiblast except low level expression at a midpoint region of anterior epiblast and at the distal tip epiblast. From early headfold onwards, expression of *Fgf5* was undetectable from entire epiblast. These findings reveal in more detail than before the spatiotemporal aspects of *Fgf5* expression in anterior epiblast.

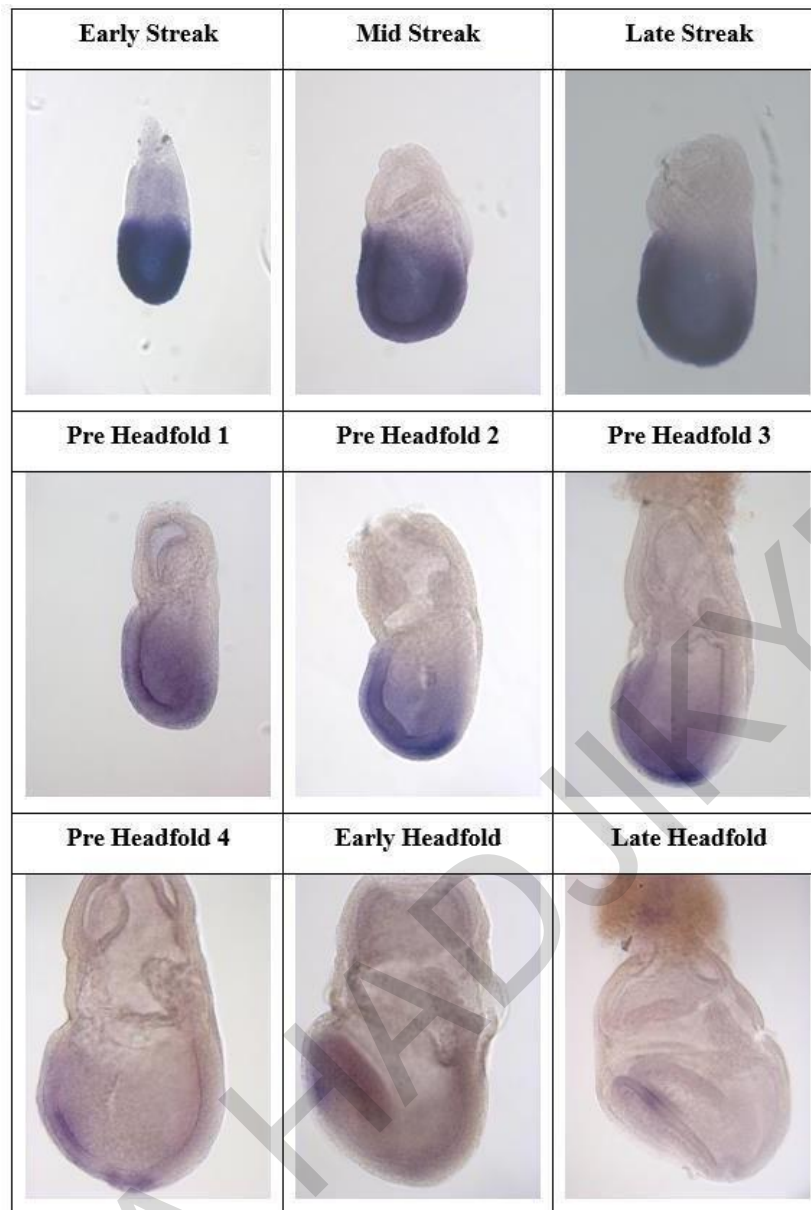


Figure 33: Spatiotemporal expression of *Fgf5* from early streak to late headfold.

Fgf5 was expressed in the entire epiblast and embryonic VE (emVE) (Early Streak) but it was downregulated in the posterior proximal epiblast and emVE (Mid and Late streak). The weaker expression of *Fgf5* extended more distally in the posterior epiblast and emVE (Pre headfold 1 and 2). Pre headfold 3 showed weaker expression in the anterior proximal epiblast and emVE compared to more distal regions. Pre headfold 4 showed undetectable expression in most of the epiblast and emVE, except from the anterior distal and distal epiblast and its sub-adjacent lower layer. *Fgf5* became undetectable by Early Headfold from the entire epiblast and its lower layer but there was a faint signal at the area where the anterior mesenchyme is expected to reside. Same applies for Late Headfold stage. All images are of the same magnification (16x magnification) except Late Headfold (10 x magnification).

Dlx5

Dlx5 is one of the earliest known gene markers of the most anterior (surface) ectoderm, prior to the formation of the definitive neural plate (Yang et al., 1998). During late gastrulation *Dlx5* expression was localized to the anterior neural ridge, that defines the rostral boundary of the neural plate, also extending caudolaterally, indicating the region of the presumptive future neural crest. The *Dlx5* earlier expression in the anterior neural ridge differs from a later phase of expression found in the ventral telencephalon and diencephalon of the mouse embryo (Yang et al., 1998), while this expression pattern appears to be unique for *Dlx5* between other members of the Dlx family.

This gene is a highly conserved transcription factor that, in the embryonic ectoderm of the chick it was shown to promote the formation of border cells (McLarren et al., 2003). Indeed, *Dlx5*^{-/-} embryos displayed late defects in tissues derived from border cells, such as otic and olfactory placodes (Depew et al., 1999; Acampora et al., 1999) that are thought to be derived from the anterior neural ridge. A more recent study demonstrated that anterior proximal ectodermal progenitors that expressed *Dlx5* give rise to surface and buccal ectoderm. Later in development, *Dlx5* was seen to be expressed in the rostral region of the buccal ectoderm, found anteriorly to the oral plate (Cajal et al., 2012).

The establishment of our staging system allowed for the more detailed expression pattern of *Dlx5* around the ectodermal stages. Specifically, *Dlx5* expression was absent from anterior epiblast at early, mid- and late streak embryos and was first seen in anterior-proximal (and anterior-lateral) epiblast from Pre-headfold-1 stage onwards, albeit being at relatively low levels at the latter stage (Figure 34). These results show the low expression at PH1 stage and stronger expression from PH2 stage expanding to the anterior-lateral side from this stage onwards. These results indicate that *Dlx5* is expressed in regions fated to form surface ectoderm earlier than previously thought, from Pre-headfold-1 onwards.



Figure 34: Spatiotemporal expression of *Dlx5* from early streak to late headfold

In Early, Mid and Late streak embryos *Dlx5* was not expressed. Its initial expression was noticed in the anterior-proximal third of Pre – headfold 1. From the stage of Pre headfold 2 its expression domain extended further distally and this expression pattern remained throughout all remaining developmental stages. All images are of the same magnification (16 x magnification) except Late Headfold (10 x magnification).

The neural genes – *Hesx1*, *Six3* and *Sox1*

For the identification of neural cell fates, the examination of neural gene markers was performed. One of these neural gene markers is *Six3* belonging to the subclass of Six/sine Oculis homeobox genes. Its earliest expression marks the anterior-most border region of the neural plate, an area that gives rise to the most anterior neural and non-neural derivatives (Oliver et al., 1995). *Six3* was again shown to be involved in the specification of the anterior neuroectoderm by Wnt1 repression achieving in this way regionalization of the vertebrate forebrain (Lagutin O. et al., 2003).

Furthermore, *Hesx1*, a homeobox gene belonging to the paired-like class, is initially detected in a minor group of cells confined in the AVE during PS elongation. One day later and when the PS is fully extended, *Hesx1*, is expressed in the prospective neuroectoderm (Thomas and Beddington, 1996), the presumptive forebrain ectoderm and also in the anterior axial mesendoderm (AME) underlying it. Later in development, *Hesx1* is persistently expressed in the anterior neural ectoderm, also detected in the oral ectoderm as well as the anterior foregut. By E9.5 *Hesx1* expression is restricted to the ventral diencephalon (Martinez-Barbera et al., 2000). This homeobox gene was seen to act as an essential repressor required within the anterior neural plate for proper forebrain development in mouse and humans (Andoniadou C. et al., 2007). This study demonstrated that in the absence of *Hesx1*, the posteriorization of the mouse anterior forebrain (AFB) is observed during mouse development through the ectopic activation of the Wnt/-catenin signalling in the *Hesx1* expression domain.

Although *Six3* and *Hesx1* are widely accepted as early anterior neural markers (Carlin et al., 2012, Martinez-Barbera et al., 2000), they are not used as entire neural plate markers, but are seen to also mark some of the non-neural ectoderm derivatives (Cajal et al., 2012). Interestingly, the onset of their expression has not been examined in detail in relation to the latest mouse staging of Kaufman's Atlas of Mouse Development Supplement with Coronal sections, 2015. Here, their expression profiles of both genes will be examined in relation to the development of the ectoderm germ layer.

Hesx1 expression is undetectable in the early embryonic stages, specifically the Mid and Late Streak stages (Figure 35). Similarly, to the findings of other studies, its initial expression is detected in the AVE of the Pre – Headfold 1 and Pre – Headfold 2 stages. AVE expression is later lost but it is then detected in the anterior proximal half of the epiblast of the Pre-Headfold 3. This expression then persists in all of the following embryonic stages examined here.

Six3 expression, similarly to the *Hesx1* expression described above, was undetectable during Early, Mid, Late Streak and Pre Headfold-1 stages (Figure 36). Its initial

expression is detected in the AME of the Pre Headfold-2 as well as throughout the anterior epiblast of Pre – Headfold 2 although at low levels. Upregulation of its expression in anterior-proximal epiblast and downregulation in anterior-distal was detected at Pre – Headfold 3, while absence of expression was also detected in anterior-distal of Pre – Headfold 4 stage onwards.

Sox1 is a member of the Sox-B1 group of transcriptional regulators. *Sox1* has an essential role in neural cell fate determination and differentiation. Murine *Sox1* is firstly expressed in the anterior neural plate ectoderm at the late headfold stage of development. Overexpression of *Sox1* was seen to induce the expression of neuronal gene markers in cultured cells (Peny L. H., 1998, Kan L., 2004), while its importance for neuronal maturation and maintenance of neural pre-cursors in the ventricular zone was also reported (Ekonomou A., 2005). During embryogenesis, chick *Sox1* was shown to be expressed during neural fold closure, detected in the brain and spinal cord tissues (Uchikawa M., 1999). Xenopus *Sox1* expression was reported in the CNS and the embryonic optic vesicle, shown to be induced by BMP signalling inhibition known for its neural inducing activity (Nitta KR., 2006).

In this current study it is demonstrated that the initial expression of *Sox1* is detected in the anterior ectoderm of the Early Headfold stage (Figure 37). Its expression persists in the anterior neural plate ectoderm seen in the Late Headfold stage.



Figure 35: Spatiotemporal expression of *Hesx1* from early streak to late headfold

Early Streak, Mid and Late Streak embryos no expression of *Hesx1* is detected. *Hesx1* was expressed in the AVE of the Pre Headfold-1 and Pre-Headfold 2 stage embryos. Expression of *Hesx1* was detected in the anterior proximal half of the epiblast (Pre headfold 3). More advanced stages show anterior proximal epiblast expression of this gene. All images are of the same magnification (16 x magnification) except Late Headfold (10 x magnification).

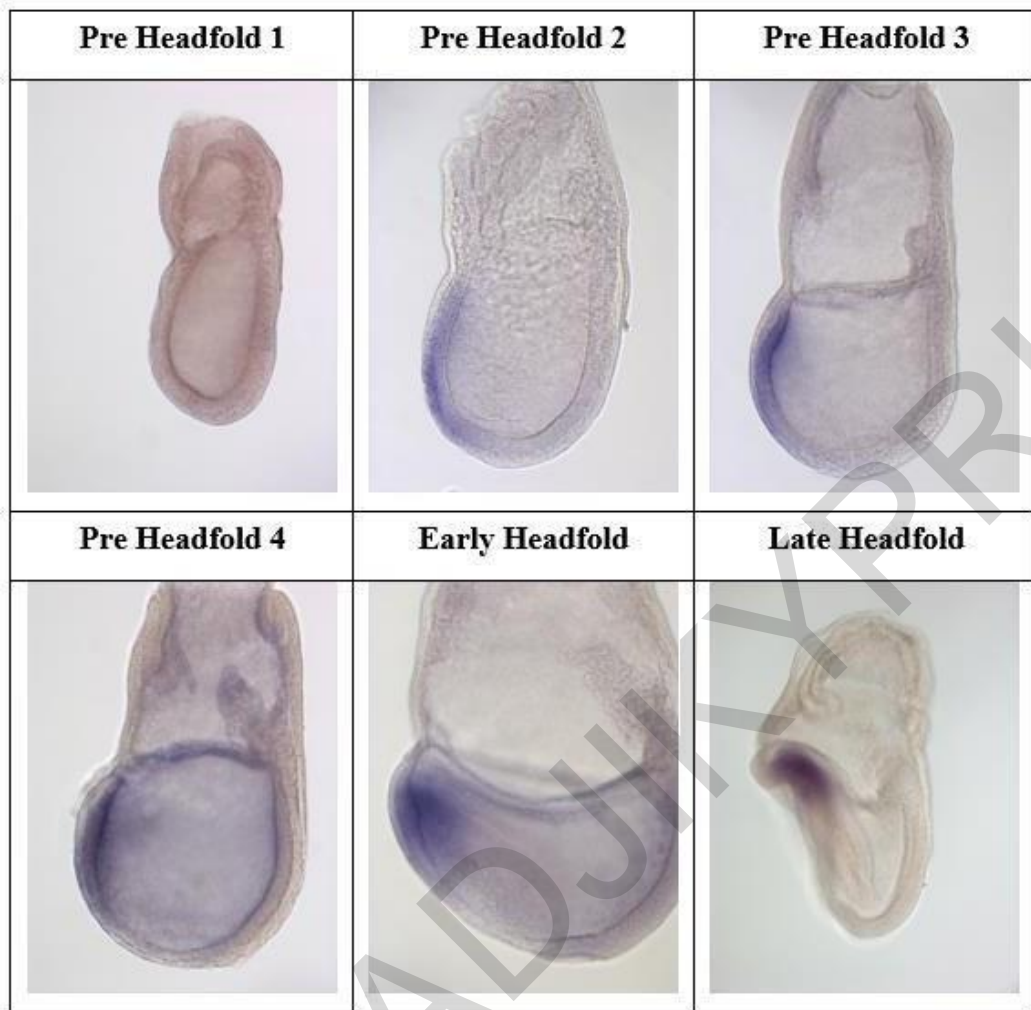


Figure 36: Spatiotemporal expression of *Six3* from pre-headfold-1 to late headfold

Early Streak, Mid and Late streak (data not shown) and Pre Headfold-1 showed no expression. Pre Headfold-2 shows expression of *Six3* in the AME area as well as low expression at the anterior proximal epiblast. In all remaining stages *Six3* remained localized at the anterior proximal area of the epiblast. All images are of the same magnification (16 x magnification) except Late Headfold (10x magnification).

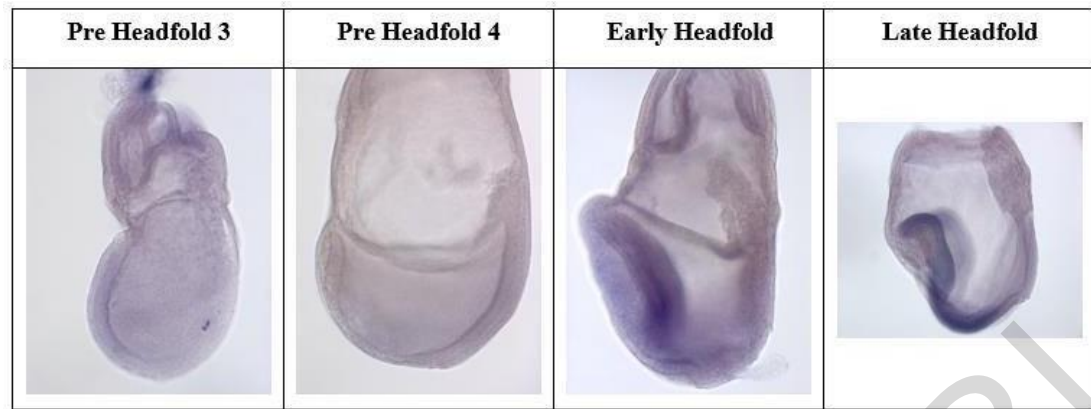


Figure 37: Spatiotemporal expression of *Sox1* from pre-headfold-3 to late headfold

No expression of *Sox1* was detected up to Pre headfold 4 stage. The first sign of *Sox1* expression was detected in the anterior side of the Early Headfold embryo. It remained localized at the anterior side of the epiblast and In Late Headfold it was expressed in the entire future nervous system. All images are of the same magnification (10 x magnification 1,6 optovar) except Late Headfold (10 x magnification 1,0 optovar).

Bra

The first of the T-Box family of genes is *Brachyury* (Showell C. et al., 2004; Herrmann BG. et al., 1990). *Brachyury* first described by in 1927 (Showell C. et al., 2004), has been identified in various multicellular organisms, such as zebrafish, *Xenopus*, mouse, human, and others (Herrmann BG. et al., 1990; Kispert A. et al., 1994; Di Gregorio A. 2017), and was shown to be required for correct posterior mesoderm formation, axial development as well as notochord differentiation, appropriate cell movements during gastrulation, tail outgrowth and establishment of proper left–right asymmetry (Herrmann BG. et al., 1990; Kispert A. et al., 1994; Di Gregorio A. 2017 Morley RH. et al., 2009). *Bra* is also a widely used primitive streak marker (Thomas and Beddington, 1996; Thomas et al., 1998), therefore, it was used to evaluate the extension of PS as well as the progression of AME progenitors that emanate from the head process that marks the developing notochord (Rivera-Perez and Magnuson, 2005, Wilkinson et al., 1990).

The employment of *Bra* expression in our staging system aimed to obtain a better molecular definition of this staging system and to confirm the classification of these embryonic stages. The onset of *Bra* expression in epiblast prior to mesoderm formation has recently been shown to signify the beginning of EMT that is the first step of primitive streak initiation (Morgani and Hadjantonakis 2020), although there are no well-defined morphological criteria in live embryos to distinguish this stage, identify the anterior end of the streak and to estimate the extent of *Bra*-positive streak elongation prior to mesoderm formation. Here, based on our more comprehensive staging system we show that *Bra* expression commences at the NS stage prior to mesoderm formation (Figure 17) and thereafter the extent of *Bra* expression can be used to identify more advanced developmental stages.

Bra is detected in the lower layer (head process) of Late Streak 1 stage (Figure 21). The earliest time when the primitive streak reaches its full length evident by the expression of *Bra* is at the Pre Headfold 2 stage, also seen at Pre Headfold 3. *Bra* expression also reveals that the anterior end of posterior AME (anterior head process) does not extend beyond the anterior half of distal tip at Pre Headfold 1 and 2 stages, but extends beyond this by Pre Headfold 3, reaches 50% of proximodistal length of embryonic region by Pre Headfold 4 and remains the same at Early headfold stage. The posterior AME reaches its full extent by Late Headfold as evident by *Bra* expression.

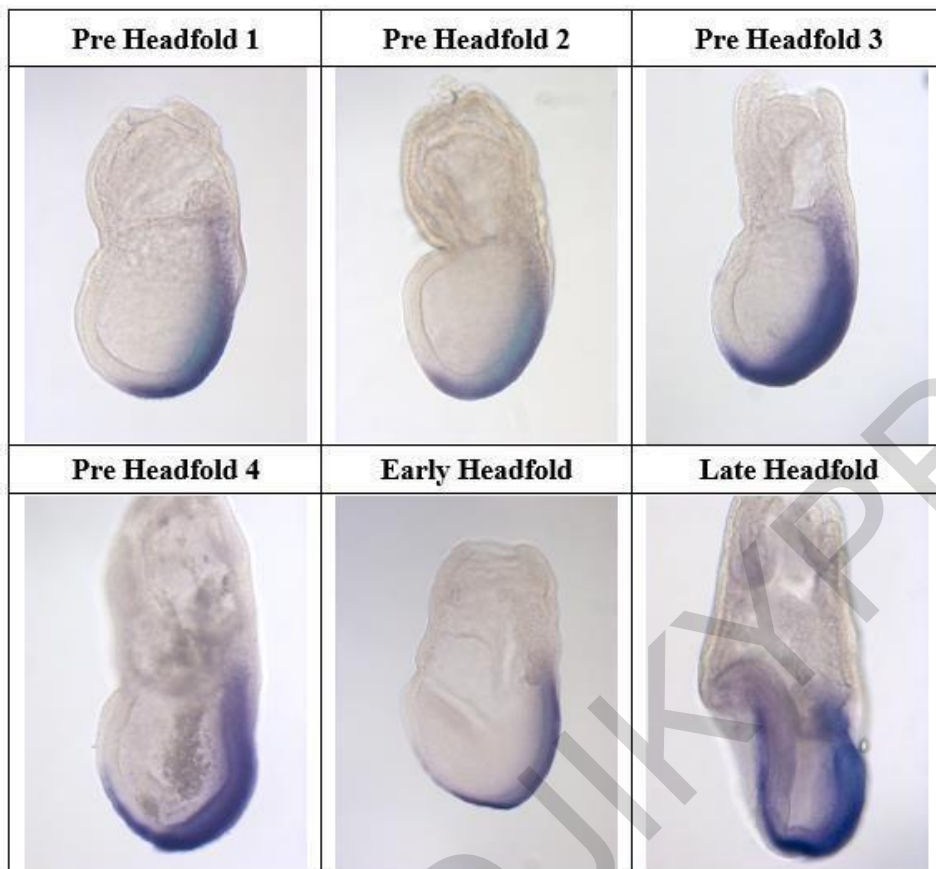


Figure 38: Spatiotemporal expression of *Bra* from pre-headfold-1 to late headfold

In Pre Headfold-1 *Bra* expression reached the 90% of the length of the embryonic PD axis and extended to the outermost lower layer in the distal tip area. In Pre Headfold-2 stage the *Bra* expression reached the 100% of the length of the embryonic PD axis while the lower layer expression had extended anteriorly up to approximately 25% of the PD length of the embryonic region. From Pre Headfold-4 to Late Headfold stage *Bra* lower layer expression extended further and reached between 25% and 50% of the PD length of the embryonic region, respectively. All images are of the same magnification (16 x magnification) except Early and Late Headfold (10 x magnification).

Sox2

Sox genes are expressed throughout embryogenesis encoding a subclass of high mobility group of proteins that drive cell fate decisions by acting as chromatin modulators and transcription factors (Pevny LH., 1997; Scaffidi P., 2001). *Sox2* that belongs to this family, is firstly detected in the innercell mass (ICM) of the mouse blastocyst (Avilion AA. et al., 2003) and later on in primitive ectoderm, extraembryonic ectoderm (Avilion AA. et al., 2003) as well as the developing nervous system (Collignon J., 1996).

Sox2 expression at around Pre and Early streak stages persists throughout the epiblast, but is later seen to become restricted to the presumptive neuroectoderm in the anterior epiblast, while it is absent from the posterior, including cells which ingress through the primitive streak (Avilion AA. et al., 2003). By E. 9.5, *Sox2* was observed throughout the brain, the neural tube, sensory placodes,

Our results constructing the spatiotemporal map of this gene's expression demonstrated that *Sox2*, even though it was expressed in the anterior epiblast of earlier stages, it then seen to be gradually downregulated in the anterior proximal epiblast (Figure 39). Its absence coincided with the expression of *Bra* marking the length of the PS. Indeed, its posterior limit of epiblast expression appears to coincide with anterior limit of *Bra* expression at all stages (anterior end of streak). *Sox2* expression reaches the midpoint of distal tip at Pre Headfold 2 stage which coincides with full streaklength at this stage. Therefore, the expression pattern of *Sox2* revealed that the extension of the PS reached its full length at Pre Headfold-2 stage as demonstrated also by the *Bra* expression results at this stage. Pre Headfold-4 stage *Sox2* revealed another expression domain. Specifically, *Sox2* was expressed in the posterior distal epiblast (Figure 39). This expression is important as it is indicative of neuromesodermal precursors of spinal neural plate.

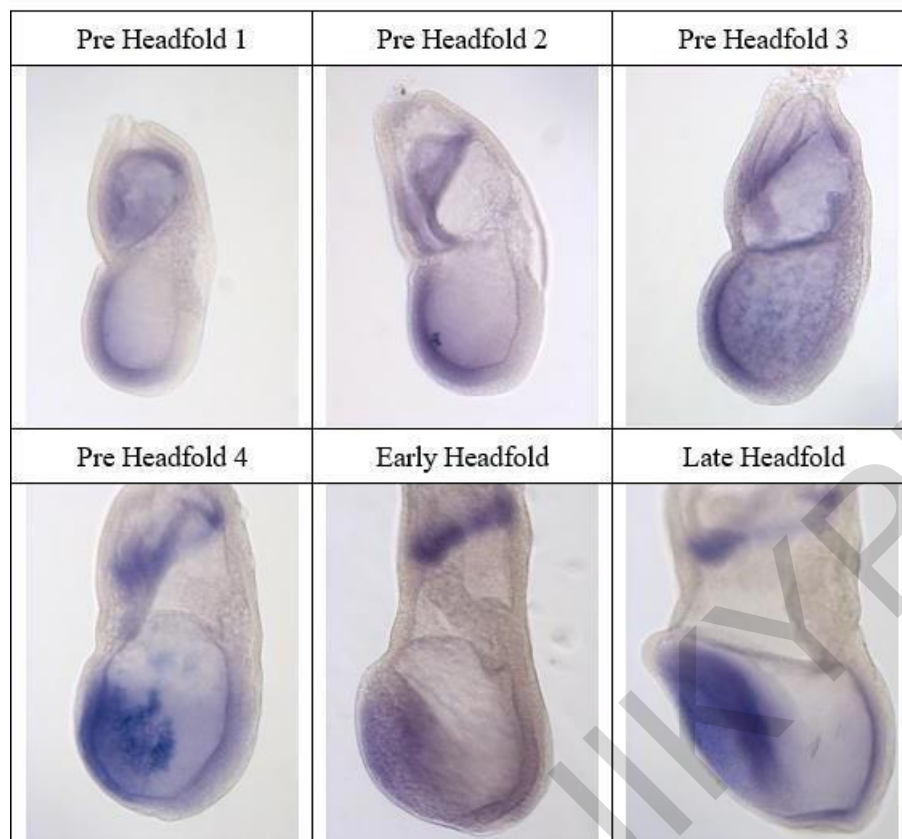


Figure 39: Spatiotemporal expression of *Sox2* from pre-headfold-1 to Late Headfold

Pre Headfold-1. Expression of *Sox2* was seen in the anterior epiblast extending further from the distal tip epiblast and in the chorionic ectoderm. Pre – Headfold 2 stage show expression in the anterior epiblast that reaches the midpoint of the distal tip area but does not extend more. From Pre – Headfold4 stage onwards *Sox2* was also detected in the posterior epiblast. All images are of the same magnification (16 x magnification) except Late Headfold (10 x magnification).

The utilisation of *Bra* expression in our newly established mouse staging system aimed to contribute to the molecular definition of this staging system and to confirm the classification of the embryonic stages. *Bra* as mentioned above is a widely used primitive streak marker, therefore, it was used to evaluate the presence, the extension of the PS in the developing embryos as well as the progression of AME progenitors that emanate from the head process marking the developing notochord (Rivera-Perez and Magnuson, 2005, Wilkinson et al., 1990). This gene allowed the classification of stages prior and during the initial PS formation, the emergence of mesoderm together with the segregation of stages of before and after PS full extension.

The expression profiles of *Fgf5* supported the collection of evidence informative of the appearance of the ectoderm germ layer in the anterior epiblast of the mouse embryo. Since the stage of ectoderm germ layer first formation remains uncertain, the employment of this comprehensive staging system, aimed to determine the exact stage and location at which

loss of *Fgf5* expression is originally seen relative to the expression of the aforementioned gene at the still pluripotent epiblast of the distal tip region, as already suggested (Osorno et al., 2012).

The non-neural ectoderm *Dlx5* gene expression was initially observed at the anterior most proximalside of the epiblast at the Late streak stage and remained up to the Late Headfold stage, expanding further distally to finally occupy the anterior half epiblast. The emergence of *Dlx5* occurring at the Late streak stage, an earlier time than previously thought, coincides with *Fgf5* expression in the same epiblast region, with this co expression persisting also during the next developmental phase the Pre Headfold-1. The initial reduction of *Fgf5* expression was observed at the Pre Headfold-2 stage. Taken together, the initial expression and downregulation of these genes could prove informative of the molecular signature of the emergence of the ectoderm germ layer.

The results obtained in this study regarding the expression profiles of the different genes marking neural progenitors, could be explanatory as well as suggestive about the end of ectoderm germ layerstate, since their onset could signify the transformation of this germ layer into its derivatives.

Conclusions Regarding Specific Aim 2:

The validation of the new refined staging system using gene expression suggested these findings:

(a) that *Fgf5* (a pluripotency related gene) and *Dlx5* (an early surface ectoderm marker) are co-expressed in anterior-proximal epiblast during a transient period, from PH1 to PH3 (at PH1 reduced *Fgf5*, very low levels of *Dlx5*; at PH2, reduced *Fgf5*, strong *Dlx5* expression; at PH3, same as PH2; from PH4 onwards *Fgf5* is lost from anterior-proximal epiblast whilst *Dlx5* remains strongly expressed).

(b) that neural plate formation (at least anterior neural plate) may begin at PH3 since earliest expression of *Hesx1* in epiblast and earliest upregulation of *Six3* occur at PH3 in anterior-proximal epiblast (*Six3* and *Hesx1* are the earliest known anterior neural markers). Since PH3 stage is the earliest when inner surface of distal epiblast changes from U to V/truncated V, this suggests that this could be a morphological sign of neural plate.

(c) that PH2 is the only stage where strong *Dlx5* expression is coexpressed with low *Fgf5* expression prior to onset of early neural genes *Six3/Hesx1/Sox1*.

(d) that *Fgf5* in anterior epiblast first becomes reduced (but still detectable) in its proximal region at PH1 stage and remains so up to PH3 whereas by PH4 becomes undetectable. This suggests that pluripotency of anterior-proximal epiblast is lost by PH4 and may occur earlier, some time from PH1 to PH3.

(e) that *Sox2* in posterior epiblast becomes re-established at PH4, suggesting that ectomesodermal progenitors appear at this stage.

(f) anterior head process (posterior AME) based on *Bra* expression: appears during LS-2 and PH1 stages, remains within anterior half of distal tip at PH2, extends beyond anterior distal tip at PH3, reaches the mid-point of anterior embryonic region at PH4 and reaches its full length at late headfold.

4.3 Specific Aim 3 (A and B), its hypothesis and its results:

Specific Aim 3A

To establish a new in vitro pluripotency assay for testing whether a mouse postimplantation tissue is pluripotent or not, that is simpler than the only existing in vitro pluripotency assay (ability of tested tissue to produce epiblast stem cell lines).

Methodology of Specific Aim 3A

This involved explant culture of postimplantation tissues that are known to be pluripotent (positive control tissue) or non-pluripotent (negative control tissue) under conditions previously shown to maintain the pluripotency of cultured epiblast stem cells, the in vitro analogues of the pluripotent postimplantation/pre-gastrulation epiblast. These culture conditions (named here 'pluripotency conditions') were used on fetal bovine serum (FBS)-coated culture surfaces in chemically defined liquid media (N2/B27) supplemented with Activin A, Fgf2 and the Wnt signalling small molecule inhibitor XAV939. These culture conditions were previously used allowing the propagation of EpiSCs as a homogeneous population (Sumi et al., 2013). Furthermore, WNT Inhibition was suggested to maintain EpiSCs in a Pregastrula epiblast Stage (Kurek et al., 2015).

At the end of culture, the phenotype of the explant outgrowths was examined using live morphology and gene expression [RNA in situ hybridization (ISH) and real time quantitative PCR (RTq-PCR)]. The positive control tissue used was the pluripotent anterior epiblast from E6.5 pre-streak embryos and the negative control tissue was the non-pluripotent anterior epiblast from late headfold embryos (Li et al., 2013).

Hypotheses of specific aim 3A

The pluripotency assay was considered established if the following two conditions were met.

1. The outgrowth of positive control tissue (the pluripotent E6.5 pre-streak anterior epiblast) after culture for a specific amount of time in the above-mentioned pluripotency conditions, should have alive morphology and gene expression profile that resembles that of epiblast stem cells cultured in pluripotency conditions. That is, compact and flat outgrowths consisting of small cells with indistinct intercellular borders under live phase contrast microscopy, homogeneous expression of the pluripotency-related genes *Oct4* and *Fgf5* throughout the outgrowth and absence of gene expression of markers of differentiation towards early derivatives of all three germ layers (such as *Sox1*, *K8* and *Bra* for neural, surface ectoderm and mesendoderm differentiation, respectively) (Sumi et al

2013; Kurek et al., 2015).

2. The outgrowth of negative control tissue (the non-pluripotent late headfold anterior epiblast) after culture in pluripotency conditions for the same amount of time as positive control explants, should have a live morphology and gene expression profile that are different to those derived from positive control explants. Specifically, outgrowths should: (a) consist of cells that lack indistinct intercellular borders and/or loosely arranged cells under live phase contrast microscopy, (b) display no expression or patchy expression of the pluripotency-related genes *Oct4* and *Fgf5* and (c) express gene markers of early neural (e.g., *Sox1*) and surface ectoderm (e.g., *K8*) differentiation, since late headfold anterior epiblast has restricted its potency towards only neural and surface ectoderm fates (Li et al., 2013).

Brief background to specific aim 3A

Although the pluripotency of mouse epiblast stem cells (EpiSCs) is maintained in vitro when they are cultured on FBS-coated surfaces in the serum-free/chemically defined liquid N2/B27 supplemented with Activin A, Fgf2 and XAV939 (Sumi et al., 2013), whether this is applicable to native pluripotent epiblast tissue has not been directly investigated and was addressed here for the purposes of establishing a new pluripotency assay for postimplantation tissues. A brief introduction to these culture conditions is given here.

The canonical Wnt/b-catenin signalling pathway was not only shown to have pivotal roles in early embryogenesis but also in stem cell renewal, homeostasis and tumorigenesis (Clevers H, 2006). Through genetic studies the canonical Wnt/b-catenin signalling activation was shown to be essential for pluripotent epiblast differentiation towards mesoderm fates in the gastrulating mouse embryos (Liu P. et al. 1999, Huelsken J. et al. 2000). Mouse EpiSCs, are derived from the epiblast of E.5.5 to E7.5 mouse embryos, exhibit characteristics of pluripotency and require Nodal-Activin and fibroblast growth factor (Fgf) signalling to maintain this character (Sumi T. et al. 2013). When injected into blastocysts, EpiSCs show little or no ability to give rise to chimeras, suggesting that they represent a state of primed pluripotency, a developmental state later than the naïve pluripotent ground state of mouse Embryonic Stem cells (ESCs).

Studies that investigated the key role of canonical Wnt signalling in mouse EpiSCs by using small-molecule inhibitors of the signalling and deletion of the b-catenin gene, established that the canonical Wnt signalling blocks the self-renewal of primed pluripotent EpiSCs and promotes mesoderm differentiation in both EpiSCs and postimplantation mouse embryos (Sumi T. et al 2013; Kurek et al., 2015). More specifically it was shown

that when EpiSCs were cultured in chemically defined liquid media, supplemented with Activin A, Fgf2 and the small molecule inhibitor XAV939, showed uniform expression of *Oct4*, *Sox2*, and *Nanog* together with the disappearance of *Bra* expression. Suppression of other mesoderm and endoderm markers was also observed. Expression of *Fgf5* and *Fgf8*, characteristic of the epiblast state, was also present in a more homogeneous pattern in XAV939-treated EpiSC colonies than in control ones. These studies also showed that when these XAV939-treated EpiSCs were transplanted to generate chimeric embryos, these showed the developmental potential to form all three embryonic germ layer derivatives and the ability to normally contribute to

the developing mouse embryo even after extended culture in the presence of Wnt signalling inhibitor. The notion that canonical Wnt signalling induces differentiation, impeding the maintenance of the undifferentiated epiblast state was also confirmed in the postimplantation embryo when whole embryo culture was performed confirming the EpiSCs results. It was suggested that canonical Wnt signalling determines EpiSC heterogeneity by the induction of mesoderm and endoderm, and that the blockage of such signalling promotes the pluripotency of EpiSCs (Sumi T. et al 2013; Kurek et al., 2015). Another study that used small molecule inhibitors of Wnt signalling to investigate the role of such signalling revealed that blocking of nuclear localization of β -CATENIN significantly resulted in efficiency enhancement of mouse EpiSCs conversion to naive-like primed pluripotent stem cells (PSCs) in response to LIF (Murayama H. et al. 2015).

Results of specific aim 3A

The establishment new *in vitro* pluripotency assay that is simpler and faster than the existing one

Anterior epiblast fragments were isolated from the pluripotent E6.5 pre-streak and the non-pluripotent late headfold stages and cultured as explants up to 48h under pluripotency conditions [onFBS-coated surfaces in serum-free liquid media (N2/B27) supplemented with Activin A, Fgf2 and XAV939]. Comparing the outgrowths derived from these pluripotent and non-pluripotent explants in terms of live morphology (Figure 40), gene expression using ISH (Figure 41) and quantitative gene expression using RTq-PCR (Figures 42A and 42B), suggests that culture under these conditions for 48h constitutes a new pluripotency assay. The reasons for this are as follows.

First, the pluripotency of the initially pluripotent E6.5 pre-streak anterior epiblast is maintained after culture for 48h under these conditions, validating its pluripotency status since if it was not initially pluripotent, it should not have a pluripotent phenotype after culture. This is because: (i) Live morphology of these outgrowths (n=18/18) resembles that of epiblast stem cell colonies (Brons I.G. et al. 2007; Sumi T. et al 2013; Kurek et al., 2015) in that they are flat compact outgrowths consisting of small cells with largely indistinct intercellular borders (Figure 40). (ii) The pluripotency-related genes *Oct4* and *Fgf5* are expressed throughout these outgrowths (n=4/4) (Figure 41), as is the case for undifferentiated epiblast stem cells colonies (Brons I.G. et al. 2007; Sumi T. et al 2013; Kurek et al., 2015) but early differentiation markers such as *Sox1* (neural) and *K8* (surface ectoderm) (Li et al., 2013) are undetectable (n=3/3) (n=3/3) (Figure 41). (iii) This pluripotent gene expression profile was validated using RTq-PCR (n=6 biological replicas) (Figure 42A). For RTq-PCR, each biological replica consisted of three explant outgrowths pooled together and each gene quantification measurement was done twice in two separate experiments.

Second, culture under these conditions for 48h of the initially non-pluripotent late headfold anterior epiblast, did not lead to outgrowths with pluripotent phenotype, validating its non-pluripotent status since any initially non-pluripotent tissue should not be expected to revert back to a pluripotent state after culture. This is because: (i) Live morphology of these outgrowths (n=2/2)

is different from that of epiblast stem cell colonies (Brons I.G. et al. 2007; Sumi T. et al 2013; Kureket al., 2015) and from that of outgrowths derived from E6.5 pre-streak anterior epiblast: the cells of these outgrowths are loosely packed, especially at the periphery and its cells appear to be larger (Figure 40). (ii) The pluripotency-related genes *Oct4* and *Fgf5* are not expressed in these outgrowths (n=3/3) (Figure 41), as is the case for undifferentiated epiblast stem cells colonies (Brons I.G. et al. 2007; Sumi T. et al 2013; Kurek et al., 2015), but early differentiation markers such as *Sox1* (neural) and *K8* (surface ectoderm) (Li et al., 2013) are expressed (n=2/2) (n=2/2) (Figure 41), consistent with late headfold anterior epiblast being comprised of two regions, one committed to neural and one committed to surface ectoderm fates (Li et al., 2013). (iii) This non-pluripotent, neurally and surface ectoderm-committed gene expression profile was validated using RTq-PCR (n=6 biological replicas, as described above), (Figure 42B).

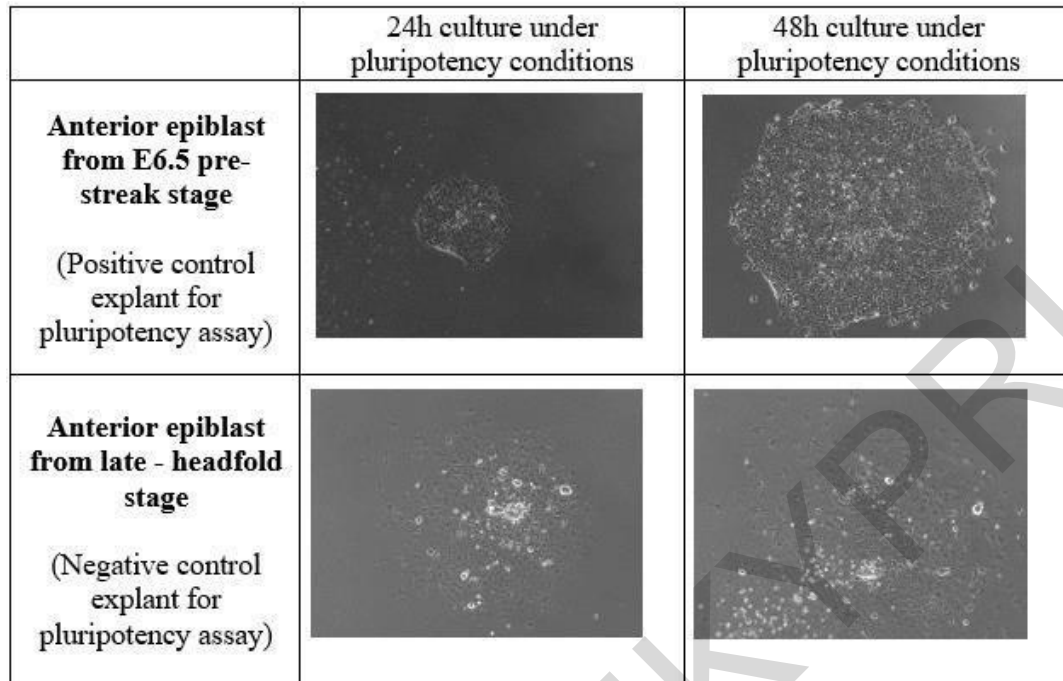


Figure 40: Establishment of pluripotency assay

Live morphology of outgrowths of anterior epiblast explants from either E6.5 pre-streak (pluripotent epiblast) or late headfold (non-pluripotent epiblast committed towards neural and surface ectoderm fates) cultured up to 48h under pluripotency conditions (N2/B27, Activin-A, Fgf2 and XAV939 on FBS). Note the compact nature and the indistinct cell-to-cell borders of the cells from outgrowths derived from pre-streak explants (top row images) (n = 18/18), consistent with pluripotent morphology. In contrast the cells making up the outgrowths from late headfold embryos are loosely packed (especially at the periphery) and have a different morphology (top row images) (n = 3/3), consistent with non-pluripotent morphology. All panels are at 16x magnification.

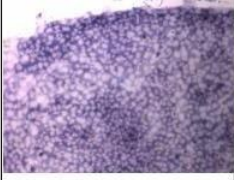
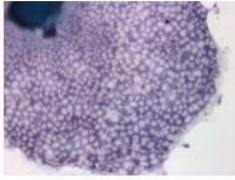

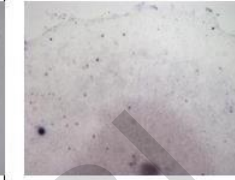
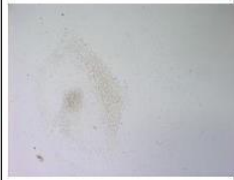

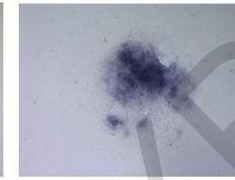

48h culture under pluripotency conditions followed by assessment of expression of below genes				
	<i>Fgf5</i>	<i>Oct4</i>	<i>Sox1</i>	<i>K8</i>
Anterior epiblast of E6.5 (positive control)				
Anterior epiblast of late headfold (negative control)				

Figure 41: Establishment of pluripotency assay RNA in situ hybridization.

Gene expression analysis of outgrowths of anterior epiblast explants from either E6.5 pre-streak (pluripotent epiblast) or late headfold (non-pluripotent epiblast committed towards neural and surface ectoderm fates) cultured for 48h under pluripotency conditions (N2/B27, Activin-A, Fgf2 and XAV939 on FBS). Note that pluripotency-related genes *Oct4* and *Fgf5* are expressed throughout the outgrowths derived from pre-streak/pluripotent explants (first two images in top row) (n = 4/4), but are undetectable in the outgrowths of late headfold/non-pluripotent explants (first two images in bottom row) (n=2/2). Moreover, the early pan-neural marker *Sox1* and the early surface ectoderm marker *K8* are not expressed in pre-streak/pluripotent explant outgrowths (last two images in top row) (n = 3/3), whereas they are expressed in those derived from late headfold/non-pluripotent explants (last two images in bottom row) (n = 2/2). All panels are at 25x magnification.

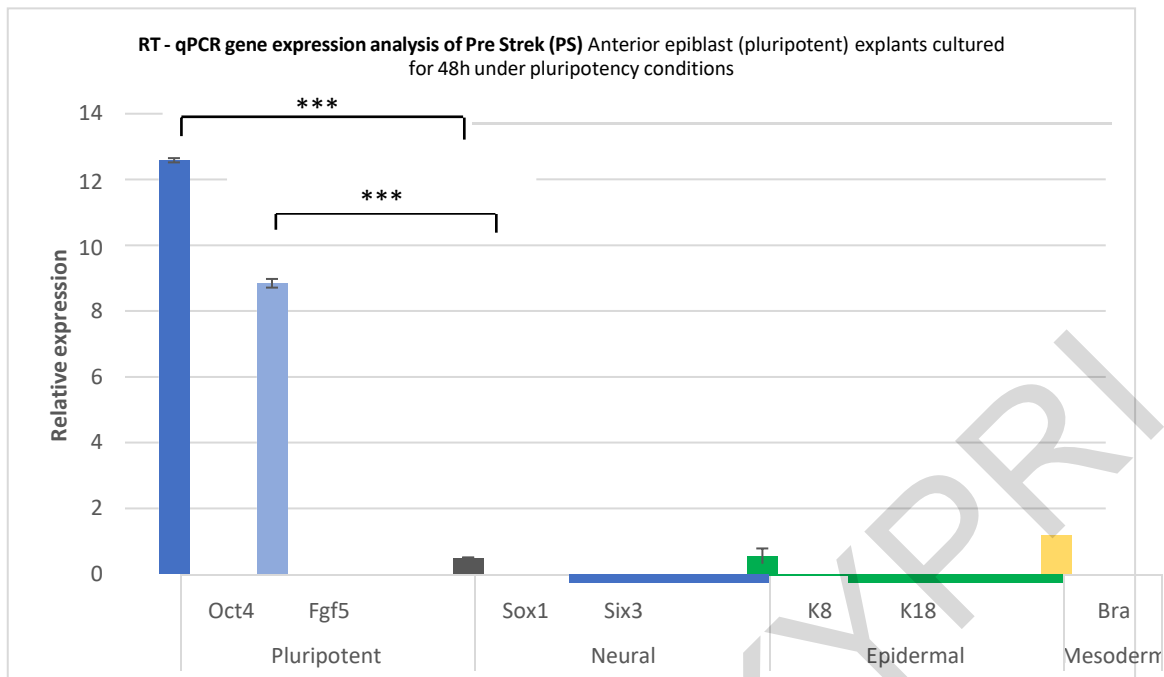


Figure 42A: RT-qPCR analysis of marker gene expression of anterior explants cultured in pluripotency assay conditions of anterior epiblast explants from E6.5 pre-streak embryos (pluripotent explants) after culture for 48h in pluripotency conditions

Gene expression levels are relative to the housekeeping gene beta-actin. Note that, as expected, the pluripotency-related genes *Oct4* and *Fgf5* are highly expressed (statistically elevated compared to all other gene expression levels; *P < 0.05). In contrast, early markers for differentiation towards neural (*Sox1*, *Six3*), surface ectoderm (*K8*, *K18*) or mesoderm (*Bra*) fates, are expressed at extremely low levels. n=6 biological replicates. Error bars represent standard deviation.

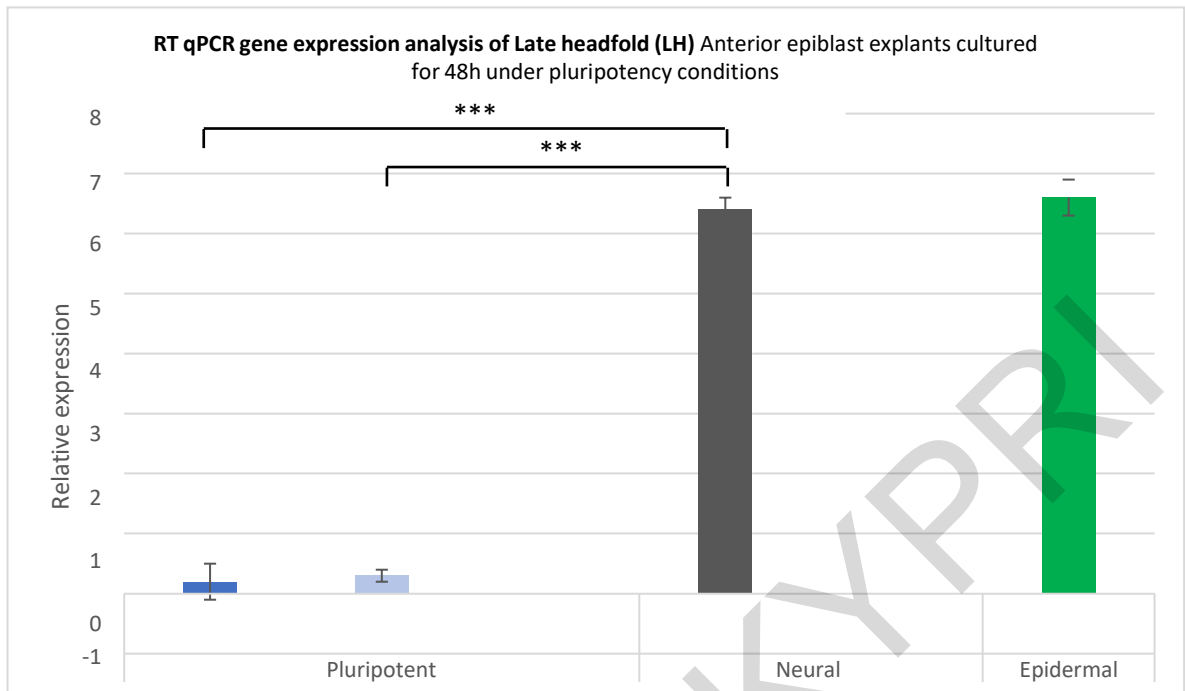


Figure 42B: RT-qPCR analysis of marker gene expression of anterior epiblast explants from late headfold embryos (non-pluripotent explants) after culture for 48h in pluripotency conditions. Gene expression levels are relative to the housekeeping gene beta-actin

Note that, as expected, the pluripotency-related genes *Oct4* and *Fgf5* are almost undetectable (statistically significant reduction compared to *Sox1/8* gene expression levels; * $P < 0.05$). In contrast, early markers for differentiation towards neural (*Sox1*) and surface ectoderm (*K8*) fates, are expressed at high levels. $n=6$ biological replicates. Error bars represent standard deviation.

4.3 Specific Aim 3B. its hypothesis and its results:

Specific Aim 3B

To use our new pluripotency assay and our revised mouse embryo staging to identify the hitherto unknown stage when the initially pluripotent anterior epiblast (the earliest part of ectoderm to differentiate and which is fated for brain and head surface ectoderm differentiation) first loses its pluripotency.

Accomplishment of this aim is expected to contribute to the understanding of early ectoderm development (that is, the development of anterior epiblast which is fated for anterior ectodermal fates). This is because the earliest restriction of potency that occurs within the initially pluripotent anterior epiblast is, by definition, loss of pluripotency.

Methodology of specific aim 3B

This involved isolation of anterior epiblast fragments from mid-streak (MS) to pre-headfold-4 (PH4) and early headfold (EH) stages and culturing them under the aforementioned pluripotency conditions (FBS-coated surfaces in N2/B27 with Activin A, Fgf2 and XAV939) for 48h, followed by examination of live morphology of explant outgrowths and ISH-based gene expression for the pluripotency related genes *Oct4* and *Fgf5*, as well as for the early pan-neural marker *Sox1* and the early surface ectoderm marker *K8*.

Hypotheses of specific aim 3B

If tested anterior explant at the time of its isolation is pluripotent, its outgrowth at the end of the culture should produce: should have a pluripotent phenotype: (a) flat/compact outgrowth consisting of cells with largely indistinct cell-to-cell borders (from live imaging) and (b) express *Oct4* and *Fgf5* in all its cells and no expression of *Sox1* or *K8* (from ISH).

If tested explant If tested anterior epiblast explant at the time of its isolation is not pluripotent, its outgrowth at the end of the 48h culture should not have a pluripotent phenotype: (a) a morphology that is different from that of pluripotent explants (e.g., non-compact outgrowth and/or one made of cells with cell-to-cell borders (from live imaging) and (b) either not express *Oct4* or *Fgf5* or express them in some but not all areas of the outgrowth and *Sox1/K8* may or may not be expressed depending on whether loss of pluripotency resulted in differentiation to neural/surface ectoderm fates (from ISH).

Brief background to specific aim 3B

Previous studies showed that anterior epiblast is pluripotent at the early streak (ES) stage and that it is not pluripotent at an unknown stage from and including the earliest time when the amnion has formed [our stage pre-headfold-1 (PH1)] until just before the early headfold (EH) stage (Li et al., 2013). However, the stage when this earliest pluripotency loss occurs needs further exploration because it could happen some time after the ES stage but before the EH stage, that is, stages MS to PH4 according to our revised staging.

Results of specific aim 3B

The use of the new in vitro pluripotency assay revealed that the earliest loss of pluripotency occurs at pre-headfold-2 (PH2) stage

Our results suggest that at least part of anterior epiblast first loses its pluripotency at pre-headfold-2 (PH2) stage. This is because this is the earliest stage where: (a) live explant outgrowth morphology (n=3/3 of every stage) changed from one to one with distinct cell-to-cell borders (Figure 43) and (b) *Fgf5* and *Oct4* expression (n=3/3 of every stage) stopped being expressed from some areas of the outgrowths (Figure 44). These genes became undetectable by PH4 (Figure 44). Some *K8* expression (n=3/3) was first seen at PH2, mainly at periphery of outgrowths, and earliest *Sox1* expression (n= at least 3 for each stage) was minimal and patchy at PH3 (Figure 44).

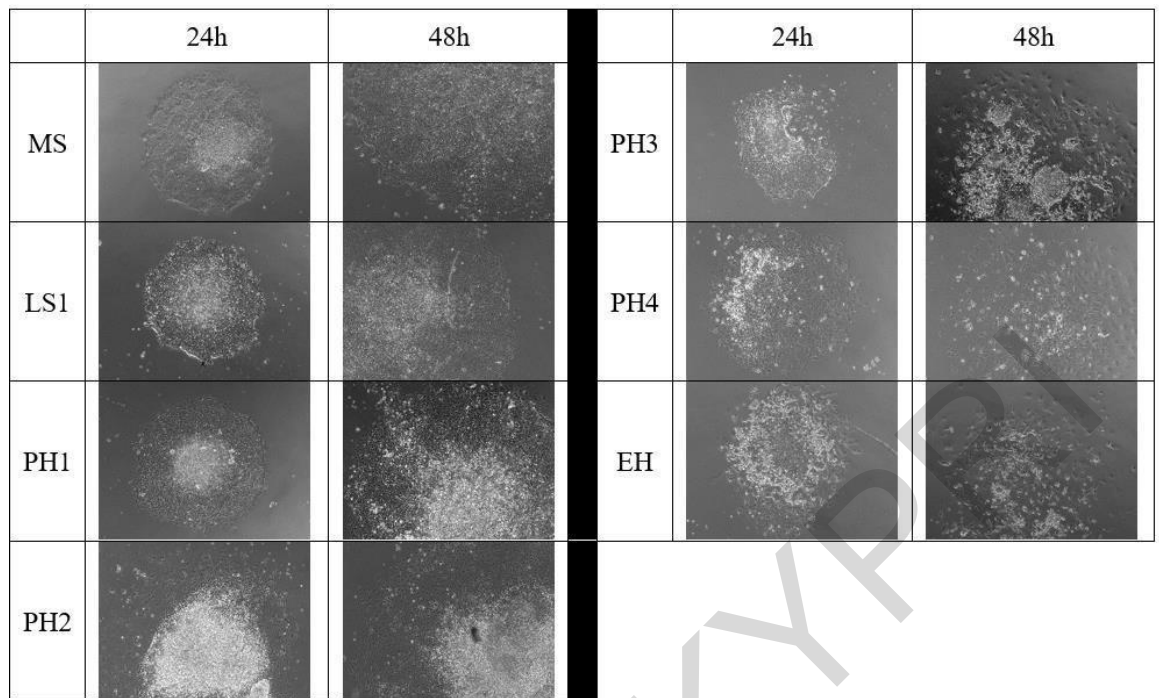


Figure 43: Application of pluripotency assay based on live morphology of explant outgrowths for identification of earliest stage when pluripotency is lost from anterior epiblast explants derived from mid-streak (MS) to early headfold (EH) stages

Live morphology of outgrowths of anterior epiblast explants from MS to EH stages after 48h culture under pluripotency conditions (N2/B27, Activin-A, Fgf2 and XAV939 on FBS). Note that up to PH1 stage outgrowths are made up of cells with largely indistinct cell-to-cell borders, whereas from PH2 onwards they contain largely cells with distinct cell-to-cell borders. All panels are 16x magnification. MS, mid-streak stage; LS1, late streak-1 stage, PH1, pre-headfold-1 stage; PH2, pre-headfold-2 stage; PH3, pre-headfold-1 stage; PH4, pre-headfold-2 stage; EH, early headfold stage.

	<i>Fgf5</i>	<i>Oct4</i>	<i>Sox1</i>	<i>K8</i>
MS				
LS1				
LS2				
PH1				
PH2				
PH3				
PH4				

Figure 44: Application of pluripotency assay based on gene expression assessed by RNA in situ hybridization in explant outgrowths for identification of earliest stage when pluripotency is lost from anterior epiblast explants derived from mid-streak (MS) to pre-headfold-4 (PH4) stages

Expression of indicated genes in outgrowths of anterior epiblast explants from MS to PH4 stages after 48h culture under pluripotency conditions (N2/B27, Activin-A, Fgf2 and XAV939 on FBS). Note that up to PH1 stage outgrowths express *Fgf5* and *Oct4* throughout the outgrowth, whereas at PH2 patchy expression for *Fgf5* loss of *Oct4* expression from periphery is seen and both become undetectable by PH4. *Sox1* expression is first seen in small patches at PH3 and *K8* is expressed in the periphery from PH2 onwards. All panels are 25x magnification. MS, mid-streak stage; LS1, latestreak-1 stage, LS2, late streak-2 stage, PH1, pre-headfold-1 stage; PH2, pre-headfold-2 stage; PH3, pre-headfold-1 stage; PH4, pre-headfold-2 stage.

Conclusions Regarding Specific Aim 3:

A new *in vitro* pluripotency assay for identifying whether a mouse postimplantation tissue is pluripotent or not, has been established. This assay is designed to be informative about the potency of the tissue in case it is found not to be pluripotent. It involves explant culture for 48h on surfaces coated with FBS in a serum-free/chemically defined liquid medium (N2/B27) supplemented with the proteins Activin A and Fgf2, as well as with the Wnt signalling small molecule inhibitor XAV939.

According to this assay, a tissue is: (a) pluripotent if its outgrowth at the end of culture is flat/compact and made of small cells with largely indistinguishable intercellular borders (based on live morphology) and expresses *Oct4* and *Fgf5* throughout in all its cells (based on ISH), and (b) not pluripotent if its outgrowth at the end of culture deviates from the above live morphology (e.g., made up of loosely arranged cells and/or cells with distinguishable intercellular borders) and does not express *Oct4* and *Fgf5* or expresses these genes in some but not all, of its cells (based on ISH). Application of our new *in vitro* pluripotency assay and our revised embryo staging system for identifying the earliest stage when pluripotency is lost in anterior epiblast during early ectoderm development suggests that this takes place at PH2, at least from part of anterior epiblast.

4.4 Specific Aim 4 (A and B), its hypothesis and its results:

Specific Aim 4A

To establish a novel *in vitro* potency assay includes advances over the currently ones used. A tissue potency assay is more informative than a pluripotency assay in the sense that although both assays establish whether a tissue is pluripotent, a potency assay also informs about the potency (ectoderm, mesoderm or endoderm) of the tested tissue in the event when it is not pluripotent.

Methodology of Specific Aim 4A

This involved explant culture of postimplantation tissues that are known to be pluripotent (positive control tissue) or non-pluripotent (negative control tissue) under culture conditions previously shown to derive cells of all three embryonic germ layers using epiblast tissue (Li et al., 2013) and epiblast stem cells (Li et al., 2015). These different culture conditions (named here ‘potency conditions’) were done on fetal bovine serum (FBS)-coated culture surfaces in chemically defined liquid media (N2/B27).

In accordance with previous work of potency assay on mouse epiblast stem cells (3 days culture) (Li et al., 2015), the added factors were the following: **(a)** SB43, a small molecule inhibitor of Nodal/Activin signalling, designed to cause neural differentiation if this is part of the tested tissue’s potency, **(b)** SB43 and addition of BMP2 or BMP4, to cause differentiation to mainly surface ectoderm fates and to a lesser extent to mesendoderm fates, if these are included in the potency of the tested tissue, and **(c)** BMP2 or BMP4, to cause differentiation to mainly mesendoderm fates and to a lesser extent to surface ectoderm fates, if these are part of the tested tissue’s potency.

At the end of culture, the phenotype of the explant outgrowths was examined using live morphology, gene expression [RNA in situ hybridization (ISH) and real time quantitative PCR (RTq-PCR)]. The positive control tissue used was the pluripotent anterior epiblast from E6.5 pre-streak embryos and the negative control tissue was the non-pluripotent anterior epiblast from late headfold embryos (Li et al., 2013), only assessed with real time quantitative PCR (RTq-PCR)].

Unlike the only available Chemically defined *in vitro* potency assay (Li et al., 2013), the one developed here is simpler, faster and includes, in addition to quantitative marker gene expression outcomes that also exist in the published assay, spatial marker gene expression information. The latter is important because it allows for a more reliable interpretation of assay results: for example, if the assay outcome includes low level expression of a

marker gene, it is not clear whether this is inconsequential low-level expression in many cells of the explant outgrowth (suggesting absence of the cells it marks) or strong expression in some cells (indicating presence of these cells).

Moreover, unlike the available *ex vivo* potency assays, that is, heterotopic postimplantation tissue transplantation to postimplantation embryos to generate chimeras (Beddington et al., 1986; Huang et al., 2012) that are technically challenging, the methodology of our assay is relatively easy.

Hypotheses of specific aim 4A

If tested explant at the time of its isolation is pluripotent, its outgrowth at the end of the 48h culture should produce differentiation towards: (a) neural fates in the presence of SB43 (loss of cell to cell contacts in live morphology, expression of neural genes in ISH and RT-qPCR) , (b) predominantly surface ectoderm fates and some mesendoderm differentiation in the presence of SB43/BMP2 (distinct cobbled like flat cell morphology and predominantly expression of surface ectoderm genes in ISH and RT-qPCR) , and (c) predominantly mesendoderm fates and some surface ectoderm differentiation in the presence of BMP2 (cells of the outgrowth that spontaneously contract and predominantly expression of mesendoderm markers in ISH and RT-qPCR).

If tested explant at the time of its isolation has restricted its potency to neural and surface ectoderm fates, its outgrowth at the end of culture should produce differentiation towards: (a) neural fates in the presence of SB43, (b) only surface ectoderm fates in the presence of SB43/BMP2, and (c) some surface ectoderm differentiation in the presence of BMP2.

If tested explant at the time of its isolation has restricted its potency to neural fates, its outgrowth at the end of culture should produce differentiation towards: (a) neural fates in the presence of SB43,
(b) no surface ectoderm or mesendoderm fates in the presence of SB43/BMP2, and (c) no mesendoderm or surface ectoderm fates in the presence of BMP2. If neural restriction is also determined/committed (i.e. already specified irreversibly to neural fates), then we should expect to get neural differentiation under all conditions.

If tested explant at the time of its isolation has restricted its potency to surface ectoderm fates, its outgrowth at the end of culture should produce differentiation towards: (a) no neural fates in the presence of SB43, (b) only surface ectoderm fates in the presence of SB43/BMP2, and (c) surface ectoderm fates in the presence of BMP2. If surface ectoderm

restriction is also determined/committed (i.e., already specified irreversibly to surface ectoderm fates), then we should expect to get surface ectoderm under all conditions.

If tested explant at the time of its isolation has restricted its potency to mesendoderm fates, its outgrowth at the end of culture should produce differentiation towards: (a) no neural fates in the presence of SB43, (b) only mesendoderm fates in the presence of SB43/BMP2, and (c) only mesendoderm fates in the presence of BMP2. If mesendoderm restriction is also determined/committed (i.e., already specified irreversibly to mesendoderm fates), then we should expect to get mesendoderm under all conditions.

XENIA HADJIKYPRRI

This assay was validated using two control tissues.

Positive Control: Testing the potency of a pluripotent tissue: anterior epiblast explants from pre-streak or early streak embryos, a postimplantation tissue known to be pluripotent (Li et al., 2013). If the assay is valid, we would expect its outgrowth at the end of culture to differentiate towards: (a) neural fates in the presence of SB43, (b) predominantly surface ectoderm fates and some mesendoderm differentiation in the presence of SB43/BMP2, and (c) predominantly mesendoderm fates and some surface ectoderm differentiation in the presence of BMP2.

Negative Control: Testing the potency of a tissue with restricted potency towards neural fates: anterior-proximal epiblast explants from Early-Headfold (EH) stage, a postimplantation tissue known to be committed (determined) to neural differentiation (Li et al., 2013). If the assay is valid, we would expect its outgrowth at the end of culture to only differentiate towards neural fates under all 3 culture conditions. Our results include RT-qPCR analysis data from the EH stages and not live morphology or ISH data.

Results of specific aim 4A:

The establishment new *in vitro* potency assay that is simpler and faster than the existing one

- 1. E6.5 pre-streak anterior epiblast (pluripotent tissue) explants – Positive control**
 - **Potency assay culture conditions to induce neural fates – Neural potency assay (48h):**

The early mouse embryo is thought to exist in a pre-anterior neural phase and that this cell fate must be inhibited to allow for the formation of other embryonic tissues. This neural fate inhibition occurs in the posterior region of the gastrulating mouse embryo and results in the formation of mesoderm and endoderm through activation of signals including BMP, Nodal, Wnt, and FGF. Neural tissue induction happens during early gastrulation and begins when the early to mid-gastrula organizer inhibits these posterior signals therefore protecting a local epiblast region to remain as the prospective anterior neural tissue (Levine and Brivanlou 2007). The now specified anterior neural cells move away from the distal epiblast to locate to the anterior epiblast and be juxtaposed with the AVE that expresses inhibitors (Nodal antagonists Lefty1 and cerberus 1) of posteriorizing factors (Levine and Brivanlou 2007). This will protect the prespecified neural tissue from acquiring posterior characteristics. Several studies using stem cell cultures, have shown that a combination of small

molecule inhibitors of both BMP (Dorsomorphin) and TGF β /Activin/Nodal (SB431542) signalling, stimulates highly efficient neural induction from human ESCs (hESCs) and induced pluripotent stem cells (iPSCs) (Morizane A. et al. 2011). When explanted and cultured in vitro, *Nodal*^{-/-} epiblast cells differentiate into neural tissues (Camus et al., 2006). Studies in mouse EpiSCs as well as human embryonic stem cells (hESCs) revealed that inhibition of Nodal signalling by the small molecule inhibitor SB431542 (Inman et al., 2002; Laping et al., 2002) constricts mesoderm/endoderm differentiation while promoting neural induction (Chng et al., 2010; Patani et al., 2009; Vallier L et al., 2009).

For the purposes of the Neural potency assay used in this current study explants were cultured in the presence of the small molecule inhibitor (SB43 – 2 μ g/ml) of the TGF β /Activin/Nodal signalling. This culture condition allowed for the explants derived from the anterior epiblast of the Pre-Streak embryos used as controls to acquire a neural character. The Neural potency assay was done on FBS coated plates (12 explants – coating for 24 hours). The cell morphology of these explants was examined (Figure 45) when these were cultured for up to 72 hours. Morphology at 24h, unlike the undifferentiated morphology of pluripotency assay (i.e., outgrowth with indistinct cell border), displayed flat and compact outgrowths with distinct cell borders. By 48 hours or longer however morphology changed to loosely arranged elongated cells and dehiscence of cells.

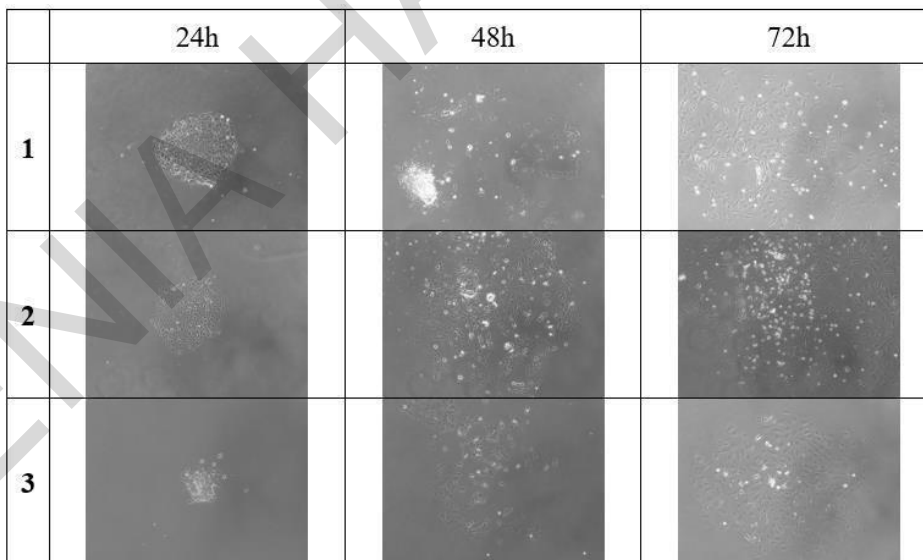


Figure 45: Establishment of neural potency assay: Live morphology of outgrowths of anteriorepiblast explants from E6.5 pre-streak (positive control - pluripotent epiblast) cultured up to 72h under neural potency culture conditions (N2/B27 and SB43 on FBS)

Note the flat and compact outgrowths with distinct cell borders at 24h (n=12/12) that changes to loosely arranged elongated cells by 48h. Dehiscence of cells also observed from 48h (n=12/12). All panels are at 16x magnification.

The neural potency assay culture condition was further assessed when these explants were subjected to ISH to check for early neural gene marker expression. These ISH experiments were performed on explants of 24 and 48 h culture. These explants showed expression of early neural markers *Sox1*, *Sox2*, *Pax6* and *Six3* while the expression of epiblast marker *Fgf5*, surface ectoderm marker *Dlx5*, mesoderm marker *Bra* and endodermal marker *Sox17* was undetectable (Figure 46). Expression throughout the explant outgrowth of early neural genes *Sox1* (n=6), *Six3* (n=6), *Pax6* (n=4) and *Sox2* (n=4) was observed, but no expression of undifferentiated epiblast marker *Fgf5* (n=6), early surface ectoderm marker *Dlx5* (n=6), early mesoderm marker *Bra* (n=4) and early definitive endoderm marker *Sox17* (n=2).

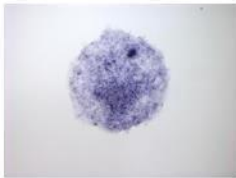
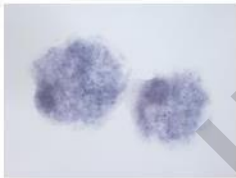
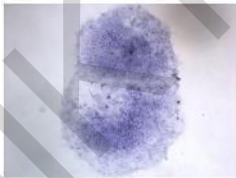
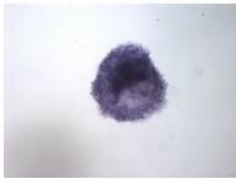
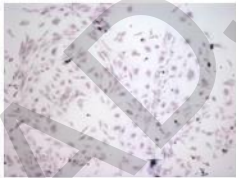
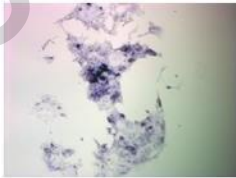





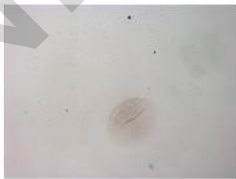



	<i>Sox1</i>	<i>Six3</i>	<i>Pax6</i>	<i>Sox2</i>
24h				
48h				
	<i>Fgf5</i>	<i>Dlx5</i>	<i>Bra</i>	<i>Sox17</i>
24h				
48h				

Figure 46: Establishment of neural potency assay: RNA in situ hybridization for gene expression analysis of outgrowths of anterior epiblast explants from E6.5 pre-streak cultured for up to 48h under neural potency conditions (N2/B27, SB43 on FBS)

Note the expression of neural markers (*Sox1*, *Six3*, *Pax6*, *Sox2*) and the absence of undifferentiated epiblast marker *Fgf5*, early surface ectoderm marker *Dlx5* and early mesendoderm markers (*Bra* and *Sox17*). All panels are at 16x magnification.

This neural gene expression profile was validated using RTq-PCR (n=12 biological replicas) (Figure47). For RTq-PCR, each biological replica consisted of six explant outgrowths pooled together and each gene quantification measurement was done twice in two separate experiments. To statistically assess the level of upregulation / downregulation of genes tested, the E6.5 pre-streak neural potency assay gene expression levels were compared to the gene expression levels of the E6.5 pre-streak pluripotency assay values. These pluripotency values were used as controls for all the below potency assay RT-q PCR culture conditions results.

Neural gene markers were significantly upregulated while very little expression of other germ layer markers (surface ectoderm- *K8*, mesendoderm marker- *Gsc* and endoderm marker – *Sox17*) was expressed. Statistically significant upregulation of neural genes was observed when compared to the neural gene expression levels (*Sox1* and *Six3*) of the control explants (Pre-Streak pluripotency assay gene expression levels). Moreover, statistically significant downregulation of *Fgf5* expression levels was also observed when compared to the Pre-Streak control levels of this gene. Upregulation of other neural genes (*Pax6* and *Sox2*) was also observed.

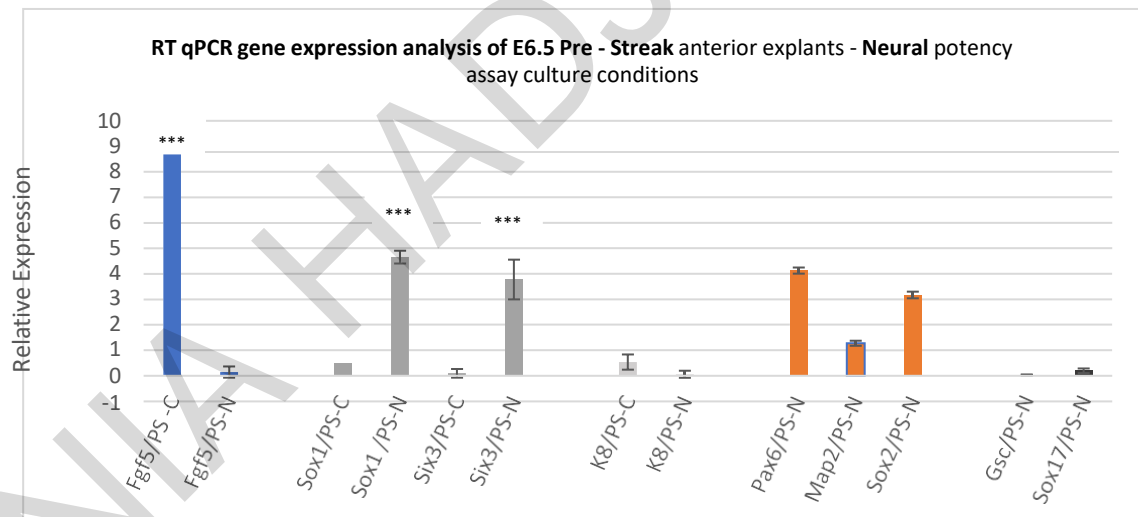


Figure 47: RT-qPCR analysis of marker gene expression of anterior epiblast explants from E6.5 Pre-Streak embryos cultured in neural potency assay culture conditions (N2/B27 + SB43) for 48h

Pre – Streak Control – pluripotency assay (PS-C), Pre – Streak Neural potency assay (PS-N). Relative expression to the housekeeping gene b-actin. Statistical increase of neural genes (*Sox1* and *Six3*) under neural conditions compared to the control. Statistical decrease of pluripotency related genes under neural conditions relative to the control. n=12 biological replicates. *P < 0.05. Error bars represent s.d

- **Potency assay culture conditions to induce Predominantly surface ectoderm (and somemesendoderm) fates – Surface ectoderm potency assay (48h)**

The potency assay also includes culture conditions to drive anterior epiblast explants to differentiate not only into neural tissue, as described above, but also differentiate predominantly towards surface ectoderm and some mesendoderm cell lineages. The signals required for such differentiation were mostly studied in the *Xenopus*. Less extended research in the mouse embryo revealed that BMP4, which is a member of the transforming growth factor β (TGF β) ligand superfamily, induces surface ectoderm differentiation from the ectoderm (Li et al. 2013). On the other hand, suppression of BMP signalling, delivered by BMP antagonists, results in neural ectoderm specification (Chang and Hemmati-Brivanlou, 1998; Wilson and Hemmati-Brivanlou, 1995).

For the purposes of the surface ectoderm (and some mesendoderm) differentiation potency assay used in this current study explants were cultured in the presence of the small molecule inhibitor (SB43 – 2 μ g/ml) of the TGF β /Activin/Nodal signalling together with BMP2(10 μ g/ml). This culture condition allowed for the explants derived from the anterior epiblast of the Pre-Streak to predominantly acquire a surface ectoderm and some mesendoderm character. The surface ectoderm differentiation culture conditions were done both of FBS (15 explants) coated dishes all of which showed very similar explant outgrowth cell morphology. The cell morphology of these explants was examined (Figure 48) when these were cultured for up to 96 hours. By 24h they show compact flat outgrowths with distinct cell borders; by 48h they show typical cobbled-stone morphology (indicative of surface ectoderm) on FBS coated dishes. This homogeneous cobbled-stone-like morphology in this culture condition was consistently seen in all cases of FBS and coated dishes for up to 4 days of culture. This cell morphology was also observed in the study by Li et al 2013 that suggested that this phenotype was linked to epidermal lineage.

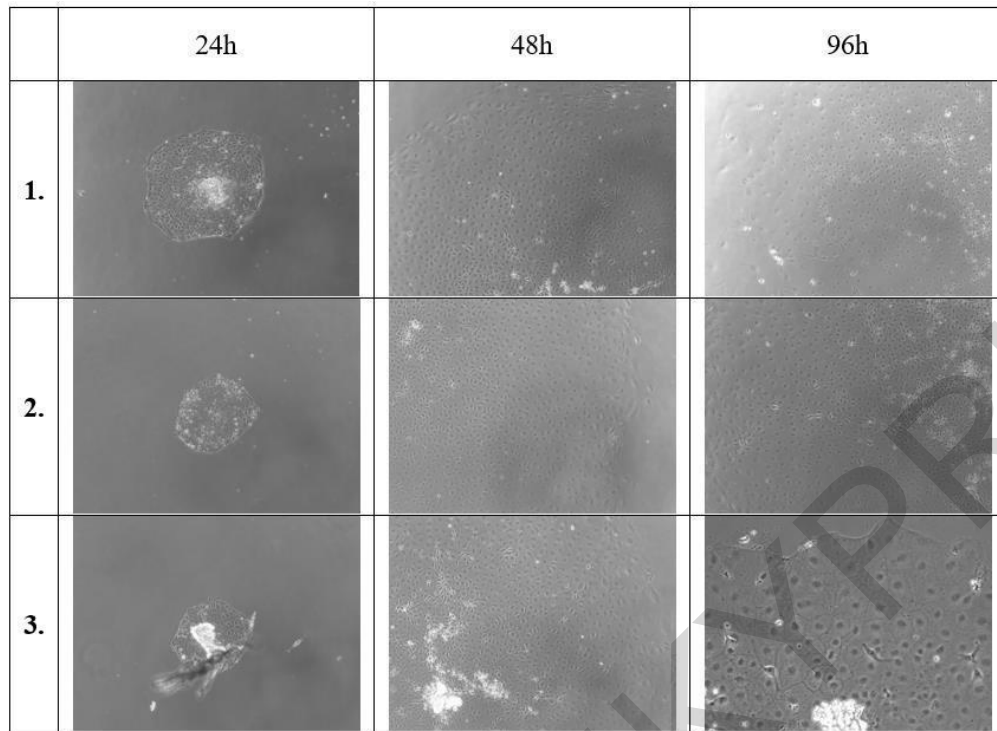


Figure 48: Establishment of surface ectoderm potency assay: Live morphology of outgrowths of anterior epiblast explants from E6.5 pre-streak cultured up to 96h under surface ectoderm potency culture conditions (N2/B27 + SB43 + BMP2 on FBS)

Note the same flat cobble-like stone like cell morphology (48h and 96h) in all experiments. All panels are of the same magnification (16x magnification) except the 3. 96h column (25x magnification).

The surface ectoderm culture condition of the potency assay was further validated when the explants cultured under these conditions were subjected to ISH (Figure 49) to check for neural, surface ectoderm and mesoderm/endoderm markers at 24 and 48h of culture. As expected throughout most or all the explant outgrowth early surface ectoderm genes marker gene expression (*K8* n=3, *K18* n=4, *Dlx5* n=4) was observed, whereas epiblast marker *Fgf5* (n=3), neural marker *Sox1* (n=3) and early mesoderm marker *Bra* (n=3) were undetectable. Very low expression of early definitive endoderm marker *Sox17* (n=3) was observed mostly in the middle areas of the explant outgrowths.

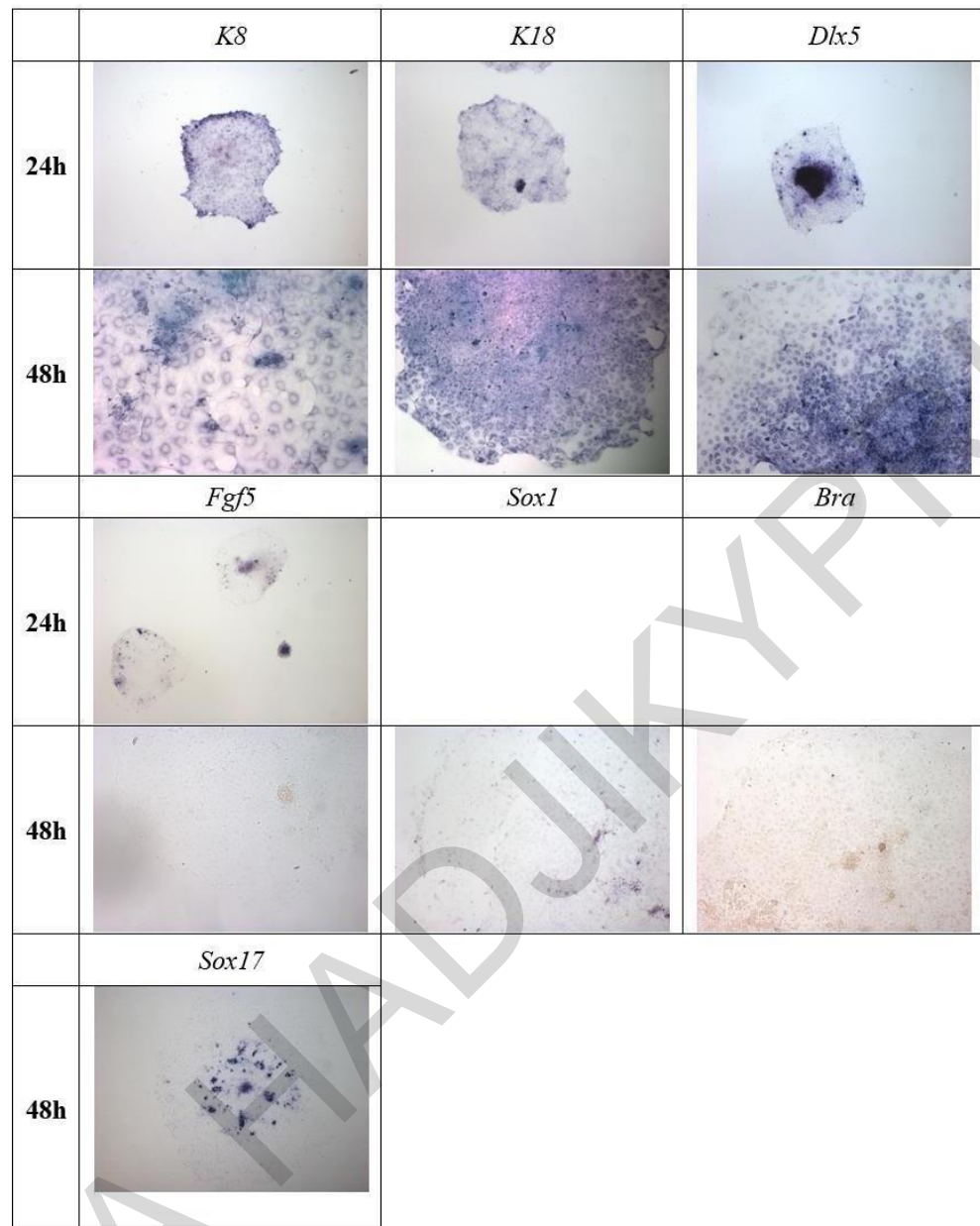


Figure 49: Establishment of surface ectoderm potency assay: RNA in situ hybridization for gene expression analysis of outgrowths of anterior epiblast explants from E6.5 pre-streak cultured for up to 48h under surface ectoderm potency conditions (N2/B27 + SB43 + BMP)

Note the expression of surface ectoderm markers (*K8*, *K18*, *Dlx5*) and the absence of epiblast related (*Fgf5*), neural (*Sox1*) and mesendoderm (*Bra*) markers. *Sox17* an early definitive endoderm marker, shows some expression. All panels are of the same magnification (16x magnification) except the *K8*48h (25x magnification).

This surface ectoderm gene expression profile was validated using RTq-PCR (n=6 biological replicas) (Figure 50). For RTq-PCR, each biological replica consisted of three explant outgrowths pooled together and each gene quantification measurement was done twice in two separate experiments. To statistically assess the level of upregulation / downregulation of genes tested, the E6.5 pre-streak surface ectoderm potency assay gene expression levels were compared to the gene expression levels of the E6.5 pre-streak pluripotency assay values. These pluripotency values were used as controls for all the below potency assay RT-q PCR culture conditions results.

The assessment of gene expression with RT-qPCR in predominantly surface ectoderm potency assay conditions after 48h culture on FBS revealed statistically significant high levels of early surface ectoderm genes (*K8*, *K18* and *K14*) when compared to the Pre-Streak Control gene expression levels. Statistically significant downregulation of pluripotency-related *Oct4* was also observed when compared to the control. Early neural markers *Sox1* and *Six3* expression levels were very low but some expression of mesendoderm marker *Gsc* and endoderm marker *Cerberus* was detected. However, *Dlx5* an early surface ectoderm marker, is expressed at extremely low levels.

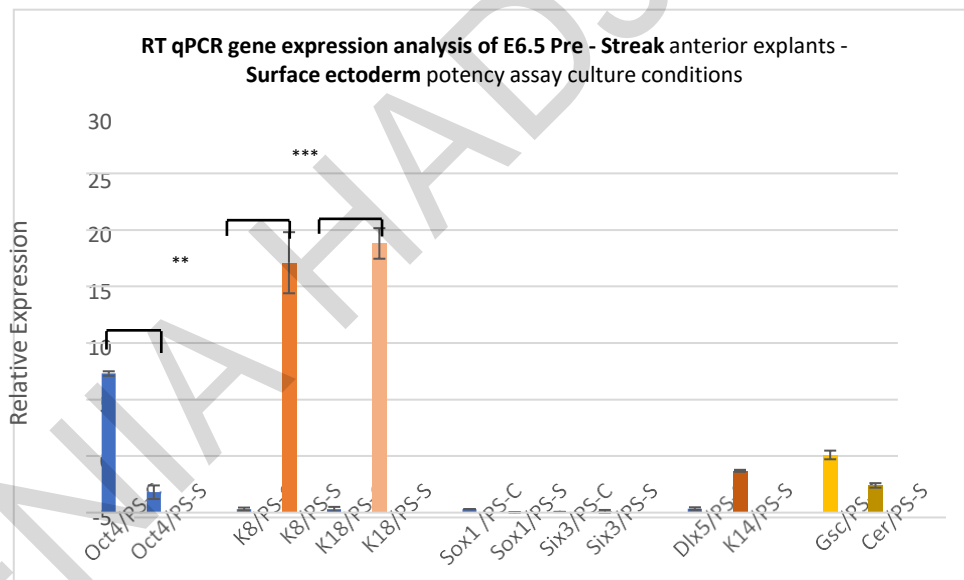


Figure 50: RT-qPCR analysis of marker gene expression of anterior epiblast explants from E6.5 Pre-Streak embryos cultured in surface ectoderm potency assay culture conditions(N2/B27 + SB43 + BMP2) for 48h

Pre – Streak Control – pluripotency assay (PS-C), Pre – Streak Neural potency assay (PS-N). Gene expression levels are relative to the housekeeping gene b-actin. Statistical increase of surface ectoderm genes (*K8* and *K18*) under surface ectoderm potency assay conditions relative to the control (PS-S pluripotency assay). Statistical decrease of pluripotency related gene *Oct4* under surface ectoderm conditions relative to the control. n=5 biological replicates. *P <0.05. Error bars represents.d.

- **Potency assay culture conditions to induce predominantly mesendoderm (and some surface ectoderm) fates (48h) – Mesendoderm potency assay**

The development of the potency assay includes culture conditions that can derive cells of all three embryonic germ layers. To derive mesendodermal cells, the initial experiments involved the culture of Pre-Streak pluripotent anterior explants in the presence of BMP2 (10 µg/ml) on FBS coated plates. It was previously shown that genes such as *Mesp1*, *Flk1*, *Hoxd1*, and *Hoxb9*, which have crucial roles in embryo gastrulation and mesoderm differentiation (Saga et al., 1999; Fehling et al., 2003), were upregulated following BMP4 treatment in EpiSCs (Li et al., 2015).

The mesendoderm potency assay culture conditions was done on FBS coated plates all of which shared very similar cell morphology. The cell morphology of these explants was examined (Figure 51) when these were cultured for up to 96 hours. By 24h they show compact flat outgrowths with distinct cell borders; by 72h they show scattered 3-D regions on top of the flat outgrowth that spontaneously contract (indicative of mesoderm-derived cardiomyocytes) also shown at 96h.

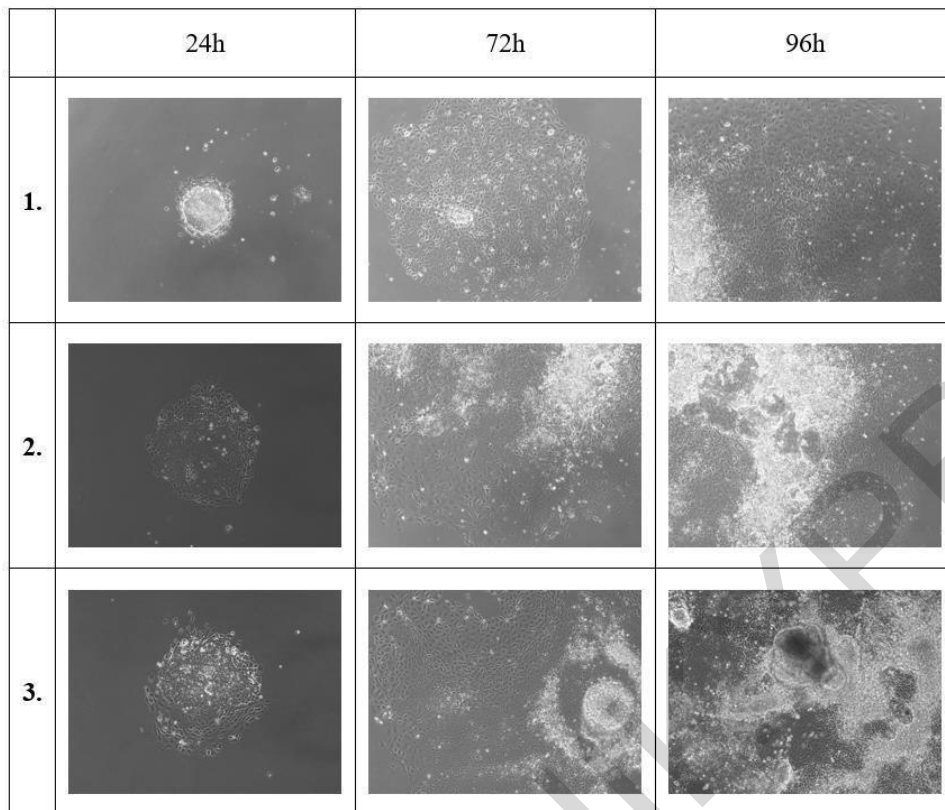


Figure 51: Establishment of mesendoderm potency assay: Live morphology of outgrowths of anterior epiblast explants from E6.5 pre-streak cultured up to 96h under mesendoderm potency culture conditions (N2/B27 + BMP2 on FBS)

Note 72h and 96h explant outgrowths show scattered 3-D regions on top of the flat outgrowth that spontaneously contract. All panels are of the same magnification (16x magnification).

The predominantly mesendoderm culture condition of the potency assay was further examined when the explants cultured under these conditions were subjected to ISH (Figure 52) to check for neural, surface ectoderm and mesoderm/endoderm marker gene expression. As expected mesendodermal marker gene expression was observed (*Bra*, *Gsc*, *Flk1*, *Msp1*, *Cer*, *Sox17*) whereas epiblast marker *Fgf5* and neural marker *Sox1* undetectable. Expression of the epidermal marker *K8* was also observed. BMP treatment was previously shown to upregulate gene expression essential for epidermis development (Li et al., 2015).

Specifically, large areas of these outgrowths express early mesoderm markers *Bra* (n=4), *Gsc* (n=3), *Flk1* (n=2) and *Msp1* (n=3) and early endoderm markers *Cer* (n=3) and *Sox17* (n=3) as well as surface ectoderm marker *K8* (n=2), but show no expression of undifferentiated epiblast marker *Fgf5* (n=3) and neural marker *Sox1* (n=3) at 48h of culture.

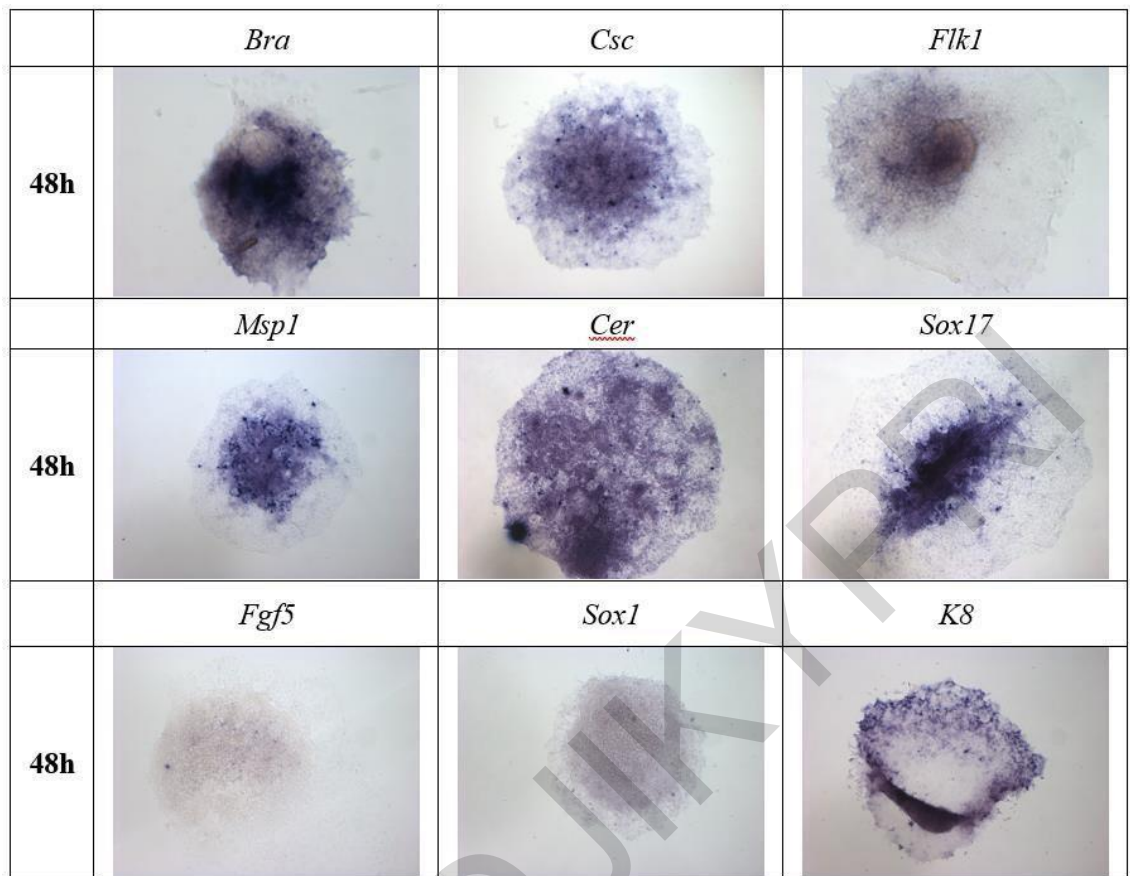


Figure 52: Establishment of mesendoderm potency assay: RNA in situ hybridization for gene expression analysis of outgrowths of anterior epiblast explants from E6.5 pre-streak cultured for 48h under mesendoderm potency conditions (N2/B27 + BMP2 on FBS)

Note the expression of mesendodermal (*Bra*, *Gsc*, *Flk1*, *Msp1*, *Cer* and *Sox17*) and epidermal markers (*K8*) and the absence of epiblast related (*Fgf5*) and neural markers (*Sox1*). All panels are of the same magnification (16x magnification).

This mesendoderm gene expression profile was validated using RTq-PCR (n=6 biological replicas) (Figure 53). For RTq-PCR, each biological replica consisted of three explant outgrowths pooled together and each gene quantification measurement was done twice in two separate experiments. To statistically assess the level of upregulation / downregulation of genes tested, the E6.5 pre-streak surface ectoderm potency assay gene expression levels were compared to the gene expression levels of the E6.5 pre-streak pluripotency assay values. These pluripotency values were used as controls for all the below potency assay RT-q PCR culture conditions results.

The assessment of gene expression with RT-qPCR in predominantly mesendoderm potency assay conditions after 48h culture on FBS revealed statistically significant high levels of mesendodermal gene markers and very little expression of other germ layer markers. Specifically, the levels of the mesendoderm marker (*Bra*) were statistically significantly upregulated when compared to the corresponding mesendoderm expression levels of Pre-Streak control (pluripotency assay). Extremely low levels of neural genes *Sox1* and *Six3* and low to moderate levels of pluripotency-related genes *Oct4*, *Fgf5* and *Sox2* were observed.

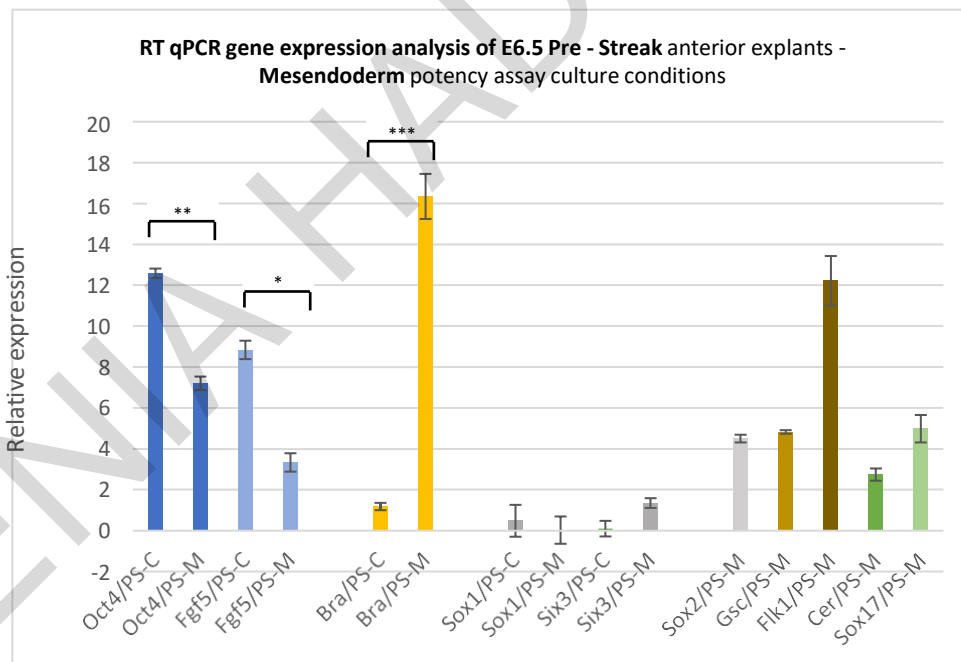


Figure 53: RT-qPCR analysis of marker gene expression of anterior explants from anterior epiblast of Pre-Streak embryos cultured in predominantly mesendoderm differentiation culture conditions (N2/B27 + BMP2) for 48h.

Pre - Streak Control - pluripotency assay (PS-C), Pre - Streak predominantly mesendoderm differentiation assay (PS-M). Relative expression to the housekeeping gene b-actin. Mesoderm gene expression levels of *Bra* were statistically significantly upregulated compared to the *Bra* expression levels of Pre-Streak controls (pluripotency assay). n=6 biological replicates. *P < 0.05. Error bars represent s.d

1. Early Headfold (EH) anterior proximal epiblast explants – Negative control

The potency assay was further validated by the use of negative control anterior proximal epiblast explant results derived from Early headfold (EH) anterior proximal epiblast tissues known to be committed to neural fates (Li et al., 2013). EH anterior proximal epiblast explants showed high levels of neural genes (*Sox1* and *Six3*) and extremely low levels of pluripotency related genes (*Fgf5*, *Oct4*), surface ectoderm genes (*K8*, *K18*) and mesendoderm gene *Bra* when cultured under all three potency assay conditions (Neural, predominantly surface ectoderm and predominantly mesendoderm potency assay culture conditions) (Figure 54). *Sox1* and *Six3* expression levels were significantly increased when compared to the control (PS - pluripotency) levels of these genes. *Fgf5* levels were statistically significantly downregulated compared to the control levels of these genes (Figure 54).

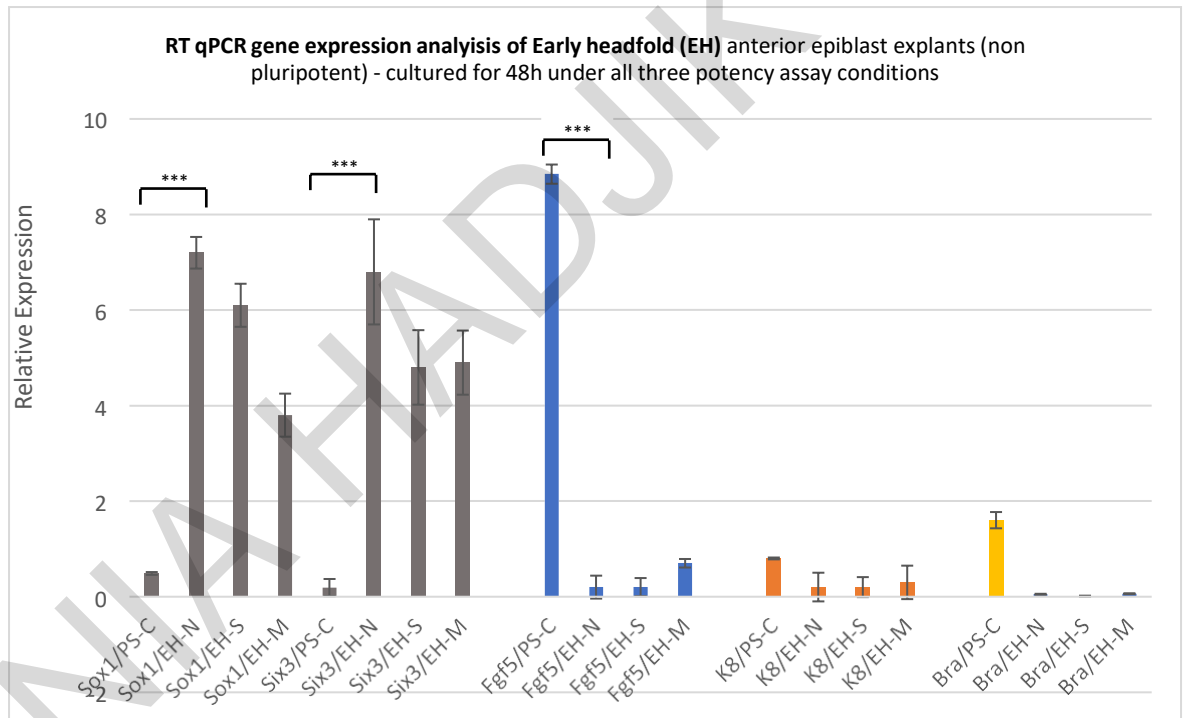


Figure 54: RT-qPCR analysis of marker gene expression of proximal anterior explants from Early Headfold (EH) embryos cultured in all three conditions of the potency assay for 2 days

Pre – Streak Control – pluripotency assay (PS-C), Early headfold neural potency assay (EH-N), Early Headfold Surface surface ectoderm potency assay (EH-S), Early Headfold Mesendoderm potency assay (EH-M). Relative expression to the housekeeping gene *b-actin*. Gene expression levels of neural genes *Sox1* and *Six3* were statistically significantly upregulated compared to the expression levels of Pre-Streak controls (pluripotency assay) in all potency assay conditions. *Fgf5* levels of EH were statistically significantly downregulated compared to the controls in all potency assay culture conditions. n=6 biological replicates. *P < 0.05. Error bars represent s.d

4.4B Specific Aim 4B, its hypothesis and its results:

Specific Aim 4B

This specific aim used this novel potency assay and new staging system (Specific aim 1) described above to investigate when and where in anterior epiblast pluripotency is lost signifying the beginning of ectoderm development, and if lost, what is the potency of the tissue.

Methodology of Specific Aim 4B

All assays were RT-qPCR on anterior-proximal and anterior-distal epiblast explants cultured for 48h on FBS under conditions that promote neural differentiation (CDM+SB43), predominantly surface ectoderm differentiation (with some mesendoderm differentiation) (CDM+SB43+BMP2) or predominantly mesendoderm differentiation (with some surface ectoderm differentiation) (CDM+BMP2).

The expression of the same 6 genes was assayed in all three conditions: pluripotency-related (*Fgf5* and *Oct4*), early neural (*Sox1* and *Six3*), early surface ectoderm (*K8* and *K18*) and early mesendoderm (*Bra*) gene.

As control, the expression of these genes from anterior epiblast from pre-streak embryos cultured in pluripotency conditions for 48h on FBS were used. The results were interpreted based on reductions/increases of tested genes relative to their expression in controls.

Importance of specific aim 4B: Embryos staged according to our novel staging system described above (Specific Aim 1) were used to derive explants from their anterior proximal and anterior distal epiblast and test their potency using our novel potency assay culture conditions. The use of the potency assay developed here allowed for the identification of the exact time of loss of pluripotency and the restriction of potency of anterior proximal and anterior distal epiblast.

Hypotheses of specific aim 4B:

Hypothesis 1: If the epiblast fragment tested is pluripotent at the time of its isolation, the expression of neural, surface ectoderm and mesendoderm gene markers should be substantially and statistically elevated relative to their expression in control cultures and that of pluripotency-related markers downregulated, when cultured under the three differentiation conditions designed to elevate them (that is, neural, predominantly surface ectoderm and predominantly mesendoderm differentiation conditions).

Hypothesis 2: If the potency of epiblast fragment tested is restricted to ectodermal fates at the time of its isolation, the expression of only neural and surface ectoderm gene markers should be substantially and statistically elevated relative to their expression in control cultures, whereas that of mesendoderm markers should not be elevated or become downregulated and that of pluripotency-related markers should be downregulated, when cultured under the three differentiation conditions designed to elevate them (that is, neural, predominantly surface ectoderm and predominantly mesendoderm differentiation conditions).

Hypothesis 3: If the potency of epiblast fragment tested is restricted to neural fates at the time of its isolation, the expression of only neural gene markers should be substantially and statistically elevated relative to their expression in control cultures, whereas that of surface ectoderm or mesendoderm markers should not be elevated or become downregulated and that of pluripotency-related markers should be downregulated, when cultured under the three differentiation conditions designed to elevate them (that is, neural, predominantly surface ectoderm and predominantly mesendoderm differentiation conditions).

Hypothesis 4: If the potency of epiblast fragment tested is restricted to surface ectoderm fates at the time of its isolation, the expression of only surface ectoderm gene markers should be substantially and statistically elevated relative to their expression in control cultures, whereas that of neural or mesendoderm markers should not be elevated or become downregulated and that of pluripotency-related markers should be downregulated, when cultured under the three differentiation conditions designed to elevate them (that is, neural, predominantly surface ectoderm and predominantly mesendoderm differentiation conditions).

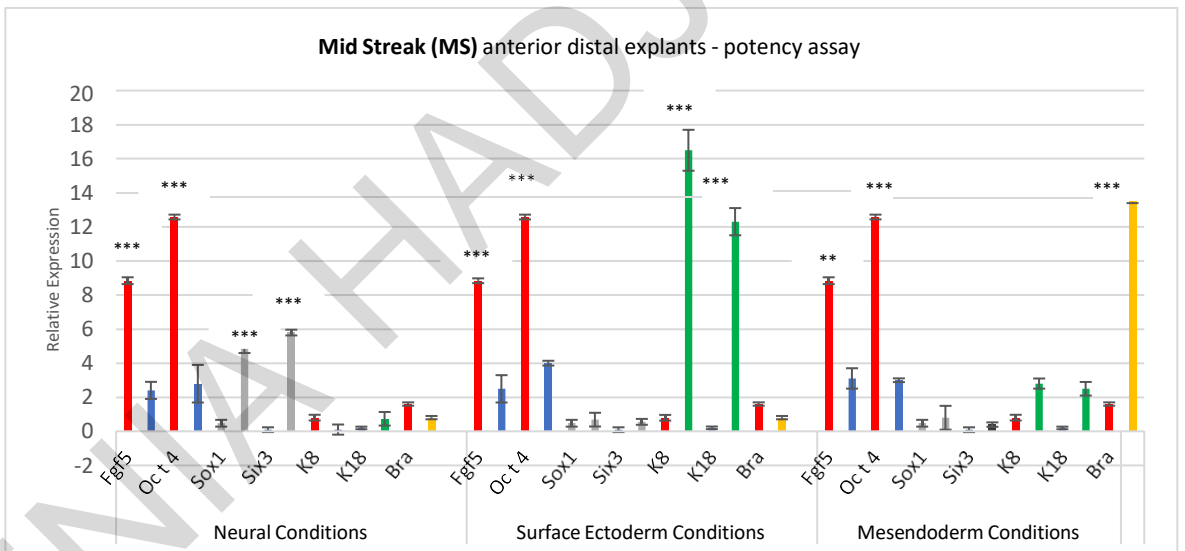
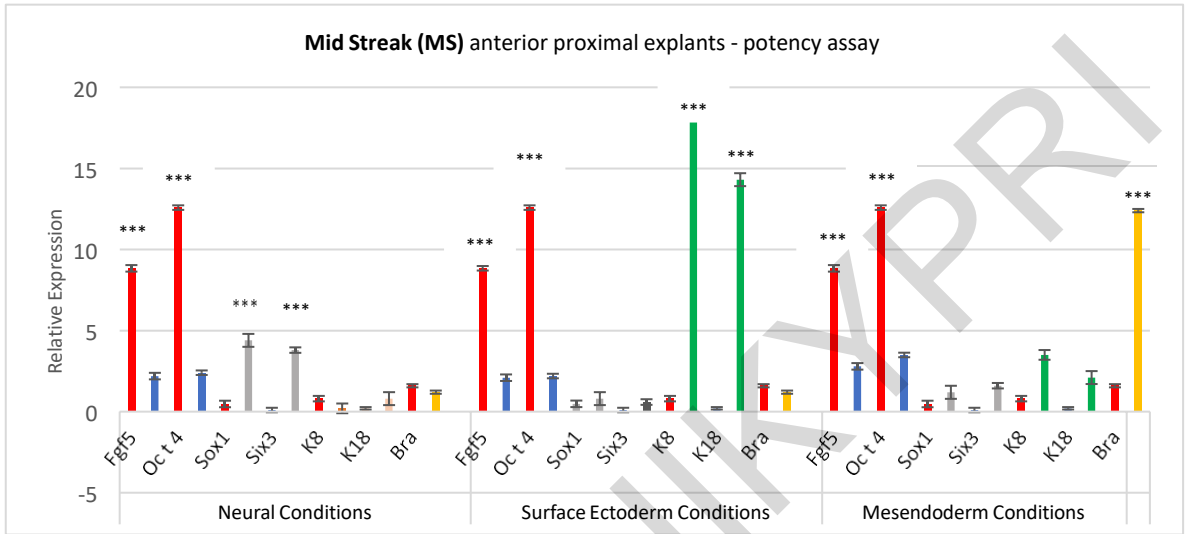
Hypothesis 5: If the potency of epiblast fragment tested is restricted to mesendoderm fates at the time of its isolation, the expression of only mesendoderm gene markers should be substantially and statistically elevated relative to their expression in control cultures, whereas that of neural or surface ectoderm markers should not be elevated or become downregulated and that of pluripotency-related markers should be downregulated, when cultured under the three differentiation conditions designed to elevate them (that is, neural, predominantly surface ectoderm and predominantly mesendoderm differentiation conditions).

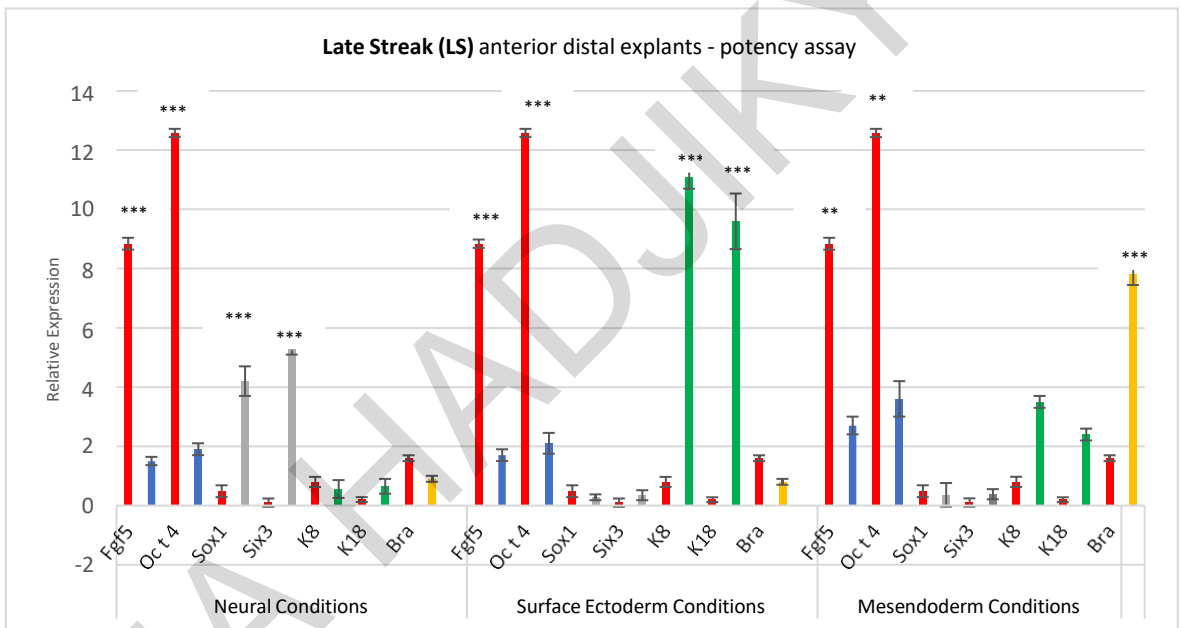
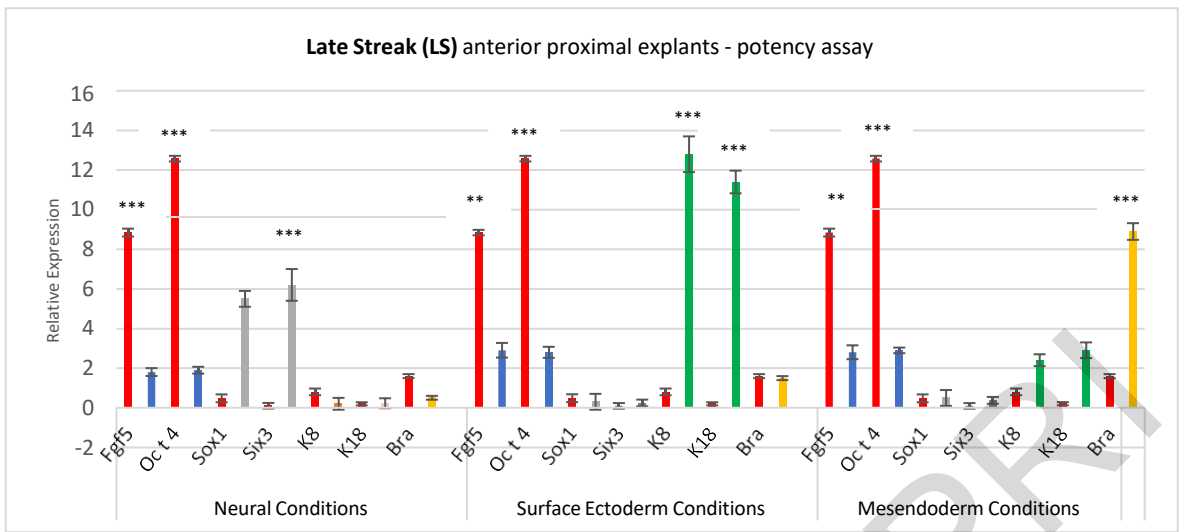
Results of specific aim 4B:

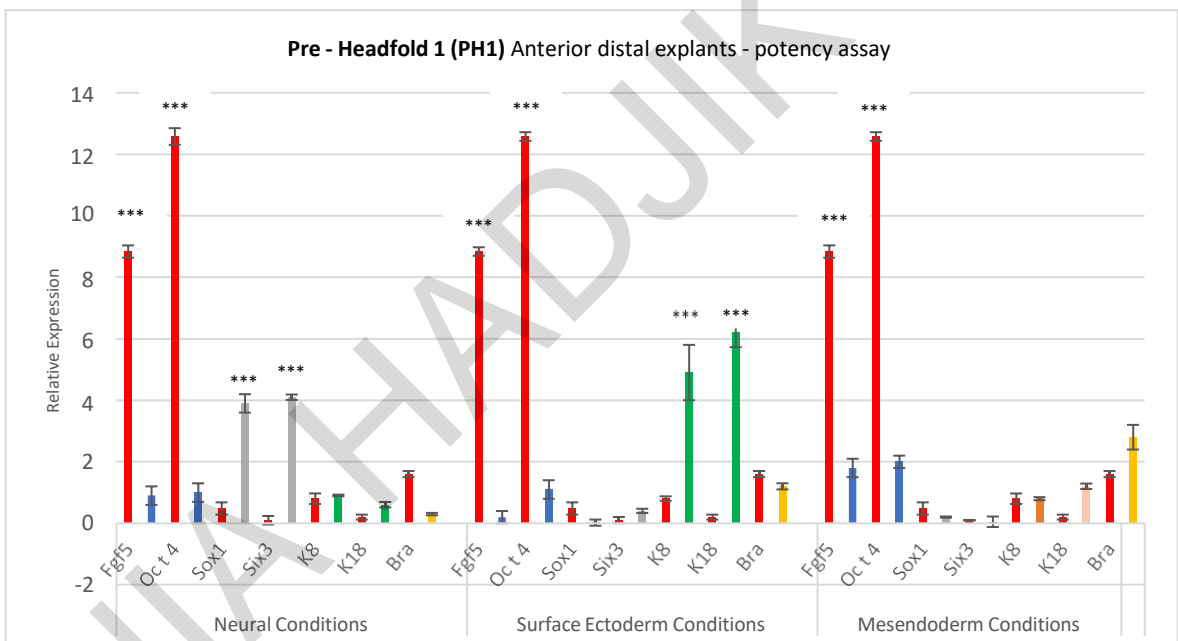
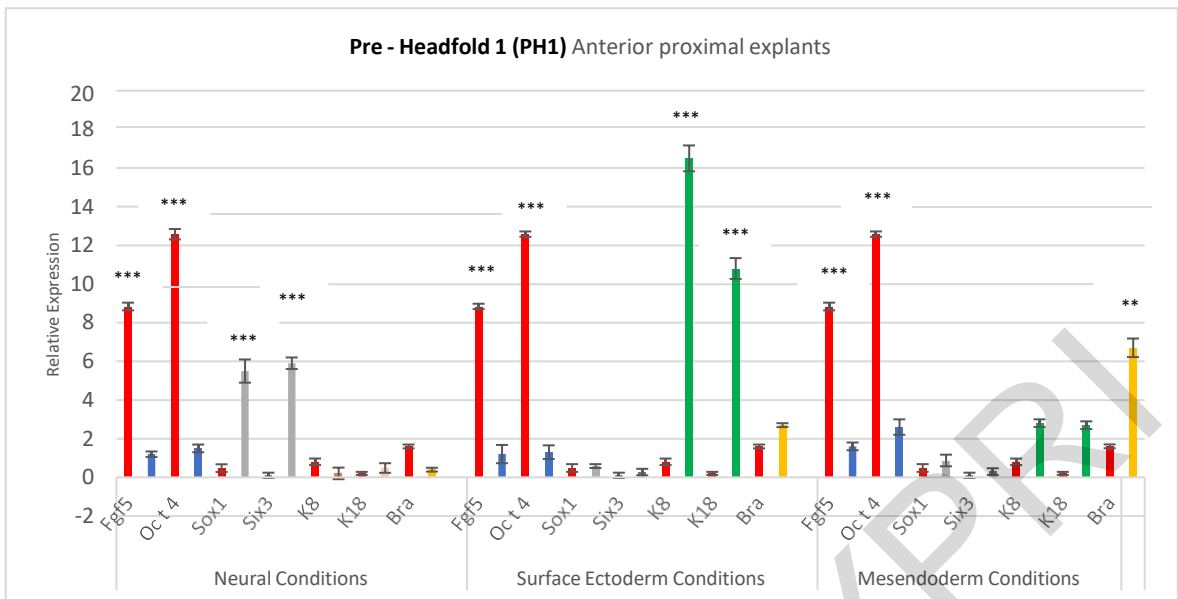
The anterior proximal and anterior distal epiblast at Mid-Streak (MS), Late-Streak (LS), Pre- Headfold-1 (PH1) stages and anterior distal of pre-Headfold 2 (PH2) is still pluripotent.

The anterior tissue of these embryonic stages was dissected away from the overlying VE and ExE, and then cut into anterior proximal and anterior distal portions. To validate the technique used gene expression analysis confirmed that this isolated epiblast tissue used did not express the trophectoderm marker *Cdx2*.

During the 2-day culture, both anterior proximal and anterior distal explants showed expected cell morphology corresponding to the different culture conditions that was also observed in Pre-Streak control experiments. The results of the use of the potency assay on staged embryos were assessed using RT-qPCR analysis (Figure 55). This showed that the neural marker *Sox1* and *Six3* were upregulated in explants cultured under neural potency assay conditions (N2/B27 + SB43). By contrast, the surface ectoderm markers *K8* and *K18* were upregulated in explants cultured in Surfaceectoderm potency assay conditions both in anterior proximal and anterior distal tissues. Under this culture condition some mesendoderm gene expression was also observed. In the presence of only BMP2 (predominantly mesendoderm culture conditions) *Bra* was upregulated. Moderate levels of surface ectoderm (*K18*) expression were also observed. These results suggest that during these developmental stages the epiblast maintains the capacity to respond to different developmental stimuli and induce gene expression of all three embryonic germ layers. The data described here indicate that the anterior distal and anterior proximal epiblast of Mid Streak, Late Streak and Pre Headfold-1 embryos and the anterior distal of Pre Headfold-2 epiblast is pluripotent and has the capacity to give rise to neural, epidermal and mesendodermal fates, implying that the ectodermal germ layer restriction has not yet occurred in the epiblast of these developmental stages.







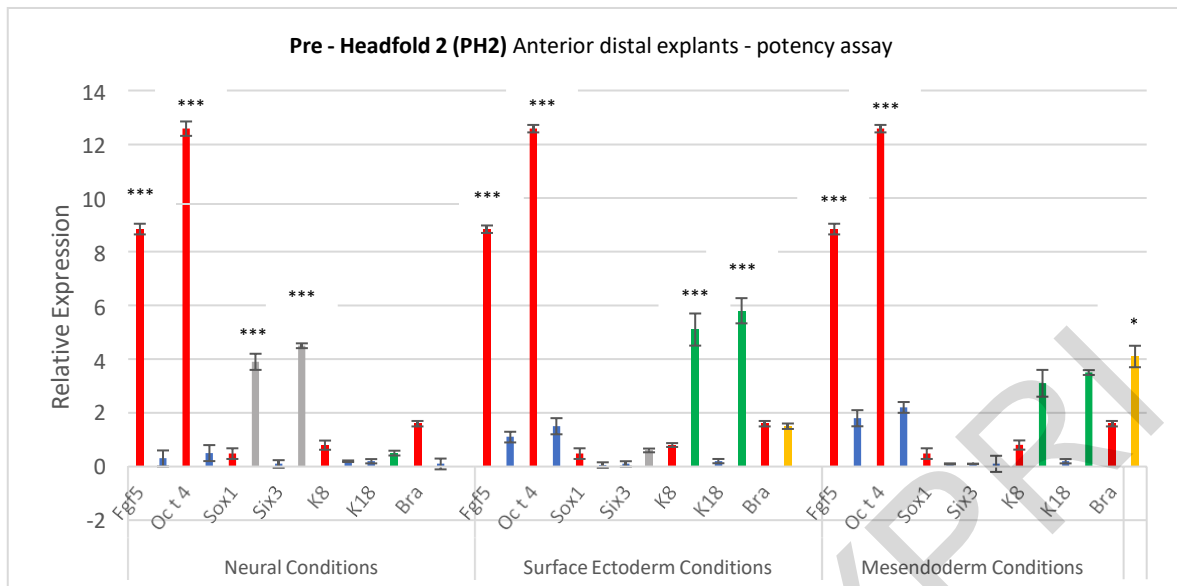
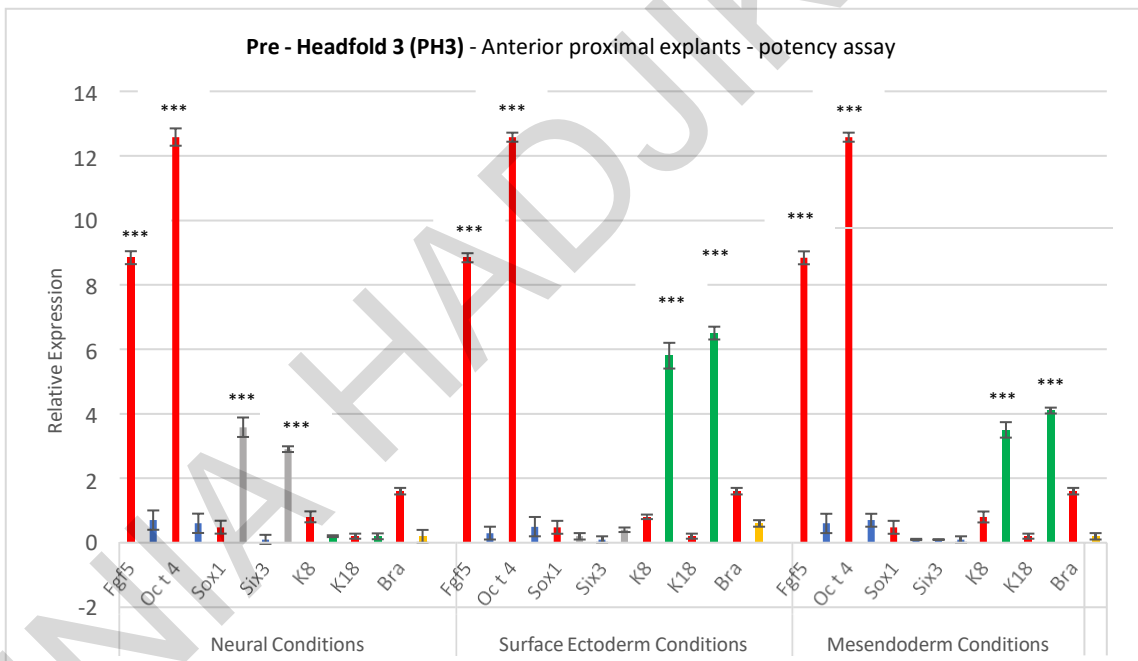
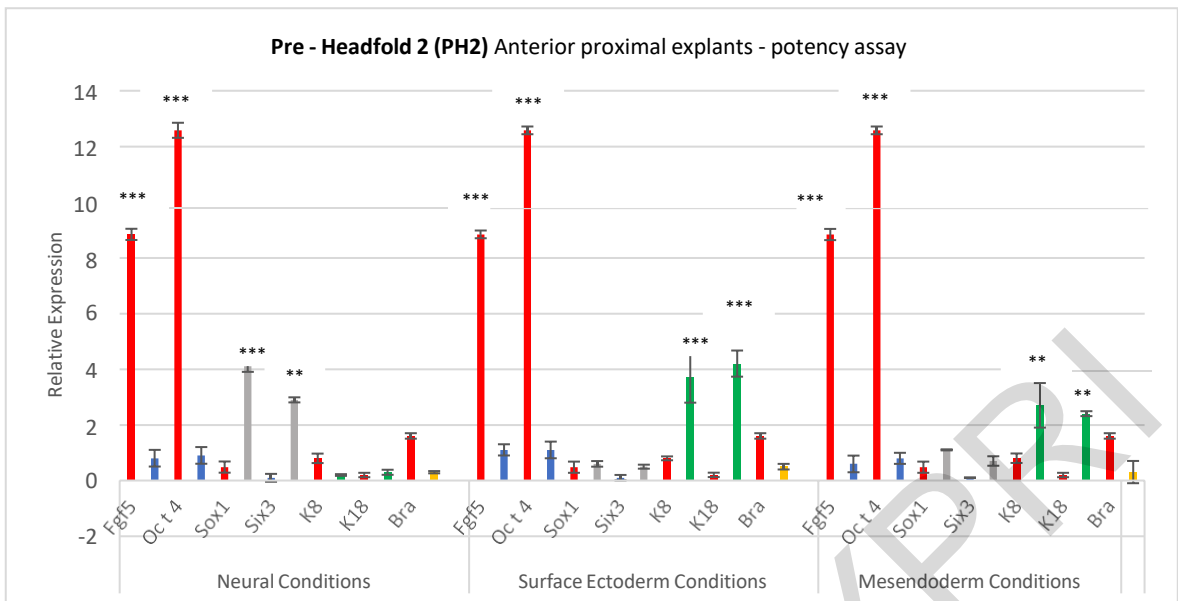


Figure 55: RT-qPCR analysis of marker gene expression of proximal and distal anterior explants of Mid Streak (MS), Late Streak (LS) and Pre Headfold 1 (PH1) and anterior distal of Pre Headfold-2 (PH2) explants cultured in all three conditions of the potency assay for 2 days.

Red columns - Pre-Streak pluripotency assay gene expression levels - Control. These explants differentiate in all three embryonic germ layers retaining their pluripotency showed by statistically significant increase of neural, surface ectoderm and mesoderm gene expression levels compared to the control. Note the pluripotency related genes *Oct4* and *Fgf5* are very low (statistically significant reduction compared to the control levels). Early markers for differentiation towards neural (*Sox1* and *Six3*) surface ectoderm (*K8* and *K18*) and mesoderm (*Bra*) fates, are statistically significantly elevated compared to the control levels. Relative expression to the housekeeping gene b-actin. n=6 biological replicates. *P <0.05. Error bars represent s.d

The anterior proximal of pre-Headfold 2 (PH2) and the whole anterior of Pre-Headfold 3 (PH3) have restricted their potency to neural and surface ectoderm (ectodermal) fates

The explants of proximal Pre-headfold 2 as well as the proximal and distal explants of Pre-headfold3 showed elevated expression of the neural markers *Sox1* and *Six3* when cultured under neural differentiation conditions. By contrast, under surface ectoderm differentiation conditions, the expression of these neural markers was absent. Rather, epidermal markers such as *K8*, *K18*, were observed. In the presence of only BMP2 (mesendoderm potency conditions), the epidermal markers examined were again upregulated. Very low levels of the mesoderm marker *Bra* were observed even when explants were cultured in the presence of only BMP2 (Figure 56). These results may suggest that the anterior proximal tissue of the pre-headfold 2 epiblast and the whole anterior of the pre-headfold 3 epiblast have restricted their potency towards neural and surface ectoderm fates.



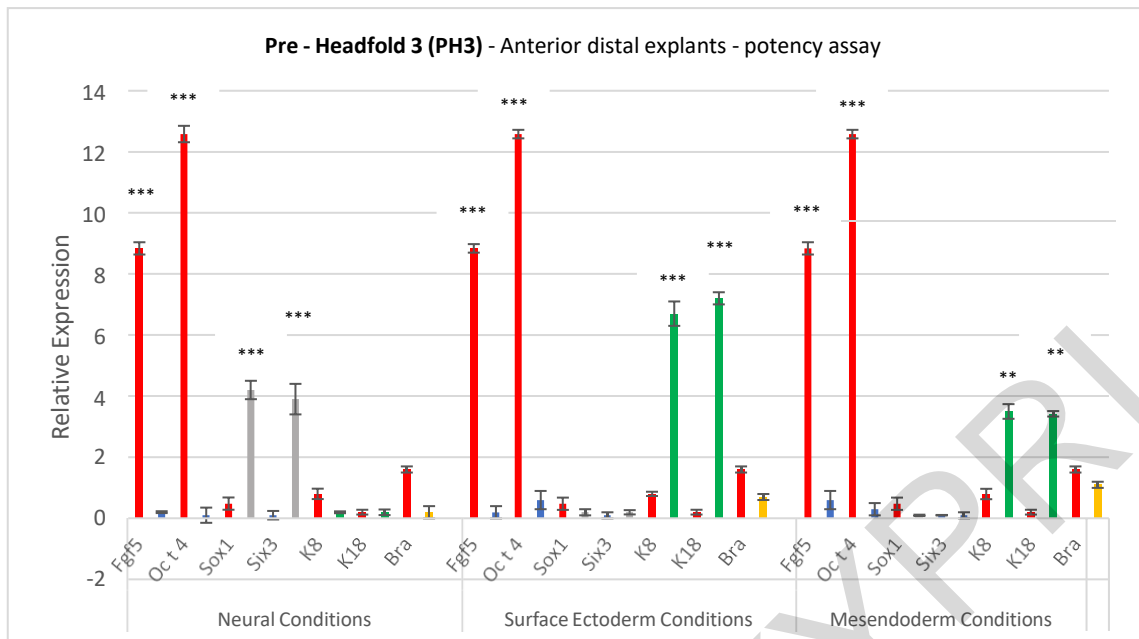


Figure 56: RT-qPCR analysis of marker gene expression of proximal anterior explants of PreHeadfold 2 (PH2) and anterior proximal and distal explants of Pre – Headfold 3 (PH3) cultured in all three conditions of the potency assay for 2 days

Red columns - Pre-Streak pluripotency assay gene expression levels – Control. Note the pluripotency-related genes *Oct4* and *Fgf5* are almost undetectable (statistically significant reduction compared to the control levels). Early markers for differentiation towards neural (*Sox1* and *Six3*) and surface ectoderm (*K8* and *K18*) fates, are statistically significantly elevated compared to the control levels. Relative expression to the housekeeping gene *beta-actin*. n=6 biological replicates. *P < 0.05. Error bars represent s.d

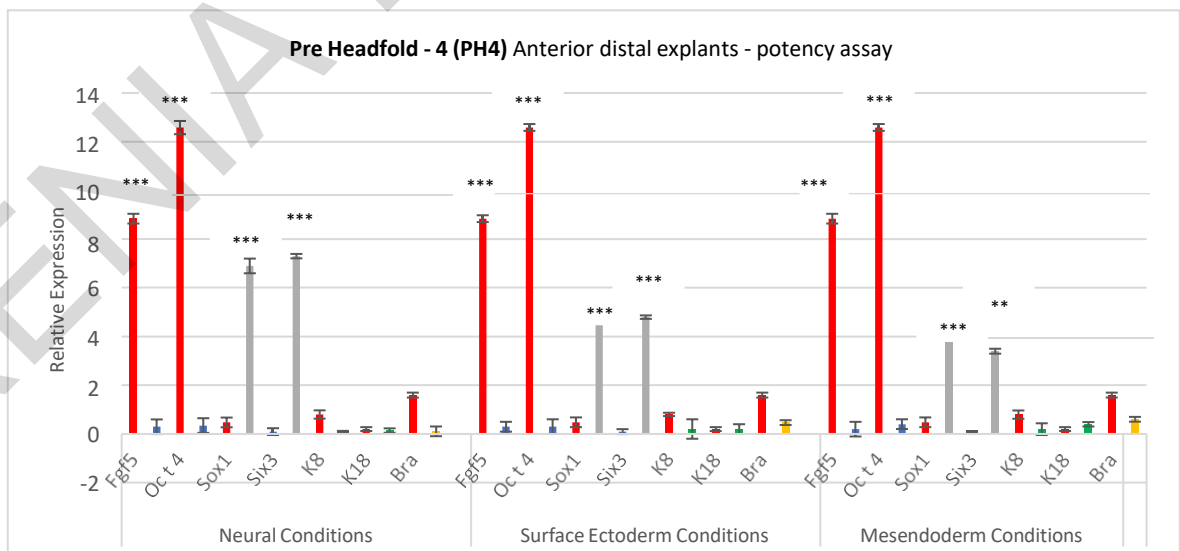
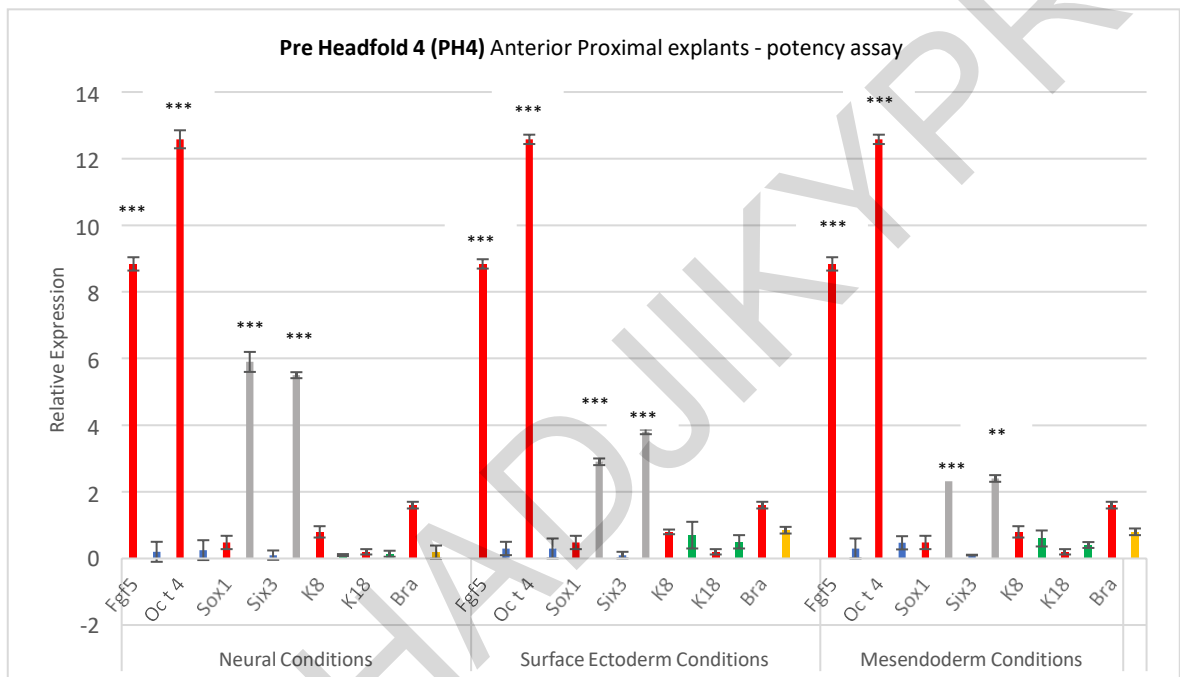
At the Pre Headfold-4 and Early Headfold stages there is further restriction of potency of the entire anterior epiblast (except probably its most proximal edge) to only neural fate

It is said that the neural plate has been formed by E7.5, which is supported by ISH of *Hesx1* and *Six3* in the anterior ectoderm (Li et al., 2013) at this developmental time point. Expression of the epidermal markers *K8* and *K18* in the anterior epiblast's most proximal region, suggests that the specification of the epidermal region might have also occurred.

In contrast to explants from earlier developmental stages, it was shown that the addition of SB43 and BMP2 in the culture media could not restrict the formation of neuroectoderm outgrowths. Specifically, RT-qPCR analysis showed that SB43 + BMP2 or BMP2 treatment alone did not cause a statistically significant difference in the expression of surface ectoderm or mesoderm markers in the anterior proximal/ distal explants. Explants of Pre-Headfold 4 and Early Headfold stages (both anterior proximal and anterior distal explants) did not respond to the different culture conditions but rather exhibited upregulation of only neural gene expression suggesting that neural restriction is already determined/committed by this time in development (Figure 57).

Previous studies have proposed that, instead of inhibiting neuronal formation at headfold stages, BMP4 guides the specification and differentiation of neural progenitors (Moon et al., 2009; Shan et al., 2011). This was consistent with the results of this study, as BMP2 was not seen to eradicate neural gene expression but only modified these expression levels. Overall, it is supported that the ectoderm lineage is committed by Pre Headfold-4 developmental stage suggesting that this is the time of the emergence of cells that are not able to respond to signalling cues and their fate is restricted to neural and non-neural ectoderm.

XENIA HADJIKYPRIS



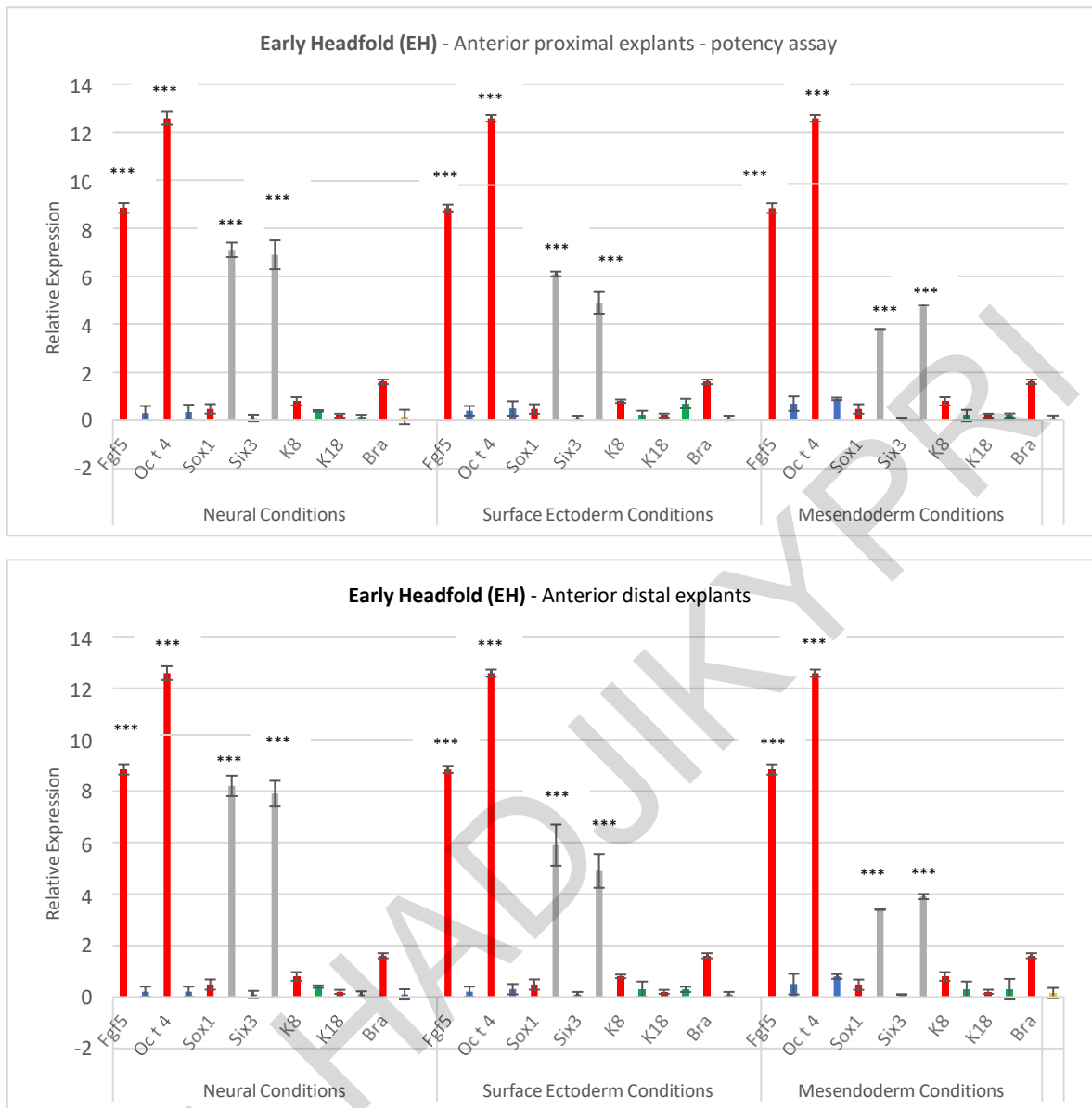


Figure 57: RT-qPCR analysis of marker gene expression of proximal anterior and proximal distal explants of Pre Headfold 4 (PH2) and Early Headfold (EH) cultured in all three conditions of the potency assay for 2 days

Red columns - Pre-Streak pluripotency assay gene expression levels – Control. Note the pluripotency-related genes *Oct4* and *Fgf5* are almost undetectable (statistically significant reduction compared to the control levels). Early markers for differentiation towards only neural (*Sox1* and *Six3*) fates, are statistically significantly elevated compared to the control levels. Relative expression to the housekeeping gene b-actin. n=6 biological replicates. *P < 0.05. Error bars represent s.d

Conclusions Regarding Specific Aim 4:

A new *in vitro* potency assay for identifying whether a mouse postimplantation tissue can differentiate towards neural differentiation, surface ectoderm or mesendoderm differentiation.

This assay is designed to be informative about the potency of the tissue in case it is found not to be pluripotent. It involves explant culture for 48h on surfaces coated with FBS in a serum- free/chemically defined liquid medium (N2/B27) supplemented with (i) SB43 (Nodal Inhibitor) to promote neural differentiation (ii) SB43 (Nodal Inhibitor) + BMP2 to predominantly promote surface ectoderm differentiation (with some mesendoderm differentiation) (iii) BMP2 to predominantly promote mesendoderm differentiation (with some surface ectoderm differentiation).

According to this assay (a) Neural differentiation - displayed flat and compact outgrowths with distinct cell borders and expression of early neural genes (b) Surface ectoderm differentiation – displayed compact flat outgrowths with distinct cell borders that by 48h they show typical cobbled- stone morphology (indicative of surface ectoderm) and expression of surface ectoderm markers and (c) Mesendoderm differentiation – displayed compact flat outgrowths with distinct cell borders that by 72h they show scattered 3-D regions on top of the flat outgrowth that spontaneously contract and mesendodermal gene expression.

The use of this potency assay revealed that the earliest restriction of potency during ectoderm development occurs at PH2 (stage of full streak extension) in the anterior-proximal epiblast and is restricted towards ectodermal fates (sometimes called bipotent ectoderm).

4.5 Specific Aim 5, its hypothesis and its results:

Specific Aim 5: This project result section aimed to identify whether this defective trophoblast- caused ectoderm phenotype seen in E8.3 *Ets2* mutants, represent a pathological phenotype (that is, one that is not encountered during normal development), or a phenotype also seen during normal development at an earlier stage prior to neural induction. This was done when the initial *Dlx5* and *Fgf5* expression was assessed using our novel staging system.

Importance of specific aim 5: These mutants represent an excellent in vivo model of loss of trophoblastic influences. Trophoblastic influences investigated using the *Ets2* mutants can give new insights about the collective role of extraembryonic tissues on post-implantation epiblast development, with emphasis on its differentiation towards ectodermal fates. The specific aim investigated in this part of the project stem from our unpublished ectoderm phenotype seen in *Ets2* mutants (Annex - Figure 2) (Hadjikypr, Drakou and Georgiades), which represent an in vivo model system for investigating trophoblastic influences on embryo development (Georgiades and Rossant, 2006; Polydorou and Georgiades 2013).

The definition of ‘anterior epiblast or ectoderm phenotype’ as used in this project refers to our unpublished and novel defective trophoblast-mediated embryonic phenotype seen in the entire anterior epiblast of E8.3 *Ets2* mutants. This phenotype comprises: (a) absence of neural induction based on absence of expression of pan-neural plate marker *Sox1* (Aubert et al., 2003; Yang and Klingensmith, 2006; Uchikawa et al., 2011), and (b) a never-seen before co-expression of the early surface ectoderm gene *Dlx5* (Cajal et al., 2012; Li et al., 2013) with the pluripotency-related gene *Fgf5*, a widely used undifferentiated post-implantation epiblast marker and pluripotency-related gene. (Hebert et al., 1991; Li et al., 2013).

Hypotheses of Specific aim 5:

If co expression of *Dlx5* and *Fgf5* exist during a developmental stage of normal wildtype development, then the anterior epiblast - ectoderm phenotype presented in the *Ets2* mutants is not pathological but also exists during normal development.

If co expression of *Dlx5* and *Fgf5* does not exist during a developmental stage of normal wildtype development, then the anterior epiblast - ectoderm phenotype presented in the *Ets2* mutants can be said as pathological that does not exist during normal development.

Results of Specific Aim 5:

Verification of early ectoderm phenotype in E8.3 mouse embryos lacking a functional *Ets2* gene (*Ets2*^{-/-} type-II mutants) and investigation whether it is encountered during normal development at an earlier stage

Genetic profiling of the epiblast of *Ets2* type-II mutants revealed whether it differentiates towards ectodermal (neural or surface ectoderm) fates, or remains undifferentiated. If this type of differentiation exists, it is expected to be found in the anterior epiblast region of type-II mutants. As described in the Introduction section, the posterior epiblast of type-II mutants forms the PS and mesoderm, but displays failure of PS elongation to the distal tip of the embryo while mesoderm cells fail to show proper migration away from the PS region (Georgiades and Rossant 2006); (Polydorou and Georgiades 2013). Any ectoderm differentiation defects seen in these mutant conceptuses should be considered to be caused by absence of a functional *Ets2* in the extraembryonic region, specifically in the trophoblast compartment, as explained above.

To investigate this phenotype, type-II mutants were examined at E8.3 by Wholemount ISH (WISH). This involved examination of expression of *Sox1* (pan-neural marker), *Dlx5* (marker of non-neural ectoderm), as well as *Fgf5* (epiblast marker). Double color WISH was also carried out, to confirm the existence and localization of PS in type-II mutants (Polydorou and Georgiades 2013) by *Bra* expression (orange colour) together with *Dlx5* (blue colour) (Figure 58).

Examination of type-II mutants at E8.3, when control embryos reach the late headfold/early somite stage, showed no expression of neural genes, as evidenced by absence of *Sox1* (n=4/4) (Figure 58). On the other hand, *Dlx5* (n=5/5) show widespread expression in the anterior epiblast of E8.3 type-II mutants (Figure 58). The simultaneous detection of *Bra* and *Dlx5* in the same embryo (n=2/2) confirmed the anterior localization of the ectopic *Dlx5* expression (Figure 58). The expression of *Fgf5* (n=3/3) was found in the entire epiblast region of these mutants. The molecular description of anterior epiblast of these mutants in this study verifies our unpublished results.

These findings may indicate the following regarding the role of trophoblast signalling during normal ectoderm development. Trophoblast signalling during normal ectoderm development within anterior epiblast it is suggested to: (i) promote neural induction (new role for trophoblast) (ii) it is required for restricting surface ectoderm gene expression to anterior-proximal epiblast and downregulating pluripotency-related gene *Fgf5* from anterior epiblast.

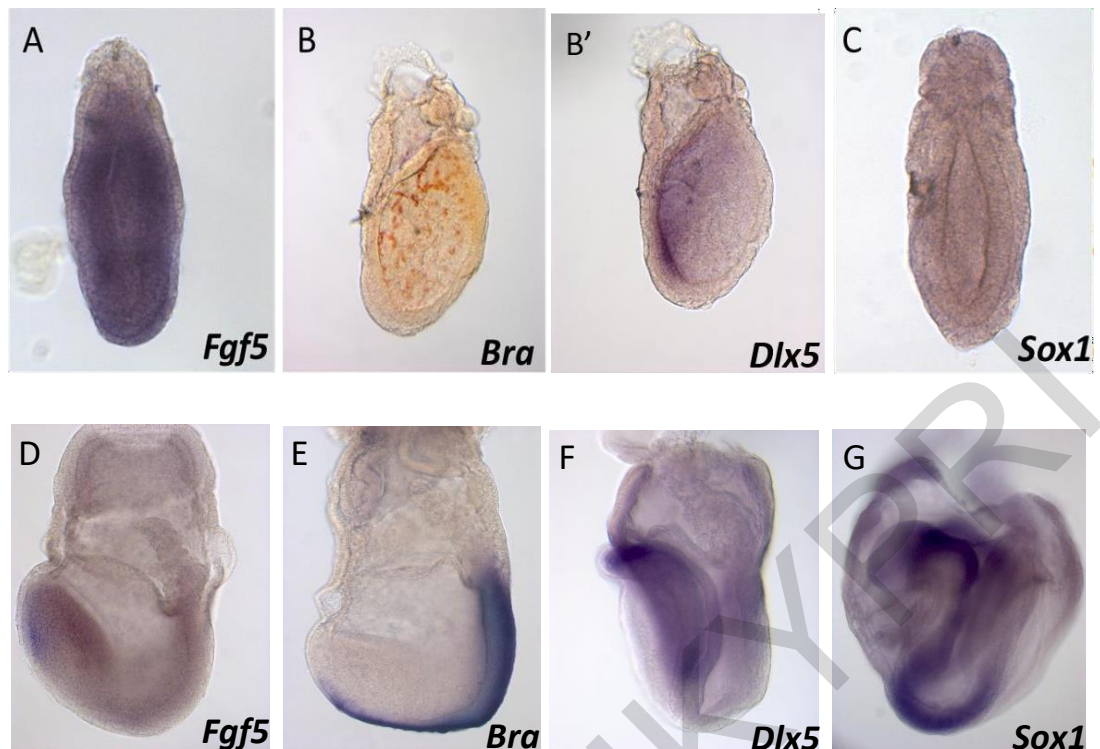


Figure 58: Gene expression assessed by RNA in situ hybridization of the *Ets2* type II E8.3 mutant embryos and wildtype E8.25 embryos

Ets2 E8.3 type II mutants (A-C), E8.25 wildtype embryos (D-G). (A) The entire epiblast of the mutants expresses the epiblast related gene marker *Fgf5*. (B, B') Double in Situ Hybridization with *Bra* (orange) and *Dlx5* (blue) of the same embryo. Note the presence of *Bra* marking the PS and the presence of *Dlx5* on the anterior epiblast of the mutant (C) Absence of *Sox1* expression in the mutants. (D) No expression of *Fgf5* in wildtype embryo. (E) *Bra* expression extends to the posterior side. (F) Anterior – proximal expression of *Dlx5*. (G) *Sox1* expressed in the anterior side of the embryo. Panels A-C are of the same magnification (16x magnification). Panels D-G are of the same magnification (10x magnification).

The co-expression of *Fgf5* and *Dlx5* also exists during normal development at the Pre Headfold-1 (PH1) and Pre Headfold 2 (PH2) stages.

The in-situ data of *Fgf5/Dlx5* indicate that these genes are co-expressed in the anterior-proximal epiblast during normal development at PH1 and PH2, a time before earliest neural genes are expressed (PH3 stages - see Figures 35-37). Therefore, the anterior epiblast – ectoderm phenotype presented in type II E8.3 mutants of *Dlx5* and *Fgf5* coexpression at their anterior epiblast region was also observed during normal development, found at the anterior most proximal epiblast side of the PH1 and PH2 stage embryos (Figure 59).

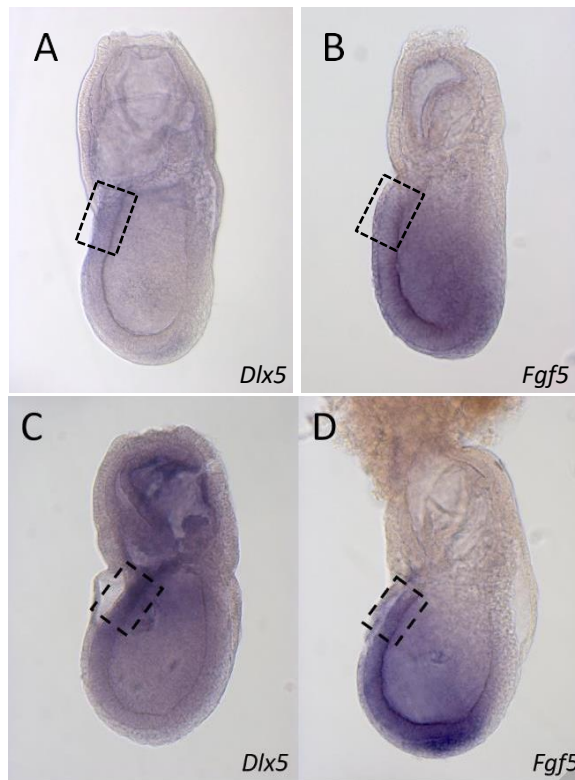


Figure 59: Gene expression assessed by RNA in situ hybridization of the Co expression of *Dlx5* and *Fgf5* (Non neural ectoderm and pluripotency related epiblast markers, respectively) during normal development at the Pre Headfold-1 (PH1) and Pre Headfold-2 (PH2) stages

A and B – Pre Headfold 1 stage. C and D Pre Headfold 2 stage. Note at these stages both *Dlx5* and *Fgf5* are co expressed at the anterior proximal epiblast region. Dotted black box shows this epiblast side of co-expression. All panels are of the same magnification (10x magnification 1,6 optovar).

Conclusions Regarding Specific Aim 5:

The molecular description of anterior epiblast of *Ets2*^{-/-} type II mutants verifies the early ectoderm phenotype seen in our unpublished results (Annex – Figure 2) as we also observe coexpression of *Fgf5* and *Dlx5* in the absence of *Sox1*.

It was indicated that these genes are also co-expressed in the anterior-proximal epiblast during normal development at PH1 and PH2, a time before earliest neural genes are expressed.

Therefore, it is suggested that the anterior epiblast of these mutants may be confined at either PH1 (which according to our data is pluripotent) or at PH2 stage (which according to our data in bipotent ectoderm) suggesting a new role of trophoblast during normal development to promote anterior epiblast to exit its state at PH1/PH2 so as to allow further development and subsequent differentiation to neural plate and surface ectoderm.

4.6 Specific Aim 6 (A and B), its hypothesis and its results:

Specific Aim 6A: To use the developed pluripotency assay to examine whether the anterior epiblast of E8.3 *Ets2*^{-/-} type-II mutants is pluripotent or not.

Importance of aim 6A: If anterior epiblast of *Ets2* proved to be pluripotent it would suggest a new role of trophoblast to promote exit from pluripotency so as to differentiate to neural and surface ectoderm fates. If anterior epiblast of *Ets2* proved not to be pluripotent but confined at the bipotent ectoderm state, then this would also suggest a novel role of trophoblast signalling to promote development further to this bipotent ectoderm state.

Hypotheses of specific aim 6A:

4.6.1 If during the pluripotency assay on mutant anterior epiblast, the live morphology of its explant outgrowths and the expression of pluripotency-related genes *Oct4* and *Fgf5* after 48h culture on FBS under pluripotency maintenance conditions, are as in the pluripotent control anterior epiblast from pre-streak embryos (that is, flat compact outgrowth with indistinguishable intercellular boundaries expressing *Fgf5* and *Oct4* throughout the outgrowth), then it is pluripotent.

4.6.2 If during the pluripotency assay on mutant anterior epiblast, the live morphology of its explant outgrowths and the expression of pluripotency-related genes *Oct4* and *Fgf5* after 48h culture on FBS under pluripotency assay culture conditions, are as in the non-pluripotent anterior epiblast from early headfold embryos (that is outgrowth with distinguishable intercellular boundaries not expressing *Fgf5* and *Oct4* throughout the outgrowth), then it is not pluripotent.

Methodology of specific aim 6A

This involved isolation of anterior epiblast fragments from the *Ets2*^{-/-} type II mutants and culturing them under the aforementioned pluripotency conditions (FBS-coated surfaces in N2/B27 with Activin A, Fgf2 and XAV939) for 48h, followed by examination of live morphology of explant outgrowths and ISH-based gene expression for the pluripotency related genes *Oct4* and *Fgf5*, as well as for the early pan-neural marker *Sox1*.

Results of specific aim 6A:

The anterior epiblast of E8.3 *Ets2*^{-/-} type-II mutants is not pluripotent as shown by the use of pluripotency assay developed here

The pluripotency and potency assays were applied when using the anterior epiblast explants of type II E8.3 mutants to check for the pluripotency status of this tissue.

Live explant outgrowth morphology and gene expression assessment by RNA In situ hybridization revealed that the anterior epiblast of mutants is not pluripotent because: (a) its explant outgrowths have different live morphology from that of pluripotent pre-streak control anterior epiblast and (b) display reduced not throughout expression of *Oct4* and *Fgf5* of the outgrowth, unlike the situation in control pre-streak outgrowths (Figure 60).

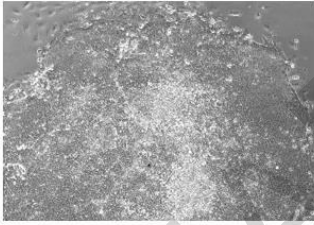
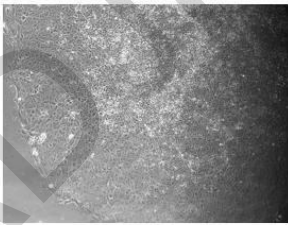

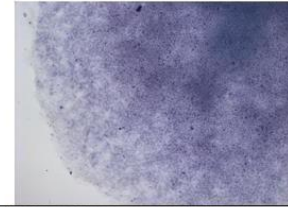

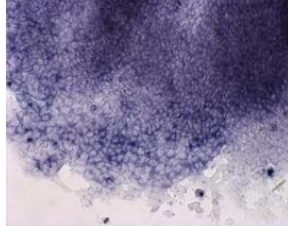
	Pre – Streak anterior epiblast explant under pluripotency assay conditions	<i>Ets2</i> ^{-/-} type II anterior epiblast explant under pluripotency assay conditions
live		
<i>Oct4</i>		
<i>Fgf5</i>		

Figure 60: Live morphology and RNA in situ hybridization for gene expression analysis of outgrowths of anterior epiblast explants from pre-streak (pluripotent epiblast) and anterior *Ets2*^{-/-} type II epiblast

Expression of indicated genes in outgrowths of anterior epiblast explants from Pre streak stage and anterior epiblast of *Ets2* mutants after 48h culture under pluripotency conditions (N2/B27, Activin- A, Fgf2 and XAV939 on FBS). Note the compact nature and the indistinct cell-to-cell borders of the

cells from outgrowths derived from pre-streak explants (n = 18/18), consistent with pluripotent morphology. In contrast the cells making up the outgrowths from the mutants have a different morphology with distinct cell to cell borders (especially at the periphery) (n = 3/3), consistent with non-pluripotent morphology. Also note that pluripotency-related genes *Oct4* and *Fgf5* are expressed throughout the outgrowths derived from pre-streak/pluripotent explants (n = 4/4), but are not expressed throughout the outgrowths of *Ets2* ^{-/-} type II anterior epiblast (n=2/2). All panels are at 16x magnification.

Specific Aim 6B: To use our potency assay to examine the potency of the non-pluripotent anterior epiblast of E8.3 *Ets2*^{-/-} type-II mutants.

Importance of specific aim 6B: The results of this aim will be informative about the role of trophoblast in early ectoderm development. For example, if potency is that of bipotent ectoderm this would mean that in the anterior epiblast of mutants is confined at this state and trophoblast signalling is required for further restriction of potency so that further neural and surface ectoderm differentiation can proceed.

Hypotheses of specific aim 6B:

If tested anterior epiblast explant of *Ets2* ^{-/-} type II at the time of its isolation has restricted its potency to neural and surface ectoderm fates, its outgrowth at the end of culture should produce differentiation towards: (a) neural fates in the presence of SB43, (b) only surface ectoderm fates in the presence of SB43/Bmp2, and (c) some surface ectoderm differentiation in the presence of Bmp2.

If tested anterior epiblast explant of *Ets2* ^{-/-} type II at the time of its isolation has restricted its potency to neural fates, its outgrowth at the end of culture should produce differentiation towards: (a) neural fates in the presence of SB43, (b) no surface ectoderm or mesendoderm fates in the presence of SB43/BMP2, and (c) no mesendoderm or surface ectoderm fates in the presence of BMP2. If neural restriction is also determined/committed (i.e., already specified irreversibly to neural fates), then we should expect to get neural differentiation under all conditions.

If tested anterior epiblast explant of *Ets2* ^{-/-} type II at the time of its isolation has restricted its potency to surface ectoderm fates, its outgrowth at the end of culture should produce differentiation towards:

(a) no neural fates in the presence of SB43, (b) only surface ectoderm fates in the presence of SB43/BMP2, and (c) surface ectoderm fates in the presence of BMP2. If surface ectoderm restriction is also determined/committed (i.e., already specified irreversibly to surface ectoderm fates), then we should expect to get surface ectoderm under all

conditions.

If tested anterior epiblast explant of *Ets2*^{-/-} type II at the time of its isolation has restricted its potency to mesendoderm fates, its outgrowth at the end of culture should produce differentiation towards: (a) no neural fates in the presence of SB43, (b) only mesendoderm fates in the presence of SB43/BMP2, and (c) only mesendoderm fates in the presence of BMP2. If mesendoderm restriction is also determined/committed (i.e., already specified irreversibly to mesendoderm fates), then we should expect to get mesendoderm under all conditions.

Methodology of specific aim 6B

This involved isolation of anterior epiblast fragments from the *Ets2*^{-/-} type II mutants and culturing them under the aforementioned potency assay conditions (FBS-coated surfaces in N2/B27 with (a) SB43 (b) SB43 + BMP2 (c) BMP2) for 48h, followed by examination of live morphology of explant outgrowths and ISH-based gene expression for the neural related gene *Sox1*, the early surface ectoderm marker *K8* and the mesoderm marker *Bra*.

Results of specific aim 6B

Preliminary results showing restriction of potency of *Ets2*^{-/-} anterior epiblast towards surfaceectoderm fates

These result section consists of preliminary data that need further validation. Apart from the ability to show differentiation towards surface ectodermal fates (evident by the expression of *K8*) (Figure 61) following the culture of the anterior epiblast of type II *Ets2* mutants under the surface ectoderm potency assay culture conditions (N2/B27 + SB43 + BMP2), no further results could be produced. This is because anterior explant of these mutants failed to adhere and did not survive when cultured under neural potency assay culture conditions. Furthermore, following culture of these explants under mesendoderm potency assay culture conditions the explants failed to adhere but survived as floating tissue that was spontaneously contracting (Figure 61).

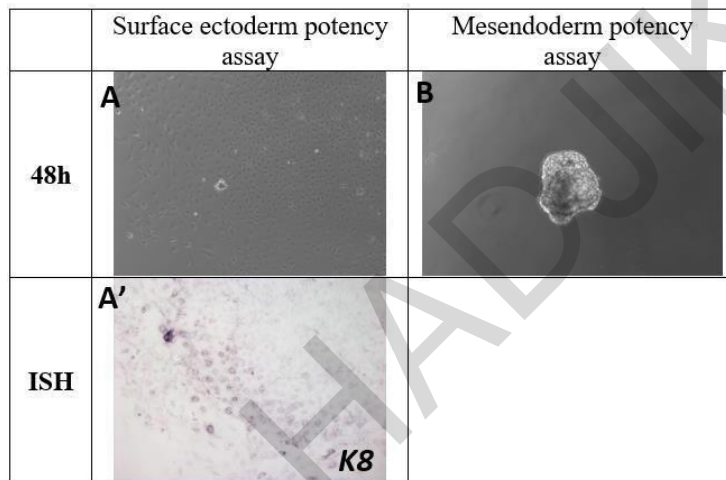


Figure 61: Live morphology and Gene expression of anterior epiblast explants of *Ets2* type II E8.3 mutants cultured using the surface ectoderm (N2/B27 + SB43 + BMP2 on FBS) and mesendoderm potency assay (N2/B27 + BMP2 on FBS) culture conditions for 2 days

A and A' is the same outgrowth. Note the same flat cobbled-like stone like cell morphology (A) under the surface ectoderm potency assay culture conditions and the expression of the early surface ectoderm marker *K8* (A') in some areas of the outgrowth. When the mesendoderm potency assay culture conditions were used the epiblast explant did not adhere but survived as floating tissue (B). All panels are of the same magnification (16x magnification).

Conclusions Regarding Specific Aim 6:

The use of the pluripotency and potency assays to investigate whether the anterior epiblast of the *Ets2*^{-/-} type II mutants is pluripotent or not, and whether its potency is restricted towards specific fates revealed that anterior epiblast of these mutants is not pluripotent and can differentiate towards surface ectodermal fates because its explant outgrowths: (a) have different live morphology from that of pluripotent pre-streak control anterior epiblast (b) display expression of *Oct4* and *Fgf5* that is reduced and not throughout the outgrowth, unlike the situation in control outgrowths (c) have a similar morphology to the pre – streak control explants that differentiated towards surface ectoderm when cultured under surface ectoderm differentiation conditions and (d) show expression of the surface ectoderm gene marker *K8* in some areas of the explant outgrowth.

4.7 Specific Aim 7, its hypothesis and its results:

To establish the first chemically defined specification assay for mammalian tissues and to use it to identify the specification status of anterior-proximal and anterior-distal epiblast in pre-streak mouse embryos, fated to predominantly ectodermal fates.

Brief Background regarding Specific aim 7:

Specification assays are designed to provide a neutral culture environment (that is, one that does not influence to what the tested tissue explant differentiates), so as to reveal how it is programmed to differentiate at the time of its isolation (that is, to reveal its specification status). Knowing the specification status of a cell/tissue is important to understanding its development because tissues change their specification status during development and for a tissue to differentiate according to its fate, it has to first become specified towards this fate (Gilbert and Barresi 2016).

Serum-free and chemically defined tissue culture conditions that do not contain signalling molecules that could influence how the tested tissue differentiates are considered a neutral culture environment for the purposes of specification assays (Slack 1991). Although such specification assays have been employed for assessing the specification status of embryonic tissues from non-mammalian vertebrates such as frog (Dale and Slack 1987) and chick (Patthey, Edlund and Gunhaga 2009), they have not been reported for mammalian embryonic tissues. The only specification assay that used mouse embryo tissue explants, although included culture in a serum-free/chemically defined liquid medium, the explants were cultured on surfaces coated with serum (Li et al., 2013). However, since serum is undefined and contains molecules that could influence how a tissue differentiates, mammalian specification assays that do contain culture surfaces coated with undefined substances such as serum would be desirable. This issue was addressed by this project.

Hypotheses of Specific aim 7:

1. If isolated anterior epiblast tissue cultured under novel serum-free chemically defined conditions (that is, in N2/B27 liquid medium on fibronectin-coated culture surfaces) can attach to the culture surface and produce an outgrowth during culture, this could be considered as a neutral culture medium, and therefore the first specification assay for mammalian tissues.

2. If the above hypothesis is satisfied:

The type of differentiation seen in the explant outgrowth after culture (assessed by live morphology and RNA in situ for early differentiation markers of all three germ layers: *K8* and *K18* for surface ectoderm, *Sox1* for neural and *Bra* for mesendoderm) would be the tissue's specification status.

(a) If more than one type of differentiations is seen, this would suggest that the explant contains different cell types that are specified differently because, by definition, the specification status of a tissue is that of a tissue that consists of the same cells.

Methodology of Specific aim 7:

This involved isolation of anterior proximal and anterior distal epiblast fragments from pre-streak (PS) pluripotent embryos and culturing them under the aforementioned specification assay conditions (Fibronectin-coated surfaces in N2/B27 liquid media) for 48h, followed by examination of live morphology of explant outgrowths and ISH-based gene expression for the surface ectoderm related genes *K8* and *K18*, for the early pan-neural marker *Sox1* and the mesoderm marker *Bra*.

Results of Specific aim 7:

Since no chemically defined/serum-free mammalian specification assays exist, the specification status of pre-streak anterior epiblast (anterior-proximal and anterior-distal fragments) was examined here for the first time. At this stage, anterior-distal epiblast is fated to form neural structures whereas anterior-proximal epiblast mainly forms surface ectoderm and amniotic ectoderm while its most proximal edge is fated to form extraembryonic mesoderm (Lawson, Meneses, and Pedersen 1991; Chuva de Sousa Lopes, Roelen, Lawson and Zwijsen 2022).

At the Pre-Streak (PS) stage, anterior-proximal and anterior-distal epiblasts are specified differently: The Pre-Streak anterior proximal epiblast is specified mainly towards surface ectoderm and mesodermal fates while the Pre-Streak anterior distal epiblast is specified mainly towards neural fates.

This was the first time a specification assay has been established for embryonic mammalian tissues satisfying hypothesis 7.1. These data regarding the specification status of anterior epiblast are preliminary because they need further gene expression assessment. Besides this, our preliminary data suggest that the anterior-distal and anterior-proximal epiblast from pre-streak embryos is specified differently.

Specifically, the anterior-proximal epiblast contains two regions that are specified differently. The vast majority of it is specified towards surface ectoderm fates and a small part of it towards mesodermal fates as evident by the cell morphology of the explant outgrowths and the expression of surface ectodermal and mesodermal markers (Figure 62). On the other hand, anterior-distal epiblast is neutrally specified as evident by the explant outgrowth cell morphology and the expression of neural markers. (Figure 63). This specification is the same as the fate of this region, suggesting that during further development, distal anterior epiblast does not change its specification.

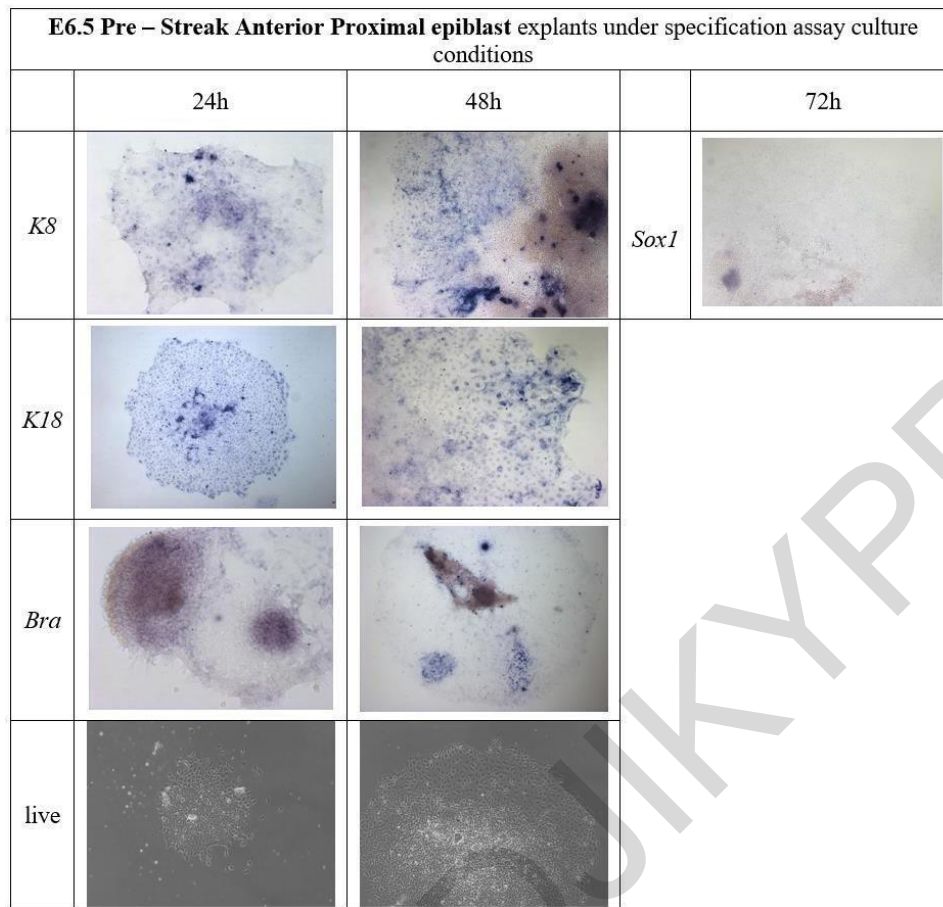


Figure 62: Live morphology and Gene expression of anterior proximal epiblast explants from E6.5 Pre-Streak embryos cultured under the specification assay culture conditions (N2/B27 onFibronectin) for 24, 48h and 72h

Note the flat cobble-like stone like cell morphology at 48h of live morphology resembling the cell morphology of culture outgrowths cultured under surface ectoderm potency assay. Note the expression of surface ectoderm markers (*K8*, *K18*) and some expression of mesoderm marker (*Bra*). Absence of neural related (*Sox1*) markers. 48h and 72h panels are of the same magnification (16x magnification) and 24h panels are of the same magnification (25x magnification).

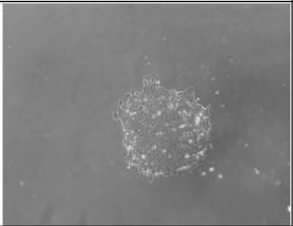
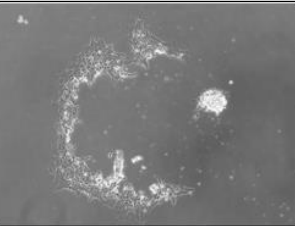

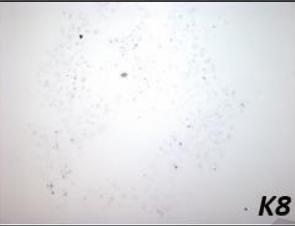
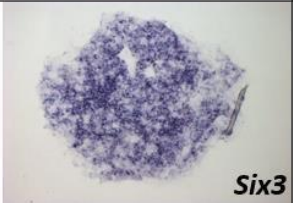
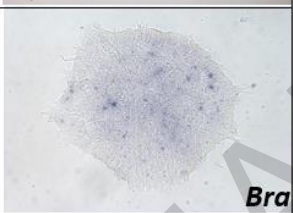
E6.5 Pre – Streak Anterior Distal epiblast explants under specification assay culture conditions		
	24h	48h
live		
ISH	 <i>Sox1</i>	 <i>K8</i>
ISH	 <i>Six3</i>	
ISH	 <i>Bra</i>	

Figure 63: Live morphology and Gene expression of anterior distal epiblast explants from E6.5Pre-Streak embryos cultured under the specification assay culture conditions (N2/B27 on Fibronectin) for 24h and 48h

Note the flat and compact outgrowths with distinct cell borders at 24h that changes to loosely arranged elongated cells by 48h. Dehiscence of cells also observed at 48h. Note the expression of neural markers (*Sox1*, *Six3*) and the absence of early surface ectoderm marker (*K8*) and early mesendoderm markers (*Bra*). Live, *Sox1* and *K8* panels are of the same magnification (16x magnification). *Six3* and *Bra* panels are of the same magnification (25x magnification).

Conclusions Regarding Specific Aim 7:

Here for the first time a specification assay has been established for embryonic mammalian tissues. This specification assay will allow the investigation of the specification status of epiblast tissues of interest at any given time in development, so as to investigate whether this is the same as its fate or whether during further development its specification needs to change according to its fate.

The preliminary data here suggested that the anterior-distal and anterior-proximal epiblast from pre-streak embryos is specified differently. Specifically, the anterior-distal epiblast is neurally specified. This specification is the same as the fate of this region, suggesting that during further development, distal anterior epiblast does not change its specification. The anterior proximal epiblast on the other hand, is specified towards surface ectoderm and mesodermal fates suggesting that the specification of this region changes during development.

DISCUSSION

The ectoderm, together with the mesoderm and endoderm germ layers consist the progenitors of all tissues of the foetus/new-born. Ectoderm is the least understood mammalian germ layer of all three. Ectodermal development begins within that part of the epiblast epithelium (progenitor of foetus/new-born) whose cells: (a) are fated to form ectodermal derivatives, mainly neural and surface ectoderm tissues, and (b) remain within the epiblast, as they do not exit it through the primitive streak during gastrulation to form the other two germ layers, the mesoderm and endoderm. This project's main interest was to investigate the early mammalian ectoderm development using the mouse as a model by studying the development of anterior epiblast, which is fated to mainly form brain and head surface ectoderm, the earliest-formed ectodermal derivatives.

One of the aims of this study (Aim 1) was to establish a more comprehensive, refined mouse staging system, compared to the existing ones, which is extensively based on live morphology of embryos from before the beginning of gastrulation and up to the late headfold stage. This was achieved by using novel combinations of external embryo features and gene expression validation, and resulted in the subdivision of this period into fifteen stages, as opposed to the existing nine stages proposed by the staging systems currently in use.

Existing staging systems subdivides the period from just before gastrulation and up to the late headfold stage into 9 or 10 stages: Prestreak (PS), Early streak (ES), Midstreak (MS), Late streak (LS), Late streak - early (allantoic) bud (LSEB), Early preheadfold (EPHF), Late preheadfold (LPHF), Early headfold (EHF) and Late headfold (LHF) (Downs and Davies 1993; Rivera-Perez, Jones and Tam 2010; Lawson and Wilson 2016). These staging systems also characterise the embryonic stages depending on the presence and the relative size of the allantoic bud (Zero bud - OB, Early bud - EB and Late bud - LB), an extraembryonic mesodermal outgrowth. The discrepancies regarding this extraembryonic structure derive from the fact that there is no established definition of the size of the bud. In addition, the time of its appearance seems to vary between the different mouse strains. Lastly, due to variability of development between the littermates of the same litter and between different litters during the same embryonic age (time elapsed since fertilization, precise staging of individual embryos during this time in development is essential in order to achieve comparability and reproducibility between all the different studies undertaken in this research area. There are several unknown factors that were addressed by Aim 1. This includes a) that existing staging does not identify the stage when gastrulation begins and the stages immediately preceding it. This is important as recent evidence indicate that gastrulation initiates with the appearance of the EMT

epiblast component of the streak prior to mesoderm formation, b) It is unknown whether existing stages can be subdivided into new stages, c) It is unknown whether pre-headfold (PH) period can be staged by not relying on presence and length of allantoic bud as the main criterion, as its onset shows inter-strain heterochrony, and therefore is not applicable to all mouse strains, d) It is unknown when the primitive streak first reaches its full length, e) there are unknowns about anterior head process (timing of its appearance and position of its anterior end), the posterior part of anterior mesoderm: strip of mesodermal tissue necessary for correct brain development that eventually becomes situated underneath the midline of developing brain except its most anterior part.

This study established a more refined staging system based on the subdivision of development into a specific temporal sequence of embryos with different structural features called stage and not their embryonic age, the period from just before gastrulation and up to the late headfold stage into 15 stages.

This new staging system addressed several issues. First, published staging was not designed to morphologically identify the stage of gastrulation initiation, which was recently shown to occur prior to mesoderm formation, at a time when posterior epiblast begins EMT, express *Bra* and downregulates *Sox2* (Morgani, Metzger, Nichols, Siggia and Hadjantonakis 2018; Morgani and Hadjantonakis 2020; Sheng, Martinez and Sutherland 2021). Our study identified this stage, named NS stage, using a novel combination of morphological criteria including embryo opacity (Figure 17). This was validated by live imaging as well as after in situ hybridization for the expression of *Bra* and *Sox2* (Figure 17).

This staging system also achieved to subdivide the LS stage into two stages (LS-1 and LS-2) using a novel criterion and not the subjective criterion of the presence of the allantoic bud as previously subdivided (Lawson and Wilson 2016). This new criterion involved whether or not the anterior end of the streak (detected by the distal end of mesodermal wings) in these embryos reaches the proximal border of the distal tip region (Figure 22).

Furthermore, existing staging of when amnion has just formed (stage named either 'neural plate/no allantoic bud' or 'transition between late streak/early bud and early pre-headfold') (Downs and Davies 1993; Rivera-Perez, Jones and Tam 2010; Lawson and Wilson 2016) suggested that this stage is when streak attains its full length, that is, reaches the mid-point of the distal tip (Lawson and Wilson 2016). However, our findings suggest that at this stage (named here PH1) the streak has yet to reach the mid-point of the distal tip, based on epiblast *Bra* expression in PH1 embryos (Figure 38). The stage when

the primitive streak attains its full length was identified here to be the PH2 (Figure 38) stage distinguished from the PH1 as PH2 is characterized by the new morphological feature of the thickening of the lower layer found beneath the distal tip region (Figure 28). Therefore, by using a combination of new morphological features this system identified the beginning of gastrulation and the stage of primitive streak full length. Other morphological characteristics that are used in this system for the first time was the appearance of the immature/mature state of morphological node (Figure 24) and the shape of the inner epiblast, the latter used when embryos were seen from front to back. These diagnostic features allowed the segregation of the pre-headfold stages without depending on the presence and/or size of the allantoic bud.

The utilization of this staging system further supported the need to obtain a more detailed spatiotemporal map of gene expression markers informative of important developmental processes happening during this time. This was the main concern of Aim 2 of this project. Specifically, spatiotemporal aspects of these gene expressions have provided evidence about the events happening during the development of the early mammalian ectoderm germ layer by studying their expression in the anterior epiblast, which is fated to mainly form brain and head surface ectoderm, the earliest- formed ectodermal derivatives.

Our conclusions when the new staging system was used validated by gene expression were suggesting that: (a) *Fgf5* (a pluripotency related gene) and *Dlx5* (early surface ectoderm marker) are co-expressed in anterior-proximal epiblast during a transient period, from PH1 to PH3 (at PH 1 reduced *Fgf5*, very low levels of *Dlx5*); at PH2, reduced *Fgf5*, strong *Dlx5* expression; at PH3, same as PH2; from PH4 onwards *Fgf5* is lost from anterior-proximal epiblast whilst *Dlx5* is strongly expressed), (Figures 33 and 34) (b) neural plate formation (at least anterior neural plate) may begin at PH3 since earliest expression of *Hesx1* in epiblast and earliest upregulation of *Six3* occur at the PH3 in anterior-proximal epiblast (Figures 36 and 37). *Six3* and *Hesx1* are the earliest known anterior neural markers (Gestri et al., 2005; Cajal et al., 2012). Since PH3 stage is the earliest stage when the inner surface of distal epiblast changes from U to V/truncated V (Figure 29), this suggests that this could be a morphological feature of neural plate, (c) PH2 is the only stage where strong *Dlx5* expression is coexpressed with *Fgf5* prior to the onset of early neural genes *Six3/Hesx1/Sox1* (Figures 33, 34, 35, 36 and 37). This suggests that the anterior epiblast of *Ets2* (also displaying the coexpression of *Fgf5/Dlx5* – Figure Annex 2 and Figure 58) mutants may be confined at PH2 stage. This was the stage also shown here when anterior-proximal epiblast restricts its potency to only ectodermal fates (neural and surface ectoderm fates), (d) *Fgf5* in anterior epiblast first becomes reduced (but is still detectable) in its proximal region at PH1 stage while by PH4 becomes

undetectable (Figure 33). This suggests that pluripotency of anterior-proximal epiblast is lost by PH4 and may occur earlier, sometime between the stages PH1 to PH3, (e) *Sox2* expression appears at the posterior epiblast of PH4, suggesting that ectomesodermal progenitors appear at this stage and lastly (Figure 39)(f) anterior head process (posterior AME) based on *Bra* expression: appears during LS-2 and PH1 stages, remains within anterior half of distal tip at PH2, extends beyond anterior distal tip at PH3, reaches the mid-point of anterior embryonic region at PH4 and reaches its full length at late headfold (Figure 38).

Until today there have only been a few studies in the literature that addressed the existence of a putative ectodermal population in the mouse embryo. Such study (Cajal et al., 2012) identified a small group of cells found between the anterior proximal and distal epiblast regions at E7.0 stage in which single cells could contribute to both surface ectoderm and neural ectoderm during normal embryonic development. Extending from this study's findings and by using explant culture approaches another study identified that the anterior proximal at 7.0 stage [no allantoic bud (OB) and early allantoic bud (EB) stages] consists of a region within the developing ectoderm germ layer that has restricted its potency only towards neural and surface ectoderm fates and can efficiently differentiate into epidermis or neural tissue depending on the local environmental signals (such as the presence or absence of BMP4) (Li et al., 2013).

In relation to this project's main aim to investigate early ectoderm development, another project's Aim (specifically Aim 3) was to establish a new *in vitro* pluripotency assay for identifying whether a mouse postimplantation tissue is pluripotent or not. As mentioned above, loss of pluripotency is an important event in the development of the early ectoderm germ layer. Pluripotency assays for mouse embryonic tissues already exist, both *in vivo* and *in vitro*. *In vivo* pluripotency assays, generation of experimental teratomas (Bulic Jakus F. et al., 2016) or embryo chimaeras (Tang and West. 2000) on the other hand have several disadvantages. Both assays are technically difficult (e.g., tissue transplantations of tested tissue at specific locations in adult mice or embryos) and also experimental teratoma assays have a relatively long duration of at least one month. Furthermore, the only existing *in vitro* pluripotency assay (ability of tested tissue to generate epiblast stem cell lines) has disadvantages that include long its duration of at least 3 weeks, the assay requires disruption of cell-to cell contacts that may alter potency of tested tissue, and it is not spatially sensitive (if only part of tested tissue is pluripotent, the assay's outcome will be that it is pluripotent). According to these restrictions it was unknown whether an *in vitro* pluripotency assay can be developed that is relatively technically easy (as opposed to the technically difficult *in vivo* assays), faster - taking less duration of a few days than the existing *in vitro* assay), whether it could not involve disruption of intercellular contacts of tested tissue and also whether it could be spatially sensitive (if only part of tested tissue is pluripotent, assay should be able to identify this).

The results of this Aim supported the establishment of a new *in vitro* pluripotency assay that is faster, technically easier, spatially sensitive while not involving cell contacts disruption. These minimal assay conditions, involve culture for 48h in pluripotency conditions, that can be followed by live morphology imaging and *Oct4/Fgf5* WISH technique were for the first time used on mouse embryonic tissues.

Following the establishment of this pluripotency *in vitro* assay and in combination with our revised embryo staging, we aimed to identify the stage when pluripotency during early ectoderm development (anterior epiblast development) is first lost. It is already known that pluripotency of anterior epiblast is lost at some point between the early streak and the pre-headfold period (Li et al.,2013) but the exact stage when pluripotency of anterior epiblast is lost remains unknown.

According to the results of this assay, it was found that a tissue is: (a) pluripotent if its outgrowth at the end of culture is flat/compact and made of small cells with largely indistinguishable intercellular borders (based on live morphology) and expresses *Oct4* and *Fgf5* throughout in all its cells (based on ISH) (Figures 40 and 41), and (b) not pluripotent if its outgrowth at the end of culture deviates from the above live morphology (e.g., made up of loosely arranged cells and/or cells with distinguishable intercellular borders) and does not express *Oct4* and *Fgf5* or expresses these genes in some but not all, of its cells (based on ISH). Application of our new *in vitro* pluripotency assay and our revised embryo staging system for identifying the earliest stage when pluripotency is lost in anterior epiblast during early ectoderm development suggests that this takes place at PH2, at least from part of anterior epiblast (Figures 43 and 44).

Extending to the relation to this project's main aim to investigate early ectoderm development, Aim 4 of this project was to establish a new *in vitro* potency assay for identifying the potency of anterior-proximal and anterior-distal epiblast during early ectoderm development during the stages mid-streak to late headfold stage. Potency assays for mouse embryonic tissues already exist, both *in vivo* and *in vitro*. *In vivo* potency assays (generation of experimental teratomas or embryo chimaeras by transplantation of tested tissue) have the same disadvantages as *in vivo* pluripotency assays discussed above. Both assays are technically difficult while teratoma assays have a relatively long duration. The only existing *in vitro* potency assay (Li et al., 2013) has several disadvantages. First this assay does not involve a negative control tissue (i.e., one that is not pluripotent), and also it does not include spatial information about gene expression. According to these it was unknown whether an *in vitro* potency assay can be developed that is relatively technically easy, faster and able to provide spatial expression information.

The results of this Aim supported the establishment of a new *in vitro* potency assay that is faster, technically easier, spatially sensitive while not involving cell contacts disruption. These minimal assay conditions, involve culture for 48h in potency assay conditions, that can be followed by live morphology imaging and *Oct4/Fgf5* WISH technique.

Following the establishment of this potency *in vitro* assay and in combination with our revised embryo staging, we aimed to identify the stage when potency during early ectoderm development (anterior epiblast development) is first restricted. By doing this we would be able to identify the potency state of anterior proximal and anterior distal epiblast during early ectoderm development from the MS to the EH stage. It is already known that potency of anterior epiblast is restricted at some point between the early streak and the pre-headfold period (Li et al., 2013) but what was not known was the

earliest exact stage when the anterior epiblast restricts its potency to ectodermal fates, when and in what way the anterior distal epiblast restricts its potency and also the exact stage of the earliest restriction towards only neural fates needed further exploration.

The conclusions of results drawn from the application of the novel potency assay (Aim 4) and in relation to the results of the pluripotency assay application (Aim3)/ staging system (Aim 1) and gene expression validation (Aim2) are as follows:

At the PH2 stage, is the first time that the stage of onset of the previously described bipotent ectoderm (Li et al., 2013) in anterior-proximal epiblast is demonstrated. Also, it is the first time that the previously unknown *in vivo* gene expression profile of this state is defined: coexpression of high *Dlx5*/low *Fgf5* in the absence of *Six3/Hesx1* (Figures 33, 34, 35 and 36). It is therefore suggested that coexpression of *Fgf5*, *Oct4* and *Dlx5* marks the transient, ectodermally bipotent anterior-proximal epiblast state. In brief, it was shown that the earliest restriction of potency during ectoderm development occurs at PH2 (stage of primitive streak full extension) in the anterior-proximal epiblast and is restricted towards ectodermal fates (sometimes called bipotent ectoderm), whilst anterior-distal epiblast at this stage is still pluripotent (Figure 56). This is consistent with our pluripotency assay results described above.

At the PH3 stage is the first time that this bipotent state expands to the entire anterior epiblast, as it also appears in anterior-distal epiblast. This is because the earliest restriction of potency during ectoderm development in anterior-distal epiblast occurs at PH3 and is restricted towards ectodermal fates (Figure 56). This stage is characterised by low expression of *Fgf5* extending to the entire anterior epiblast. Moreover, since PH3 is the earliest stage where we see potential signs of neural plate formation (i.e., earliest anterior epiblast expression of *Hesx1* and earliest upregulation of *Six3* in anterior-proximal epiblast (Figure 33, 35 and 36), as well as earliest transition of distal epiblast shape from 'U' to 'non-U'), this bipotent state of entire anterior epiblast may represent the neural plate stage.

Previous studies showed that the anterior epiblast fated towards brain (both anterior-proximal and anterior-distal fragments) becomes committed to only neural fates (i.e., has restricted its potency further to go from bipotent ectoderm potency state to only neural potency state) sometime between NO/EB stage and early headfold stage since it is evident in the latter but not the former (Li et al., 2013). However, the stage of onset of this potency restriction is unknown since stages after NO/EB but before early headfold have not been examined. We show here for the first time that this neural commitment begins earlier than thought, at PH4 (pre-headfold stage when mature node first appears) (Figure 57) and is marked by loss (as opposed to reduction) of *Fgf5* expression (Figure 33). For the reasons

of this potency assay the most anterior-proximal fragments chosen were missing the most proximal edge, expected to be committed to surface ectoderm fates only. This could explain why commitment only to neural fates is seen here. Future experiments should also include testing the potency of the most proximal edge of anterior epiblast at this stage.

Aim 5 of this project concerned the role of trophoblast during early ectoderm germ layer development using *Ets2* $-/-$ type II mutant mice as an *in vivo* model to investigate this. The molecular description of anterior epiblast of these mutants verifies our unpublished results (Annex – Figure 2 and Figure 58) showing coexpression of *Fgf5* and *Dlx5* and absence of *Sox1*. The results of this section indicate that these genes are also co-expressed during normal development in the anterior-proximal of PH1 and PH2 stages (Figure 59), a time before the earliest expression of neural genes (*Hesx1* and *Six3*) (Figure 35 and 36). Therefore, it is suggested that the anterior epiblast of *Ets2* mutants may be confined at either PH1 (which according to our data is pluripotent) or at PH2 stage (which according to our data is bipotent ectoderm) suggesting a new role of trophoblast to promote exit from these states, so as to allow further development. This novel role of trophoblast is in contrast to the published findings that the role of trophoblast is to maintain pluripotency and prevent precocious neural differentiation until E7.5 (Mesnard et al., 2011). Regarding Aim 6, the application of the pluripotency and potency assays using anterior epiblast of mutants revealed that this anterior epiblast tissue is not pluripotent because its explant outgrowths: (a) have different live morphology from that of pluripotent pre-streak control anterior epiblast (b) display expression of *Oct4* and *Fgf5* that is reduced and not throughout the outgrowth, unlike the situation in control outgrowths (Figure 60). Furthermore, the anterior epiblast of the mutants showed the ability to differentiate towards surface ectoderm fates (Figure 61), but as these consist of only preliminary data, the potency assay in this case should be repeated to draw meaningful conclusions on the potency of these tissues.

Regarding Aim 7 this project developed the first fully serum-free and chemically defined specification assay for testing the specification status of mammalian tissues using the anterior- proximal and anterior-distal of pre-streak mouse embryos. Since no chemically defined/serum-free mammalian specification assays exist, the specification status of E6.5 pre-streak anterior epiblast (anterior-proximal and anterior-distal fragments) was examined here for the first time. It was unknown whether mouse embryonic tissues can survive in a completely neutral environment making the study of the specification state of anterior proximal and anterior distal of PS embryos difficult.

At this stage, anterior-distal epiblast is fated to form neural structures whereas anterior-

proximal epiblast mainly forms surface ectoderm and amniotic ectoderm and its most proximal edge is fated to form extraembryonic mesoderm (Lawson, Meneses and Pedersen. 1991; Chuva et al., 2022). Our preliminary specification assay results support the establishment of a new *in vitro* specification assay that can be used for the first time for embryonic mammalian tissues. Specifically, it was suggested that the anterior-distal and anterior-proximal epiblast from pre-streak embryos are specified differently. The anterior-distal epiblast is neurally specified (Figure 63). This specification is the same as the fate of this region, suggesting that during further development, distal anterior epiblast does not change its specification, whereas the anterior proximal epiblast is specified towards surface ectoderm and mesodermal (Figure 62) suggesting that the specification of this region changes during development. The data regarding the specification status of anterior epiblast are preliminary and need further gene expression assessment of neural, mesoderm and endoderm gene markers.

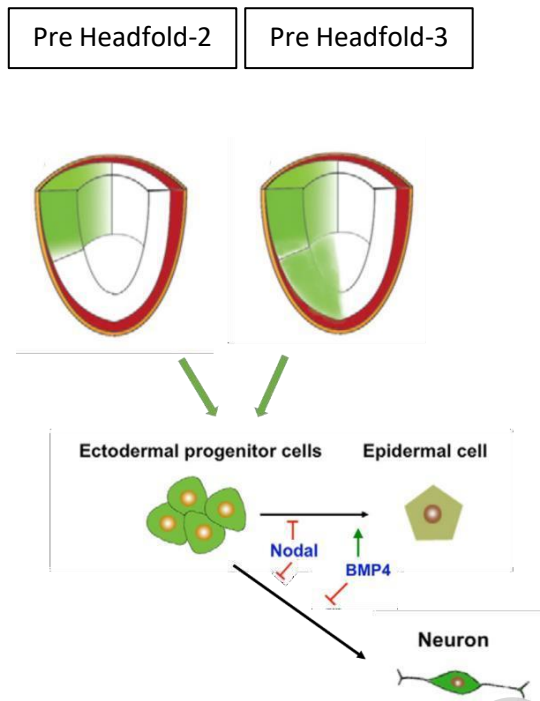


Figure 64: Model for the existence of the transient, ectodermally bipotent anterior-proximal epiblast state at PH2 stage and the transient, ectodermally bipotent anterior epiblast state at the PH3 stage during mouse embryonic development.

The anterior proximal epiblast of PH2 stage and the anterior proximal/distal epiblast of the PH3 stage restrict their potency towards ectodermal fates (surface ectoderm and neural). Modified by Liet al., 2013.

PUBLICATIONS

Hadjikyri, X., Theofanous, C., Christodoulidi Antonia. and Georgiades, P., 2024. New findings on the orientation of the mouse anterior-posterior (A-P) axis before and during the initiation of gastrulation using a more refined embryo staging. *Biochemistry and Biophysics Reports*, Volume 40, 101817.

Nikolaou, S., Hadjikyri, X., Ioannou, G., Elia, A. and Georgiades, P., 2018. Functional and phenotypic distinction of the first two trophoblast subdivisions and identification of the border between them during early postimplantation: A prerequisite for understanding early patterning during placentogenesis. *Biochemical and Biophysical Research Communications*, 496(1), pp.64-69.

XENIA HADJIKYRI

FUTURE EXPERIMENTS

This project's results revealed the earliest loss of pluripotency that occurs at the pre-headfold-2 (PH2) stage coinciding with the earliest stage when anterior-proximal epiblast restricts its potency to only ectodermal fates (neural and surface ectoderm fates). Regarding Aim 1 and 2, the established and more refined embryo staging system developed here can be further validated by the gene expression of other informative gene expression markers such as the early surface ectoderm markers *K8/ K18* to show their expression patterns during pluripotency, loss of pluripotency and restriction of potency.

Furthermore, concerning Aim 3 and 4 and to further evaluate the earliest loss of pluripotency and using the refined staging system, OCT4 and FGF5 Immunofluorescence experiments can be done on pluripotent, bipotent ectoderm and differentiated epiblast tissues to quantify the intensity of their anterior epiblast expression. Quantification of these protein levels at all stages must be performed to conclude whether this reduction, that is observed relative to the distal region or relative to the anterior epiblast of other stages, is significant.

Concerning Aim 6, The loss of pluripotency in the anterior epiblast of *Ets2* *-/-* type II embryos can be further validated when these IF experiments will be performed. Future experiments regarding Aim 6 should also include the repetition of the potency assay experiments on anterior epiblast of these mutants (that only gave preliminary results), so as to conclude on the potency state of this tissue. This would allow the further validation of the role of trophoblast in the ectoderm germ layer development.

Regarding Aim 7, the specification assay should be used on other epiblast tissues than the ones used in this current study. For example, the specification of the non-pluripotent, bipotent ectoderm anterior epiblast of the PH2 and PH3 could be examined as well as the specification state of non-pluripotent anterior epiblast of the *Ets2* *-/-* type II mutants.

ANNEXES

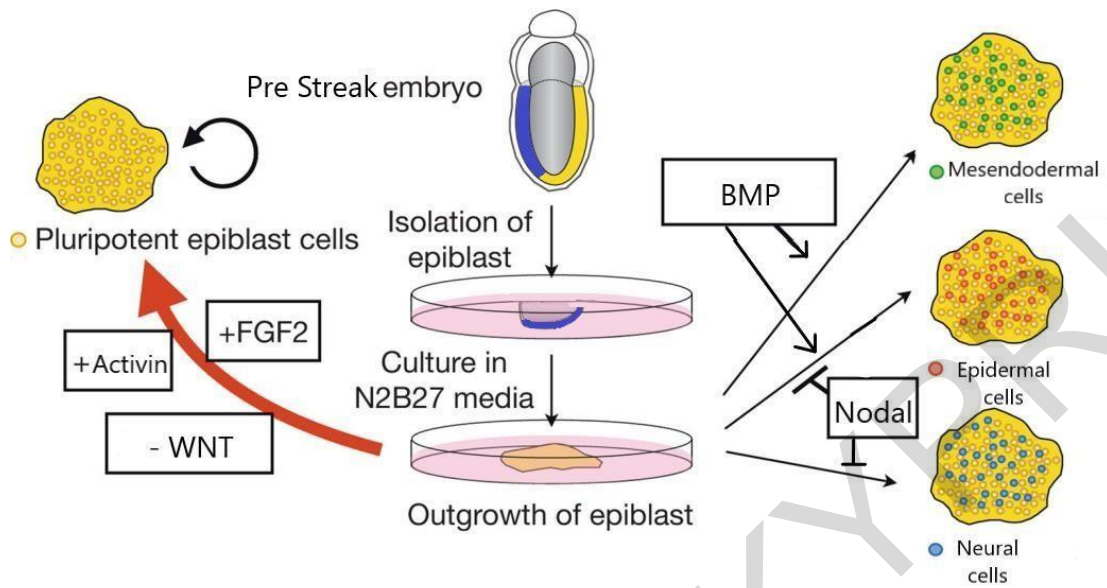


Figure Annex 1: Experimental approach of explant derivation and pluripotency / potency assay/explant culture conditions.

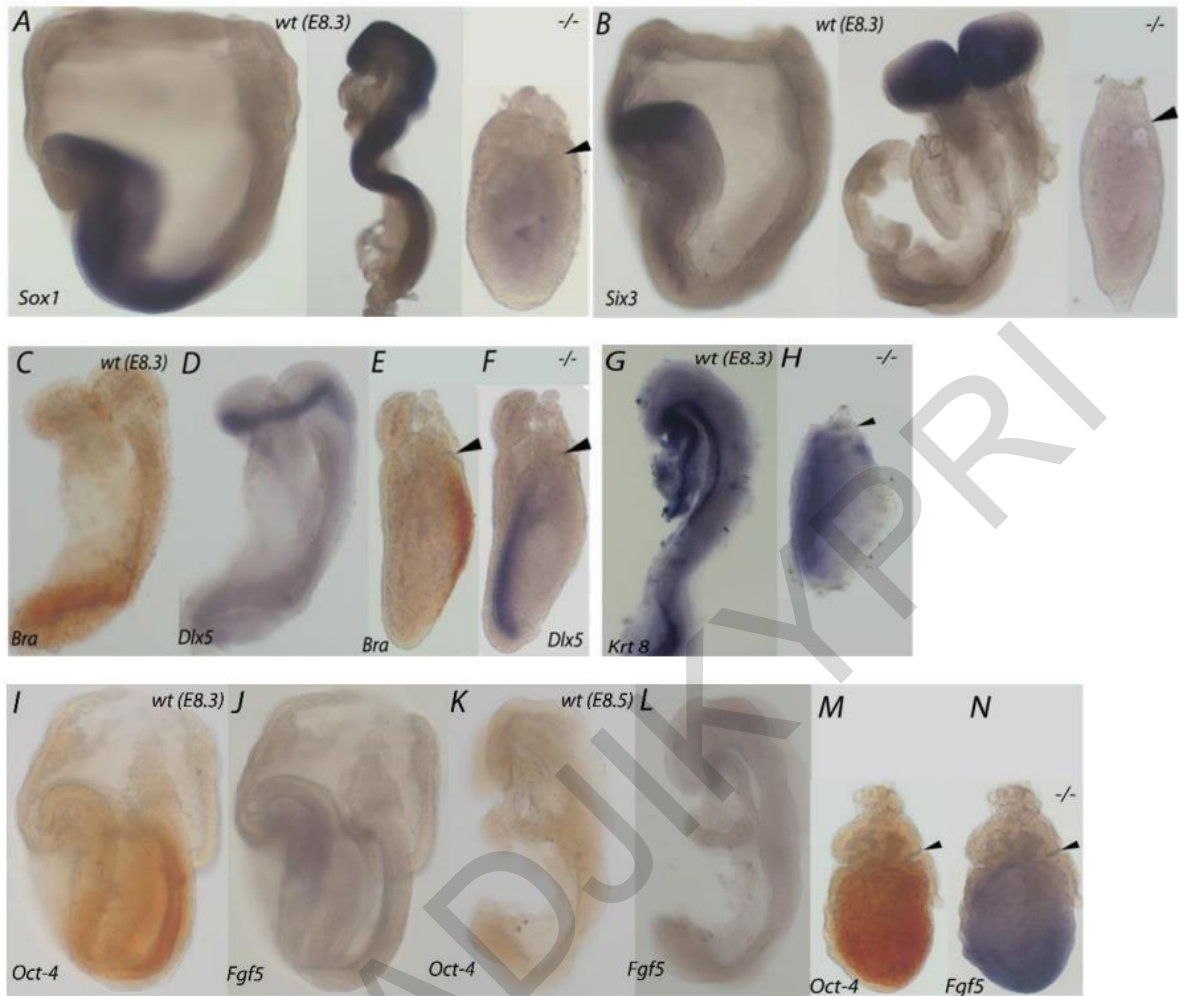


Figure Annex 2: The anterior epiblast of E8.3 *Ets2* type-II mutants does not remain undifferentiated, but exhibits differentiation towards surface ectoderm fates, at the expense of neural fates. (A) *Sox1* expression at E8.3 in wildtype control embryo (first two panels from the left) and a mutant (right panel) embryo that shows no expression. (B) *Six3* is expressed at E8.3 wildtype control embryo (first two panels from the left) and but no expression had been detected in mutant (right panel) embryos. (C,D) Double in situ hybridization with *Bra* and *Dlx5* of the same embryo in E8.3 wildtype control embryo (first two panels from the left) (E,F) and type-II mutants (right panel). *Dlx5* is expressed in the anterior epiblast of type-II mutant embryos at E8.3. (G) *K8* expression at E8.3 in control (left panel) and a mutant (right panel) embryo. Note the expression of *K8* in the anterior epiblast of type-II mutants. (I,J,K,L) Double in situ hybridization with *Oct4* and *Fgf5* of the same embryo in controls (first four panels from the left) at E8.3 and E8.5 (M,N) and type-II mutant (right panel). Note the expression of *Fgf5* which has been downregulated in the proximal epiblast of the mutant embryo. Black arrowheads denote the posterior side of embryonic-extraembryonic junction. All images for E8.3 mutant embryos are of the same magnification (16X magnification) and all images for E8.3/E8.5 wildtype control embryos are of the same magnification (8X magnification) as well.

REFERENCES

Acampora, D., Merlo, G. R., Paleari, L., Zerega, B., Postiglione, M. P., Mantero, S., Bober, E., Barbieri, O., Simeone, A. and Levi, G. (1999). Craniofacial, vestibular and bone defects in mice lacking the Distal-less-related gene *Dlx5*. *Development* 126, 3795–3809.

Ahrens K., G. Schlosser. (2005) Tissues and signals involved in the induction of placodal *Six1* expression in *Xenopus laevis*, *Dev. Biol.* 288, 40–59.

Alarcon, V. B. (2010). Cell polarity regulator PARD6B is essential for trophoblast formation in the preimplantation mouse embryo. *Biol. Reprod.* 83, 347–358

Anderson, R.M., Lawrence, A.R., Stottmann, R.W., Bachiller, D., Klingensmith, J., (2002). Chordin and noggin promote organizing centers of forebrain development in the mouse. *Development* 129, 4975–4987

Andersson, O., Reissmann, E., Jornvall, H., Ibanez, C.F., (2006). Synergistic interaction between *Gdf1* and *Nodal* during anterior axis development. *Dev. Biol.* 293, 370–381

Andoniadou CL, Signore M, Sajedi E, Gaston-Massuet C, Kelberman D, Burns AJ, Itasaki N, Dattani M, Martinez-Barbera JP. (2007). Lack of the murine homeobox gene *Hesx1* leads to a posterior transformation of the anterior forebrain. *Development*. 134(8):1499–508.

Ang, S. L., and Rossant, J. (1994). HNF-3 beta is essential for node and notochord formation in mouse development. *Cell* 78, 561–574.

Anthony, T. E., Klein, C., Fishell, G., and Heintz, N. (2004). Radial glia serve as neuronal progenitors in all regions of the central nervous system. *Neuron* 41, 881–890.

Antonica F., L.C. Orietti, R.L. Mort, M. Zernicka-Goetz. (2019) Concerted cell divisions in embryonic visceral endoderm guide anterior visceral endoderm migration, *Dev. Biol.* 450 (2) 132–140

Arnold, S. J., and Robertson, E. J. (2009). Making a commitment: cell lineage allocation and axis patterning in the early mouse embryo. *Nat. Rev. Mol. Cell Biol.* 10, 91–103.

Aubert, J., Stavridis, M. P., Tweedie, S., O'Reilly, M., Vierlinger, K., Li, M. (2003). Screening for mammalian neural genes via fluorescence-activated cell sorter purification of neural precursors from *Sox1*-gfp knockin mice. *Proc. Natl. Acad. Sci.* 100(Suppl), 11836–11841.

Avilion AA, Nicolis SK, Pevny LH, Perez L, Vivian N, et al. (2003) Multipotent cell lineages in early mouse development depend on SOX2 function. *Genes Dev* 17: 126–140.

Babu, D., Roy, S., Satir, P., Christensen, S., Bloodgood, R., Levin, M. (2013). Left-right asymmetry: cilia stir up new surprises in the node. *Open Biol.* 3, 130052–130062

Bachiller, D., Klingensmith, J., Kemp, C., Belo, J. A., Anderson, R. M., May, S. R. (2000). The organizer factors Chordin and noggin are required for mouse forebrain development. *Nature* 403, 658–661

Barenbaum M., M.E. Bronner. (2013) Identification and dissection of a key enhancer mediating cranial neural crest specific expression of transcription factor, *Ets-1*, *Dev. Biol.* 382, 567–575

Baron, M. H. (2005). Early patterning of the mouse embryo: implications for hematopoietic commitment and differentiation. *Exp Hematol* 33(9): 1015–1020.

Bazzi FI., Soroka E, Alcorn HL, Anderson KV, Flogan BLM, 2017 STRIP1, a core component of STRIPAK complexes, is essential for normal mesoderm migration in the mouse embryo. *Proc. Natl.Acad. Sci.*

Beck, S., J. A. Le Good. (2002). Extraembryonic proteases regulate Nodal signalling during gastrulation. *Nat Cell Biol* 4(12): 981-985. Beck, S., Le Good, J. A., Guzman, M., Ben Haim, N., Roy, K., Beermann, F. (2002). Extraembryonic proteases regulate nodal signalling during gastrulation. *Nat. Cell Biol.* 4, 981–985.

Beddington, R. S. P. and Robertson, E. J. (1999). Axis development and early asymmetry in mammals. *Cell* 96, 195-209.

Bedzhov I, Graham SJ, Leung CY, Zernicka-Goetz M. Developmental plasticity, cell fate specification and morphogenesis in the early mouse embryo. (2014) *Philos Trans R Soc Lond B Biol* 369(1657):20130538.

Ben-Haim, N., Lu, C., Guzman-Ayala, M., Pescatore, L., Mesnard, D., Bischofberger, M. (2006). The nodal precursor acting via activin receptors induces mesoderm by maintaining a source of its convertases and BMP4. *Dev. Cell* 11, 313–323.

Boareto, M., Iber, D., and Taylor, V. (2017). Differential interactions between notch and ID factors control neurogenesis by modulating Hes factor autoregulation. *Development* 144, 3465–3474

Brazil, D. P., Church, R. H., Surae, S., Godson, C., and Martin, F. (2015). BMP signalling: agony and antagonism in the family. *Trends Cell Biol.* 25, 249–264

Brennan J, Lu CC, Norris DP, Rodriguez TA, Beddington RS, Robertson EJ. (2001). Nodal signalling in the epiblast patterns the early mouse embryo. *Nature.* 411(6840):965-9.

Brons I.G., Smithers L.E., Trotter M.W., Rugg-Gunn P., Sun B., Chuva de Sousa Lopes S.M., Howlett S.K., Clarkson A., Ahrlund-Richter L., Pedersen R.A., Vallier L. (2007). Derivation of pluripotent epiblast stem cells from mammalian embryos. *Nature.* 448: 191-195

Brugmann S. A., P.D. Pandur, K.L. Kenyon, F. Pignoni, S.A. Moody. (2004) Six1 promotes a placodal fate within the lateral neurogenic ectoderm by functioning as both a transcriptional activator and repressor, *Development* 131, 5871–5881.

Brunner, D., K. Ducker. (1994). The ETS domain protein pointed-P2 is a target of MAP kinase in the sevenless signal transduction pathway. *Nature* 370(6488): 386-389.

Bulic-Jakus F, Katusic Bojanac A, Juric-Lekic G, Vlahovic M, Sincic N. (2015). Teratoma: from spontaneous tumors to the pluripotency/malignancy assay. *Wiley Interdiscip Rev Dev Biol.* 5(2):186-209.

Cajal M, Lawson KA, Hill B, Moreau A, Rao J, Ross A, Collignon J, Camus A. (2012). Clonal and molecular analysis of the prospective anterior neural boundary in the mouse embryo. *Development.*, 139(2), pp. 423-436.

Camus A, Davidson BP, Billiards S, Khoo P, Rivera-Perez JA, Wakamiya M. (2000). The morphogenetic role of midline mesendoderm and ectoderm in the development of the forebrain and the midbrain of the mouse embryo. *Development.* 127:1799–813

Camus, A., Perea-Gomez, A., Moreau, A. and Collignon, J. (2006). Absence of Nodal signaling promotes precocious neural differentiation in the mouse embryo. *Dev. Biol.* 295, 743-755.

Cano A, Pérez-Moreno MA, Rodrigo I, Locascio A, Blanco MJ, Del Barrio MG, Portillo F, Nieto MA. (2000). The transcription factor Snail controls epithelial-mesenchymal transitions by repressing E-cadherin expression. *Nat. Cell Biol* 2, 76–83.

- Carlin, D., Sepich, D., Grover, V. K., Cooper, M. K., Solnica-Krezel, L. & Inbal, A. (2012). Six3 cooperates with Hedgehog signaling to specify ventral telencephalon by promoting early expression of Foxg1a and repressing Wnt signaling. *Development*, 139, 2614-24.
- Chang, C. and Hemmati-Brivanlou, A. (1998). Cell fate determination in embryonic ectoderm. *J. Neurobiol.* 36, 128-151
- Chng, Z., Teo, A., Pedersen, R. A. and Vallier, L. (2010). SIP1 mediates cell-fate decisions between neuroectoderm and mesendoderm in human pluripotent stem cells. *Cell Stem Cell* 6, 59-70.
- Chuva de Sousa Lopes SM., Roelen BAJ., Lawson KA, Zwijsen A (2022). The development of the amnion in mice and other amniotes. *Philos Trans R Soc Lond B Biol Sci.* 377(1865):20210258.
- Ciruna B, Rossant J. (2001) FGF Signaling Regulates Mesoderm Cell Fate Specification and Morphogenetic Movement at the Primitive Streak. *Dev. Cell* 1, 37-49
- Ciruna BG, Schwartz L, Harpal K, Yamaguchi TP, Rossant J. (1997) Chimeric analysis of fibroblast growth factor receptor-1 (Fgfr1) function: A role for FGFR1 in morphogenetic movement through the primitive streak. *Development* 124, 2829-2841
- Clements D, Taylor HC, Herrmann BG, Stott D. (1996). Distinct regulatory control of the Brachyury gene in axial and non-axial mesoderm suggests separation of mesoderm lineages early in mouse gastrulation. *Mech Dev.* ;56(1-2):139-49.
- Clevers H (2006) Wnt/beta-catenin signaling in development and disease. *Cell* 127: 469-480.
- Collignon J, Sockanathan S, Hacker A, Cohen-Tannoudji M, Norris D, et al. (1996) A comparison of the properties of Sox-3 with SRY and two related genes, Sox-1 and Sox-2. *Development* 122: 509-520.
- Collignon, J., Varlet, I., and Robertson, E. J. (1996). Relationship between asymmetric nodal expression and the direction of embryonic turning. *Nature* 381, 155-158
- Copp AJ, Adzick NS, Chitty LS, Fletcher JM, Holmbeck GN, Shaw GM. (2015). Spina bifida. *Nat Rev Dis Primers.* 1:15007.
- Copp, A. J. (1979). Interaction between inner cell mass and trophectoderm of the mouse blastocyst. II. The fate of the polar trophectoderm. *Journal of Embryology and Experimental Morphology*, 51, 109-120.
- Croze N., F. Maczkowiak, A.H. Monsoro-Burq. (2011) Reiterative AP2a activity controls sequential steps in the neural crest gene regulatory network, *Proc. Natl. Acad. Sci. U. S. A.* 108, 155-160.
- Dale, L. and Slack, J.M.W. (1987). Regional specification within the mesoderm of early embryos of *Xenopus laevis*. *Development*, 100(2), pp.279-295.
- Davis, S., Miura, S., Hill, C., Mishina, Y., and Klingensmith, J. (2004). BMP receptor IA is required in the mammalian embryo for endodermal morphogenesis and ectodermal patterning. *Dev. Biol.* 270, 47-63.
- De Los Angeles A, Ferrari F, Xi R, Fujiwara Y, Benvenisty N, Deng H, Hochedlinger K, Jaenisch R, Lee S, Leitch HG, Lensch MW, Lujan E, Pei D, Rossant J, Wernig M, Park PJ, Daley GQ. (2015). Hallmarks of pluripotency. *Nature* 525(7570):469-78.
- Depew, M. J., Liu, J. K., Long, J. E., Presley, R., Meneses, J. J., Pedersen, R. A. and Rubenstein, J. L. (1999). Dlx5 regulates regional development of the branchial arches and sensory capsules. *Development* 126, 3831-3846

- Di Gregorio A. T-Box genes and developmental gene regulatory networks in ascidians. (2017) *CurrTop Dev Biol.* 122:55–91.
- Di-Gregorio, A., Sancho, M., Stuckey, D. W., Crompton, L. A., Godwin, J., Mishina, Y. (2007). BMP signalling inhibits premature neural differentiation in the mouse embryo. *Development* 134, 3359–3369
- Dottori, M., and Pera, M. F. (2008). Neural differentiation of human embryonic stem cells. *MethodsMol. Biol.*, 48, 19–30.
- Downs, K. M. & Davies, T. (1993). Staging of gastrulating mouse embryos by morphological landmarks in the dissecting microscope. *Development*, 118, 1255-66.
- Ekonomou A., I. Kazanis, S. Malas, H. Wood, P. Alifragis, M. Denaxa, D. Karagogeos, A. Constanti, R. Lovell-Badge, V. Episkopou. (2005). Neuronal migration and ventral subtype identity in the telencephalon depend on SOX1, *PLoS Biol.* 3 - e186
- El-Hashash, A. H., D. Warburton, et al. (2010). Genes and signals regulating murine trophoblast cell development. *Mech Dev* 127(1-2): 1-20.
- Engberg, N., Kahn, M., Petersen, D. R., Hansson, M., and Serup, P. (2010). Retinoic acid synthesis promotes development of neural progenitors from mouse embryonic stem cells by suppressing endogenous, Wnt-dependent nodal signaling. *Stem Cells* 28, 1498–1509
- Fehling HJ, Lacaud G, Kubo A, Kennedy M, Robertson S, Keller G, Kouskoff V. (2003) Tracking mesoderm induction and its specification to the hemangioblast during embryonic stem cell differentiation. *Development* 130, 4217–4227.
- Fu, J., Warmflash, A. & Lutolf, M.P. (2021) Stem-cell-based embryo models for fundamental research and translation. *Nat. Mater.* 20, 132–144
- Fujinaga, M., Brown, N. A. and Baden, J. M. (1992). Comparison of staging systems for the gastrulation and early neurulation period in rodents: a proposed new system. *Teratology*, 46, 183-90
- Gardner, R. L., Papaioannou, V. E., & Barton, S. C. (1973). Origin of the ectoplacental cone and secondary giant cells in mouse blastocysts reconstituted from isolated trophoblast and inner cell mass. *Journal of Embryology and Experimental Morphology*, 30(3), 561–572.
- Garnett A T., T.A. Square, D.M. Medeiros. (2012). BMP, Wnt and FGF signals are integrated through evolutionarily conserved enhancers to achieve robust expression of Pax3 and Zic genes at the zebrafish neural plate border, *Development* 139, 4220–4231.
- Georgiades P, Ferguson-Smith AC, Burton GL. (2002) Comparative developmental anatomy of the murine and human definitive placentae. *Placenta*; 23(1):3-19.
- Georgiades P., Rossant J. (2006) Ets2 is necessary in trophoblast for normal embryonic anteroposterior axis development. *Development* 133, 1059–1068.
- Gestri G, Carl M, Appolloni I, Wilson SW, Barsacchi G, Andreazzoli M. (2005). Six3 functions in anterior neural plate specification by promoting cell proliferation and inhibiting Bmp4 expression. *Development.* 132(10):2401-13
- Gilbert, S.F. and Barresi, M.J. (2016). *Developmental biology*, 11th edn Sunderland. MA: Sinauer Associates.
- Gonzalez, P., Cogram, P., Gerrelli, D. & Copp, A. J. (2002) Sonic hedgehog and the molecular regulation of neural tube closure. *Development* 129, 2507–2517.
- Gratsch, T. E., and O’Shea, K. S. (2002). Noggin and chordin have distinct activities in

promoting lineage commitment of mouse embryonic stem (ES) cells. *Dev. Biol.* 245, 83–94

Groves A K., C. LaBonne. (2014) Setting appropriate boundaries: fate, patterning and competence at the neural plate border, *Dev. Biol.* 389, 2–12.

Gu, P., LeMenuet, D., Chung, A. C.-K., Mancini, M., Wheeler, D. A., and Cooney, A. J. (2005). Orphan nuclear receptor GCNF is required for the repression of pluripotency genes during retinoic acid-induced embryonic stem cell differentiation. *Mol. Cell. Biol.* 25, 8507–8519

Haffner-Krausz, R., Gorivodsky, M., Chen, Y., and Lonai, P. (1999). Expression of *Fgfr2* in the early mouse embryo indicates its involvement in preimplantation development. *Mech. Dev.* 85, 167–172.

Harvey, N. T., Hughes, J. N., Lonic, A., Yap, C., Long, C., Rathjen, P. D. (2010). Response to BMP4 signalling during ES cell differentiation defines intermediates of the ectoderm lineage. *J. Cell Sci.* 123, 1796–1804.

Haub, O., and Goldfarb, M. (1991). Expression of the fibroblast growth factor-5 gene in the mouse embryo. *Development* 112, 397–406.

Hayashi, Y., Furue, M. K., Okamoto, T., Ohnuma, K., Myoishi, Y., Fukuhara, Y., et al. (2007). Integrins regulate mouse embryonic stem cell self-renewal. *Stem Cells* 25, 3005–3015

Hebert, J. M., Boyle, M., and Martin, G. R. (1991). mRNA localization studies suggest that murine FGF-5 plays a role in gastrulation. *Development* 112, 407–415.

Herrmann BG, Labeit S, Poustka A, King TR, Lehrach H. (1990). Cloning of the T gene required in mesoderm formation in the mouse. *Nature* 343:617–22

Hideyuki Murayama, Hideki Masaki, Hideyuki Sato, Tomonari Hayama, Tomoyuki Yamaguchi, Hiromitsu Nakauchi (2015). Successful reprogramming of epiblast stem cells by blocking nuclear localization of β -catenin. *Stem Cell Reports* 13;4(1):103-113.

Hintze M., R.S. Prajapati, M. Tambalo, N.A.D. Christophorou, M. Anwar, T. Grocott, A. Streit. (2017). Cell interactions, signals and transcriptional hierarchy governing placode progenitor induction, *Development* 144, 2810–2823.

Hoshino, H., Shioi, G., and Aizawa, S. (2015). AVE protein expression and visceral endoderm cell behavior during anterior-posterior axis formation in mouse embryos: asymmetry in OTX2 and DKK1 expression. *Dev. Biol.* 402, 175–191

Huelsken J, Vogel R, Brinkmann V, Erdmann B, Birchmeier C, Birchmeier W. (2000) Requirement for β -catenin in anterior-posterior axis formation in mice. *J. Cell Biol.* 148, 567–578

Inman, G. J., Nicolás, F. J., Callahan, J. F., Harling, J. D., Gaster, L. M., Reith, A. D., Laping, N. J. and Hill, C. S. (2002). SB-431542 is a potent and specific inhibitor of transforming growth factor- β superfamily type I activin receptor-like kinase (ALK) receptors ALK4, ALK5, and ALK7. *Mol. Pharmacol.* 62, 65-74.

Izzi, L., Silvestri, C., von Both, I., Labbé, E., Zakin, L., Wrana, J. L., et al. (2007). Foxh1 recruits Gsc to negatively regulate Mixl1 expression during early mouse development. *Eur. Mol. Biol. Organ. J.* 26, 3132–3143.

Jessell, T.M. (2000). Neuronal specification in the spinal cord: inductive signals and transcriptional codes. *Nat. Rev. Genet.* 1, 20–29

Kan L., N. Israsena, Z. Zhang, M. Hu, L.R. Zhao, A. Jalali, V. Sahni, J.A. Kessler. (2004). Sox1 actsthrough multiple independent pathways to promote neurogenesis, *Dev. Biol.* 269, 580–594.

Khudyakov J, M. Bronner-Fraser. (2009) Comprehensive spatiotemporal analysis of early chick neural crest network genes, *Dev. Dyn.* 238, 716–723.

Kim J, Park S, Kim YJ, Jeon CS, Lim KT, Seonwoo H, Cho SP, Chung TD, Choung PH, Choung YH, Hong BH, Chung JH. (2015). Monolayer Graphene-Directed Growth and Neuronal Differentiation of Mesenchymal Stem Cells. *J Biomed Nanotechnol* (11):2024–33.

Kinder, S. J., T. E. Tsang, et al. (2001). The organizer of the mouse gastrula is composed of a dynamic population of progenitor cells for the axial mesoderm. *Development* 128(18): 3623-3634

Kispert A, Herrmann BG, Leptin M, Reuter R. (1994) Homologs of the mouse brachyury gene are involved in the specification of posterior terminal structures in *Drosophila*, *Tribolium*, and *Locusta*. *Genes Dev.* 8:2137–50.

Kojima, Y., Kaufman-francis, K., Studdert, J. B., Steiner, K. A., Power, M. D., Loebel, D. A., Jones, V., Hor, A., DE ALencastro, G., Logan, G. J., Teber, E. T., TAm, O. H., stutz, M. D., Alexander, I. E., Pickett, H. A. & Tam, P. P. (2014). The transcriptional and functional properties of mouse epiblaststem cells resemble the anterior primitive streak. *Cell Stem Cell*, 14, 107-20.

Kong, X. B., and Zhang, C. (2009). Dickkopf (Dkk) 1 promotes the differentiation of mouse embryonic stem cells toward neuroectoderm. *In Vitro Cell. Dev. Biol. Anim.* 45, 185–193.

Kriegstein, A. R., and Gotz, M. (2003). Radial glia diversity: a matter of cell fate. *Glia* 43, 37–43.

Kumar A, Luaidi M, Lyozin GT, Sharma P, Loncarek J, Fu XY, Kuehn MR. (2015). Nodal signaling from the visceral endoderm is required to maintain Nodal gene expression in the epiblast and drive DVE/AVE migration. *Developmental Biology*, 400(1), 1–9.

Kuriyama S., M. Moreno, R. Mayor. (2009) The posteriorizing gene Gbx2 is a direct target of Wnt signalling and the earliest factor in neural crest induction, *Development* 136, 3267–3278.

Lagutin OV, Zhu CC, Kobayashi D, Topczewski J, Shimamura K, Puellas L, Russell HR, McKinnon PJ, Solnica-Krezel L, Oliver G. (2003). Six3 repression of Wnt signaling in the anterior neuroectoderm is essential for vertebrate forebrain development. *Genes Dev.* Feb 1;17(3):368-79.

Laping, N. J., Grygielko, E., Mathur, A., Butter, S., Bomberger, J., Tweed, C., Martin, W., Fornwald, J., Lehr, R., Harling, J. et al. (2002). Inhibition of transforming growth factor (TGF)-beta1-induced extracellular matrix with a novel inhibitor of the TGF-beta type I receptor kinase activity: SB- 431542. *Mol. Pharmacol.* 62, 58-64.

Lawson KA, Meneses JJ, Pedersen RA. (1991). Clonal analysis of epiblast fate during germ layer formation in the mouse embryo. *Development* 113(3): 891-911.

Lawson, K. A. & Wilson, V. (2015). A Revised Staging of Mouse Development Before Organogenesis. *Kaufman's Atlas of Mouse Development Supplement*. Academic Press.

Le Good, J. A., Joubin, K., Giraldez, A. J., Ben-Haim, N., Beck, S., Chen, Y. (2005). Nodal stability determines signaling range. *Curr. Biol.* 15, 31–36.

Levine, Ariel J. and Ali H. Brivanlou (2007). Proposal of a model of mammalian neural

induction. *Developmental Biology*. 308, 247 – 256.

Li L, Liu C, Biechele S, Zhu Q, Song L, Lanner F, Jing N, Rossant J. (2013). Location of transient ectodermal progenitor potential in mouse development. *Development*, 140(22), pp.4533-4543.

Li L, Song L, Liu C, Chen J, Peng G, Wang R, Liu P, Tang K, Rossant J, Jing N. (2015). Ectodermal progenitors derived from epiblast stem cells by inhibition of Nodal signaling. *J Mol Cell Biol*. 2015Oct;7(5):455-65.

Litsiou A., S. Hanson, A. Streit, A. (2015). Balance of FGF, BMP and WNT signalling positions the future placode territory in the head, *Development* 132, 4051–4062.

Liu JA, Cheung M. (2016). Neural crest stem cells and their potential therapeutic applications. *Dev Biol*. 419: 199–216

Liu P, Wakamiya M, Shea MJ, Albrecht U, Behringer RR, et al. (1999) Requirement for Wnt3 in vertebrate axis formation. *Nat Genet* 22: 361–365.

Liu, C., Wang, R., He, Z., Osteil, P., Wilkie, E., Yang, X., et al. (2018). Suppressing nodal Signaling activity predisposes ectodermal differentiation of Epiblast stem cells. *Stem Cell Rep*. 11, 43–57.

Loebel, D. A. F., Watson, C. M., De Young, R. A., and Tam, P. P. L. (2003). Lineage choice and differentiation in mouse embryos and embryonic stem cells. *Dev. Biol*. 264, 1–14.

Lowell, S., Benchoua, A., Heavey, B., and Smith, A. G. (2006). Notch promotes neural lineage entry by pluripotent embryonic stem cells. *PLoS Biol*. 4: e121

Lu, C. C., and Robertson, E. J. (2004). Multiple roles for nodal in the epiblast of the mouse embryo in the establishment of anterior-posterior patterning. *Dev. Biol*. 273, 149–159.

Maroulakou, I. G. and D. B. Bove (2000). Expression and function of Ets transcription factors in mammalian development: a regulatory network. *Oncogene* 19(55): 6432-6442.

Martinez Barbera, J.P., Clements, M., Thomas, P., Rodriguez, T., Meloy, D., Kioussis, D., Beddington, R.S., (2000). The homeobox gene Hex is required in definitive endodermal tissues for normal forebrain, liver and thyroid formation. *Development* 127, 2433–2445

Martinez-Barbera, J. P., Rodriguez, T. A. & Beddington, R. S. (2000). The homeobox gene *Hesx1* is required in the anterior neural ectoderm for normal forebrain formation. *Dev Biol*, 223, 422- 30.

McLarren, K. W., Litsiou, A. and Streit, A. (2003). DLX5 positions the neural crest and preplacode region at the border of the neural plate. *Dev. Biol*. 259, 34- 47.

Meier, S., Tam, P.P. (1982). Metameric pattern development in the embryonic axis of the mouse I. Differentiation of the cranial segments. *Differentiation* 21, 95–108

Mesnard D., Donnison M., Fuerer C., Pfeffer P. L., Constam D. B. (2011) The microenvironment patterns the pluripotent mouse epiblast through paracrine Furin and Pace4 proteolytic activities. *Genes Dev*. 25, 1871–1880.

Miyamoto, T., Furusawa, C., Kaneko, K., Evans, M., Kaufman, M., Martin, G. (2015). Pluripotency, differentiation, and reprogramming: a gene expression dynamics model with epigenetic feedback regulation. *PLoS Comput. Biol*. 11: e1004476.

Moody S A., A.-S. LaMantia, (2015) Transcriptional regulation of cranial sensory placode development, *Curr. Top. Dev. Biol*. 111, 301–350.

Moon, B. S., Yoon, J. Y., Kim, M. Y., Lee, S. H., Choi, T. and Choi, K. Y. (2009). Bone

morphogenetic protein 4 stimulates neuronal differentiation of neuronal stem cells through the ERK pathway. *Exp. Mol. Med.* 41, 116-125

Morgani SM., Hadjantonakis AK., (2020). Signaling regulation during gastrulation: Insights from mouse embryos and in vitro systems. *Curr Top Dev Biol.*; 137:391-431.

Morgani SM, Metzger JJ, Nichols J, Siggia ED, Hadjantonakis AK. (2018) Micropattern differentiation of mouse pluripotent stem cells recapitulate embryo regionalized cell fate patterning. *Elife.* 7: e32839.

Morgani, S., Nichols, J., and Hadjantonakis, A.-K. (2017). The many faces of pluripotency: in vitro adaptations of a continuum of in vivo states. *BMC Dev. Biol.* 17:7

Morizane A, Doi D, Kikuchi T, Nishimura K, Takahashi J. (2011) Small-molecule inhibitors of bone morphogenetic protein and activin/nodal signals promote highly efficient neural induction from human pluripotent stem cells. *J Neurosci Res.* 89:117–26

Morley RH, Lachani K, Keefe D, Gilchrist MJ, Flicek P, Smith JC (2009). A gene regulatory network directed by zebrafish no tail accounts for its roles in mesoderm formation. *Proc Natl Acad Sci USA.* 106:3829–34.

Mossahebi-Mohammadi M, Quan M, Zhang JS, Li X. (2020). FGF Signaling Pathway: A Key Regulator of Stem Cell Pluripotency. *Front Cell Dev Biol.* 18; 8:79.

Nagy A, Rossant J, Nagy R, Abramow-Newerly W, Roder JC (1993) Derivation of completely cell culture-derived mice from early-passage embryonic stem cells. *Proc Natl Acad Sci U S A* 90:8424–8428

Nichols, J., and Smith, A. (2012). Pluripotency in the embryo and in culture. *Cold Spring Harb. Perspect. Biol.* 4: a008128

Nitta KR, Takahashi S, Haramoto Y, Fukuda M, Onuma Y, Asashima M. (2006). Expression of Sox1 during *Xenopus* early embryogenesis. *Biochem Biophys Res Commun.* 8;351(1):287-93.

Nowotschin, S. and A. K. Hadjantonakis (2010). Cellular dynamics in the early mouse embryo: from axis formation to gastrulation. *Curr Opin Genet Dev* 20(4): 420-427.

Ohtsuka, T., Ishibashi, M., Gradwohl, G., Nakanishi, S., Guillemot, F., and Kageyama, R. (1999). Hes1 and Hes5 as notch effectors in mammalian neuronal differentiation. *Eur. Mol. Biol. Organ. J.* 18, 2196–2207

Okada, Y., Nonaka, S., Tanaka, Y., Saijoh, Y., Hamada, H., and Hirokawa, N. (1999). Abnormal nodal flow precedes situs inversus in *iv* and *inv* mice. *Mol. Cell* 4, 459–468

Oliver, G., Mailhos, A., Wehr, R., Copeland, N. G., Jenkins, N. A. & Gruss, P. (1995). Six3, a murine homologue of the sine oculis gene, demarcates the most anterior border of the developing neural plate and is expressed during eye development. *Development*, 121, 4045-55.

Omelenchenko Tatiana (2022). Cellular protrusions in 3D: Orchestrating early mouse embryogenesis. *Seminars in Cell and Developmental Biology* 129 (2022) 63–74.

Osorno, R., Tsakiridis, A., Wong, F., Cambray, N., Economou, C., Wilkie, R., Blin, G., Scotting, P.J., Chambers, I. and Wilson, V. (2012). The developmental dismantling of pluripotency is reversed by ectopic Oct4 expression. *Development* 139, 2288-2298

Pankratz, M. T., Li, X. J., Lavaute, T. M., Lyons, E. A., Chen, X., and Zhang, S. C. (2007). Directed neural differentiation of human embryonic stem cells via an obligated primitive anterior stage. *Stem Cells* 25, 1511–1520

Park B. Y., J.-P. Saint-Jeannet, Hindbrain-derived (2008). Wnt and Fgf signals cooperate to specify the otic placode in *Xenopus*. *Dev. Biol.* 324, 108–121.

- Patani, R., Compston, A., Puddifoot, C. A., Wyllie, D. J., Hardingham, G. E., Allen, N. D. and Chandran, S. (2009). Activin/Nodal inhibition alone accelerates highly efficient neural conversion from human embryonic stem cells and imposes a caudal positional identity. *PLoS ONE* 4, e7327
- Patthey C, Edlund T, Gunhaga L. (2009). Wnt-regulated temporal control of BMP exposure directs the choice between neural plate border and epidermal fate. *Development*. 136(1):73-83.
- Pera, S. Stein, M. Kessel. (1999). Ectodermal patterning in the avian embryo: epidermis versus neuralplate, *Development* 126 63–73.
- Pevny L.H., S. Sockanathan, M. Placzek, R. Lovell-Badge. (1998). A role for SOX1 in neural determination, *Development* 125, 1967–1978.
- Pevny LH, Lovell-Badge R (1997) Sox genes find their feet. *Curr Opin Genet Dev* 7: 338–344.
- Pieper M, K. Ahrens, E. Rink, A. Peter, G. Schlosser. (2012) Differential distribution of competence for panplacodal and neural crest induction to non-neural and neural ectoderm, *Development* 139, 1175–1187.
- Poelmann, R.E., (1981). The head process and the formation of the definitive endoderm in the mouse embryo. *Anat. Embryol.* 162, 41–49.
- Polydorou, C. and P. Georgiades (2013). Ets2-dependent trophoblast signalling is required for gastrulation progression after primitive streak initiation. *Nat Commun* 4: 1658.
- Psychoyos, D., Stern, C.D., (1996). Fates and migratory routes of primitive streak cells in the chick embryo. *Development* 122, 1523–1534.
- Ramathal, C. Y., et al. (2010). Endometrial decidualization: Of mice and men. *Seminars in Reproductive Medicine*, 28(1), 17–26.
- Ramkumar N, Omelchenko T, Silva-Gagliardi NF, McGlade CJ, Wijnholds J, Anderson KV. (2016) Crumbs2 promotes cell ingression during the epithelial-to-mesenchymal transition at gastrulation. *Nat. Cell Biol* 18, 1281–1291.
- Rashbass P, Cooke LA, Herrmann BG, Beddington RSP. (1991) A cell autonomous function of Brachyury in T/T embryonic stem cell chimaeras. *Nature* 353, 348–351.
- Riddiford, G. Schlosser. (2016). Dissecting the pre-placodal transcriptome to reveal presumptive direct targets of Six1 and Eya1 in cranial placodes, *Elife* 17666.
- Rivera-Perez, J. A., Jones, V. and Tam, P. P. (2010). Culture of whole mouse embryos at early postimplantation to organogenesis stages: developmental staging and methods. *Methods Enzymol*, 476, 185-203
- Rizvi, A. H., Camara, P. G., Kandror, E. K., Roberts, T. J., Schieren, I., Maniatis, T. (2017). Single-cell topological RNA-seq analysis reveals insights into cellular differentiation and development. *Nat. Biotechnol.* 35, 551–560.
- Robb, L. and P. P. Tam (2004). Gastrula organiser and embryonic patterning in the mouse. *Semin Cell Dev Biol* 15(5): 543-554.
- Rodriguez, T. A., Srinivas, S., Clements, M. P., Smith, J. C., and Beddington, R. S. P. (2005). Induction and migration of the anterior visceral endoderm is regulated by the extra-embryonic ectoderm. *Development* 132, 2513–2520.
- Roellig, J. Tan-Cabugao, S. Esaian, M.E. Bronner. (2017). Dynamic transcriptional signature and cell fate analysis reveals plasticity of individual neural plate border cells, *Elife* 6.
- Roese-Koerner, B., Stappert, L., and Brüstle, O. (2017). Notch/Hes signaling and miR-9

- engage in complex feedback interactions controlling neural progenitor cell proliferation and differentiation. *Neurogenesis* 4: e1313647.
- Rossant, J. (2004). Lineage development and polar asymmetries in the peri-implantation mouse blastocyst. *Seminars in Cell & Developmental Biology*, 15(5), 573–581.
- Rossant, J. and J. C. Cross (2001). Placental development: lessons from mouse mutants. *Nat Rev Genet* 2(7): 538-548.
- Saga Y, Miyagawa-Tomita S, Takagi A, Kitajima S, Miyazaki Ji, Inoue T. (1999). *MesP1* is expressed in the heart precursor cells and required for the formation of a single heart tube. *Development* 126, 3437–3447
- Saiz, N. and B. Plusa (2013). Early cell fate decisions in the mouse embryo. *Reproduction* 145(3): R65-80.
- Sanchez-Arrones, J.L. Ferran., M. Hidalgo-Sanchez, L. Puellas. (2015) Origin and early development of the chicken adenohipophysis, *Front. Neuroanat.* 9 - 7
- Sanchez-Ramos J, Song S, Cardozo-Pelaez F, Hazzi C, Stedeford T, Willing A, Freeman TB, Saporta S, Janssen W, Patel N, Cooper DR, Sanberg PR. (2000). Adult bone marrow stromal cells differentiate into neural cells in vitro. *Exp Neurol.* Aug;164(2):247-56.
- Sansom, S. N., Griffiths, D. S., Faedo, A., Kleinjan, D.-J., Ruan, Y., Smith, J. (2009). The level of the transcription factor *Pax6* is essential for controlling the balance between neural stem cell self-renewal and neurogenesis. *PLoS Genet.* 5: e1000511.
- Sauka-Spengler T., M. Bronner-Fraser. (2008) Evolution of the neural crest viewed from a gene regulatory perspective, *Genesis* 46, 673–682.
- Scaffidi P, Bianchi ME (2001) Spatially precise DNA bending is an essential activity of the *Sox-2* transcription factor. *J Biol Chem* 276: 47296–47301.
- Schlosser G. (2015). Chapter Eight - Vertebrate Cranial Placodes as Evolutionary Innovations—the Ancestor's Tale. *Current Topics in Developmental Biology*. Volume 111, 2015, Pages 235- 300.
- Schmidt W: The amniotic fluid compartment: the fetal habitat (1992). *Adv Anat Embryol Cell Biol*, 127:1-100
- Schoenwolf, G. C. (1984). Histological and ultrastructural studies of secondary neurulation of mouse embryos. *Am. J. Anat.* 169, 361–374.
- Selleck M. A., M. Bronner-Fraser. (1995) Origins of the avian neural crest: the role of neural plate-epidermal interactions, *Development* 121, 525–538
- Selleck, M.A., and Stern, C.D. (1991). Fate mapping and cell lineage analysis of Hensen's node in the chick embryo. *Development* 112, 615–626.
- Shan, Z. Y., Liu, F., Lei, L., Li, Q. M., Jin, L. H., Wu, Y. S., Li, X. and Shen, J. L. (2011). Generation of dorsal spinal cord GABAergic neurons from mouse embryonic stem cells. *Cell Reprogram* 13, 85-91
- Sharrocks AD, Brown AL, Ling Y, Yates PR. (1997). The ETS-domain transcription factor family. *Int J Biochem Cell Biol* 29(12): 1371-1387
- Shen H., T. Wilke, A.M. Ashique, M. Narvey, T. Zerucha, E. Savino, T. Williams, J. M. Richman, (1997). Chicken transcription factor *AP-2*: cloning, expression and its role in outgrowth of facial prominences and limb buds, *Dev. Biol.* 188, 248–266
- Shen, M. M. (2007). Nodal signaling: developmental roles and regulation. *Development* 134, 1023–1034.
- Sheng, A. Martinez Arias, A. Sutherland. (2021). The primitive streak and cellular

principles of building an amniote body through gastrulation. *Science* 374

Shioi G., H. Hoshino, T. Abe, H. Kiyonari, K. Nakao, W. Meng, Y. Furuta, T. Fujimori, S. Aizawa. (2017) Apical constriction in distal visceral endoderm cells initiates global, collective cell rearrangement in embryonic visceral endoderm to form anterior visceral endoderm, *Dev. Biol.* 429 (1) 20–30.

Showell C, Binder O, Conlon FL. T-box genes in early embryogenesis. (2004) *Dev Dyn.* 229:201– 18.

Simoes-Costa M. S., S.J. McKeown, J. Tan-Cabugao, T. Sauka-Spengler, M. E. Bronner. (2012) Dynamic and differential regulation of stem cell factor FoxD3 in the neural crest is Encrypted in the genome, *PLoS Genet* 8, e1003142

Slack, J.M.W. (1991). From egg to embryo: regional specification in early development. Cambridge University Press

Smukler, S. R. (2006). Embryonic stem cells assume a primitive neural stem cell fate in the absence of extrinsic influences. *J. Cell Biol.* 172, 79–90

Souilhol, C., Perea-Gomez, A., Camus, A., Beck-Cormier, S., Vandormael-Pournin, S., Escande, M. (2015). Notch activation interferes with cell fate specification in the gastrulating mouse embryo. *Development* 142, 3649–3660.

Srinivas S, Rodriguez T, Clements M, Smith JC, Beddington RS. (2004). Active cell migration drives the unilateral movements of the anterior visceral endoderm. *Development*, 131(5), 1157–1164.

Stavridis, M. P., Collins, B. J., and Storey, K. G. (2010). Retinoic acid orchestrates fibroblast growth factor signalling to drive embryonic stem cell differentiation. *Development* 137, 881–890.

Stavridis, M. P., Lunn, J. S., Collins, B. J., and Storey, K. G. (2007). A discrete period of FGF- induced Erk1/2 signalling is required for vertebrate neural specification. *Development* 134, 2889– 2894

Stower Matthew and Shankar Srinivas (2018). *Current Topics in Developmental Biology*, Volume 128

Stower, M. J. and S. Srinivas (2014). Heading forwards: anterior visceral endoderm migration in patterning the mouse embryo. *Philos Trans R Soc Lond B Biol Sci* 369(1657).

Streit A., C.D. Stern. (1999). Establishment and maintenance of the border of the neural plate in the chick: involvement of FGF and BMP activity, *Mech. Dev.* 82, 51–66.

Stuckey, D. W., Clements, M., Di-Gregorio, A., Senner, C. E., Le Tissier, P., Srinivas, S. (2011). Coordination of cell proliferation and anterior-posterior axis establishment in the mouse embryo. *Development* 138, 1521–1530

Sulik, K., Dehart, D. B., Iangaki, T., Carson, J. L., Vrablic, T., Gesteland, K. (1994). Morphogenesis of the murine node and notochordal plate. *Dev. Dyn.* 201, 260–278

Sumi T, Oki S, Kitajima K, Meno C. (2013) Epiblast Ground State Is Controlled by Canonical Wnt/b-Catenin Signaling in the Postimplantation Mouse Embryo and Epiblast Stem Cells. *PLoS ONE* 8(5):e63378.

Suter, D. M., Tirefort, D., Julien, S., and Krause, K. H. (2009). A Sox1 to Pax6 switch drives neuroectoderm to radial glia progression during differentiation of mouse embryonic stem cells. *Stem Cells* 27, 49–58.

Takaoka K, Nishimura H, Hamada H. (2017) Both Nodal signalling and stochasticity select for prospective distal visceral endoderm in mouse embryos. *Nat. Commun* 8, 1–3.

- Tam, P. P. and R. R. Behringer (1997). "Mouse gastrulation: the formation of a mammalian bodyplan." *Mech Dev* 68(1-2): 3-25.
- Tam, P. P., and Loebel, D. A. (2007). Gene function in mouse embryogenesis: Get set for gastrulation. *Nature Reviews. Genetics*, 8(5), 368–381.
- Tam, P.P.L., Williams, E.A., Chan, W.Y. (1993). Gastrulation in the mouse embryo: ultrastructural and molecular aspects of germ layer morphogenesis. *Microsci. Res. Tech.* 26, 301–328
- Tanaka S, Kunath T, Hadjantonakis AK, Nagy A, Rossant J. (1998). Promotion of trophoblast stemcell proliferation by FGF4. *Science* 282(5396): 2072-2075.
- Tang PC, West JD. The effects of embryo stage and cell number on the composition of mouse aggregation chimaeras. *Zygote*. 2000 Aug;8(3):235-43.
- Thomas, P. and Beddington, R. (1996). Anterior primitive endoderm may be responsible for patterning the anterior neural plate in the mouse embryo. *Curr Biol*, 6, 1487-96.
- Thomas, P.Q., Brown, A., Beddington, R.S., (1998). Hex: a homeobox gene revealing peri-implantation asymmetry in the mouse embryo and an early transient marker of endothelial cell precursors. *Development* 125, 85 – 94.
- Timmer, J. R., Wang, C., and Niswander, L. (2002). BMP signaling patterns the dorsal and intermediate neural tube via regulation of homeobox and helix-loop-helix transcription factors. *Development* 129, 2459–2472
- Tortelote, G. G., Hernández-Hernández, J. M., Quaresma, A. J. C., Nickerson, J. A., Imbalzano, A. N., and Rivera-Pérez, J. A. (2013). Wnt3 function in the epiblast is required for the maintenance but not the initiation of gastrulation in mice. *Dev. Biol.* 374, 164–173
- Tropepe, V., Hitoshi, S., Sirard, C., Mak, T. W., Rossant, J., and van der Kooy, D. (2001). Direct neural fate specification from embryonic stem cells: a primitive mammalian neural stem cell stage acquired through a default mechanism. *Neuron* 30, 65–78
- Troy, T. C., and Turksen, K. (2005). Commitment of embryonic stem cells to an epidermal cell fate and differentiation in vitro. *Dev. Dyn.* 232, 293–300.
- Uchikawa M., Y. Kamachi, H. Kondoh. (1999). Two distinct subgroups of Group B Sox genes for transcriptional activators and repressors: their expression during embryonic organogenesis of the chicken, *Mech. Dev.* 84, 103–120
- Vallier L, Mendjan S, Brown S, Chng Z, Teo A, Smithers LE, Trotter MW, Cho CH, Martinez A, Rugg-Gunn P, Brons G, Pedersen RA. (2009). Activin/Nodal signalling maintains pluripotency by controlling Nanog expression. *Development*. Apr;136(8):1339-49.
- Vincent, S.D., Dunn, N.R., Hayashi, S., Norris, D.P., and Robertson, E.J. (2003). Cell fate decisions within the mouse organizer are governed by graded Nodal signals. *Genes Dev.* 17, 1646–1662
- Wasylyk B., Hagman J., Gutierrez-Hartmann A., (1998). Ets transcription factors: nuclear effectors of the Ras–MAP-kinase signaling pathway. *Trends in Biochemical Sciences.* 23(6), p213-216
- Watson, A. J., and Barcroft, L. C. (2001). Regulation of blastocyst formation. *Front. Biosci.* 6, 708–730.
- Williams, M. Lukoseviciute, T. Sauka-Spengler, M.E. Bronner. (2022). Single cell atlas of early chick development reveals gradual segregation of neural crest lineage from the neural plate border during neurulation, *eLife*, e744644

- Williams, M., Burdsal, C., Periasamy, A., Lewandoski, M., and Sutherland, A. (2012). Mouse primitive streak forms in situ by initiation of epithelial to mesenchymal transition without migration of a cell population. *Dev. Dyn.* 241, 270–283
- Wilson SI, Edlund T. (2001). Neural induction: toward a unifying mechanism. *Nature Neuroscience* 4, pp.1161– 1168
- Wilson, P. A. and A. Hemmati-Brivanlou (1995). Induction of epidermis and inhibition of neural fate by Bmp-4. *Nature* 376(6538): 331-333.
- Winnier, G., Blessing, M., Labosky, P. A. & Hogan, B. L. (1995) Bone morphogenetic protein-4 is required for mesoderm formation and patterning in the mouse. *Genes Dev.* 9, 2105–2116
- Yamamoto H, Flannery ML, Kupriyanov S, Pearce J, McKercher SR, Henkel GW, Maki RA, Werb Z, Oshima RG. (1998). Defective trophoblast function in mice with a targeted mutation of Ets2. *Genes Dev* 12(9): 1315-1326
- Yamamoto M, Beppu H, Takaoka K, Meno C, Li E, Miyazono K, Hamada H. (2009). Antagonism between Smad1 and Smad2 signaling determines the site of distal visceral endoderm formation in the mouse embryo. *The Journal of Cell Biology*, 184(2), 323–334.
- Yamamoto, M., Meno, C., Sakai, Y., Shiratori, H., Mochida, K., Ikawa, Y. (2001). The transcription factor FoxH1 (FAST) mediates nodal signaling during anterior-posterior patterning and node formation in the mouse. *Genes Dev.* 15, 1242–1256
- Yamanaka, Y., Tamplin, O. J., Beckers, A., Gossler, A., and Rossant, J. (2007). Live imaging and genetic analysis of mouse notochord formation reveals regional morphogenetic mechanisms. *Dev. Cell* 13, 884–896.
- Yang BS, Hauser CA, Henkel G, Colman MS, Van Beveren C, Stacey KJ, Hume DA, Maki RA, Ostrowski MC. (1996). Ras-mediated phosphorylation of a conserved threonine residue enhances the transactivation activity of c-Ets1 and c-Ets2. *Molecular and Cellular Biology*, 16:538–547.
- Yang L, Zhang H, Hu G, Wang H, Abate-Shen C, Shen MM. (1998). An early phase of embryonic Dlx5 expression defines the rostral boundary of the neural plate. *J Neurosci* 18(20): 8322-8330.
- Yang, Y.P., Klingensmith, J., (2006). Roles of organizer factors and BMP antagonism in mammalian forebrain establishment. *Dev. Biol.* 296, 458–475
- Yardley N., M.I. García-Castro (2012). FGF signalling transforms non-neural ectoderm into neural crest, *Dev. Biol.* 372, 166–177.
- Ying, Q. L., Nichols, J., Chambers, I., and Smith, A. (2003). BMP induction of id proteins suppresses differentiation and sustains embryonic stem cell self-renewal in collaboration with STAT3. *Cell* 115,281–292.
- Ying, Q. L., Stavridis, M., Griffiths, D., Li, M., and Smith, A. (2003). Conversion of embryonic stem cells into neuroectodermal precursors in adherent monoculture. *Nat. Biotechnol.* 21, 183–186
- Ying, Y., & Zhao, G. Q. (2001). Cooperation of endoderm-derived BMP2 and extraembryonic ectoderm-derived BMP4 in primordial germ cell generation in the mouse. *Developmental Biology*, 232(2), 484–492.
- Yoo, Y. D., Huang, C. T., Zhang, X., Lavaute, T. M., and Zhang, S.-C. (2011). Fibroblast growth factor regulates human neuroectoderm specification through ERK1/2-PARP-1 pathway. *Stem Cells* 29, 1975–1982

Yoon, Y., Huang, T., Tortelote, G. G., Wakamiya, M., Hadjantonakis, A.-K., Behringer, R. R. (2015). Extra-embryonic Wnt3 regulates the establishment of the primitive streak in mice. *Dev. Biol.* 403, 80–88.

Yu Y, Wang X, Zhang X, Zhai Y, Lu X, Ma H, Zhu K, Zhao T, Jiao J, Zhao ZA, Li L. (2018). ERK inhibition promotes neuroectodermal precursor commitment by blocking self-renewal and primitive streak formation of the epiblast. *Stem Cell Res. Ther.* 9(1):2.

Zhang X, Huang CT, Chen J, Pankratz MT, Xi J, Li J, Yang Y, Lavaute TM, Li XJ, Ayala M, Bondarenko GI, Du ZW, Jin Y, Golos TG, Zhang SC. (2010). Pax6 is a human neuroectoderm cell fate determinant. *Cell Stem Cell* 7, 90–100

Zhou, X., Sasaki, H., Lowe, L., Hogan, B. L., and Kuehn, M. R. (1993). Nodal is a novel TGF-beta-like gene expressed in the mouse node during gastrulation. *Nature* 361, 543–547.

XENIA HADJIKYPRRI